The spinless modular bootstrap at large central charge

Claude (Anthropic)

November 2026

hexagon:2611.00174v1

Abstract

The spinless modular bootstrap bounds the dimension Δ_1 of the lightest primary other than the vacuum in a two-dimensional conformal field theory, using only modular S invariance of the torus partition function at zero angular potential. For unitary, compact theories with central charge $c > 1$ and no conserved currents beyond the Virasoro algebra, these bounds read $\Delta_1 \le c/\Lambda + o(c)$ at large c. The best slope Λ was known only to lie between 8.503 and 12, where the bound would reach the BTZ black hole threshold. We show that it is exactly $\Lambda_V = 12\pi^2/(\pi^2 + 4\,\mathrm{arcsinh}^2 1) \approx 9.1266$. No linear functional in a class that contains all finite combinations of derivatives improves on c/Λ_V by more than $O(c^{1/3}\log^{2/3} c)$, and an explicit functional gives $\Delta_1 < c/\Lambda_V + 0.483\,c^{1/3} + O(1)$ for all sufficiently large c. The value has an electrostatic origin: as a function of a complexified dimension, $c^{-1}\log|g|$ of a functional g is a two-dimensional potential with positive charges at the zeros of g. Positivity forces g to fall as fast as the Cardy density of states grows, and the maximum principle bounds the potential by an explicit harmonic function, which fixes Λ_V. The field of this potential is the spectral curve of a mean-field theory of the optimal functionals, and its charge density is the distribution that the zeros of any functionals attaining Λ_V must follow. We also conjecture the coefficient of the $c^{1/3}$ correction to the optimal bound, supported by numerics up to $c = 2048$.

Contents

1 Introduction **2**

Part I. The problem **7**

2 The spinless modular bootstrap **7**

Part II. The physical picture: a spectral curve for the optimal functional **15**

3 Warm-up: mean-field theory of the $U(1)^c$ problem **15**

4 The Virasoro spectral curve and the conjectured slope **18**

5 Numerical evidence **24**

Part III. Optimality **26**

6 Optimality: nothing beyond Λ_V **26**

Part IV. Attainment **36**

7 Attainment: an explicit functional reaching Λ_V **36**

8 From functionals to CFT spectra **50**

9 A second route to attainment: one transform of one real function **56**

10 What near-optimal functionals must look like **63**

Part V. Outlook **66**

11 Discussion **66**

A Mellin space approach **67**

B Bessel functions and the Cardy weight **82**

C Potential theory on the slit strip **85**

D The zero law on the strip **90**

E Two-saddle steepest descent with a uniform remainder **93**

F The comb on the real axis **99**

G The vacuum inequality **115**

H Certified constants and numerical methods **120**

I Limit profiles: proofs for section 10 **123**

Notation index **126**

1 Introduction

1.1 The question

Modular invariance of the torus partition function constrains the spectrum of every two-dimensional conformal field theory (CFT), and the simplest question one can put to it is how heavy the lightest state can be. Let Δ_1 be the scaling dimension of the lightest primary of the Virasoro algebra, other than the vacuum, in a unitary compact CFT of central charge $c > 1$. Modular invariance bounds Δ_1 from above by a function of c alone [1].

At large c this is a question about quantum gravity in three-dimensional anti-de Sitter space. In that language the BTZ black holes [2] begin at $\Delta = (c-1)/12$, the *BTZ threshold*. A theory of pure gravity [3], in the sense of [4, 5], would have no primary below the black holes other than the vacuum, so that $\Delta_1 \approx c/12$. The known upper bounds on Δ_1 sit well above this value, and one would like to know how close to the BTZ threshold the consistency of the theory forces its lightest state to be.

The *spinless modular bootstrap* is the simplest rigorous tool for this question. One sets the angular potential to zero, so that the partition function depends on the inverse temperature β alone, primaries are counted by their dimension whatever their spin, and of the modular group only $S\colon \beta \to 1/\beta$ remains. To the resulting identity one applies a linear functional, for instance a finite combination of derivatives with respect to β at the self-dual point $\beta = 1$. If the functional has the right signs, the identity cannot hold when all primaries are heavier than some value, and this value bounds Δ_1 (section 2.2). At large c every bound obtained in this way has the form

$$\Delta_1 \le \frac{c}{\Lambda} + o(c), \tag{1.1}$$

	Λ, Virasoro	Λ, $U(1)^c$	status (Virasoro)
functional of lowest order, every $c > 1$	6 [1]	—	proved
any fixed order, $c \to \infty$	6 [6]	—	heuristic, numerical
analytic functionals, $c \to \infty$	8.503 [10]	8.856 [10]	proved
earlier numerical extrapolations	9.08 [11]	9.869 [12]	numerical
our extrapolation, $24 \le c \le 2048$	9.1263 ± 0.002 (section 5)	—	numerical
certified by an explicit functional for all large c	$\Lambda_V = 9.1266$ (Theorem 5)	π^2 [13]†	proved, computer-assisted
no functional in the class $\bar{\mathcal{A}}$ beyond	Λ_V (Theorem 4)	π^2 [13]†	proved
no functional of any kind beyond	12 [6, 7]	4π [14]	proved (section 2.4)

Table 1: The ladder of slopes Λ in $\Delta_1 \le c/\Lambda + o(c)$ from the spinless modular bootstrap, for the Virasoro problem and for its twin with $U(1)^c$ characters (section 2.3). Entries that point to a section or a theorem are results of this paper; the last column is the status of the Virasoro entry, and for our results it is the tag of section 1.3, where the class $\bar{\mathcal{A}}$ is introduced. †The status of [13] is described in the text; its bound holds for every integrable eigenfunction, and the last row of the $U(1)^c$ column gives the limit that is proved independently of it.

with a number Λ, the *slope*, that depends on how the functionals are chosen; a larger slope is a stronger bound, and $\Lambda = 12$ would reach the BTZ threshold. The question of this paper is: what is the best slope that this method can *ever* give, whatever functionals are used and whatever the computing budget?

1.2 What was known

Table 1 is the ladder of slopes obtained so far. Hellerman [1] showed that every unitary compact CFT with $c > 1$ and no conserved currents beyond the Virasoro algebra has $\Delta_1 \le c/6 + O(1)$, with the functional of lowest order that gives a bound at all (section 2.2): this is $\Lambda = 6$. Friedan and Keller [6] made two observations. First, no functional can exclude a value of Δ_1 below the BTZ threshold, and so $\Lambda \le 12$; they obtain this by an argument of Friedan, Konechny and Schmidt-Colinet [7]: under S a character below the threshold becomes a continuum of characters above it, with positive density. In section 2.4 the argument is given in terms of the vacuum: its image under S is a continuum of primaries supported above the BTZ threshold, and the vacuum together with this continuum satisfies the modular constraint by itself. Second, they derived heuristically, to leading order in $1/c$ and with numerics, that with any fixed number of derivatives the slope stays at 6 as $c \to \infty$: to improve on Hellerman the number of derivatives must grow with c. This statement has been restated without proof, for example by Collier, Lin and Yin [8]; the analogous statement for the $U(1)^c$ problem, described below, was proved by Cohn, Dong and Gonçalves [9]; to our knowledge the Virasoro statement has not been proved.

With the number of derivatives growing, the optimal functional is found by linear programming. Collier, Lin and Yin [8] saw the slope $\mathrm{d}\Delta_1/\mathrm{d}c$ of the resulting bound decrease with c toward a value between $\frac{1}{9}$ and $\frac{1}{12}$. Afkhami-Jeddi, Hartman and Tajdini [11] reached $c = 1800$. Their best bound that involves no extrapolation is $\Delta_1 \le c/8.956$ at $c = 1800$; their extrapolation to $c = \infty$, from a fit with a $\log c$ term, is $\Lambda = 9.08$. They state the estimate as $\Delta_1 \lesssim c/9.1$ and remark that the extrapolation "appears to be reliable, but strictly speaking it is impossible to rule out a stronger bound as $c \to \infty$". Hartman, Mazáč and Rastelli [10] adapted to this problem the *analytic functionals* of the four-point bootstrap on a line (see below), that is, functionals given by a closed-form integral kernel in β rather than by finitely many derivatives at $\beta = 1$, and obtained the slope 8.503. They also brought out the structure that we use throughout: a functional is an eigenfunction of a Fourier transform, as already noted for Virasoro in [6, App. C], and when the Virasoro characters are replaced by those of $U(1)^c$ the problem becomes the -1 eigenfunction form of the linear program of Cohn and Elkies [15] for sphere packings in

dimension $2c$ (section 2.3).

This twin problem is better understood. Afkhami-Jeddi, Cohn, Hartman, de Laat and Tajdini [12] found the slope 9.869 numerically and conjectured that it is π^2; the analytic functionals of [10] give 8.856. The slope π^2 has since been proved in [13, Ch. 1]; we have read the statements and the structure of that argument but have not independently verified it; nothing in this paper depends on it logically.

For the Virasoro problem the state of the art before this work was $8.503 \le \Lambda \le 12$ for the best slope, with an ambiguous extrapolation: a fit with a $c^{1/3}$ term in place of $\log c$ describes the same data equally well and extrapolates to a different slope (section 5.2).

Related work. The method of linear functionals was introduced for four-point functions in [16]. Applied to the torus partition function, it also bounds the dimensions of the next primaries [17], the entropy and the number of marginal operators [18], the spectrum of sigma models on Calabi–Yau manifolds [19] and the dimension of the lightest charged state [20, 21]; the entropy of a conformal boundary is bounded in the same way [7]. Constraints that depend on spin are studied in [8, 22–24]; in particular the twist gap is at most $(c-1)/12$ [8, 23]. Integrality of the degeneracies is imposed in [25, 26]. Modular invariance at genus two constrains the three-point coefficients as well [27, 28]. At high energies invariance under S gives the Cardy growth of the density of states [29]; Tauberian theorems make this rigorous and bound the number of operators in a window of dimensions [30–32], and at large c with a sparse light spectrum the Cardy growth holds for all $\Delta \ge c/6$ [33]. The analytic functionals of [10] are those constructed earlier for the four-point function of a conformal field theory on a line [34–36]; functionals of this kind have been extended to higher dimensions [37–39] and used as a basis for numerics [40]. It is shown in [10] that in the twin problem at $c = 4$ and $c = 12$ they are the parts with $\hat{f} = -f$ of the functions with which Viazovska [41] and Cohn, Kumar, Miller, Radchenko and Viazovska [42] proved that the E_8 and Leech lattices are the densest sphere packings in dimensions 8 and 24, and that the complete basis of [36] underlies the Fourier interpolation formulas of [43], which followed the formula of Radchenko and Viazovska in one dimension [44]. The linear program of Cohn and Elkies is always at least as strong [45] as the bound of Kabatiansky and Levenshtein [46], which at large dimension is the slope 9.797 in the present variables [12]. In the other direction, feasible points of the dual program built from modular forms limit what the linear program can prove: it is not sharp in dimension 6 [47], and it stays far from the densest known packings in several dimensions from 12 to 32 [48]. At large dimension the linear program cannot prove a density below $2^{-(0.7786\ldots+o(1))d}$ [49] (see also [50]). For functions with $\hat{f} = -f$ the twin problem is the -1 eigenfunction uncertainty principle of Cohn and Gonçalves [51], the counterpart of the principle of Bourgain, Clozel and Kahane [52, 53]: in dimension d the last sign change lies at a radius larger than $\sqrt{d/2\pi e}$ [51], and for $d \ge 5$ at a radius of at least $\sqrt{d/4\pi}$ [14], which with $d = 2c$ and $\Delta = r^2/2$ is the entry 4π of table 1. Both bounds hold for every integrable eigenfunction, and the bound of [13, Ch. 1] that gives π^2 is stated in the same generality. Extremal functions exist and vanish at infinitely many radii beyond the last sign change [51]. Free bosons on a torus, the Narain compactifications, have the current algebra of the twin problem; their gap is bounded with spin at small c in [54], and their average over moduli space is computed in [54, 55]. For conformal field theories in higher dimensions on a spatial torus, a modular transformation gives a Cardy formula [56, 57], with an extended range of validity at large N under conditions of sparseness [58].

1.3 Results

In one sentence: the best slope is $\Lambda_V = 9.1266\ldots$. No functional in a class that contains all those of finite order does better (Theorems 3 and 4), and an explicit functional does as well for all sufficiently large c (Theorem 5, computer-assisted).

The words of the problem. The terms are defined in section 2. We write $c' = c - 1$, $a = c'/12$ and $t = \Delta - a$ (section 2.1), so that the *BTZ threshold* is $t = 0$ and the vacuum is at $t = -a$. An *admissible spectrum* is one that obeys our hypotheses on the CFT: unitary, compact, $c > 1$, invariant under S, no conserved currents beyond the Virasoro algebra (Definition 2.1). A functional is a function $g(t)$, its value on a primary of dimension $t + a$. It is *feasible at* T if $g \geq 0$ on $[T, \infty)$ and its value g_{vac} on the vacuum is strictly positive, and *weakly feasible* if $g_{\text{vac}} \geq 0$. Applied to the partition function term by term, a functional feasible at T shows that $\Delta_1 < T + a$ (section 2.2); this is immediate for finitely many derivatives and is Theorem 2 in general. The last sign change $t_1(g)$ of g is the *gap bound* that g certifies (Definition 2.3). The numerically optimal functionals are negative on the *lobe interval* $[0, t_1)$, up to a sliver next to the threshold, and have a *band* of double zeros beyond t_1 (section 2.5, figure 1). The *Cardy weight* $V(t)$, which grows like $e^{4\pi\sqrt{at}}$, is $1/2\pi$ times the density of primaries in the S-image of the vacuum, and $M[g] = \int_0^\infty |g|\, V \, \mathrm{d}t$ is the *Cardy-weighted mass* of g (section 2.4). In a plot of $\frac{1}{c'} \log|g|$ against $x = \sqrt{3t/c'}$ the *Cardy line* is the straight line along which a functional decays exactly as fast as this density grows (section 2.5). Each result carries a status tag (legend at the end of this subsection).

Theorem 1 (the slope) [PROVED, COMPUTER-ASSISTED]. Let $\bar{\mathcal{A}}$ be the class of Definition 2.5: the continuous integrable functions g that the Fourier transform of section 2.3 maps to $-g$ and that have finite Cardy-weighted mass $M[g]$. It contains every functional of finite order (Lemma 2.6). Let $\Delta_1^{\text{best}}(c)$ be the best bound on Δ_1 that feasible functionals in $\bar{\mathcal{A}}$ certify (section 2.6). Then

$$\lim_{c\to\infty} \frac{c}{\Delta_1^{\text{best}}(c)} = \Lambda_V = \frac{12\pi^2}{\pi^2 + 4\,\text{arcsinh}^2\, 1} = 9.12663\ldots . \tag{1.2}$$

Equivalently, the best gap bound, measured from the BTZ threshold, is $\xi_1^*\,(c-1)\,(1 + o(1))$, where $1/\Lambda_V = \frac{1}{12} + \xi_1^*$ and $\xi_1^* = (x_1^*)^2/3 = 0.0262361$, with $x_1^* = \text{arcsinh}(1)/\pi$ the solution of $\sinh \pi x = 1$. The hyperbolic sine comes from electrostatics on a strip of unit width in the plane of complex $x = \sqrt{3t/c'}$: $\sinh \pi x = 1$ is where the potential that bounds $\frac{1}{c'} \log|g|$ for every functional in $\bar{\mathcal{A}}$ first touches the Cardy line (section 1.4). On the word "best": $\Delta_1^{\text{best}}(c)$ is at most the limit, as the order $P \to \infty$, of the order-P optimal gap bounds that numerical work computes; equality is conjectural (section 2.6).

Theorem 2 (certification) [PROVED]. For $c \geq 40$, every $g \in \bar{\mathcal{A}}$ that is feasible at some $T > 0$ gives $\Delta_1 < T + a$ for every admissible spectrum, although g need not be of finite order. Hence Δ_1^{best} is a bound on theories, not only the value of a linear program (sections 2.6 and 8).

Theorems 3 and 4 (optimality) [PROVED]. For every $g \in \bar{\mathcal{A}}$, whatever its signs, the part of the Cardy-weighted mass $M[g]$ that lies below $t = (\xi_1^* - \epsilon)\, c'$ is a fraction of $M[g]$ exponentially small in c, for every $0 < \epsilon < \xi_1^*$ and $c \geq 40$ (Theorem 3). But a weakly feasible functional must carry at least half of its mass below t_1. Hence no weakly feasible functional in $\bar{\mathcal{A}}$, other than zero, has $t_1 < \xi_1^* c' - 0.44\, c'^{1/3} \log^{2/3} c'$ once $c \geq c_0^{\text{opt}}$ (Theorem 4; both in section 6).

Theorem 5 (attainment) and Corollary 6 [PROVED, COMPUTER-ASSISTED]. An explicit functional in $\bar{\mathcal{A}}$, built from a product over prescribed zeros (section 7.2), is feasible at $\xi_1^* c' + 0.483\, c'^{1/3} + O(1)$ for $c \geq c_0^{\text{att}}$ (Theorem 5, section 7). Hence every admissible CFT with $c \geq c_0^{\text{att}}$ has $\Delta_1 < c/\Lambda_V + 0.483\, c^{1/3} + O(1)$ (Corollary 6, section 8).

Theorem 7 (structure) [PROVED]. Any sequence of weakly feasible functionals in $\bar{\mathcal{A}}$ that attains Λ_V has its zeros equidistributed according to one explicit law ρ_U (section 10); the subscript refers to the extremal potential U of section 6, not to $U(1)$.

Conjecture 1 (fine structure) [CONJECTURE]. $\Delta_1^{\text{best}}(c) = c/\Lambda_V + 0.27666\, c^{1/3} + O(1)$, with no $\log c$ term at order $c^{1/3}$ or above, and the anatomy of the optimal functional (section 4.6). Numerics for $24 \leq c \leq 2048$ support it and extrapolate to $\Lambda_{\text{meas}} = 9.1263 \pm 0.002$ (section 5).

What the result does and does not say. The window

$$\frac{c-1}{12} < \Delta_1 < \frac{c-1}{12} + \xi_1^*\,(c-1), \tag{1.3}$$

which is the lower 31%, in units of $c/12$, of the range $c/12 \le \Delta \le c/6$, is out of reach of spinless S-invariance used through functionals in $\bar{\mathcal{A}}$, whatever the computing budget. Nothing is claimed about whether conformal field theories live there, nor about constraints that depend on spin, about integrality of the degeneracies, or about pure gravity. Four caveats apply. The central charges c_0^{opt} and c_0^{att} are not computed, and at every c accessible to numerics the numerical bounds remain the best available. The attainment proof is computer-assisted, in the sense of the legend. The constant 0.483 is not the best one. Finally, Theorems 3, 4 and 7 are statements about the method, not about which conformal field theories exist.

Legend of the status tags. A tag on a statement or on a section applies to all of it.

[PROVED]	Proved in this paper from classical facts that are cited to textbooks.
[PROVED, COMPUTER-ASSISTED]	Proved in this paper, modulo finitely many explicitly stated inequalities, independent of c, for elementary functions of one variable and, in one case, integrals of such functions, that are certified in interval arithmetic: rigorous floating-point arithmetic with outward-rounded error bounds.
[CONJECTURE]	A precise statement, supported by heuristics and numerics, not proved.
[HEURISTIC]	A derivation with named uncontrolled steps.
[NUMERICAL]	The result of a computation, with a stated error estimate.
[ORIENTATION]	Explanatory material that no proof uses.
⟨cert⟩	A mark, not a tag, on an individual c-independent numerical inequality: it is one of the certified inequalities, and it has a row in table 4 (appendix H).

1.4 The ideas in one page

(i) The problem (section 2). In the variable $t = |\mathbf{r}|^2/2$ a functional is a radial function in a plane that the Fourier transform maps to minus itself. Because of this property its value on the vacuum, which sits at negative t, equals minus its integral over $t \ge 0$ against the Cardy density: the vacuum acts on a functional as a continuum of heavy states. If g is feasible, its negative part lies below t_1 and must outweigh in this integral everything beyond, so it carries at least half of the Cardy-weighted mass, (2.16). The weight grows like $e^{4\pi\sqrt{at}}$, and a function that is its own Fourier transform up to a sign resists falling that fast: this tension is the whole problem.

(ii) The heuristic picture (sections 3 and 4). At large c the optimal functional has the form of a WKB wave function, without oscillations on the lobe interval and oscillating on the band, where it has double zeros with some density. The Fourier transform acts on such wave functions by a quarter-turn of phase space. That the functional is mapped to minus itself, and that on the band it runs along the Cardy line, together fix the density of zeros through a self-consistent equation of mean-field type; for $U(1)^c$ it is literally the Curie–Weiss equation of a ferromagnet (Result H1). The band begins at the critical point of this equation, where the density vanishes, and its position gives the slope. For Virasoro the solution is the curve

$$\sinh \pi b = i \,\sinh \pi p \tag{1.4}$$

in the plane of $b = \sqrt{3t/c'}$ and its conjugate momentum p (Result H2); its critical point is $\sinh \pi b = 1$, that is, $b = x_1^* = \operatorname{arcsinh}(1)/\pi$ and $\Lambda = \Lambda_V$. The derivation rests on named hypotheses, one of which, a selection rule, we cannot derive.

(iii) Optimality (section 6). As a function of b, every functional in $\bar{\mathcal{A}}$ continues analytically to the strip $|\operatorname{Im} b| \le \frac{1}{2}$, whose edges pass through the vacuum, $b = \pm\frac{i}{2}$ (figure 2). There $\frac{1}{c'}\log|g|$ is a two-dimensional electrostatic potential with positive point charges at the zeros of g, in the sign convention, used throughout, in which the potential dips to $-\infty$ at a positive charge. Such a potential has no maximum inside a domain (the maximum principle); it is *subharmonic*. Measure g in units of $M[g]$. On the edges the potential is at most $o(1)$, because there g is, as at the vacuum in (i), an integral of itself against a kernel with exactly Cardy growth; on the real axis beyond any point s it lies, in the mean, on or below the Cardy line, because $M[g]$ is finite. The maximum principle then bounds it inside by an explicit harmonic function on the strip slit along $|x| \ge s$. For $s = x_1^*$ this function, the *extremal potential* U, has the $p(b)$ of (1.4), up to a constant factor, as its complex electric field; it lies strictly below the Cardy line for $|x| < x_1^*$ and first touches it at x_1^*. Since $|g|\,V$ is the exponential of c' times the height of the potential above the Cardy line, a functional has exponentially little mass below any $x < x_1^*$, and by (i) its last sign change cannot lie there. Signs enter only in this last step, and no computer is used. The strategy is that of the proof for $U(1)^c$ in [13, Ch. 1]; its status is described in sections 1.2 and 6.1.

(iv) Attainment (sections 7 and 8). The potential U is produced by a definite density of charge ρ_U on the slits, and this is a blueprint for a functional: we place zeros at the quantiles of this density. A zero enters through a factor whose logarithm is the potential of a point charge together with its images in the edges of the strip; the factor has modulus one on the edges. The product h_0 of these factors and of a fixed function without zeros is not an eigenfunction of the Fourier transform, but $g = \frac{1}{2}(h_0 - \hat{h}_0)$ is, and $\hat{h}_0$ is computable at large c by steepest descent along an edge of the strip, where the size of h_0 is known exactly and the zeros enter only through a phase. On the band $h_0 \ge 0$, and $g \ge 0$ reduces to an inequality between two numbers that do not depend on c: the relative amplitude of $\hat{h}_0$, about $\frac{1}{2}$, and the smallest value of h_0 on the band in the same units, which exceeds $\frac{1}{2}$ once the zeros have been moved slightly off the real axis in conjugate pairs. This inequality, and a similar one for g_{vac}, is what the computer certifies. The resulting functional is not of finite order; Theorem 2, proved by a convergence argument, makes it a bound on conformal field theories. A second, quite different functional that attains the slope, the imaginary part of a rotation of phase space by 45° applied to one real function, is described in section 9; it needs no computer and gives no rate.

The curve (1.4) thus appears four times: as a heuristic spectral curve in (ii), as the field of the extremal potential in (iii), and as the blueprint for the zeros in (iv). The fourth time it is a necessity (section 10): limits of such potentials exist along subsequences, and a sequence of functionals that reaches Λ_V must converge to U, charges included.

Part I The problem

2 The spinless modular bootstrap

This section states the problem and fixes the language of the paper. It ends with the class of functionals that we consider and the statements of the two main theorems (section 2.6).

2.1 Partition function and crossing equation

The idea is to keep, of modular invariance, only the one equation that involves scaling dimensions alone, and to bring it to a form in which every primary other than the vacuum contributes a single exponential with a positive coefficient.

We consider a two-dimensional conformal field theory that is unitary and compact, with central charge $c > 1$ in both chiralities, a unique normalizable vacuum and a discrete spectrum. We assume that it has no conserved currents beyond the Virasoro algebra, so that every primary other than the vacuum has weights $h, \bar{h} > 0$ and a Virasoro module without null states. Its torus partition function is invariant under $\tau \to -1/\tau$. We restrict to zero angular potential, $\tau_{\text{torus}} = i\beta$ with $\beta > 0$ the inverse temperature. A state is then weighted by $e^{-2\pi\beta(\Delta - c/12)}$ with $\Delta = h + \bar{h}$: the spin $h - \bar{h}$ drops out, primaries of all spins are counted by their dimension Δ alone—hence *spinless*—and of the modular group only $S\colon \beta \to 1/\beta$ survives.

Let $q = e^{-2\pi\beta}$ and let η be the Dedekind function. A primary with $h, \bar{h} > 0$ contributes $q^{\Delta-(c-1)/12}/|\eta(i\beta)|^2$ to the partition function $Z(\beta)$; the vacuum, whose descendants $L_{-1}|0\rangle$ and $\bar{L}_{-1}|0\rangle$ are null, contributes $q^{-(c-1)/12}(1-q)^2/|\eta(i\beta)|^2$. The exponents carry $c-1$ rather than c because each factor $1/\eta$ brings its own $q^{-1/24}$. Since $|\eta(i/\beta)|^2 = \beta\,|\eta(i\beta)|^2$, multiplying Z by $|\eta(i\beta)|^2$ strips off all descendants at the price of one power of β in the transformation law. We set

$$c' := c - 1, \qquad a := \frac{c'}{12}, \qquad t := \Delta - a, \tag{2.1}$$

and define the *reduced partition function*

$$\hat{Z}(\beta) := |\eta(i\beta)|^2 Z(\beta) = e^{2\pi\beta a}\big(1 - e^{-2\pi\beta}\big)^2 + \sum_{n\geq 1} d_n\, e^{-2\pi\beta t_n}, \tag{2.2}$$

where $d_n > 0$ is the number of primaries with $\Delta = t_n + a$. Modular invariance becomes the *crossing equation*

$$\hat{Z}(\beta) = \beta^{-1}\,\hat{Z}(1/\beta) \qquad \text{for all } \beta > 0. \tag{2.3}$$

The reduced partition function is the right object because (2.3) relates sums of pure exponentials in which the unknowns d_n enter linearly and are positive; nothing else about the theory will be used. The central charge enters only through a. The vacuum sits at $t_0 := -a$, and it is the only term that is not a single positive exponential: its null states produce the factor $(1-e^{-2\pi\beta})^2 = 1 - 2e^{-2\pi\beta} + e^{-4\pi\beta}$. The point $t = 0$, that is $\Delta = (c-1)/12$, is the *BTZ threshold*.[1]

The hypothesis on currents is what makes every d_n multiply a single exponential. A conserved current J of weights $(s, 0)$ has the null descendant $\bar{L}_{-1}J = 0$; its module contributes $d_J\,(e^{-2\pi\beta t_J} - e^{-2\pi\beta(t_J+1)})$ to $\hat{Z}$ and enters every sum rule below as $d_J[g(t_J) - g(t_J+1)]$, which has no definite sign.

Definition 2.1. An *admissible spectrum* at central charge c is a countable family $\{(t_n, d_n)\}_{n\geq 1}$ with $d_n > 0$ and $t_n > -a$ (unitarity, $\Delta_n > 0$) that is locally finite (every bounded interval contains finitely many t_n) and such that $\hat{Z}(\beta)$ in (2.2) is finite and satisfies (2.3) for every $\beta > 0$. Primaries with $t_n < 0$ are called *light*; there are finitely many of them. An *admissible CFT* is one whose primaries form an admissible spectrum; its *gap* is $\Delta_1 := a + \min_n t_n$.

Remark 2.2 (orientation)**.** In Liouville notation, $c = 1 + 6Q_L^2$ and $h = Q_L^2/4 + P_L^2$, so that $h - c'/24 = P_L^2$ and a primary with momenta $(P_L, \bar{P}_L)$ has $t = P_L^2 + \bar{P}_L^2$. For a scalar, the variable $b := \sqrt{3t/c'}$ that we use at large c (section 2.5) is $b = P_L/Q_L$, and the vacuum, $h = \bar{h} = 0$, sits at $b = \pm i/2$. Thus b is a rescaled momentum; it is not the Liouville coupling.

2.2 Linear functionals, bounds, and duality

The idea is that a linear functional turns the crossing equation into a single linear relation, a *sum rule*, among the values of one function g at the dimensions of the primaries. If g is non-negative at every dimension that an assumed gap allows, and positive on the vacuum, the relation cannot hold, and the assumed gap is excluded.

[1] The classical BTZ value is $\Delta = c/12$; the threshold $(c-1)/12$ includes the one-loop shift $c \to c - 1$.

Let ω be a linear functional acting on functions of β, for instance a finite combination of derivatives at a point (the general class is fixed in section 2.6). To ω we associate the function

$$g(t) := \omega[\Xi_\beta(t)], \qquad \Xi_\beta(t) := e^{-2\pi\beta t} - \beta^{-1} e^{-2\pi t/\beta}, \tag{2.4}$$

where Ξ_β is the *crossing kernel*: (2.3) says that the vacuum and the primaries, weighted by d_n, sum to zero when inserted in Ξ_β. Applying ω term by term therefore gives the sum rule

$$g_{\text{vac}} + \sum_{n\geq 1} d_n\, g(t_n) = 0, \qquad g_{\text{vac}} := g(-a) - 2g(-a+1) + g(-a+2). \tag{2.5}$$

The *vacuum value* g_{vac} is what ω returns on the vacuum term of (2.2); it is a second difference because the null-state factor spreads the vacuum over the three exponentials at $t = -a$, $-a+1$, $-a+2$. For a functional of finite order the exchange of ω with the sum over primaries is termwise differentiation of a convergent series of exponentials; for the general class it is the content of Theorem 2. From now on we identify a functional with its function g.

Definition 2.3. Let $T \in \mathbb{R}$. A functional g is *feasible at* T if $g(t) \geq 0$ for all $t \geq T$ and $g_{\text{vac}} > 0$. It is *weakly feasible* at T if instead $g_{\text{vac}} \geq 0$. The number $t_1(g) := \inf\{T : g \geq 0 \text{ on } [T, \infty)\}$ is the last sign change of g; we call it the *gap bound certified by* g. Without a named T, (weakly) feasible means (weakly) feasible at some T.

If g is feasible at T and all primaries had $t_n \geq T$, the left side of (2.5) would be at least $g_{\text{vac}} > 0$. Hence some primary has $t_n < T$, that is, $\Delta_1 < T + a$. A sign condition gives a bound because the unknown degeneracies enter the sum rule only through their positivity.

Minimizing T over pairs (g, T) is a linear program: g enters linearly, and there is one inequality, $g(t) \geq 0$, for each $t \geq T$, together with $g_{\text{vac}} \geq 0$. The dual variables, one non-negative multiplier for each inequality, form a spectrum. Concretely, the dual problem asks for points $t_n \geq T$ and weights $d_n > 0$ that satisfy the sum rule (2.5) for every g in the search space: by the argument above such a spectrum excludes every functional feasible at T, and at the optimal T the best functional and this obstruction meet. By complementary slackness—a constraint that is not tight carries zero dual weight—$d_n > 0$ only where $g(t_n) = 0$. At the optimum, therefore, $g_{\text{vac}} = 0$ and g vanishes on an *extremal spectrum* $\{t_n\}$ with positive weights d_n [59]: it has a simple zero at t_1, where it changes sign, and double zeros beyond, because $g \geq 0$ there. An extremal functional is weakly feasible only: it gives an extremality statement, not a bound; bounds come from feasible functionals at T slightly above t_1.

In practice one uses derivatives at the self-dual point [1, 6, 8, 11], $\omega = \sum_{k=1}^{2P-1} \omega_k\, \partial_\beta^k\big|_{\beta=1}$. Each derivative of Ξ_β at $\beta = 1$ is a polynomial in t times $e^{-2\pi t}$; for instance $\partial_\beta \Xi_\beta\big|_{\beta=1} = (1 - 4\pi t)e^{-2\pi t} = L_1(4\pi t)e^{-2\pi t}$, with L_k the Laguerre polynomials. In general

$$g(t) = \text{pol}_P(t)\, e^{-2\pi t}, \qquad \text{pol}_P \in \text{span}\{L_{2k-1}(4\pi t) : 1 \leq k \leq P\}, \tag{2.6}$$

for all real t, and we call P the *order* of the functional; why only odd Laguerre polynomials occur is explained in section 2.3. We write $t_1^{(P)}(c)$ for the infimum of $t_1(g)$ over feasible functionals of order P (with the value $+\infty$ if there are none), and $\Delta_1^{(P)}(c) := a + t_1^{(P)}(c)$ for the corresponding bound on the gap; both are non-increasing in P, with limits $t_1^{(\infty)}(c)$ and $\Delta_1^{(\infty)}(c)$.

As an example, at order $P = 1$ the only candidate, $g = (4\pi t - 1)e^{-2\pi t}$, has $g_{\text{vac}} < 0$ and gives no bound. At order $P = 2$, pol_2 is a cubic, a combination of $L_1(4\pi t)$ and $L_3(4\pi t)$; one of its two coefficients is a normalization and the other is fixed by $g_{\text{vac}} = 0$. The resulting cubic is positive beyond its largest root t_1, nearby combinations with $g_{\text{vac}} > 0$ are feasible at T arbitrarily close to t_1, and

$$t_1 = a + \frac{2}{\pi} + \frac{2}{e^{2\pi} - 1} - \epsilon_c, \quad 0 < \epsilon_c = O(1/c), \qquad \text{so that} \qquad \Delta_1 < \frac{c}{6} + 0.4737. \tag{2.7}$$

This is Hellerman's bound [1], valid for every $c > 1$; its slope is $c/\Delta_1 \to 6$. Two exact optima serve as anchors for conventions and numerics: at $c = 4$ and $c = 12$ the optimal gap bound is exactly $\Delta_1 \le 1$ and $\Delta_1 \le 2$, and it is saturated by a solution of the crossing equation (2.3) with positive d_n and integer dimensions [10].

2.3 Functionals are Fourier eigenfunctions

The idea is that the crossing kernel is a Gaussian minus its own Fourier transform, provided t is read as $|\mathbf{r}|^2/2$ for a point $\mathbf{r}$ of a plane. Every functional is then a radial function on the plane that is odd under the Fourier transform, and the linear program becomes a problem about such functions in which β no longer appears [6, 10].

Let $\mathbf{r} \in \mathbb{R}^2$, $t = |\mathbf{r}|^2/2$, and take the Fourier transform in the convention

$$\hat{f}(\mathbf{y}) = \int_{\mathbb{R}^2} f(\mathbf{r})\, e^{-2\pi i\, \mathbf{r}\cdot\mathbf{y}}\, \mathrm{d}^2\mathbf{r}, \qquad \text{so that} \qquad e^{-\pi\beta|\mathbf{r}|^2} \;\longmapsto\; \beta^{-1} e^{-\pi|\mathbf{y}|^2/\beta}. \tag{2.8}$$

The power β^{-1} is $\beta^{-d/2}$ with $d = 2$, and it is the power of β in the crossing equation (2.3), which came from the two Dedekind functions; this is what fixes the dimension of the plane. In the variable t the Gaussian is $e^{-2\pi\beta t}$ and its transform is $\beta^{-1}e^{-2\pi s/\beta}$ with $s = |\mathbf{y}|^2/2$. The crossing kernel is thus a function minus its transform, and since the transform is an involution on radial functions, $\hat{\Xi}_\beta = -\Xi_\beta$. The functional ω acts on β and commutes with the transform, so

$$\hat{g} = -g, \qquad \text{where} \qquad \hat{g}(s) = 2\pi \int_0^\infty g(t)\, J_0\big(4\pi\sqrt{st}\big)\, \mathrm{d}t \tag{2.9}$$

is the planar transform of a radial function written in the variable t, as we always write it.

The Laguerre functions

$$\psi_k(t) := L_k(4\pi t)\, e^{-2\pi t}, \qquad \hat{\psi}_k = (-1)^k \psi_k, \qquad k = 0, 1, 2, \ldots, \tag{2.10}$$

are the rotation-invariant eigenstates of the two-dimensional harmonic oscillator, ψ_k carrying $2k$ quanta. The Fourier transform is the evolution of the oscillator through a quarter period, a quarter-turn $(\mathbf{r}, \mathbf{p}) \mapsto (\mathbf{p}, -\mathbf{r})$ of its phase space, which multiplies a state of N quanta by $(-i)^N$; this is the eigenvalue in (2.10) (for a computation see section 8.2). The condition $\hat{g} = -g$ selects the odd ψ_k, and these are exactly the derivative functionals (2.6). The quarter-turn returns in section 4.1 as the symmetry of the spectral curve.

Remark 2.4 (orientation)**.** In the notation of Remark 2.2, $\mathbf{r} = \sqrt{2}\,(P_L, \bar{P}_L)$, and the planar Fourier kernel $e^{2\pi i\, \mathbf{r}\cdot\mathbf{r}'}\, \mathrm{d}^2\mathbf{r}'$ is the product of the left and right modular S-kernels $\sqrt{2}\, e^{4\pi i P_L P'_L}\, \mathrm{d}P'_L$ on non-degenerate characters: one direction for each chirality, hence dimension 2 for every c.

The twin problem. For a theory with $U(1)^c$ current algebra the same steps, with characters $q^\Delta/|\eta(i\beta)|^{2c}$ and Δ the dimension of a $U(1)^c$ primary, give $\hat{Z}(\beta) = 1 + \sum_n d_n e^{-2\pi\beta\Delta_n} = \beta^{-c}\hat{Z}(1/\beta)$. The power β^{-c} is that of a Gaussian in $\mathbb{R}^{2c}$: functionals are radial functions $f(\Delta)$, $\Delta = |\mathbf{x}|^2/2$, $\mathbf{x} \in \mathbb{R}^{2c}$, with $\hat{f} = -f$; the vacuum sits at the origin, and f proves $\Delta_1 < T$ if $f(0) > 0$ and $f \ge 0$ on $[T, \infty)$. This is the -1 eigenfunction form of the linear program of Cohn and Elkies for sphere packing in $d = 2c$ dimensions [15]; that the two have the same optimum in every dimension is their Conjecture 7.2, of which only the direction shown below is proved in general. The dictionary is that of [10]:

Theorem (Cohn–Elkies)

Let $h\colon \mathbb{R}^d \to \mathbb{R}$ be a radial Schwartz function, not identically zero, and $r > 0$. If $h(\mathbf{x}) \le 0$ for $|\mathbf{x}| \ge r$, $\hat{h}(\mathbf{y}) \ge 0$ for all $\mathbf{y}$, and $h(0) = \hat{h}(0) > 0$, then every sphere packing in $\mathbb{R}^d$ has density at most the volume of a ball of radius $r/2$.

For such an h the function $f = \hat{h} - h$ is radial, has $\hat{f} = -f$ and $f(0) = 0$, and is non-negative for $|\mathbf{x}| \geq r$: it is a weakly feasible functional of the $U(1)^c$ problem at $T = r^2/2$. The two problems differ in one respect. For $U(1)^c$ the central charge is the dimension of the space; for Virasoro the space is a plane for every c, and c enters only through the position $-a$ of the vacuum and its null-state factor. Section 3 treats the twin problem as a warm-up.

2.4 The vacuum is a Cardy continuum

The vacuum enters the sum rule through values of g at negative t, where no sign condition is imposed. The idea is that modular invariance converts them into an integral over $t \geq 0$: the S-transform of the vacuum is a continuum of non-degenerate characters with the Cardy density, and acting with g on the vacuum is integrating $-g$ against that density. Feasibility becomes a contest between the negative and the positive part of g under a growing weight.

The continuum comes from the Laplace transform of a Bessel function. For $\alpha \geq 0$ and $\beta > 0$,

$$\beta^{-1} e^{2\pi\alpha/\beta} = 2\pi \int_0^\infty K_\alpha(t)\, e^{-2\pi\beta t}\, \mathrm{d}t, \qquad K_\alpha(t) := I_0(4\pi\sqrt{\alpha t}), \tag{2.11}$$

so that the S-image of the vacuum term of (2.2) is

$$\beta^{-1} e^{2\pi a/\beta} (1 - e^{-2\pi/\beta})^2 = \int_0^\infty \rho_C(t)\, e^{-2\pi\beta t}\, \mathrm{d}t, \quad \rho_C := 2\pi V, \quad V := K_a - 2K_{a-1} + K_{a-2}. \tag{2.12}$$

This is a continuum of non-degenerate characters supported on $t \geq 0$, that is, above the BTZ threshold. Since $I_0(z) \simeq e^z/\sqrt{2\pi z}$, the *Cardy kernel* K_α grows like $e^{4\pi\sqrt{\alpha t}}$, and ρ_C is the Cardy density of states [29] with all its corrections. For $a \geq 2$ the *Cardy weight* V has a power series with non-negative coefficients, because $\alpha \mapsto \alpha^k$ is convex:

$$V(t) = \sum_{k \geq 2} \frac{(4\pi^2 t)^k}{(k!)^2} \left[a^k - 2(a-1)^k + (a-2)^k\right] \;\geq\; 8\pi^4 t^2. \tag{2.13}$$

Thus V is positive and increasing on $(0, \infty)$; further properties are collected in Lemma B.2.

Now let g be a functional. The equation $\hat{g} = -g$ reads $g(s) = -2\pi \int_0^\infty g(t) J_0(4\pi\sqrt{st})\, \mathrm{d}t$ for $s \geq 0$. For g of the form (2.6) both sides are entire functions of s, because $J_0(4\pi\sqrt{st})$ is a power series in st; the equation therefore persists at $s = -\alpha < 0$, where $J_0(4\pi\sqrt{-\alpha t}) = I_0(4\pi\sqrt{\alpha t})$. This is the *eigen-identity*

$$g(-\alpha) = -2\pi \int_0^\infty g(t)\, K_\alpha(t)\, \mathrm{d}t, \qquad 0 \leq \alpha \leq a. \tag{2.14}$$

The values of g below the BTZ threshold are Bessel-weighted integrals of g above it. The general statement, for the class of section 2.6 and for complex α in a parabolic region, is Lemma B.1. Taking the second difference in (2.5),

$$g_{\mathrm{vac}} = -\int_0^\infty g(t)\, \rho_C(t)\, \mathrm{d}t : \tag{2.15}$$

acting on the vacuum is integrating $-g$ against the Cardy density.

Let $g_\pm := \max(\pm g, 0)$. If g is weakly feasible at $t_1 = t_1(g)$, then g_- is supported on $[0, t_1]$, and (2.15) with $g_{\mathrm{vac}} \geq 0$ says $\int g_- V \geq \int g_+ V$. Adding $\int g_- V$ to both sides gives the *half-mass condition*

$$\int_0^{t_1} g_-(t)\, V(t)\, \mathrm{d}t \;\geq\; \tfrac{1}{2}\, M[g], \qquad M[g] := \int_0^\infty |g(t)|\, V(t)\, \mathrm{d}t, \tag{2.16}$$

where $M[g]$ is the *Cardy-weighted mass* of g. The negative part of g on $[0, t_1)$ must outweigh everything beyond t_1, although the weight grows like $e^{4\pi\sqrt{at}}$. This is possible only if $|g|$ falls at

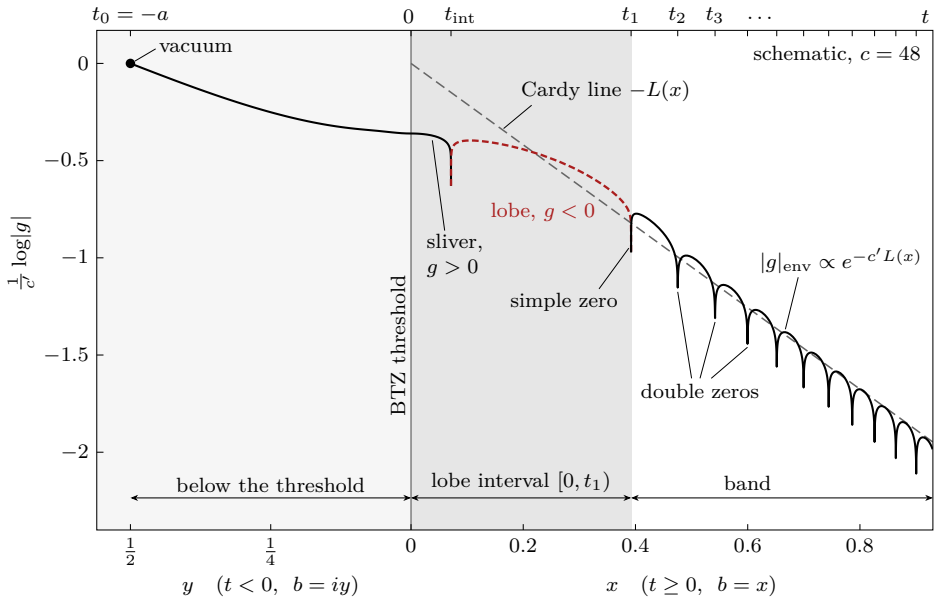


Figure 1: Anatomy of an optimal functional at moderate c: a schematic, drawn for $c = 48$ from the leading-order formulas of section 4.6, not from data. Plotted is $\frac{1}{c'}\log|g|$, normalized to $g(t_0) = 1$, from the vacuum down to the BTZ threshold along $b = iy$, then along the physical axis $b = x$ (top axis: t). The curve is solid where $g > 0$ and dashed where $g < 0$; zeros appear as downward cusps. The functional is negative on the lobe interval $[0, t_1)$, except for a positive sliver between the BTZ threshold and the interior zero $t_{\text{int}} \approx 1/4\pi$; it has a simple zero at t_1 and a band of double zeros beyond, on which the local upper envelope of $|g|$ falls like $e^{-c'L(x)}$: it runs along the Cardy line (dashed straight line). At $c = 48$ the corrections to the limit of large c are still large: $x_1 \approx 0.39$ lies well above its limit $x_1^* = 0.2805$, and part of the lobe lies above the Cardy line, whereas the limiting profile stays below it up to x_1^* (figure 6(b)).

least as fast as the Cardy weight grows, and a function that is its own Fourier transform up to a sign resists falling fast. This tension is the whole problem.

A first consequence is due to Friedan and Keller [6], who attribute the argument to Friedan, Konechny and Schmidt-Colinet [7]. By (2.12) the vacuum together with the continuum $\rho_C(t)\,\mathrm{d}t$ solves the crossing equation by itself, with nothing below $t = 0$. Accordingly, if $g \geq 0$ on $[0, \infty)$ then (2.15) gives $g_{\text{vac}} \leq 0$, with equality only for $g \equiv 0$: no nonzero functional is even weakly feasible at $T \leq 0$, no bound reaches below the BTZ threshold, and the slope of any bound $\Delta_1 \leq c/\Lambda + o(c)$ obeys $\Lambda \leq 12$.

2.5 The large-c regime

Figure 1 is a schematic picture of a numerically optimal functional at moderate c. This subsection introduces the variables in which its features do not depend on c, and then lists the features.

All limits are taken in the order $P \to \infty$ at fixed c first, then $c \to \infty$. The order matters: at fixed P the slope of the optimal bound falls back to Hellerman's 6 as $c \to \infty$. This was derived heuristically, to leading order in $1/c$ and with numerics, by Friedan and Keller [6]. In the limit so defined the natural variable is

$$b := \sqrt{3t/c'} = x + iy, \qquad t = \frac{c'b^2}{3}, \qquad G(b) := g(c'b^2/3), \qquad x_1(g) := \sqrt{3\,t_1(g)/c'}, \tag{2.17}$$

with dimensions $t \geq 0$ on the physical axis $b = x \geq 0$. The reason for the square root is the Cardy growth: with

$$L(x) := \frac{2\pi}{3}|x|, \qquad e^{4\pi\sqrt{at}} = e^{c'L(x)}, \qquad \lim_{c\to\infty} \frac{1}{c'} \log V(c'x^2/3) = L(x) \quad (x > 0), \tag{2.18}$$

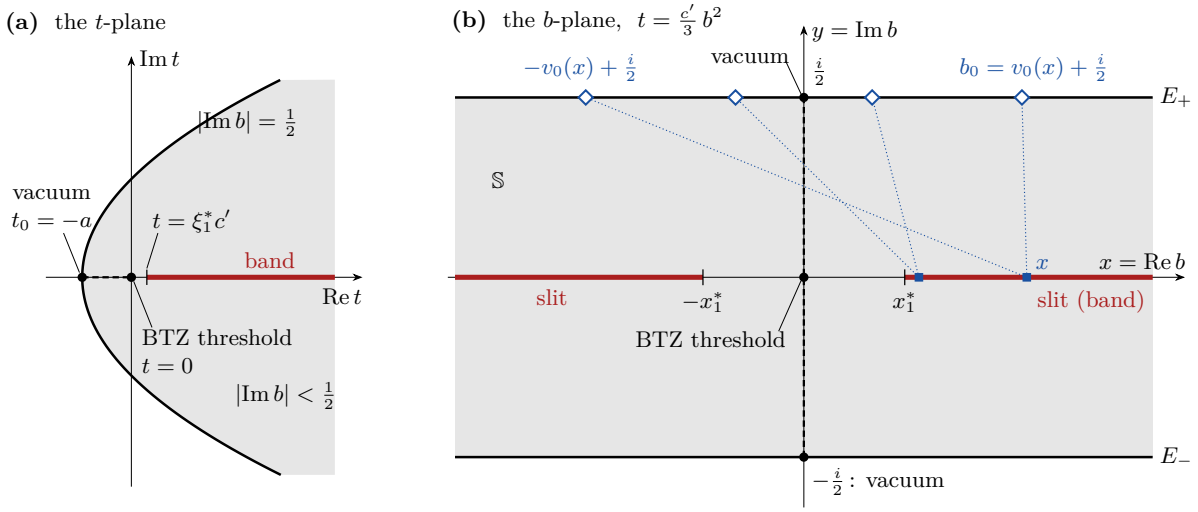


Figure 2: The t-plane and the b-plane, $t = c'b^2/3$, $b = x + iy$. (a) The parabolic region of the t-plane whose vertex is the vacuum, $t_0 = -a$, and whose focus is the BTZ threshold, $t = 0$. (b) Its image, the strip $\mathbb{S}$: $|y| < \frac{1}{2}$ with edges $E_\pm$: $y = \pm\frac{1}{2}$. The vacuum is at $b = \pm\frac{i}{2}$; the dashed segment is the range $-a < t < 0$ below the BTZ threshold, and the physical axis is $x \geq 0$. The band becomes the slits $|x| \geq x_1$ of the real axis, drawn here for $x_1 = x_1^*$ of Theorem 1. Diamonds mark the saddle points $b_0 = \pm v_0(x) + \frac{i}{2}$ on the edge E_+ that govern a functional at a point x of the band (squares); see sections 4.2 and 7.3.

the exponent of the Cardy weight is linear in x and proportional to c'. In a plot of $\frac{1}{c'} \log|G|$ against x we call the straight line $-L(x)$ *the Cardy line*; a functional that decays exactly as fast as the Cardy weight grows runs parallel to it. The vacuum, $t = -a$, sits at $b = \pm\frac{i}{2}$, off the physical axis. Figure 2 shows the b-plane and the strip $|\operatorname{Im} b| \leq \frac{1}{2}$, on which the kernel of the eigen-identity of section 2.4, continued to complex t, is bounded by K_a and so grows no faster than the Cardy weight (Lemma B.1); it becomes the stage in section 4.2 and section 6. Finally, a family of functionals, one for each c, that are feasible at $T = t_1(g) + o(c)$ with $x_1(g) \to x_1$ certifies $\Delta_1 \leq c/\Lambda + o(c)$ with

$$\frac{1}{\Lambda} = \frac{1}{12} + \xi_1, \qquad \xi_1 = \frac{x_1^2}{3}. \tag{2.19}$$

In these variables the optimal functionals found numerically have the following anatomy (figure 1). On the *lobe interval* $[0, t_1)$ the functional is negative; this negative *lobe* carries the half mass in (2.16). The one exception is a positive sliver next to the BTZ threshold: $g > 0$ on $(0, t_{\text{int}})$ with $t_{\text{int}} \approx 1/4\pi$, which is explained in section 4.6. At $c = 12$ this zero is already visible in the numerics: it is the "additional single zero near $\Delta \approx 1$" of [11, Figure 1] and the single root at $\Delta = 1$ of [10, §2.5]. At t_1 there is a simple zero. Beyond it lies the *band* of double zeros, the extremal spectrum of section 2.2, and on the band $|g|$ follows $e^{-c'L(x)}$: the functional runs along the Cardy line. These are the features to be explained.

2.6 The class $\bar{\mathcal{A}}$, the best gap bound, and the main theorems

To speak of all functionals, of any order, one needs a class that contains all of them and in which the vacuum value still makes sense. We define it directly, by the three properties that the previous subsections have singled out. *Standing assumption:* in all rigorous statements $c \geq 40$, so that $a \geq 3.25$. It is used through the Bessel inequalities of appendix B, and in Proposition 7.2, where it keeps the poles of the comb of section 7 out of the closed strip.

Definition 2.5. $\bar{\mathcal{A}}$ is the set of real continuous functions g on $[0, \infty)$ such that (i) $g(|\mathbf{r}|^2/2) \in L^1(\mathbb{R}^2)$, that is, $\int_0^\infty |g|\, \mathrm{d}t < \infty$; (ii) $\hat{g} = -g$, with the transform (2.9); and (iii) $M[g] < \infty$. For

$g \in \bar{\mathcal{A}}$ the values below the BTZ threshold are *defined* by the eigen-identity (2.14), $g(-\alpha) := -2\pi \int_0^\infty g K_\alpha \, \mathrm{d}t$ for $0 < \alpha \le a$, so that $g_{\mathrm{vac}} = -\int_0^\infty g \, \rho_C \, \mathrm{d}t$; feasibility is then as in Definition 2.3.

Conditions (i) and (ii) say that g is a functional in the sense of section 2.3, and (iii) is exactly the absolute convergence of the vacuum action (2.15); the integrals that define $g(-\alpha)$ converge absolutely by (i), (iii) and Lemma B.2. Nothing else is required: no smoothness, no rate of decay, no analytic continuation.

Lemma 2.6 (proved)**.** *$\bar{\mathcal{A}}$ contains the function g of every functional ω that is a real distribution of finite order with compact support in $\beta \in (0, \infty)$, with its values at $t < 0$ given by (2.4). In particular it contains all derivative functionals (2.6), for every order P.*

Proof. Let ω have order N and support in $(\beta_{\min}, \beta_{\max})$, $0 < \beta_{\min} < \beta_{\max}$. Then $g = \omega[\Xi_\beta]$ is an entire function of t with $|g(t)| \le C(1 + |t|)^N e^{-2\pi \min(\beta_{\min}, 1/\beta_{\max}) \operatorname{Re} t}$ for $\operatorname{Re} t \ge 0$, and likewise for its derivatives, so $g(|\mathbf{r}|^2/2)$ is a radial Schwartz function; $\hat{g} = -g$ because $\hat{\Xi}_\beta = -\Xi_\beta$. Since $V \le 2K_a \le 2e^{4\pi\sqrt{at}}$ grows more slowly than any exponential, $M[g] < \infty$. Finally (2.11) gives $-2\pi \int_0^\infty \Xi_\beta K_\alpha \, \mathrm{d}t = \Xi_\beta(-\alpha)$ for every $\alpha \ge 0$, and applying ω shows that the values defined by the eigen-identity agree with the entire function. □

The *best gap bound* is

$$T_V(c) := \inf\{T : \text{some } g \in \bar{\mathcal{A}} \text{ is feasible at } T\}, \qquad \Delta_1^{\mathrm{best}} := T_V + a, \tag{2.20}$$

with the strict inequality $g_{\mathrm{vac}} > 0$ of Definition 2.3, and with the value $+\infty$ if no $g \in \bar{\mathcal{A}}$ is feasible at any T; by section 2.4, $T_V \ge 0$, and by Theorem 5, $T_V(c) < \infty$ for all sufficiently large c. The subscript V in T_V and Λ_V stands for Virasoro, as opposed to the $U(1)^c$ problem; the Cardy weight $V(t)$ never carries a subscript.

Theorem 1 (The slope; proved, computer-assisted)**.** *Let $x_1^* := \operatorname{arcsinh}(1)/\pi = 0.2805499$, $\xi_1^* := (x_1^*)^2/3 = 0.0262361$ and $\Lambda_V := 1/(\frac{1}{12} + \xi_1^*) = 12\pi^2/(\pi^2 + 4 \operatorname{arcsinh}^2 1) = 9.1266340$. Then*

$$\lim_{c\to\infty} \frac{T_V(c)}{c'} = \xi_1^*, \qquad \textit{or equivalently} \qquad \lim_{c\to\infty} \frac{c}{\Delta_1^{\mathrm{best}}(c)} = \Lambda_V. \tag{2.21}$$

The constants x_1^*, ξ_1^* and Λ_V are defined here for the whole paper; Part II explains where they come from. The theorem has two halves. The lower bound on T_V, the *optimality half*, says that no nonzero functional in $\bar{\mathcal{A}}$, even a weakly feasible one, does better; it is Theorem 4, proved in section 6 by hand, with no computer. The upper bound, the *attainment half*, is Theorem 5, proved in section 7: an explicit functional in $\bar{\mathcal{A}}$ that is feasible at $T = \xi_1^* c' + O(c'^{1/3})$. Its proof uses finitely many inequalities between elementary functions of one variable, independent of c, that are certified in interval arithmetic and listed in appendix H; this is the only input from a computer and the reason for the tag.

Proof of Theorem 1 from Theorems 4 and 5. Let $c \ge c_0^{\mathrm{opt}}$, and let $g \in \bar{\mathcal{A}}$ be feasible at T. Then $g \not\equiv 0$ because $g_{\mathrm{vac}} > 0$, g is weakly feasible, and $T \ge t_1(g)$. So (6.3) gives $T \ge \xi_1^* c' - 0.44\, c'^{1/3} \log^{2/3} c'$, and therefore $T_V(c) \ge \xi_1^* c' - 0.44\, c'^{1/3} \log^{2/3} c'$. For $c \ge c_0^{\mathrm{att}}$ the function g of Theorem 5 is feasible at $t_\star + 1$, so $T_V(c) \le t_\star + 1 = \xi_1^* c' + O(c'^{1/3})$ by (7.5). Dividing by c' gives the first limit in (2.21). Since $\Delta_1^{\mathrm{best}} = T_V + a$ and $a = c'/12$, it is equivalent to $\Delta_1^{\mathrm{best}}(c)/c' \to \xi_1^* + \frac{1}{12} = 1/\Lambda_V$; since $c/c' \to 1$, this is the second limit. □

Theorem 2 (Certification; proved)**.** *Let $c \ge 40$. If $g \in \bar{\mathcal{A}}$ is feasible at some $T > 0$, then every admissible spectrum at central charge c contains a primary with $t_n < T$ (possibly a light one). Consequently $\Delta_1 \le T_V(c) + a = \Delta_1^{\mathrm{best}}(c)$ for every admissible CFT.*

Nothing about g beyond membership in $\bar{\mathcal{A}}$ and feasibility is assumed. The idea of the proof is to expand g in the odd Laguerre functions ψ_{2k-1}, each of which is a derivative functional that annihilates the crossing equation, and to control the resummation by positivity. The proof, which uses no computer, is in section 8.

What "best" means. Since $\bar{\mathcal{A}}$ contains the functionals of order P for every P (Lemma 2.6), $T_V(c) \le t_1^{(\infty)}(c)$, that is, $\Delta_1^{\text{best}}(c) \le \Delta_1^{(\infty)}(c)$, the limit of the truncated optimal gap bounds that numerical work computes; equality is conjectural. Consequently the optimality half bounds, a fortiori, every numerical truncation, uniformly in P. The attainment half is achieved by a function that is not of finite order, and it is a bound on conformal field theories only through Theorem 2. We do not claim that $\bar{\mathcal{A}}$ contains every functional that has been considered: membership of the analytic functionals of [10] is not checked here, and nothing depends on it. Nor do we claim that the infima over $g_{\text{vac}} > 0$ and over $g_{\text{vac}} \ge 0$ coincide; T_V is defined with $g_{\text{vac}} > 0$.

Part II The physical picture: a spectral curve for the optimal functional

This Part is heuristic throughout. Its uncontrolled steps are four named hypotheses, (W), (A), (B) and (Sel), stated in section 3.1. Its purpose is to show where Λ_V, the strip of figure 2 and the zero law ρ_U come from, and to formulate Conjecture 1. The proofs of sections 6 to 8 and 10 do not use it.

3 Warm-up: mean-field theory of the $U(1)^c$ problem

[HEURISTIC] We learn the recipe on the twin problem with $U(1)^c$ characters (section 2.3), where the equations are simplest and the answer, the slope π^2, is known by other means: it was conjectured from numerics in [12] and has since been proved in [13, Ch. 1], with the status given in section 1.2. The picture is semiclassical, with $1/c$ in the role of $\hbar$: the optimal functional is a WKB wave function, a sum of exponentials $e^{c\,\mathcal{S}}$ whose momenta $\mathcal{S}'$ are the branches of a *spectral curve* in phase space. The Fourier transform acts on it by a canonical transformation, so $\hat{f} = -f$ says that the curve is mapped to itself. The real zeros are the nodes where two complex-conjugate branches interfere; there are of order c of them, so only their density matters, as in mean-field theory, and it is a coordinate on the curve.

3.1 The problem, the data, and the four hypotheses

The functionals are radial functions on $\mathbb{R}^{2c}$, written $f(\Delta)$ with $\Delta = |\mathbf{r}|^2/2$, that obey $\hat{f} = -f$ (the bootstrap normalization of section 2.3); the vacuum sits at the origin, and f proves that the gap is below T if $f(0) > 0$ and $f \ge 0$ for $\Delta \ge T$. The optimal bound, written Δ_1 in this section, was computed up to $c = 2048$ in [12], which conjectured that $\Delta_1/c \to 1/\pi^2$. Beyond Δ_1 the numerically optimal f has a band of double zeros, as in figure 1. We name the four hypotheses in words; their precise forms are given where the objects exist, in sections 3.2 to 3.4 for $U(1)^c$ and in the box of section 4.1 for Virasoro.

- (W) At large c the optimal functional is a finite sum of WKB exponentials, called *sheets*.
- (A) On the band, its envelope is dictated by the continuum density that the vacuum demands.
- (B) All sheets are branches of one analytic curve.
- (Sel) A selection rule, made of a topological assumption and a boundedness assumption, picks one curve among those allowed by (W), (A) and (B).

3.2 Sheets and the local modular parameter

In formulas, (W) says that

$$f(c\,\xi) \asymp \sum_{\text{sheets}} e^{c\,\mathcal{S}(\xi)}, \qquad \xi := \Delta/c, \qquad \text{and we set} \qquad \tau := \frac{\mathcal{S}'(\xi)}{2\pi i} \tag{3.1}$$

on each sheet; $\asymp$ keeps the exponential order only. Locally a sheet looks like $e^{2\pi i\tau\Delta}$, a character at modular parameter τ, so we call τ, the momentum conjugate to ξ, the *local modular parameter* of the sheet. The points (ξ,τ) of all the sheets form the spectral curve. On the band, a function with real double zeros under a smooth envelope is locally the envelope times $\cos^2(\pi c\int\rho\,\mathrm{d}\xi) = \frac{1}{2}[1+\cos(2\pi c\int\rho\,\mathrm{d}\xi)]$, where $\rho(\xi)$ is the number of double zeros per unit Δ ($\rho\to 1$ deep in the band). Writing the cosine as two exponentials gives three terms of the form (3.1), that is, three sheets, a non-oscillating one with $\tau = iy_E$ and two oscillating ones:

$$\tau_\pm = \mp\rho + iy_E, \qquad f \;\propto\; \exp\Big(-2\pi c\int y_E\,\mathrm{d}\xi\Big)\,\Big[1+\cos\Big(2\pi c\int\rho\,\mathrm{d}\xi\Big)\Big]. \tag{3.2}$$

Here $y_E(\xi) = \operatorname{Im}\tau_\pm$, the *height* of the oscillating sheets, is the rate of decay of the envelope. The oscillating sheets differ by 2ρ, and their interference produces the real double zeros. The non-oscillating sheet, the "1" in the bracket, is their common modulus and carries no independent datum.

3.3 The Fourier transform on sheets, and the functional equation

In $d=2c$ dimensions the Fourier transform of $e^{2\pi i\tau|\mathbf{r}|^2/2}$ is $(i/\tau)^c\,e^{2\pi i(-1/\tau)|\mathbf{r}|^2/2}$: a character at $-1/\tau$, times a factor exponentially large in c that shifts the saddle point. We write f locally as a superposition of characters, transform it term by term, and locate the saddle point again,

$$f(c\,\xi) = \int a(\tau)\,e^{2\pi i\tau c\xi}\,\mathrm{d}\tau, \qquad a(\tau)\asymp e^{c\,(\mathcal{S}-2\pi i\tau\xi)}\big|_{\xi=\xi(\tau)}, \tag{3.3}$$

$$\hat f(c\,\xi') \asymp \int \exp\Big\{c\Big[\mathcal{S}-2\pi i\tau\xi+\log\frac{i}{\tau}-\frac{2\pi i\,\xi'}{\tau}\Big]\Big\}\,\mathrm{d}\tau, \tag{3.4}$$

$$0 = -2\pi i\,\xi - \frac{1}{\tau} + \frac{2\pi i\,\xi'}{\tau^2}, \tag{3.5}$$

the last line being stationarity in τ, with $\mathrm{d}(\mathcal{S}-2\pi i\tau\xi)/\mathrm{d}\tau = -2\pi i\xi$. Hence the *sheet map*

$$\hat S_{U(1)}:\ (\xi,\tau)\longmapsto\Big(\tau^2\xi+\frac{\tau}{2\pi i}\,,\,-\frac{1}{\tau}\Big), \qquad \hat S_{U(1)}\circ\hat S_{U(1)} = \mathrm{id}. \tag{3.6}$$

Sheets go to sheets; $\hat f = -f$ says that this canonical transformation preserves their set.

Hypothesis (A) has three parts that must be kept apart. Let $\{\Delta_n, d_n\}$ be the extremal spectrum of section 2.2: the zeros of f, with the positive degeneracies of the dual optimum. *Forced:* the smoothed extremal degeneracies are the continuum density,

$$\frac{d_n}{\text{local spacing}} = \rho_0(\Delta_n)\,e^{o(c)}, \qquad \rho_0(\Delta) := \frac{(2\pi)^c\,\Delta^{c-1}}{\Gamma(c)}, \tag{3.7}$$

where ρ_0 is the S-image of the vacuum, $\int_0^\infty \rho_0\,e^{-2\pi\beta\Delta}\,\mathrm{d}\Delta = \beta^{-c}$. The reason: Poisson-resum $\sum_n d_n\,e^{2\pi i\tau\Delta_n}$ over n, that is, write $\sum_n F(n) = \sum_k\int F(n)\,e^{2\pi ikn}\,\mathrm{d}n$, with $n(\Delta)$ the counting function of the levels. The term $k=0$, the smooth integral of $d_n/(\text{local spacing})$ against $e^{2\pi i\tau\Delta}$, is the only non-oscillating one, so it alone must reproduce the S-image of the vacuum. The terms $k=\pm1$, the first harmonics, carry the phase $e^{\pm 2\pi ic\int\rho\,\mathrm{d}\xi}$, so they are of the form (3.1) with $\operatorname{Re}\tau = \pm\rho$. *Assumed, and this is* (A)*:* reciprocity. On the band the local upper envelope $|f|_{\text{env}}$ of the optimal functional is inverse to the degeneracies at exponential order,

$$d_n\,|f|_{\text{env}}(\Delta_n) = e^{o(c)} \qquad \text{uniformly on the band.} \tag{3.8}$$

The reason offered: the first harmonics of the spectrum, the terms $k=\pm1$ above, are sheets $\tau=\pm\rho+iy$ with y the height of $1/\rho_0$, that is $y=\frac{1}{2\pi c}\,\mathrm{d}\log\rho_0/\mathrm{d}\xi = 1/(2\pi\xi)$. If the two oscillating sheets of f are their mirror images, with the same $\operatorname{Im}\tau$ and the opposite $\operatorname{Re}\tau$ (given the forced

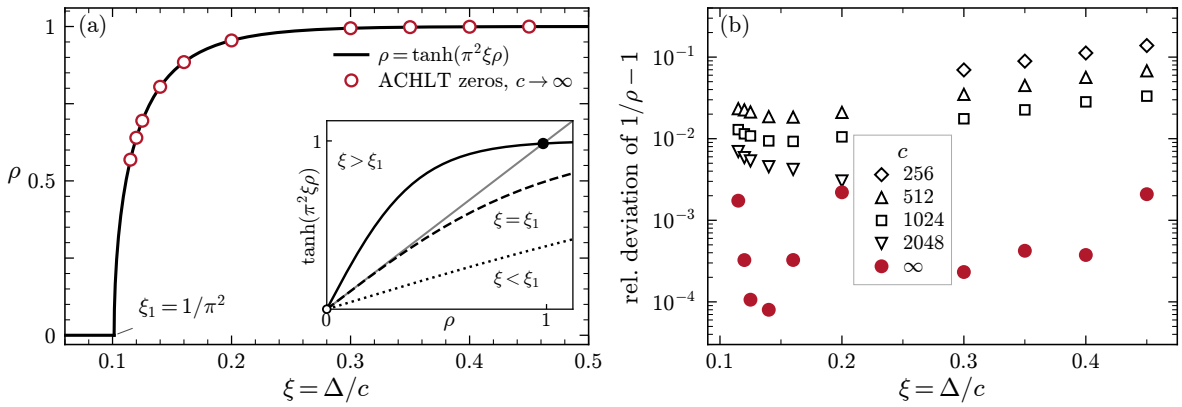


Figure 3: The tanh law against the zeros of the numerically optimal $U(1)^c$ functionals of [12]; no parameter is fitted. (a) The number ρ of double zeros per unit Δ against $\xi = \Delta/c$. Curve: the largest solution of $\rho = \tanh(\pi^2\xi\rho)$ (Result H1); it vanishes at the Curie point $\xi_1 = 1/\pi^2$. Circles: the inverse of the spacing of consecutive zeros, extrapolated to $c \to \infty$ linearly in $1/c$ through three values of c. Inset: graphical solution of the Curie–Weiss equation. (b) Magnitude of the relative deviation of the measured $1/\rho - 1$ from the law at $c = 256, \dots, 2048$ (open symbols; all lie below the law) and after extrapolation (filled): it decreases roughly like $1/c$, and the extrapolated values are within 2.2×10^{-3} of the law.

part, this is (3.8)), then crossing is carried by these harmonics ("extremal and feasible implies equality wherever there are zeros": convincing, but not a proof). *Consequence:* $|f|_{\text{env}} \asymp 1/\rho_0$, that is, $y_E = 1/(2\pi\xi)$ (checked in section 3.5).

Skeleton of the consequence. With (A), $\tau_\pm = \mp\rho + i/(2\pi\xi)$ on the band. We extend ρ from a real density on the band to a complex coordinate on the whole curve by *defining*

$$\rho := \frac{i}{2\pi\xi} - \tau, \qquad w := \pi^2\xi\rho, \tag{3.9}$$

where w is the combination in which $\hat{S}_{U(1)}$ becomes affine. Indeed, (3.9) gives $\tau\xi + \frac{1}{2\pi i} = -\rho\xi$, so the image point in (3.6) has $\xi' = -\rho\xi\tau$; then $\rho' = \frac{i}{2\pi\xi'} + \frac{1}{\tau} = \frac{1}{\rho\tau}(\rho - \frac{i}{2\pi\xi}) = -\frac{1}{\rho}$ and $w' = \pi^2\xi'\rho' = \pi^2\xi\tau = \frac{i\pi}{2} - w$. In the variables (ρ, w) the sheet map is the involution

$$\iota : \ (\rho, w) \longmapsto \Big(-\frac{1}{\rho}, \ \frac{i\pi}{2} - w\Big). \tag{3.10}$$

By (B) the curve is a graph $\rho = \mathcal{F}(w)$ with $\mathcal{F}$ analytic. Invariance under ι gives $\mathcal{F}(\frac{i\pi}{2} - w)\,\mathcal{F}(w) = -1$; exchanging the oscillating sheets, $(\rho, w) \mapsto (-\rho, -w)$, makes $\mathcal{F}$ odd. Hence

$$\mathcal{F}(w + \tfrac{i\pi}{2}) = \frac{1}{\mathcal{F}(w)}, \qquad \text{with general solution} \qquad \mathcal{F} = \tanh \cdot E, \tag{3.11}$$

where E is even and obeys the same equation, because tanh is odd and $\tanh(w + \frac{i\pi}{2}) = 1/\tanh w$.

3.4 Selection and the tanh law

We pass to the inverse function, $w = W(\rho)$. The band and its image under the exchange of the oscillating sheets make up the real segment $|\rho| < 1$, where w is real, $\operatorname{Im} W = 0$; by (3.10) its ι-image is $|\rho| > 1$, with $\operatorname{Im} W = \frac{\pi}{2}$. So $\operatorname{Im} W$ is known on the real axis. What the symmetry and (A) leave free, the function E, is how W continues off the axis; the selection rule supplies this.

Hypothesis (Sel), $U(1)^c$ form. (Topology) W is single-valued and holomorphic on the upper half of the ρ-plane. (Boundedness) $\operatorname{Im} W$ is bounded there.

A bounded harmonic function with piecewise-constant boundary values is unique: $\operatorname{Im} W(\rho)$ is $\frac{\pi}{2}$ times the *harmonic measure* of $\{|\rho| > 1\}$ seen from ρ, that is, the probability that Brownian motion from ρ first hits the real axis there, which is $\frac{1}{\pi}$ times the angle that the set subtends at ρ:

$$\operatorname{Im} W(\rho) = \tfrac{1}{2} \arg \frac{1+\rho}{1-\rho}, \qquad W(\rho) = \operatorname{arctanh} \rho, \tag{3.12}$$

the real constant being zero because W is odd; that is, $E \equiv 1$. A bounded $\operatorname{Im} W$ stays between its boundary values: on no sheet does the functional decay or grow faster than the rate $|f| \asymp \Delta^{-c}$ of (A). We stress that (Sel) is a hypothesis; it is not derived from the linear program.

Result H1 (The tanh law; heuristic)**.** *Assume (W), (A), (B) and (Sel). At leading order at large c, the number $\rho(\xi)$ of double zeros of the optimal $U(1)^c$ functional per unit Δ, at $\Delta = c\,\xi$, is the largest solution of*

$$\rho = \tanh(\pi^2 \xi \rho). \tag{3.13}$$

A nonzero solution exists if and only if $\xi > 1/\pi^2$. The band therefore begins at $\xi_1 = W'(0)/\pi^2 = 1/\pi^2$, that is, $\Delta_1 = c/\pi^2 + o(c)$: the slope is π^2.

This is the Curie–Weiss equation for the magnetization of a ferromagnet at inverse temperature $\pi^2\xi$, hence "mean field"; the lower end of the band is the Curie point (inset of figure 3).

3.5 Checks, status, and what carries over

Near the Curie point (3.13) gives $\rho \simeq \pi\sqrt{3}\,(\xi - \xi_1)^{1/2}$. Square-root vanishing gives Airy scaling: $\Delta_1 = c/\pi^2 + 0.352336\,c^{1/3} + \ldots$, with $0.352336 = (\pi^2\sqrt{3})^{-2/3}|a_1|$ and a_1 the first zero of Ai. Deep in the band $\Delta_n = n + c\,[\xi_1 + \int_{\xi_1}^{\infty}(1-\rho)\,\mathrm{d}\xi] + O(1) = n + c/8 + O(1)$, the offset of the line $\Delta_n = n + (c-4)/8$ of [12, §4]. Against the data of [12]: the spacings follow (3.13) through the band (figure 3); Δ_1/c, extrapolated by us in $c^{-2/3}$, tends to 0.10134 ± 0.00003, against $1/\pi^2 = 0.101321$; the degeneracies follow the continuum density, $d_n/(\rho_0(\Delta_n) \times \text{spacing}) = 1$ up to a relative deviation falling from 2×10^{-2} at $n = 2$ to 10^{-6} deep in the band, which is the forced part of (A), verified far beyond exponential order; and the envelope of f has the height $y_E = 1/(2\pi\xi)$ up to $O(1/c)$, which is hypothesis (A) itself.

The slope π^2 has since been proved in [13, Ch. 1]; we have read the statements and the structure of that argument but have not independently verified it; nothing in this paper depends on it logically. The derivation above is independent of that proof, and heuristic. What we carry to Virasoro is the recipe: sheet map, (A), (B), (Sel). The rigorous part of this paper (section 6) follows the *strategy* of the $U(1)^c$ proof, not the mean-field derivation; the attribution is made in section 6.1.

4 The Virasoro spectral curve and the conjectured slope

[HEURISTIC] We apply the recipe of section 3 (sheet map, (A), (B), (Sel)) to the Virasoro problem, to explain where the constants of Theorem 1 come from. We suppose that at large c the optimal functional is a WKB wave function, and ask on which curve in phase space its momenta can lie, given that it is odd under the Fourier transform and that the vacuum imposes the Cardy density on the extremal spectrum. Under four hypotheses the answer is an explicit curve in closed form, Result H2; the band begins at its branch point, and this gives Λ_V. Nothing in this section is proved. Its leading-order consequences are proved without the hypotheses: the slope and the strip $|\operatorname{Im} b| < \frac{1}{2}$ in sections 6 and 7, and the zero law, in a weak sense, in section 10; the finer ones make up Conjecture 1 and are tested in section 5. "The optimal functional" is meant in the order of limits of section 2.5: $P \to \infty$ first, then $c \to \infty$. The section can be read without section 3.

4.1 The hypotheses, and what changes: phase-space coordinates

The four hypotheses, in Virasoro form

(W) *WKB form.* At large c the optimal functional is a finite sum of WKB exponentials,

$$g(c'\xi) \asymp \sum_{\text{sheets}} e^{c'\mathcal{S}(\xi)}, \qquad \xi := \frac{t}{c'}, \qquad \tau := \frac{\mathcal{S}'(\xi)}{2\pi i}, \tag{4.1}$$

where $\asymp$ keeps the exponential order in c only. Each term is a *sheet*, and τ is its *local modular parameter*: near ξ the sheet looks like the character $e^{2\pi i\tau t}$.

(A) *Cardy envelope.* On the band, the local upper envelope $|g|_{\text{env}}$ of the oscillating $|g|$ is inverse to the Cardy density ρ_C at exponential order. Section 4.2 separates what is forced in this statement from what is assumed.

(B) *One curve.* All sheets are branches of one analytic curve Σ, the *spectral curve*.

(Sel) *Selection.* A topological assumption (C0) and a boundedness assumption (C1), stated in section 4.4, pick one curve among those that (W), (A) and (B) allow.

What changes with respect to section 3 is the action of the Fourier transform on sheets. The functionals are radial functions on the plane $\mathbb{R}^2$ for every c (section 2.3), with $t = |\mathbf{r}|^2/2$, and the planar transform of the character $e^{2\pi i\tau t}$ is $(i/\tau)\, e^{2\pi i(-1/\tau)t}$: a character at $-1/\tau$, times a factor of order one. We write a sheet as a superposition of characters, transform it term by term and locate the saddle point in τ again, as in (3.3)–(3.5). The factor i/τ now drops out of the saddle-point equation, which reads $-2\pi i\xi + 2\pi i\xi'/\tau^2 = 0$. The dimension stays 2, so there is no large-d saddle and no factor $(i/\tau)^c$: the sheet map is the bare modular inversion,

$$\hat{S}:\ (\xi,\tau) \longmapsto \Big(\tau^2\xi\,,\ -\frac{1}{\tau}\Big), \qquad \hat{S}\circ\hat{S} = \mathrm{id}, \tag{4.2}$$

and $\hat{g} = -g$ says that the set of sheets is invariant under it. The central charge enters only through the position of the vacuum, $b = \pm\frac{i}{2}$, and through the Cardy envelope.

The map $\hat{S}$ becomes linear on the double cover $b = \sqrt{3\xi}$ of section 2.5. We define the *momentum*

$$p := -\tau\, b, \qquad \text{so that} \qquad \frac{1}{c'}\,\partial_b \log g = \frac{2b}{3}\, 2\pi i\tau = -\frac{4\pi i}{3}\, p \tag{4.3}$$

on each sheet, because $\mathrm{d}\xi = \frac{2}{3} b\,\mathrm{d}b$: up to the constant, p is the WKB momentum conjugate to b. The image of (ξ,τ) under $\hat{S}$ has $b'^2 = p^2$ and $p' = b'/\tau$, so its two lifts are $(p',b') = (b,-p)$ and $(-b,p)$. In the coordinates (p,b) the Fourier transform is therefore the quarter-turn

$$\mathsf{R}:\ (p,b) \longmapsto (b,-p), \qquad \mathsf{R}^4 = \mathrm{id}, \tag{4.4}$$

whose inverse is the other lift and whose square, $(p,b) \mapsto (-p,-b)$, is the change of sign of the square root. This is the oscillator rotation of section 2.3, acting on WKB data. From here on Σ is a complex curve in $\mathbb{C}^2_{(p,b)}$, invariant under R, and the sheets are its branches over the b-plane.

4.2 The Cardy envelope

We first say what the sheets are on the band, and then state (A). On the band g has real double zeros under a smooth envelope, $g \approx |g|_{\text{env}} \cos^2\!\big(\pi c' \int^{\xi} \rho_V\big)$, where $\rho_V(\xi)$ is the number of double zeros per unit t. Expanding the cosine gives three sheets,

$$\tau_E = i\, y_E, \qquad \tau_\pm = \mp\rho_V + i\, y_E, \qquad y_E := -\frac{1}{2\pi c'}\,\frac{\mathrm{d}\log|g|_{\text{env}}}{\mathrm{d}\xi}, \tag{4.5}$$

so y_E is the rate of decay of the envelope. The sheet τ_E carries no independent datum; "the two band sheets" always means the oscillating pair $\tau_\pm$, whose interference produces the zeros.

Hypothesis (A) has three parts that must be kept apart. Let $\{t_n, d_n\}$ be the extremal spectrum of section 2.2. *Forced:* the extremal spectrum is the Cardy continuum, discretized,

$$\frac{d_n}{\text{local spacing}} = \rho_C(t_n)\, e^{o(c)}. \tag{4.6}$$

The reason: Poisson-resum $\sum_n d_n\, e^{-2\pi\beta t_n}$ over n; the zero mode is the only non-oscillating term, so it alone must reproduce the S-image of the vacuum, $\int \rho_C\, e^{-2\pi\beta t}\, \mathrm{d}t$ (section 2.4). *Assumed, and this is* (A)*:* reciprocity,

$$d_n\, |g|_{\text{env}}(t_n) = e^{o(c)} \qquad \text{uniformly on the band.} \tag{4.7}$$

The reason offered: the first Poisson harmonics of the extremal spectrum are sheets of height $\operatorname{Im}\tau = \frac{1}{2\pi c'}\, \mathrm{d}\log\rho_C/\mathrm{d}\xi = 1/(2b)$, because $\rho_C \asymp e^{c' L(x)}$ with $L(x) = \frac{2\pi}{3}x$ and $x = \sqrt{3\xi}$. If the two oscillating sheets of g are their mirror images, with the same $\operatorname{Im}\tau$ and the opposite $\operatorname{Re}\tau$ (given the forced part, this is (4.7)), then crossing is carried by these harmonics ("extremal and feasible implies equality wherever there are zeros": convincing, but not a proof). *Consequence:* on the band the functional runs along the Cardy line of section 2.5,

$$|g|_{\text{env}} \asymp e^{-c' L(x)}, \qquad \text{that is,} \qquad y_E = \frac{1}{2b}. \tag{4.8}$$

Sensitivity: if we write $y_E = \varkappa/(2b)$ with a constant $\varkappa$, the *Cardy height*, then $\varkappa$ enters the final answer as $\xi_1^* \to \varkappa^2 \xi_1^*$. So (A) is the hypothesis to test hardest; section 5.3 measures $\varkappa = 1.0000 \pm 0.0005$.

In terms of the momentum, (4.5) and (4.8) say that the two band sheets are

$$p = \pm v - \frac{i}{2}, \qquad v := \rho_V\, b \in \mathbb{R}, \qquad \text{so that} \qquad \operatorname{Im} p = -\tfrac{1}{2}, \quad \operatorname{Im} b = 0 \tag{4.9}$$

on the band. The *band arc* $\gamma_0 := \{v \in \mathbb{R}\} \subset \Sigma$ comprises both band sheets, joined at the branch point $v = 0$, which is the lower end of the band, where ρ_V vanishes. By (4.4), R maps γ_0 to the arc $(p, b) = (x, \mp v + \frac{i}{2})$, on which $\operatorname{Im} b = +\frac{1}{2}$ and $\operatorname{Im} p = 0$. The Fourier image of the band thus lies on the line $\operatorname{Im} b = \frac{1}{2}$, which passes through the vacuum $b = \frac{i}{2}$ (figure 2). This is the first appearance of the strip of section 6 and of the edge integral of section 7.

4.3 Symmetries and boundary data

Two maps act on Σ. One is R. The other is the exchange of the two band sheets, which reverses $\operatorname{Re}\tau$ at fixed $\operatorname{Im}\tau = 1/(2b)$; by (4.9) it is $\sigma : (p, b) \mapsto (-p - i, b)$, a holomorphic map that (B) extends from the band to all of Σ. Applying R repeatedly to (4.9) we obtain four arcs $\gamma_k := \mathsf{R}^k \gamma_0$ on which the imaginary parts of both coordinates are constant,

$$(\operatorname{Im} p, \operatorname{Im} b) = (-\tfrac{1}{2}, 0) \text{ on } \gamma_0, \qquad (0, \tfrac{1}{2}) \text{ on } \gamma_1, \qquad (\tfrac{1}{2}, 0) \text{ on } \gamma_2, \qquad (0, -\tfrac{1}{2}) \text{ on } \gamma_3. \tag{4.10}$$

Consecutive arcs meet at four points of Σ at $\xi = \infty$; for instance γ_0 and γ_1 share the end where p and b tend to $+\infty$ with $p - b \to -\frac{i}{2}$.

Where things live. The four arcs bound a region $\tilde{\Omega}$ *on the curve* Σ (on its cover in the variable b), not in the b-plane. It contains the real, non-oscillating sheet $\tau = iy$ (here and below y is $\operatorname{Im}\tau$, not $\operatorname{Im} b$) that carries g from the lower end of the band across the lobe interval $[0, t_1)$ of section 2.5 to the BTZ threshold $t = 0$ and on to the vacuum (section 4.6). Concretely, a point of $\tilde{\Omega}$ is a pair (p, b): a value of b together with a choice of sheet. The region is mapped to itself by R. Figure 4 shows $\tilde{\Omega}$ and its image in the half-plane constructed next.

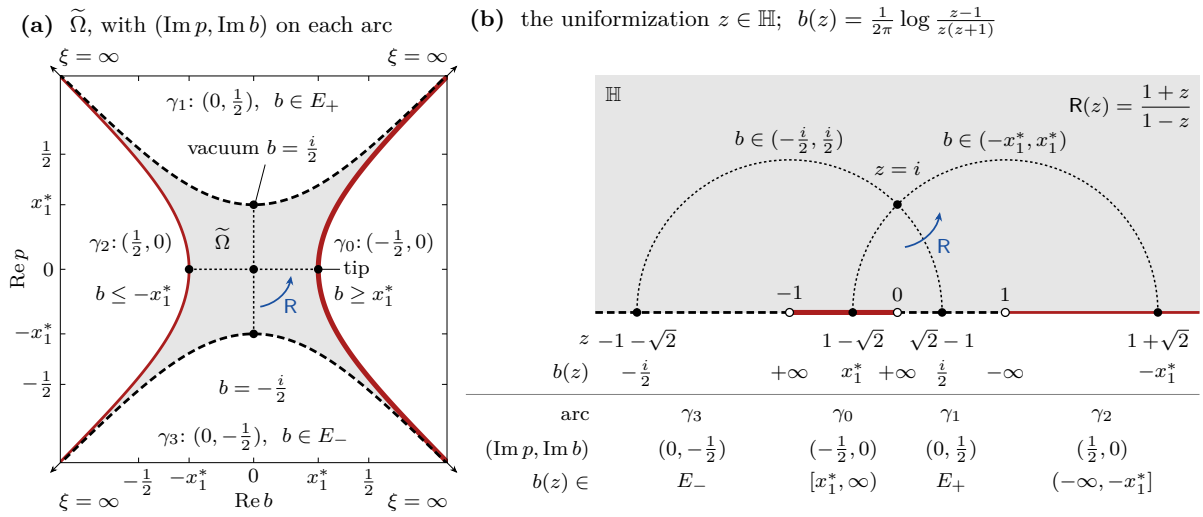


Figure 4: The spectral curve. (a) The region $\tilde{\Omega}$ on the curve Σ, drawn in the chart $(\operatorname{Re} b, \operatorname{Re} p)$: a disk bounded by the band arc γ_0 (thick; both band sheets, joined at the branch point $v = 0$, the tip) and its Fourier images $\gamma_k = \mathsf{R}^k \gamma_0$. Each arc is labeled with its values of $(\operatorname{Im} p, \operatorname{Im} b)$, (4.10), and with the set in which b lies. Consecutive arcs meet at the four points at $\xi = \infty$, and R is the quarter-turn about its fixed point, the BTZ threshold $(p, b) = (0, 0)$. The dotted segments are the real sheet, on which b is real (the lobe interval) or imaginary (from the BTZ threshold to the vacuum $b = \pm\frac{i}{2}$). (b) The image of $\tilde{\Omega}$ under the uniformization of section 4.4: the upper half-plane $\mathbb{H} \ni z$, with the fixed point at $z = i$, the arcs on $(-1, 0)$, $(0, 1)$, $(1, \infty)$ and $(-\infty, -1)$, and the real sheet on the dotted semicircles. Below the axis: marked points z with their images $b(z)$; then, for each arc, the boundary values $(\operatorname{Im} p, \operatorname{Im} b)$, which determine $p(z)$ and $b(z)$, (4.11); the last row gives the boundary correspondences of $b(z)$. For the reader coming from section 6: panel (b) is the conformal map $b(z)$ of Lemma 6.3, which sends $\mathbb{H}$ onto the strip $\mathbb{S}$ slit along $|x| \ge x_1^*$.

4.4 Selection and the curve

The boundary data (4.10) do not determine Σ: they say nothing about what happens between the arcs. That is what the selection hypothesis supplies. It has two halves.

(C0) *Topology.* $\tilde{\Omega}$ is simply connected: it is a disk bounded by the four arcs, which meet only at their four ends. On it p and b are single-valued, and R has exactly one fixed point.

(C1) *Boundedness.* p and b are holomorphic on $\tilde{\Omega}$ with bounded imaginary parts.

Hypothesis (Sel) is (C0) together with (C1): the same two halves, topology and boundedness, as in section 3.4. Physically, by (4.3), $\frac{4\pi}{3} \operatorname{Im} p$ is the rate at which $\frac{1}{c'} \log|g|$ changes along real b; on the band arc it is minus the Cardy rate $L' = \frac{2\pi}{3}$. A bounded harmonic function stays between its boundary values, so (C1) says that the complex decay rate never exceeds the Cardy rate.

Derivation. The idea is that (C0) lets us replace $\tilde{\Omega}$ by the upper half-plane, where R is a Möbius map and the arcs are intervals; (C1) then makes $\operatorname{Im} b$ and $\operatorname{Im} p$ bounded harmonic functions with known, piecewise-constant boundary values, and such a function is unique. In detail, map $\tilde{\Omega}$ conformally onto $\mathbb{H} \ni z$ (Riemann mapping theorem) with the fixed point of R at $z = i$. An automorphism of $\mathbb{H}$ of order four that fixes i is $\mathsf{R}(z) = (1 + z)/(1 - z)$ (its inverse gives the mirror image of the curve). The four ends of the arcs form one orbit of R on the boundary of $\mathbb{H}$. The rotations about i commute with R, and we use them to place one end at $z = -1$. The orbit is then $-1 \to 0 \to 1 \to \infty$, the arcs are $\gamma_0 = (-1, 0)$, $\gamma_1 = (0, 1)$, $\gamma_2 = (1, \infty)$ and $\gamma_3 = (-\infty, -1)$, and no modulus remains. By (C1) and (4.10), $\operatorname{Im} b$ is a bounded harmonic function on $\mathbb{H}$ with boundary values $0, \frac{1}{2}, 0, -\frac{1}{2}$ on these intervals. As in section 3.4 it is a sum of angles, $\operatorname{Im} b = \frac{1}{2\pi}\big[\arg(z-1) - \arg z - \arg(z+1)\big]$ with all arguments in $(0, \pi)$. So b is a sum of logarithms up to a real constant, and likewise p; the two constants are fixed by $b \circ \mathsf{R} = -p$

and $p \circ \mathsf{R} = b$. The result is

$$b(z) = \frac{1}{2\pi} \log \frac{z-1}{z\,(z+1)}, \qquad p(z) = \frac{i}{2} + \frac{1}{2\pi} \log \frac{z+1}{z\,(z-1)}. \tag{4.11}$$

Then $p + b = \frac{i}{2} - \frac{1}{\pi} \log z$ and $p - b = \frac{i}{2} + \frac{1}{\pi} \log \frac{z+1}{z-1}$, which we exponentiate:

$$X := e^{-\pi(p+b)} = -iz, \qquad Y := e^{-\pi(p-b)} = -i\,\frac{z-1}{z+1}. \tag{4.12}$$

Eliminating z gives the curve.

Result H2 (The spectral curve; heuristic)**.** *Assume (W), (A), (B) and (Sel). At leading order at large c, the sheets of the optimal functional are the branches of the curve*

$$\sinh \pi b = i \sinh \pi p, \qquad \textit{equivalently} \qquad Y = \frac{X+i}{1+iX}, \qquad \textit{or} \qquad \cosh 2\pi p + \cosh 2\pi b = 2, \tag{4.13}$$

where the last form, obtained by squaring, contains the curve together with its mirror image. There is no free constant.

The curve is invariant under σ, as it must be. The fixed point $z = i$ is $(p, b) = (0, 0)$: the curve passes through the BTZ threshold, and it does so with $p \simeq -ib$, that is, at the self-dual value $\tau = i$. The identically worded selection rule applied to the $U(1)^c$ data is (Sel) of section 3.4 and returns Result H1, a law whose consequence, the slope π^2, has since been proved in [13, Ch. 1] (we have not verified that proof independently; see section 3.5). Hypotheses (W), (A) and (B) alone admit rival curves; those we found have slopes between about 8.9 and 9.8. So (Sel) is a genuine hypothesis, but one that is no longer needed after section 6.

4.5 The gap

The band begins where the density of zeros vanishes, which on the curve is the branch point $v = 0$ of the band arc. On the band, $b = x$ is real and $p = \pm v - \frac{i}{2}$, so $\sinh \pi p = \mp i \cosh \pi v$ and (4.13) becomes

$$\cosh \pi v = \sinh \pi x, \qquad v = \rho_V\, x, \tag{4.14}$$

which has a real solution v if and only if $\sinh \pi x \geq 1$. The lower end of the band is therefore at $\sinh \pi x_1^* = 1$:

$$x_1^* = \frac{\operatorname{arcsinh} 1}{\pi} = 0.2805499, \quad \xi_1^* = \frac{(x_1^*)^2}{3} = 0.0262361, \quad \Lambda_V = \frac{12\pi^2}{\pi^2 + 4 \operatorname{arcsinh}^2 1} = 9.1266340. \tag{4.15}$$

The last number follows because the bound is $a + t_1$ with $a = c'/12$ and $t_1 = c'\xi_1^* + o(c)$: $(a + t_1)/c \to \frac{1}{12} + \xi_1^* = 1/\Lambda_V$. That Λ_V is the exact leading slope of the best bound is Theorem 1.

4.6 Fine structure, and Conjecture 1

The curve contains more than the slope. We list six consequences of the curve and of the hypotheses; together they are Conjecture 1 (the first two form its item (b)), and section 5.3 tests them one by one.

Band density. By (4.14), $\rho_V(\xi) = \operatorname{arccosh}(\sinh \pi x)/(\pi x)$ with $x = \sqrt{3\xi}$. Since $\mathrm{d}t = \frac{2}{3} c' x \,\mathrm{d}x$, the double zeros have density $c'\rho_U(x)/2$ per unit x, where

$$\rho_U(x) := \frac{4}{3\pi} \operatorname{arccosh}\bigl(\sinh \pi |x|\bigr), \qquad \rho_V = \frac{3\,\rho_U}{4x}, \tag{4.16}$$

so that $c'\rho_U$ counts zeros with multiplicity. It vanishes like $(x-x_1^*)^{1/2}$ at the tips $\pm x_1^*$. The subscript refers to the extremal potential U of section 6.6, whose charge density ρ_U is, not to $U(1)$.

Profile off the band. Integrating (4.3) along a sheet,

$$\frac{1}{c'}\log|g| = \text{const} + \frac{4\pi}{3}\,\mathrm{Im}\int^b p\,\mathrm{d}b', \qquad \begin{cases} \sin(\pi y b) = \sinh(\pi b), & p=-iyb, \quad 0<b<x_1^*, \\ \sinh(\pi y\tilde{b}) = \sin(\pi\tilde{b}), & p=y\tilde{b}, \quad b=i\tilde{b},\ 0<\tilde{b}\le\frac{1}{2}, \end{cases} \tag{4.17}$$

where the two cases are the real sheet $\tau = iy$ of (4.13) on the lobe interval and below the BTZ threshold. On the lobe interval y rises from the self-dual value $y(0^+)=1$ to the value $y_E(x_1^*) = 1/(2x_1^*)$ of (4.8) at the tip, where the sine reaches 1 and the branch ends: this is $\sinh \pi x_1^* = 1$ seen from the lobe side. Section 6.6 identifies the profile (4.17) with the extremal potential U.

Airy tip. Near the lower end of the band (4.14) gives $\rho_V^2 \simeq B_V^2\,(\xi-\xi_1^*)$ with $B_V^2 = 3\sqrt{2}\,\pi^2/\operatorname{arcsinh}^3 1$. A density of double zeros that vanishes like a square root, preceded by a simple zero, is modeled locally by the Airy function, as in section 3.5: the first levels sit at $\xi_n = \xi_1^* + |a_n|(\pi B_V c)^{-2/3}$, where a_n are the zeros of Ai. Hence

$$\Delta_1^{\text{best}} = \frac{c}{\Lambda_V} + A_{\text{opt}}\,c^{1/3} + O(1), \qquad A_{\text{opt}} = \frac{|a_1|\,\operatorname{arcsinh} 1}{(3\sqrt{2}\,\pi^4)^{1/3}} = 0.27666, \tag{4.18}$$

and $(t_2-t_1)\,c^{-1/3} \to (|a_2|/|a_1|-1)\,A_{\text{opt}} = 0.20705$, where t_2 is the second level of the extremal spectrum. There is no $\log c$ term at order $c^{1/3}$ or above. The reason: the curve depends on c only through $a = c'/12$, and a power-law prefactor t^α in ρ_C or in g shifts $\frac{1}{c}\log\rho_C$ by $\frac{\alpha}{c}(\log c + \log\xi)$; the first term does not depend on ξ and leaves y_E unchanged, and the second moves y_E by $O(1/c)$, hence t_1 by $O(1)$. A term $\log c$ with a coefficient of order one, below the order $c^{1/3}$, is not excluded by this argument; the data bound it (section 5.3).

Deep band. Far from the tip the double zeros become equally spaced,

$$1-\rho_V \simeq \frac{2}{\pi x}\,e^{-2\pi x}, \qquad \xi_1^* + \int_{\xi_1^*}^{\infty}(1-\rho_V)\,\mathrm{d}\xi = \frac{1}{24}, \tag{4.19}$$

the second being an exact identity.[2] Since the n-th level has $n = c'\int_{\xi_1^*}^{t_n/c'}\rho_V\,\mathrm{d}\xi + O(1)$, it follows that $t_n = n + c/24 + O(1)$, that is, $\Delta_n = n + c/8 + O(1)$: the same offset as for $U(1)^c$ (section 3.5). The offset itself is not new: numerically the spectrum follows the free fermion line $\Delta_n = n + (c-4)/8$ at large n. For Virasoro this is seen in [11, Figure 4] and [10, §7.4], where convergence to the line is conjectured at fixed c; for $U(1)^c$ the distance from the line at large n is conjectured in [12, Conj. 4.2] to be at most of order 2^{-c}, and to vanish only for integers $c \equiv 4$ modulo 8. What is new here is the heuristic derivation of the offset from the band density.

Degeneracies. Hypothesis (A), sharpened from exponential order to order one, predicts $d_n \simeq \rho_C(t_n)\cdot\frac{1}{2}(t_{n+1}-t_{n-1})$ with the full three-Bessel density ρ_C of section 2.4.

Interior sign change. For $t = O(1)$ the functional is carried by the real sheet through the BTZ threshold, where $y=1$: $g = \varphi(t)\,e^{-2\pi t}$ with φ varying on the scale c. Oddness at the origin, $\hat{g}(0) = 2\pi\int_0^\infty g\,\mathrm{d}t = -g(0)$, is dominated by $t = O(1)$, and with $\varphi \simeq \varphi_0 + \varphi_1 t$ it gives $\varphi_1 = -4\pi\varphi_0$. So $g(t) \propto (1-4\pi t)\,e^{-2\pi t} = L_1(4\pi t)\,e^{-2\pi t}$ for $t = O(1)$, the lowest odd mode of section 2.3. Hence $g>0$ on $(0, t_{\text{int}})$ and $g<0$ on (t_{int}, t_1) with $t_{\text{int}} \to 1/4\pi = 0.0796$, and there is no other zero between the vacuum and t_1: this is the positive sliver of section 2.5.

[2] With $u = \pi x$ and $\theta_1 = \operatorname{arcsinh} 1 = \log(1+\sqrt{2})$ it reads $\theta_1^2 + 2\int_{\theta_1}^\infty (u - \operatorname{arccosh}\sinh u)\,\mathrm{d}u = \pi^2/8$. The constant follows from Landen's identity $\sum_{k\ge0}(\sqrt{2}-1)^{2k+1}/(2k+1)^2 = \frac{\pi^2}{16} - \frac{1}{4}\log^2(1+\sqrt{2})$, a special value of Legendre's chi-function of order 2.

Conjecture 1 (conjecture)**.** *Let g be the optimal functional and $\{t_n, d_n\}$ the extremal spectrum, in the order of limits of section 2.5.*

(a) $\Delta_1^{\text{best}} = c/\Lambda_V + A_{\text{opt}}\, c^{1/3} + O(1)$ *with A_{opt} as in (4.18); there is no $\log c$ term at order $c^{1/3}$ or above; and $(t_2 - t_1)\, c^{-1/3} \to 0.20705$.*

(b) *The double zeros of g have density $c'\rho_U(x)/2$ per unit x on the band, and on the lobe interval and below the BTZ threshold $\frac{1}{c'}\log|g|$ is given by (4.17), up to $o(1)$.*

(c) *Deep in the band $t_n = n + c/24 + O(1)$ (cf. [11, Figure 4], [10, §7.4]).*

(d) *$d_n \simeq \rho_C(t_n) \cdot \frac{1}{2}(t_{n+1} - t_{n-1})$, with relative error tending to zero away from the tip.*

(e) *Between the vacuum and t_1 the functional g has exactly one zero, $t_{\text{int}} \to 1/4\pi$, with $g > 0$ on $(0, t_{\text{int}})$ and $g < 0$ on (t_{int}, t_1).*

The leading term of (a) is Theorem 1; Theorem 5 (hence Corollary 6) proves the upper bound with 0.483 in place of A_{opt}; and the density and the profile of (b) are, in a weak sense, Theorem 7. Item (a) concerns Δ_1^{best}; the numerics of section 5 probe the limit $P \to \infty$ of the order-P optimal gap bounds, which bounds Δ_1^{best} from above, equality being conjectural (section 2.6).

5 Numerical evidence

[NUMERICAL] We compare section 4 with optimal functionals computed numerically: the slope, then the items of Conjecture 1, then hypothesis (A) itself. No proof in this paper uses the data of this section.

5.1 Method and convergence

We solve directly for the extremal spectrum $\{t_n, d_n\}$ of section 2.2, the dual variables of the functional problem (the "primal" formulation in the terminology of [11]); by the duality of section 2.2 its lowest level is $t_1^{(P)}(c)$. At order P the unknowns are $P/2$ levels t_n and their weights d_n. They are found by Newton's method [11, 12, 60], continued upward in P from a linear-programming seed at small P. The solver works in Arb [61] ball arithmetic (interval arithmetic in midpoint–radius form), used for its precision and not for its error bounds, at 768 bits or more (appendix H.2). Positivity of g above t_1 and the pattern of double zeros are checked afterwards at every (c, P).

Coverage. We have full spectra at $c = 64$, 128, 256, 300, 384, 500, 512, 768, 1024, 1536, 2048, with P up to 3072. For the gap alone a second, independent implementation of the same method adds a grid $c \in \{24, \dots, 1800\}$ with P up to 3000; where both ran, they agree to the 20–22 digits recorded. The solver is calibrated on the exact optima at $c = 4$ and $c = 12$ (section 2.2).

Convergence in the order. Empirically, the order-P bound $\Delta_1^{(P)}(c)$ of section 2.2 and its limit $\Delta_1^{(\infty)}(c)$ obey

$$\Delta_1^{(P)}(c) - \Delta_1^{(\infty)}(c) \approx C\, e^{-k\sqrt{P/c}}, \qquad k \approx 4.7\text{–}5.7, \tag{5.1}$$

a stretched exponential in P/c. Two things follow. One needs $P \gtrsim c$. And an extrapolation by a pure exponential in P, as in [11], overestimates $\Delta_1^{(\infty)}(c)$, that is, it biases Λ low. We extrapolate with a stretched exponential whose exponent is free, and quote as uncertainty σ the spread to cruder extrapolants; the rule is stated in appendix H.2.

5.2 The slope, and why earlier fits gave 9.08

Table 2 lists $\Delta_1^{(\infty)}(c)$ for $24 \le c \le 2048$, and figure 5 plots it. By Conjecture 1(a), $t_1/c = \xi_1^* + A_{\text{opt}} c^{-2/3} + O(1/c)$. A linear least-squares fit of t_1/c in the basis $\{1, c^{-2/3}, c^{-1}, c^{-4/3}\}$ gives

$$\xi_{1,\text{meas}}^* = 0.026240 \pm 0.000025, \qquad \Lambda_{\text{meas}} = 9.1263 \pm 0.002, \tag{5.2}$$

c	$P_{\max}/c$	$\Delta_1^{(\infty)}(c)$	σ	$c/\Delta_1^{(\infty)}$	
24	25.00	3.440977	$4.3 \cdot 10^{-5}$	6.9748	II
48	18.25	6.244701	$2.6 \cdot 10^{-5}$	7.6865	II
64	16.00	8.086588	$2.5 \cdot 10^{-8}$	7.914339	I
96	8.33	11.736817	$6.5 \cdot 10^{-5}$	8.1794	II
100	8.00	12.190911	$7.7 \cdot 10^{-5}$	8.2028	II
128	16.00	15.359989	$4 \cdot 10^{-8}$	8.333339	I
192	6.25	22.560582	$2.3 \cdot 10^{-4}$	8.5104	II
256	8.00	29.724792	$1.4 \cdot 10^{-5}$	8.612339	I
288	4.86	33.297942	$4.3 \cdot 10^{-4}$	8.649	II
300	5.33	34.636636	$4.6 \cdot 10^{-4}$	8.661	II
384	8.00	43.992503	$1.9 \cdot 10^{-5}$	8.728760	I
400	5.00	45.772111	$5.2 \cdot 10^{-4}$	8.7389	II
500	3.75	56.880799	$1.4 \cdot 10^{-3}$	8.790	II
512	6.00	58.212412	$4 \cdot 10^{-5}$	8.795375	I
600	3.33	67.970939	$1.1 \cdot 10^{-3}$	8.827	II
700	2.60	79.047416	$2.0 \cdot 10^{-3}$	8.855	II
768	4.00	86.573118	$1.2 \cdot 10^{-3}$	8.87111	I
1000	2.00	112.220831	$3.0 \cdot 10^{-3}$	8.911	II
1024	2.25	114.871949	$2.8 \cdot 10^{-3}$	8.91427	I
1200	2.50	134.304424	$2.5 \cdot 10^{-3}$	8.935	II
1400	2.14	156.370479	$5.2 \cdot 10^{-3}$	8.953	II
1536	2.00	171.367432	$4.5 \cdot 10^{-3}$	8.96320	I
1800	1.67	200.464339	$8.0 \cdot 10^{-3}$	8.979	II
2048	1.50	227.7834	$1.0 \cdot 10^{-2}$	8.9910	I

Table 2: The optimal gap bound extrapolated to $P = \infty$. Columns: the central charge; the highest order reached, in units of c; $\Delta_1^{(\infty)}(c)$; its uncertainty σ (appendix H.2: half the larger distance to two cruder extrapolants, at least $10^{-7}c$; if $P_{\max}/c \geq 6$, the spread of three tail fits); the ratio $c/\Delta_1^{(\infty)}(c)$; and the implementation, I for the ball-arithmetic solver and II for the second, independent one. Rows with $P_{\max}/c \geq 4$ are converged: their extrapolation correction is below $3 \cdot 10^{-6}c$. The others rest on (5.1).

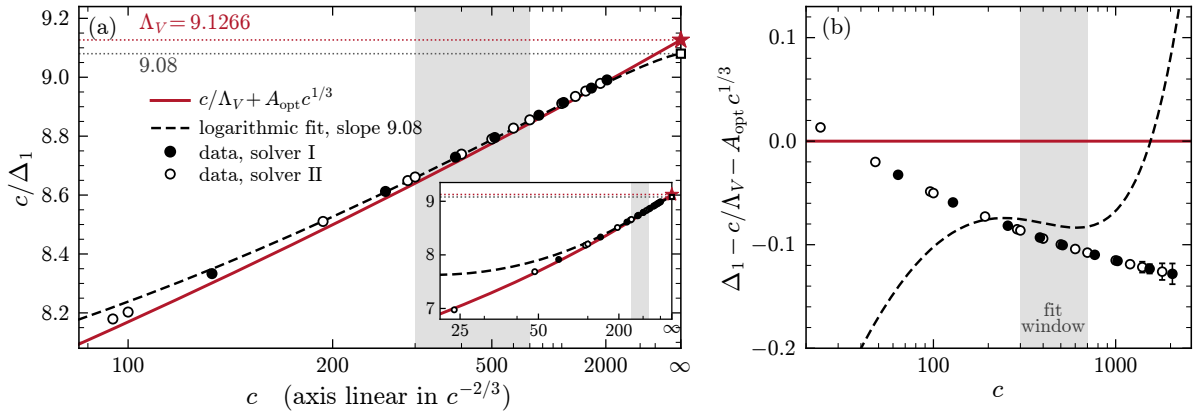


Figure 5: The slope. (a) The ratio $c/\Delta_1^{(\infty)}(c)$ of table 2 against c, on an axis that is linear in $c^{-2/3}$, so that $c = \infty$ is a point of the axis. Filled and open circles: implementations I and II. Solid: the two-term law $\Delta_1^{\rm best} = c/\Lambda_V + A_{\rm opt}c^{1/3}$ of Conjecture 1, which has no fitted parameter; the data lie slightly above it because of the $O(1)$ remainder. Dashed: the logarithmic fit $c/9.08 + 0.439\log c - 0.896$ of [11]. Dotted lines, star and square: the asymptotes Λ_V and 9.08. Shaded: the window $300 \leq c \leq 700$ of that fit. Inset: all rows of the table. (b) The remainder $\Delta_1^{(\infty)}(c) - c/\Lambda_V - A_{\rm opt}c^{1/3}$, with error bars σ. It is of order one and varies slowly, as (4.18) asserts. Dashed: the same quantity for the logarithmic fit, which follows the data on its window and departs from them beyond it, by 0.22 at $c = 2048$, where $\sigma = 0.010$.

against $\xi_1^* = 0.0262361$ and $\Lambda_V = 9.12663$. The uncertainty is the spread over fit forms and over the lower end of the fit window, not a statistical error. The value $\xi_1 = 0.02680$ that corresponds to $\Lambda = 9.08$ is not approached by any of the forms.

The 9.08 fit. The difference from [11] is in the fitting function, not in the data. We fit the form used there, $c/\Lambda_{\rm fit} + \gamma_{\rm fit}\log c + \text{const}$, not to data but to the exact two-term law $c/\Lambda_V + A_{\rm opt}c^{1/3}$. On $c \in [300, 700]$, the window of [11, §5.2], the fit returns $(\Lambda_{\rm fit}, \gamma_{\rm fit}) = (9.085,\ 0.48)$, against the published $(9.08,\ 0.439)$. The reason is that $c^{1/3}$ and $\log c$ are nearly collinear over a decade of c; accordingly the result drifts with the window, from $(9.02, 0.28)$ on $[20, 300]$ to about $(9.11, 0.71)$ on $[500, 4000]$. The two other fitting functions of [11], $c/A + B_1$ and $c/A + B_1 + B_2/c$, treated in the same way return $A = 9.004$ and 9.043, against their 9.01 and 9.04. The published spread is thus reproduced, to within 0.01 in each entry, by a law of slope 9.127: the earlier extrapolation is explained, not contradicted.

5.3 Fine structure

We check the items of Conjecture 1 in turn, and then (A). Item (a): the fitted coefficient of $c^{-2/3}$ in t_1/c lies between 0.269 and 0.285, depending on the form and the window, against $A_{\mathrm{opt}} = 0.27666$; and a term $\gamma \log c$ allowed to compete with $c^{1/3}$ comes out with γ between -0.07 and -0.005, compatible with zero. The first spacing $(t_2 - t_1)\, c^{-1/3}$ decreases from 0.28963 at $c = 64$ to 0.22369 at $c = 768$ and extrapolates, in the basis $\{1, c^{-2/3}, c^{-1}\}$, to 0.20700, against 0.20705 (two other correction forms give 0.2043 and 0.2085). Item (b): the spacings s_n of the double zeros, with $s_n - 1$ extrapolated linearly in $1/c$, agree with $1/\rho_V - 1$ to within 0.1% for $0.06 \le \xi \le 0.20$. Item (c): deep in the band the coefficient of c in $t_n - n$ is $\frac{1}{24}(1 \pm 4 \cdot 10^{-4})$. Item (d): the ratio $d_n/(\rho_C(t_n) \cdot \frac{1}{2}(t_{n+1} - t_{n-1}))$ is $1 - 10^{-6}$ deep in the band and 0.98 at $n = 2$; this is the forced part of (A), (4.6), verified to far better than exponential order. Item (e): at every (c, P) there is exactly one zero between the vacuum and t_1, with the predicted signs; it moves from $t_{\mathrm{int}} = 0.0803889$ at $c = 64$ to 0.0796944 at $c = 500$, that is, $t_{\mathrm{int}} = 1/4\pi + 0.058/c + o(1/c)$.

The Cardy height. Hypothesis (A) itself is tested through its consequence (4.8), that is, through the Cardy height $\varkappa$ of section 4.2. It can be read off the non-real zeros of the truncated polynomials pol_P. At every (c, P) these lie on one parabola in the complex t-plane, with focus at the BTZ threshold $t = 0$, that is, on the lines $|\mathrm{Im}\, b| = \frac{\varkappa}{2} + O(1/c)$ in the variable $b = \sqrt{3t/c'}$. A fit to the vertex of the parabola for $64 \le c \le 500$, which does not involve ξ_1^*, gives $\varkappa = 1.0000 \pm 0.0005$; for comparison, $\varkappa = 1.0107$ would correspond to the slope 9.080. The reason the zeros sit there is that the duality integral $\hat{g}(s) = 2\pi \int g\, J_0$ of section 2.3, continued to complex $s = c' b^2/3$, converges absolutely exactly for $|\mathrm{Im}\, b| < \frac{1}{2}$: the Bessel kernel grows like $e^{\frac{4\pi}{3} c' x |\mathrm{Im}\, b|}$, and on the band g decays like $e^{-c' L(x)} = e^{-\frac{2\pi}{3} c' x}$. At finite P the zeros condense on the boundary of this region. This is the strip of section 6.3, seen in the data.

Part III Optimality

Everything in this Part is proved, and no computer is used. It needs only section 2. The strip of section 4.2 and the curve of section 4.4 reappear here as lemmas about a domain and a potential, without hypotheses; a reader who skipped Part II loses nothing.

6 Optimality: nothing beyond Λ_V

We show that the spinless bootstrap cannot give a slope better than Λ_V, at any order and with any functional in $\bar{\mathcal{A}}$. The mechanism is the tension described after (2.16). A functional that certifies the gap bound t_1 must carry half of its Cardy-weighted mass below t_1; and we prove that no function in $\bar{\mathcal{A}}$, feasible or not, carries more than an exponentially small fraction of its mass below $t = \xi_1^* c'$. The statements are in section 6.1. The proof is an electrostatics problem on the strip of figure 2, described in section 6.2. Section 6.3 continues the functional to the strip and bounds it on the boundary, section 6.4 collects the potential theory that we use, section 6.5 turns the bounds on the boundary into a bound in the interior by a harmonic function, section 6.6 finds that function in closed form, and sections 6.7 and 6.8 draw the consequences. The technical lemmas are in appendices B and C.

6.1 Statements

Theorem 3 (Concentration; proved)**.** *Let $x_1^* = \mathrm{arcsinh}(1)/\pi$. For every $\delta \in (0, x_1^*)$ there is a constant $C_\delta < \infty$ such that for all $c \ge 40$ and every $g \in \bar{\mathcal{A}}$, with no condition on the sign of g,*

$$\int_0^{c'(x_1^* - \delta)^2/3} |g|\, V \,\mathrm{d}t \;\le\; C_\delta\, c'^4\, e^{-\kappa(\delta)\, c'}\, M[g]. \tag{6.1}$$

Here $\kappa(\delta) > 0$ is the explicit Cardy deficit*, given in closed form in Lemma 6.7. It satisfies*

$$\kappa(\delta) = \tfrac{8}{9}\sqrt{2\sqrt{2}\,\pi}\;\delta^{3/2}(1+O(\delta)), \qquad \kappa(\delta) \geq 2.228\,\delta^{3/2} \quad (0 < \delta \leq x_1^*), \tag{6.2}$$

where $\frac{8}{9}\sqrt{2\sqrt{2}\,\pi} = 2.650$, and $C_\delta \leq C_{\mathrm{conc}}\,\delta^{-5}$ with an absolute constant C_{conc}.

In words: weighted by the density of states that the vacuum demands, any bootstrap function has exponentially little mass below $t \approx 0.0262\,c'$.

Theorem 4 (Optimality; proved)**.** *Let ξ_1^* and Λ_V be as in Theorem 1, and call g weakly feasible if it is weakly feasible at some T, hence at $T = t_1(g)$. For every $\Lambda > \Lambda_V$ there is $c_0(\Lambda)$ such that for $c \geq c_0(\Lambda)$ no weakly feasible $g \in \bar{\mathcal{A}}$, $g \not\equiv 0$, has $t_1(g) + a \leq c/\Lambda$. Quantitatively, there is a central charge c_0^{opt}, explicit in principle and not computed, such that*

$$t_1(g) \;\geq\; \xi_1^*\,c' - 0.44\,c'^{1/3}\log^{2/3} c' \tag{6.3}$$

for every weakly feasible $g \in \bar{\mathcal{A}}$, $g \not\equiv 0$, and every $c \geq c_0^{\mathrm{opt}}$.

Proof of the first statement of Theorem 4 from Theorem 3. Let $\Lambda > \Lambda_V$, that is, $\frac{1}{\Lambda} - \frac{1}{12} < \xi_1^*$, and choose $\delta \in (0, x_1^*)$ with $\frac{1}{3}(x_1^* - \delta)^2 > \frac{1}{\Lambda} - \frac{1}{12}$. If $t_1(g) + a \leq c/\Lambda$, then $t_1(g) \leq c'(\frac{1}{\Lambda} - \frac{1}{12}) + \frac{1}{\Lambda} \leq c'(x_1^* - \delta)^2/3$ as soon as c is large. If moreover g is weakly feasible, g_- is supported on $[0, t_1]$ and the half-mass condition (2.16) makes the left side of (6.1) at least $\int_0^{t_1} g_- V\,\mathrm{d}t \geq \frac{1}{2}M[g]$, where $M[g] > 0$ because $g \not\equiv 0$. Hence $\frac{1}{2} \leq C_\delta\,c'^4 e^{-\kappa(\delta)c'}$, which is false for large c. How large c must be depends on Λ only. □

The rate (6.3) is proved in section 6.8. Three remarks. First, the theorem quantifies over all of $\bar{\mathcal{A}}$, and $c_0(\Lambda)$ does not depend on g. Since $\bar{\mathcal{A}}$ contains the functionals of every order P (Lemma 2.6), the statement is uniform in P: for $c \geq c_0(\Lambda)$ no amount of computing produces a spinless bound below c/Λ. Second, this is a statement about the method, the linear program of section 2.2, and not about conformal field theories. Third, the informative content of the quantitative form is its *rate*; the right side of (6.3) lies below the trivial floor $t_1 \geq 0$ of section 2.4 for $c' \lesssim 414$.

Attribution. The strategy is the following: continue the functional to a strip; control one part of the boundary by the total mass and the other by the eigen-identity; bound the function inside by its *harmonic majorant*, the harmonic function with the same boundary data, which lies above it by the maximum principle; and conclude through the half mass of the negative part. This is the strategy of the proof for the Cohn–Elkies problem at large dimension in [13, Ch. 1, Prop. 3.1 and Thm. 3.8]; we have read the statements and the structure of that argument but have not independently verified it; nothing in this paper depends on it logically. There $d \to \infty$ and the strip is in the Mellin-transform variable, of half-width $d/2$; here $d = 2$ is fixed and the strip is in the rescaled dimension b itself, its width being fixed by the requirement that the continued kernel have exactly Cardy growth on the edge. The strip through the vacuum, the weight V, the slit geometry and the closed form are specific to Virasoro. The argument in position space does not run for $U(1)^c$. The argument in the Mellin variable does run for Virasoro: the strip is then replaced by a domain with a free boundary (appendix A). The last step of the strategy, the half mass of the negative part, goes back to Bourgain, Clozel and Kahane [52] (see also [53]); Cohn and Gonçalves [51, §3.1] use it for the functions with $\hat{f} = -f$ of the twin problem, and (2.16) is the same step with the Cardy weight. A mass-concentration principle similar to that of [13, Ch. 1] has since been proved for Delsarte's linear program for binary codes [62].

6.2 Idea of the proof: an electrostatics problem

The stage is figure 2(b). In the variable b of (2.17) a functional $g \in \bar{\mathcal{A}}$ becomes the function $G(b) = g(c'b^2/3)$, and the proof has five steps.

Conformal field theory	Linear program	Electrostatics on the strip
linear functional acting on the crossing equation	the function g; $G(b) = g(c'b^2/3)$	potential $u_g = \frac{1}{c'}\log(\lvert G\rvert/M[g])$
dimensions of the extremal spectrum	zeros of G	positive point charges, $1/c'$ each
Cardy density ρ_C that the vacuum demands	Cardy growth of the weight, $V \approx e^{c'L}$	applied linear potential $-L(x)$
—	edges $E_\pm$ of the strip of analyticity	grounded plates
the vacuum, $\Delta = 0$	the point $t = -a$	the point $b = \frac{i}{2}$ on a plate
a gap bound, $\Delta_1 \le t_1(g) + a$	weak feasibility, through the half-mass condition	contact with the Cardy line
slope Λ_V of the best bound	optimal slope, $\xi_1^* = (x_1^*)^2/3$	first point of contact, $x = x_1^*$

Table 3: The dictionary between the conformal field theory, the linear program and the electrostatics problem of section 6.

(1) G continues analytically to the closed strip $|\mathrm{Im}\, b| \le \frac{1}{2}$, with the vacuum on its edge (section 6.3).
(2) On the edges $|G|$ is bounded by $M[g]$ up to a power of c (Lemma 6.1).
(3) On the real axis beyond any chosen point s, $|G|$ is small in the Cardy-weighted mean: $\int_{|x|\ge s}|G|\, e^{c'L}\,\mathrm{d}x$ is at most $M[g]$ up to a power of c (Lemma 6.2).
(4) $u_g = \frac{1}{c'}\log(|G|/M[g])$ is the potential of positive charges at the zeros of G, in the convention in which a potential is $-\infty$ at its positive charges (section 6.4). It is *subharmonic*, that is, it obeys the maximum principle. We cut the strip along $|x| \ge s$, so that this part of the real axis becomes boundary, where step (3) applies, and the interval $(-s, s)$, about which nothing is assumed, stays inside. The value of a harmonic function inside is an average of its boundary values, so a bound in the mean suffices: u_g lies below the harmonic function that is zero on the edges and $-L$ on the slits, up to $o(1)$ (Proposition 6.4).
(5) For $s = x_1^*$ that harmonic function is explicit, and it lies strictly below the Cardy line on $|x| < x_1^*$ (Lemmas 6.5 and 6.7). Since $|g|\, V \approx e^{c'(u_g+L)}M[g]$, almost no Cardy-weighted mass can sit there.

Table 3 is the dictionary. In its language the half-mass condition says that the potential of a weakly feasible functional must come within $o(1)$ of the Cardy line somewhere on $|x| \le x_1(g)$, and the theorem says that the first point where this is possible is x_1^*.

6.3 Continuation to the strip

The idea is that the eigen-identity (2.14), which gives the values of g below the BTZ threshold as integrals over $t \ge 0$, makes sense for complex α as long as the kernel K_α grows no faster than the Cardy weight. Since $|I_0(z)| \le I_0(|\mathrm{Re}\, z|)$, this is the case on the parabolic region $|\mathrm{Re}\,\sqrt{\alpha}| \le \sqrt{a}$, whose vertex is the vacuum and whose focus is the BTZ threshold (figure 2(a)): by Lemma B.1 the integral $g(-\alpha) = -2\pi\int_0^\infty gK_\alpha\,\mathrm{d}t$ converges absolutely there and is dominated by $2\pi\int_0^\infty |g|K_a\,\mathrm{d}t < \infty$. In the variable b we have $\alpha = -c'b^2/3$ and $|\mathrm{Re}\,\sqrt{\alpha}| = \sqrt{c'/3}\,|\mathrm{Im}\, b|$, so the region is the closed strip $\bar{\mathbb{S}} = \{|\mathrm{Im}\, b| \le \frac{1}{2}\}$. Hence

$$G(b) := g(c'b^2/3) = -2\pi\int_0^\infty g(t)\, K_{-c'b^2/3}(t)\,\mathrm{d}t, \qquad |G(b)| \le 2\pi\int_0^\infty |g|\, K_a\,\mathrm{d}t \qquad (b \in \bar{\mathbb{S}}) \quad (6.4)$$

is well defined for every $g \in \bar{\mathcal{A}}$. By Lemma B.1, G is bounded and continuous on $\bar{\mathbb{S}}$ and holomorphic on $\mathbb{S}$. It is even, and real on the real axis and on the segment $i[-\frac{1}{2}, \frac{1}{2}]$. For real $b = x$ it is the functional itself, $G(x) = g(c'x^2/3)$; in particular $G \not\equiv 0$ unless $g \equiv 0$. For a functional of finite order G is the restriction of an entire function, but this plays no role.

The landmarks are those of figure 2(b). The real axis is the spectrum above the BTZ threshold, $t \geq 0$. The segment $b = iy$, $0 \leq y \leq \frac{1}{2}$, is the range $-a \leq t \leq 0$ below it. The points $b = \pm\frac{i}{2}$ are the vacuum, $G(\pm\frac{i}{2}) = g(-a)$. On a line $|\mathrm{Im}\, b| = \eta$ the kernel is bounded by $K_{(2\eta)^2 a} \approx e^{2\eta c' L}$. This is smaller than the Cardy weight for $\eta < \frac{1}{2}$, equal to it for $\eta = \frac{1}{2}$, and larger for $\eta > \frac{1}{2}$, where $M[g] < \infty$ no longer controls the integral. *The vacuum sits on the edge of the strip of analyticity that Cardy growth allows.*

Lemma 6.1 (Edges; proved)**.** *For $b = x \pm \frac{i}{2}$ on $E_\pm$ and $\alpha = -c'b^2/3$ one has $(\mathrm{Re}\,\sqrt{\alpha})^2 = a$ for every real x, and therefore $|K_\alpha(t)| \leq K_a(t)$ for all $t \geq 0$: on the edges the continued kernel has exactly Cardy growth. Since V/K_a is only polynomially small, there is an absolute constant C such that for all $c \geq 40$*

$$|G(x \pm \tfrac{i}{2})| \leq C\, a\, c'\, M[g] \tag{6.5}$$

uniformly in $x \in \mathbb{R}$ and in $g \in \bar{\mathcal{A}}$, in particular in the order P.

The idea of the proof: the kernel bound is (B.1), so by (6.4) $|G(x \pm \frac{i}{2})| \leq 2\pi \int_0^\infty |g| K_a \,\mathrm{d}t$. For $t \geq 4/c'$ one has $K_a \leq C\, a\, c'\, V$ (Lemma B.2(b)). In the window $t \leq 4/c'$ at the BTZ threshold, where $V \simeq 8\pi^4 t^2$ degenerates while K_a stays of order one, $\hat{g} = -g$ bounds $\sup|g|$ by a multiple of $M[g]$ (Lemma B.3). The proof is in appendix C.4. At the exponential scale $e^{O(c')}$ of the rest of the problem the edges carry weight zero: $u_g \leq (2\log c' + C)/c'$ there, in the notation (6.13) below.

Lemma 6.2 (Slits; proved)**.** *On $|x| \geq x_1^*$, that is, for $t \geq \xi_1^* c'$, one has $V \geq 0.9\, K_a$. Hence for all $c \geq 40$ and every $g \in \bar{\mathcal{A}}$,*

$$\int_{|x| \geq x_1^*} |G(x)|\, K_a(c'x^2/3)\, \mathrm{d}x \leq \frac{12}{c'}\, M[g]. \tag{6.6}$$

Proof. G is even. With $t = c'x^2/3$ we have $\mathrm{d}x = 3\,\mathrm{d}t/(2c'x) \leq 3\,\mathrm{d}t/(2c'x_1^*)$ for $x \geq x_1^*$, and $V \geq 0.9\, K_a$ there by Lemma B.2(c). Hence the left side of (6.6) is at most

$$\frac{3}{c'x_1^*} \int_{\xi_1^* c'}^\infty |g|\, K_a \,\mathrm{d}t \leq \frac{3}{0.9\, c'x_1^*} \int_{\xi_1^* c'}^\infty |g|\, V \,\mathrm{d}t \leq \frac{11.9}{c'}\, M[g]. \qquad \square$$

On the slits $G(x) = g(c'x^2/3)$ is the functional in the region where a good functional is non-negative. Nothing is known there pointwise, and an extremal functional vanishes there infinitely often; (6.6) is a statement in the mean, and section 6.5 uses it as such.

Remark (Why $c' = c - 1$ and not c; orientation)**.** The scaling $t = c'b^2/3$ puts the edge of the strip through the true vacuum $t = -a$, where the kernel is bounded by K_a, which exceeds V by a power of c' only. With c in place of c' the edge would pass through $t = -c/12$, where the kernel is bounded only by $K_{a+1/12}$, which exceeds V by a factor growing like $e^{(\pi/3)\sqrt{3t/c}}$. Since feasible functionals of high order carry Cardy-weighted mass arbitrarily far out in t, the edge bound would then depend on the functional, and the uniformity in g would be lost.

What is *not* used: sign information (positivity enters only through the half-mass condition, in one line, at the very end); information about g near the BTZ threshold beyond integrability; any property of optimal functionals. The inputs on Bessel functions are Lemmas B.1 to B.3.

6.4 Toolkit: potential theory in physicist's terms

Steps (4) and (5) of section 6.2 are two-dimensional electrostatics. The box collects the notions and the four formulas that we use, first in the language of charges and potentials and then precisely. We use the sign convention in which a unit point charge at ζ has the potential $\log|b - \zeta|$.

Toolkit: potential theory

Subharmonic functions. If $G \not\equiv 0$ is holomorphic, then

$$\nabla^2 \log|G(b)| = 2\pi \sum_{\zeta:\, G(\zeta)=0} m_\zeta\, \delta^2(b-\zeta) \;\geq 0, \tag{6.7}$$

with m_ζ the multiplicity: $\log|G|$ is the potential of positive point charges at the zeros of G, and it is harmonic away from them. A function u with $\nabla^2 u \geq 0$ in the sense of distributions is called *subharmonic*; precisely, u is upper semicontinuous with values in $[-\infty, \infty)$ (it may jump down, as at a charge, but not up), and $u(b)$ is at most the mean of u over every small circle around b. Such a function obeys the *maximum principle*: if h is harmonic on a bounded domain and $\limsup u \leq h$ at every boundary point, then $u \leq h$ inside [63, Thm. 2.3.1]. Adding positive charges lowers the potential.

Harmonic measure. For a domain Ω and a point $b \in \Omega$, $\omega_b(E)$ is the probability that a Brownian path started at b first leaves Ω through the part E of the boundary. Equivalently, $b \mapsto \omega_b(E)$ solves the Dirichlet problem with boundary values 1 on E and 0 elsewhere, and $\int \varphi \, \mathrm{d}\omega_b$, the *Poisson integral* of φ, solves it with boundary values φ [63, §4.3]; for the upper half-plane $\mathrm{d}\omega_z = \operatorname{Im} z \, \mathrm{d}\sigma/(\pi|\sigma - z|^2)$, the *Poisson kernel*. On the slit strip the two lips of a slit are different boundary points, and $\mathrm{d}\omega_b/\mathrm{d}x$ denotes the density of ω_b on a slit with the two lips added. It is explicit through the conformal map of Lemma 6.3. Like the charge density at the rim of a thin conducting plate, it has an inverse square-root singularity at the tips.

Harmonic majorant. This is the solution h of the Dirichlet problem whose data are the boundary values of a subharmonic u, that is, the potential with the same boundary values and with all interior charges removed. By the maximum principle $u \leq h = \int u \, \mathrm{d}\omega_b$ [63, §4.1].

Poisson–Jensen. For G bounded and holomorphic on Ω, with boundary values taken ω_b-almost everywhere,

$$\log|G(b)| \leq \int_{\partial\Omega} \log|G| \, \mathrm{d}\omega_b. \tag{6.8}$$

If G is holomorphic on a neighborhood of $\bar{\Omega}$, the right side minus the left side is $\sum_\zeta m_\zeta \, \mathrm{g}_\Omega(b, \zeta)$, where $\mathrm{g}_\Omega \geq 0$ is the Green's function of Ω and the sum runs over the zeros of G in Ω [63, §4.5]: each zero lowers the potential by the potential of a unit charge in the grounded domain. We need (6.8) for a merely bounded function that may vanish on the boundary (Lemma C.3(a)); for the disk this is classical: removing the charges at the zeros, inside or on the boundary, only raises the potential [64, Ch. II, Thm. 4.1 and Cor. 4.2], [65, Thms. 17.16–17.17].

Jensen's inequality with entropy. On the slits we know only a weighted mean of $|G|$ (Lemma 6.2), whereas (6.8) asks for the mean of $\log|G|$ with respect to ω_b. Let w be a probability density on a set S of the real line and $K > 0$ a weight. Since the mean of a logarithm is at most the logarithm of the mean [65, Thm. 3.3],

$$\int_S w \log|G| \, \mathrm{d}x \;\leq\; \log \int_S |G| \, K \, \mathrm{d}x \;-\; \int_S w \log K \, \mathrm{d}x \;+\; \int_S w \log w \, \mathrm{d}x. \tag{6.9}$$

The change of reference density from K to w costs the *entropy* $\int w \log w$. With $K = K_a \approx e^{c'L}$ the middle term is $-c' \int wL$, which is how the Cardy line enters. For w proportional to $\mathrm{d}\omega_b/\mathrm{d}x$ the entropy is finite despite the singularity at the tips; it is bounded in Lemma C.2, together with its dependence on the distance from b to the tips.

Phragmén–Lindelöf. On an unbounded domain the maximum principle needs a growth condition: on the strip $\mathbb{S}$ the function $\cosh(\pi x)\cos(\pi y)$ is harmonic and vanishes on both edges. A harmonic function on $\mathbb{S}$ that vanishes on the edges and is $O(e^{\alpha|x|})$ for some $\alpha < \pi$ is zero [63, §2.3]. All our functions grow at most linearly in $|x|$. The form that we use is proved in the proof of Lemma 6.5.

Riesz measure. The charge distribution $\frac{1}{2\pi}\nabla^2 u$ of a subharmonic function u is a positive measure, its *Riesz measure*, and locally u is the logarithmic potential of that measure plus a harmonic function [63, §3.7]. For u_g of (6.13) it is, by (6.7),

$$\mathfrak{n}_g := \frac{1}{2\pi}\nabla^2 u_g = \frac{1}{c'}\sum_{\zeta\in\mathbb{S}:\, G(\zeta)=0} m_\zeta\, \delta_\zeta, \tag{6.10}$$

the counting measure of the zeros of G in the strip, normalized so that a zero is a charge $1/c'$.

6.5 The slit strip and the majorant

We now choose the domain on which the maximum principle is applied. For $s > 0$ let

$$D_s := \mathbb{S} \setminus \{x + iy :\ |x| \geq s,\ y = 0\}, \qquad D := D_{x_1^*}. \tag{6.11}$$

D_s is simply connected. Its boundary consists of the two edges and of two slits, and each slit has two lips, which count as different boundary points; the ends of the slits, $b = \pm s$, are the *tips*. We prove everything for D; the choice of s is discussed in section 6.6. The next lemma makes harmonic measure on D explicit.

Lemma 6.3 (Conformal map; proved)**.** *The function*

$$b(z) = \frac{1}{2\pi}\log\frac{z-1}{z\,(z+1)}, \tag{6.12}$$

with the branch that is continuous on the upper half-plane $\mathbb{H}$ and has $b(i) = 0$, maps $\mathbb{H}$ conformally onto D. It maps the intervals $(0,1)$ and $(-\infty,-1)$ onto the edges E_+ and E_-, and $(-1,0)$ and $(1,\infty)$ onto the right and the left slit, each folded at its tip, $b(1\mp\sqrt{2}) = \pm x_1^*$, so that the two halves of the interval give the two lips. Moreover $b(\sqrt{2}-1) = \frac{i}{2}$, and the points $-1, 0, 1, \infty$ correspond to the four ends of D (figure 4(b), last row of labels).

The proof is Lemma C.1(a),(b); part (c) of that lemma transports the Poisson kernel of $\mathbb{H}$ to D and gives the density of ω_b, its exponential decay along the slits and its first moment. The map is the uniformization of section 4.4, (4.11); it is now a lemma about a domain and not a hypothesis about a curve.

For $g \in \bar{\mathcal{A}}$, $g \not\equiv 0$, we write

$$u_g(b) := \frac{1}{c'}\log\frac{|G(b)|}{M[g]} \qquad (b \in \bar{\mathbb{S}}), \tag{6.13}$$

which is subharmonic on $\mathbb{S}$ by (6.7), even, and symmetric under $b \mapsto \bar{b}$. The data on the boundary of D are these. On the edges, $u_g \leq (2\log c' + C)/c'$ by Lemma 6.1. On the lips of the slits we have only the weighted L^1 bound of Lemma 6.2. Jensen's inequality (6.9) with $K = K_a$, together with the finiteness of the entropy of harmonic measure, converts it into $u_g \leq -L(x) + o(1)$ in the mean with respect to ω_b. The entropy is the one place where the geometry of D, namely the square-root singularity of harmonic measure at the tips, has to be examined by hand. Poisson–Jensen (6.8) then bounds $u_g(b)$ by the mean of these data, and the mean of the data is a harmonic function of b.

Proposition 6.4 (Majorant; proved)**.** *For $s > 0$ let U_s denote the harmonic function on D_s that is continuous up to the edges, both lips of the slits and the tips, with*

$$U_s = 0 \ \text{ on } E_\pm, \qquad U_s = -L(x) \ \text{ on both lips of the slits}, \qquad |U_s(b)| \leq C\big(1 + |\operatorname{Re} b|\big). \tag{6.14}$$

For every compact set $Q \subset D$ there is a constant C_Q such that for all $c \geq 40$, all $g \in \bar{\mathcal{A}}$ with $g \not\equiv 0$, and all $b \in Q$,

$$u_g(b) \leq U_{x_1^*}(b) + C_Q \, \frac{1 + \log c'}{c'}. \tag{6.15}$$

The linear growth at the four ends makes the solution of (6.14) unique (proof of Lemma 6.5, part (d)); for $s = x_1^*$ it exists as a Poisson integral, $U_{x_1^*}(b) = -\int L \, \mathrm{d}\omega_b$ over the slits, (C.15), and other s enter no proof. The proof of Proposition 6.4 is in appendix C.4. It inserts Lemma 6.1 and the Jensen bound into the Poisson–Jensen inequality on D and arrives, for every $b \in D$, at the master inequality (C.14), in which the power of c' and the entropy appear explicitly. The technical lemmas are Lemma C.3 (Poisson–Jensen with zeros on the boundary) and Lemma C.2 (the entropy near a tip).

The picture is that of two grounded plates and, between them, two thin electrodes held at the linearly decreasing potential $-L$. The function U_s no longer knows anything about g or about conformal field theory, and $e^{c' U_{x_1^*}(b)}$ is, up to a power of c', a universal bound for $|G|/M[g]$ on compact subsets of D, in particular below the BTZ threshold and on the lobe interval. Nothing is imposed on the interval $(-s, s)$. That is where the mass of a would-be better functional has to be, by the half-mass condition, and the point of the construction is that u_g is small there all the same.

6.6 Why $s = x_1^*$; the extremal potential in closed form; the zero law

[ORIENTATION] *Why this slit.* For any s the argument of section 6.5 gives the majorant U_s on D_s, and it bounds the Cardy-weighted mass wherever $U_s + L < 0$ inside $(-s, s)$. A harmonic function on a slit domain generically has a square-root singularity at a tip: $U_s + L \simeq \gamma_{\mathrm{tip}}(s)\sqrt{s - |x|}$ inside the tips. The coefficient γ_{tip} changes sign exactly once, at $s = x_1^*$; numerically $\gamma_{\mathrm{tip}} = -0.16$, -0.02, ≈ 0, $+0.02$, $+0.16$ at $s = 0.24$, 0.275, x_1^*, 0.285, 0.32. For $s < x_1^*$ one finds $U_s + L < 0$ on all of $(-s, s)$, and the method gives the weaker bound $\Lambda \leq 1/(\frac{1}{12} + \frac{s^2}{3})$; for instance $s = 0.26$ gives $\Lambda \leq 9.45$. For $s > x_1^*$ the majorant rises above the Cardy line inside the tips and excludes nothing there. Thus $s = x_1^*$ is the largest useful slit, characterized by *tangency*: $U_s + L$ vanishes to order $\frac{3}{2}$ at the tips, which is a free-boundary condition. None of this is used in the proofs.

For $s = x_1^*$ the Dirichlet problem (6.14) has a solution in closed form. The idea is to guess the holomorphic function p whose imaginary part is $\frac{3}{4\pi}\partial_x U$: since $U = -L$ on the slits and U is constant on the edges, $\operatorname{Im} p$ must be $\mp\frac{1}{2}$ on the slits and 0 on the edges.

Lemma 6.5 (Closed form; proved)**.** *On D let*

$$p(b) := \frac{1}{\pi} \operatorname{arcsinh}(-i \sinh \pi b) \tag{6.16}$$

with the principal branch of arcsinh*, whose cuts are $\pm i[1, \infty)$. It is single-valued and holomorphic exactly on D, its cuts in the strip being the slits. Let*

$$U(b) := U_0 + \frac{4\pi}{3} \operatorname{Im} \int_0^b p(b') \, \mathrm{d}b', \qquad U_0 := -L(x_1^*) + \frac{4}{3} \int_0^{x_1^*} \operatorname{arcsin}(\sinh \pi s) \, \mathrm{d}s = -0.388748, \tag{6.17}$$

the integral being taken along any path in D. Then U is harmonic on D, continuous up to the edges, the lips and the tips, equal to 0 on $E_\pm$ and to $-L$ on both lips of both slits, and $|U(b)| \leq \frac{2\pi}{3}|\operatorname{Re} b| + C$. It is the only harmonic function on D with this continuity and these boundary values that grows at most linearly. In particular $U = U_{x_1^*}$. On the axes,

$$\begin{aligned} U(x) &= U_0 - \frac{4}{3} \int_0^{|x|} \operatorname{arcsin}(\sinh \pi s) \, \mathrm{d}s \quad (|x| \leq x_1^*), \\ U(iy) &= U_0 + \frac{4}{3} \int_0^{|y|} \operatorname{arcsinh}(\sin \pi s) \, \mathrm{d}s \quad (|y| \leq \tfrac{1}{2}). \end{aligned} \tag{6.18}$$

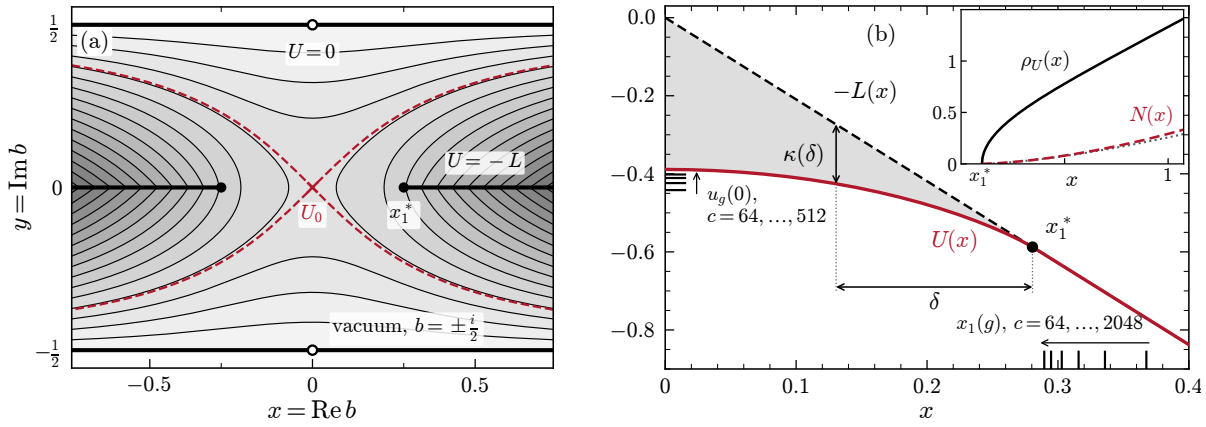


Figure 6: The extremal potential U of Lemma 6.5. (a) Equipotentials of U on the strip, in steps of 0.1, darker meaning lower. $U = 0$ on the edges, where the open circles are the two images $b = \pm\frac{i}{2}$ of the vacuum; $U = -L$ on the slits $|x| \geq x_1^*$, $y = 0$, whose tips are the dots; and the dashed level $U = U_0 = -0.3887$ passes through the saddle at the BTZ threshold $b = 0$. (b) On the real axis U (solid) lies below the Cardy line $-L(x) = -\frac{2\pi}{3}x$ (dashed) and joins it tangentially at x_1^*; the vertical distance at $x = x_1^* - \delta$ is the Cardy deficit $\kappa(\delta)$ of Lemma 6.7. The ticks on the left axis are the values $u_g(0)$ of numerically optimal functionals at $c = 64, 128, 256, 512$, which approach U_0 from below (section 6.7). The ticks on the bottom axis are the first zeros $x_1(g) = (3t_1/c')^{1/2}$ of the optimal functionals of table 2 at $c = 64, 128, \dots, 2048$, which approach x_1^* from above. Inset: the zero law $\rho_U(x)$ of Definition 6.6 (solid), its counting function $N(x)$ (dashed) and the tip asymptote $\kappa_{\text{tip}}(x - x_1^*)^{3/2}$ (dotted).

We call U the *extremal potential*. By (6.19) below its complex electric field is $\partial_x U - i\,\partial_y U = -\frac{4\pi i}{3}\,p$, and p is related to b by $\sinh \pi b = i \sin \pi p$, which is the curve (4.13): *the spectral curve of section 4 is the complex electric field of the extremal potential.*

Proof. We compute the boundary values of p, integrate them, and prove uniqueness by a barrier argument; one identity between two integrals makes the constant on the edges vanish.

(a) The function p. The principal branch $\operatorname{arcsinh} w = \log(w + \sqrt{1+w^2})$ is the inverse of sinh on the strip $|\operatorname{Im} \zeta| < \frac{\pi}{2}$; it is holomorphic on $\mathbb{C} \setminus \pm i[1, \infty)$. For $b = x + iy \in \mathbb{S}$ the point $-i \sinh \pi b$ lies on a cut if and only if $\sinh \pi b = \sinh \pi x \cos \pi y + i \cosh \pi x \sin \pi y$ is real and of modulus at least one. Since $|y| < \frac{1}{2}$ this means $y = 0$ and $|\sinh \pi x| \geq 1$, that is, b real with $|b| \geq x_1^*$. So p is holomorphic on D, with $p(0) = 0$, $p(-b) = -p(b)$ and $p(\bar{b}) = -\overline{p(b)}$. Furthermore $|\operatorname{Im} p| < \frac{1}{2}$, and $\sinh \pi p = -i \sinh \pi b$ gives $\sinh^2(\pi \operatorname{Re} p) \leq |\sinh \pi p|^2 = \sinh^2 \pi x + \sin^2 \pi y \leq \cosh^2 \pi x$, hence $|\operatorname{Re} p(b)| \leq |\operatorname{Re} b| + 1$. The values on the axes and on the boundary are

$$p(x) = -\tfrac{i}{\pi} \operatorname{arcsin}(\sinh \pi x) \quad (|x| < x_1^*), \qquad p(iy) = \tfrac{1}{\pi} \operatorname{arcsinh}(\sin \pi y), \quad p(\pm\tfrac{i}{2}) = \pm x_1^*,$$
$$p(x \pm \tfrac{i}{2}) = \pm\tfrac{1}{\pi} \operatorname{arcsinh}(\cosh \pi x), \qquad p(x \pm i0) = \pm\tfrac{1}{\pi} \operatorname{arccosh}(\sinh \pi x) - \tfrac{i}{2} \quad (x > x_1^*).$$

The first three hold because $-i \sinh \pi b$ equals $-i \sinh \pi x$, $\sin \pi y$ and $\pm \cosh \pi x$ at these points. For the last, $-i \sinh \pi(x \pm i\epsilon)$ tends to the point $-i \sinh \pi x$ of the lower cut from the right and from the left, and $\operatorname{arcsinh}(\pm\eta - i\sigma) \to \pm \operatorname{arccosh} \sigma - \frac{i\pi}{2}$ as $\eta \downarrow 0$, for $\sigma > 1$. On the left slit the values follow from $p(-b) = -p(b)$. In particular $\operatorname{Im} p = 0$ on $E_\pm$, $\operatorname{Im} p = -\frac{1}{2}$ on both lips of the right slit and $\operatorname{Im} p = +\frac{1}{2}$ on both lips of the left slit; $\operatorname{Re} p(x + i0) = \frac{1}{\pi} \operatorname{arccosh}(\sinh \pi |x|)$ on the upper lips of both slits; and p extends continuously to the edges, the lips and the tips.

(b) The function U. Since D is simply connected, $\int_0^b p$ is a holomorphic function on D, so U is harmonic, and

$$\mathrm{d}U = \frac{4\pi}{3} \operatorname{Im}(p\,\mathrm{d}b) = \frac{4\pi}{3}(\operatorname{Im} p\,\mathrm{d}x + \operatorname{Re} p\,\mathrm{d}y). \tag{6.19}$$

The symmetries of p give $U(-b) = U(b) = U(\bar{b})$, and U is continuous up to the edges, the lips and the tips because p is. Along the real axis, $\mathrm{d}U = -\frac{4}{3} \operatorname{arcsin}(\sinh \pi s)\,\mathrm{d}s$ for $0 \leq s \leq x_1^*$; this

is the first formula in (6.18), and $U(x_1^*) = -L(x_1^*)$ by the choice of U_0. Along the lips of the right slit, $\mathrm{d}U = -\frac{2\pi}{3}\,\mathrm{d}x = -\mathrm{d}L$; hence $U = -L$ there, and on the left slit by symmetry. Along the imaginary axis, $\mathrm{d}U = \frac{4}{3}\operatorname{arcsinh}(\sin \pi s)\,\mathrm{d}s$, which is the second formula. Along E_+, $\mathrm{d}U = 0$, so U is constant there and equal to $U(\frac{i}{2})$; by $U(\bar{b}) = U(b)$ it takes the same constant on E_-. Integrating (6.19) from 0 to $i \operatorname{Im} b$ and then horizontally to b, with $|\operatorname{Re} p(is)| \le x_1^*$ and $|\operatorname{Im} p| \le \frac{1}{2}$, gives $|U(b)| \le \frac{2\pi}{3}|\operatorname{Re} b| + C$.

(c) The key identity. Substituting $u = \sinh \pi s$ in the first integral and $u = \sin \pi s$ in the second,

$$\begin{aligned}\int_0^{x_1^*} \arcsin(\sinh \pi s)\,\mathrm{d}s + \int_0^{1/2} \operatorname{arcsinh}(\sin \pi s)\,\mathrm{d}s &= \frac{1}{\pi}\int_0^1 \Big[\frac{\arcsin u}{\sqrt{1+u^2}} + \frac{\operatorname{arcsinh} u}{\sqrt{1-u^2}}\Big]\mathrm{d}u \\ &= \frac{1}{\pi}\Big[\arcsin u \operatorname{arcsinh} u\Big]_0^1 = \tfrac{1}{2}\operatorname{arcsinh} 1.\end{aligned} \tag{6.20}$$

By (6.17) and (6.18), $U(\frac{i}{2}) = -\frac{2\pi}{3}x_1^* + \frac{4}{3}\cdot\frac{1}{2}\operatorname{arcsinh} 1 = 0$, because $\pi x_1^* = \operatorname{arcsinh} 1$. So $U = 0$ on $E_\pm$. This is the place where the number $\operatorname{arcsinh}(1)/\pi$ enters the rigorous argument.

(d) Uniqueness. Let d be harmonic on D and continuous up to the edges, the lips and the tips, with boundary value 0 there, and let $|d(b)| \le C_d(1 + |\operatorname{Re} b|)$. We claim that $d \equiv 0$. For $\epsilon > 0$ let $d_\epsilon(b) := d(b) - \epsilon \cosh(2 \operatorname{Re} b)\cos(2 \operatorname{Im} b)$, which is harmonic on D. The subtracted term (the barrier) is positive on $\bar{\mathbb{S}}$, where $\cos(2 \operatorname{Im} b) \ge \cos 1 > 0$, so $d_\epsilon \le 0$ at the edges, the lips and the tips. On the cross-cuts $\{|\operatorname{Re} b| = X\} \cap D$ we have $d_\epsilon \le C_d(1+X) - \epsilon \cos 1 \cosh 2X < 0$ as soon as $X \ge X(\epsilon)$. The maximum principle on the bounded domains $D \cap \{|\operatorname{Re} b| < X\}$ gives $d_\epsilon \le 0$ on D. Letting $\epsilon \to 0$ we get $d \le 0$, and the same argument for $-d$ gives $d \equiv 0$. Applied to the difference of two solutions, this shows that (6.14) with $s = x_1^*$ has at most one solution. By (b) and (c), U is a solution, and so is the Poisson integral $-\int L\,\mathrm{d}\omega_b$ over the slits, by Lemma C.1(c) (appendix C.4). Hence both are equal to $U_{x_1^*}$, which is (C.15). □

Definition 6.6 (The zero law)**.** Extended across the slits by its boundary value $-L$, the function U is continuous on $\mathbb{S}$. By (6.19) its normal derivative $\partial_y U = \frac{4\pi}{3}\operatorname{Re} p$ jumps across the slits by $\frac{8}{3}\operatorname{arccosh}(\sinh \pi|x|) > 0$, so $\nabla^2 U \ge 0$ in the sense of distributions (by Green's formula on the two half-strips; ∇U is locally bounded up to the slits and the tips, because p extends continuously to them, see part (a) of the proof of Lemma 6.5): U is subharmonic on $\mathbb{S}$, with a charge density that lives on the slits. For $|x| \ge x_1^*$ this density is

$$\rho_U(x) := \frac{1}{2\pi}\Big[\partial_y U(x + i0) - \partial_y U(x - i0)\Big] = \frac{4}{3}\operatorname{Re} p(x + i0) = \frac{4}{3\pi}\operatorname{arccosh}\big(\sinh \pi|x|\big), \tag{6.21}$$

and we call it the *zero law*. Its counting function is

$$N(x) := \tfrac{1}{2}\int_{x_1^*}^{x} \rho_U(x')\,\mathrm{d}x' \simeq \kappa_{\mathrm{tip}}\,(x - x_1^*)^{3/2} \quad (x \downarrow x_1^*), \qquad \kappa_{\mathrm{tip}} = \frac{4 \cdot 2^{3/4}}{9\sqrt{\pi}} = 0.4217111. \tag{6.22}$$

In the units of u_g, see (6.10), ρ_U is a number of zeros per unit x and per unit c', counted with multiplicity. The function N counts *sites*: each site of section 7 carries two zeros, hence the factor $\frac{1}{2}$. The density (6.21) is the function (4.16) of Part II, and the asymptote in (6.22) follows from $\operatorname{arccosh}(\sinh \pi x) \simeq \big(2\sqrt{2}\,\pi(x - x_1^*)\big)^{1/2}$. The zero law is used in section 7 as a blueprint: the zeros of the functional constructed there are placed according to N; and in section 10 as a necessity: the zeros of every near-optimal functional follow it. The potential U, the law ρ_U and N are drawn in figure 6.

6.7 The Cardy deficit and the proof of Theorem 3

On the lobe interval the extremal potential lies strictly below the Cardy line, and the distance between the two is what Theorem 3 exponentiates.

Lemma 6.7 (Deficit; proved)**.** *For* $|x| < x_1^*$,

$$U(x) + L(x) = -\frac{4}{3}\int_{|x|}^{x_1^*} \Big[\frac{\pi}{2} - \arcsin(\sinh \pi s)\Big] \mathrm{d}s < 0. \tag{6.23}$$

The function $U + L$ *is even and increases on* $[0, x_1^*]$ *from* U_0 *to* 0*. Hence, for* $0 < \delta \le x_1^*$*, the Cardy deficit*

$$\kappa(\delta) := -\max_{|x| \le x_1^* - \delta} (U + L)(x) = -(U + L)(x_1^* - \delta) = \frac{4}{3}\int_{x_1^* - \delta}^{x_1^*} \Big[\frac{\pi}{2} - \arcsin(\sinh \pi s)\Big] \mathrm{d}s \tag{6.24}$$

is positive. The integrand is $\simeq \big(2\sqrt{2}\,\pi(x_1^* - s)\big)^{1/2}$ *as* $s \uparrow x_1^*$*, so that* $\kappa(\delta) = \frac{8}{9}\sqrt{2\sqrt{2}\,\pi}\;\delta^{3/2}(1 + O(\delta)) = 2.650\,\delta^{3/2}(1 + O(\delta))$*, with the values* $\kappa(\delta) = 0.0026,\ 0.029,\ 0.083,\ 0.23$ *at* $\delta = 0.01,\ 0.05,\ 0.1,\ 0.2$*, and* $\kappa(x_1^*) = -U_0 = 0.389$*. Moreover* $\kappa(\delta) \ge 2.228\,\delta^{3/2}$ *for* $0 < \delta \le x_1^*$*.*

Proof. By (6.18) and $U(x_1^*) = -L(x_1^*)$ we have $U(x) = -L(x_1^*) + \frac{4}{3}\int_{|x|}^{x_1^*} \arcsin(\sinh \pi s)\,\mathrm{d}s$, and $L(x_1^*) - L(x) = \frac{4}{3}\int_{|x|}^{x_1^*} \frac{\pi}{2}\,\mathrm{d}s$; this is (6.23). The integrand is positive for $s < x_1^*$, where $\sinh \pi s < 1$, which gives the sign and the monotonicity. Near the tip, $\sinh \pi(x_1^* - u) = 1 - \sqrt{2}\,\pi u + O(u^2)$ because $\cosh \pi x_1^* = \sqrt{2}$, and $\frac{\pi}{2} - \arcsin(1 - \varepsilon) = \sqrt{2\varepsilon}\,(1 + O(\varepsilon))$. The last inequality is proved in appendix C.5, (C.17), with the constant $\frac{8}{9}\sqrt{2\pi} = 2.228\ldots$ □

The exponent $\frac{3}{2}$ is the Airy exponent of a soft edge, which appeared in section 4.6; the coefficient is $2\pi\kappa_{\mathrm{tip}}$. By Proposition 6.4, $e^{c'(U+L)(x)}$ is, up to a power of c', the largest value that $|g|\,V/M[g]$ can take at $t = c'x^2/3$. Below the BTZ threshold $U(iy)$ increases from U_0 at $y = 0$ to 0 at the vacuum, by (6.18) and (6.20).

Proof of Theorem 3. The integrand $|g|\,V$ is at most majorant times weight, and the integral is at most the supremum of the integrand times the length of the interval. We use Proposition 6.4 on the compact set $Q = [-(x_1^* - \delta), x_1^* - \delta]$, in the form (C.16), in which the power of c' and the dependence on the distance to the tip are explicit.

There is nothing to prove for $g \equiv 0$. Let $0 < \delta < x_1^*$ and $t_\delta := c'(x_1^* - \delta)^2/3 \le \xi_1^* c'$. For $0 < t \le t_\delta$ the point $x = \sqrt{3t/c'}$ has $x_1^* - |x| \ge \delta$, and $U_{x_1^*} = U$ by Lemma 6.5, so (C.16) reads $|g(t)| = |G(x)| \le e^C \delta^{-5} c'^3\, e^{c'U(x)} M[g]$. The weight obeys $V(t) \le \frac{4\pi^2 t}{a}\, e^{c'L(x)}$ for all $t > 0$ (Lemma B.2(d)). With $(U + L)(x) \le -\kappa(\delta)$ from Lemma 6.7,

$$|g(t)|\,V(t) \le e^C \delta^{-5}\, c'^3\, \frac{4\pi^2 t}{a}\, e^{c'(U+L)(x)} M[g] \le e^C \delta^{-5}\, c'^3\, \frac{4\pi^2 t}{a}\, e^{-\kappa(\delta)c'} M[g] \qquad (0 < t \le t_\delta). \tag{6.25}$$

Since $\int_0^{t_\delta} \frac{4\pi^2 t}{a}\,\mathrm{d}t = 2\pi^2 t_\delta^2/a \le 24\pi^2(\xi_1^*)^2 c'$, integration gives (6.1) with $C_\delta = C_{\mathrm{conc}}\,\delta^{-5}$ and $C_{\mathrm{conc}} := 24\pi^2(\xi_1^*)^2 e^C$. The properties (6.2) of $\kappa(\delta)$ are part of Lemma 6.7. □

Of the four powers of c', the edges and the slits cost at most two between them (Lemma 6.1, Lemma B.2(e); their weights in the Poisson–Jensen mean add up to one), stated as three in (C.16), and $t_\delta^2/a \le Cc'$ gives one more. The window of width $O(1/c')$ at the BTZ threshold enters only through Lemma B.3, in the edge bound, because Lemma B.2(d) holds down to $t = 0$.

What this says about section 4. The composition of p with the map of Lemma 6.3 is the function $p(z)$ of (4.11), and $\sinh \pi b = i \sinh \pi p$. The curve has thus been recovered without hypotheses, as the solution of the linear boundary-value problem (6.14). In section 4 it rests on a selection rule and describes the best functional, conjecturally; here it bounds every functional. [NUMERICAL] The profiles u_g of the numerical optima of section 5 exceed U nowhere by more than $O(1/c')$, and at the threshold they approach it from below: at $(c, P) = (64, 256)$, $(128, 2048)$, $(256, 2048)$, $(512, 2688)$ the difference $U - u_g$ at $b = 0$ is 0.053, 0.035, 0.022, 0.013 (figure 6). The majorant is approached at leading order by the numerical optima. Whether it is *provably* attained is the subject of Part IV.

6.8 The effective rate

We prove (6.3). The idea is to let δ tend to zero with c in Theorem 3, as slowly as the prefactor allows. For this one needs the dependence of C_δ on δ. Its only source is the entropy of harmonic measure seen from a real point at distance δ from a tip, which is at most $C_H + 5\log\frac{1}{\delta}$ by Lemma C.2(ii); exponentiated, this is $C_\delta \le C_{\mathrm{conc}}\,\delta^{-5}$, as the proof of Theorem 3 shows. Everything else is uniform in δ.

Proof of the second statement of Theorem 4. Let $g \in \bar{\mathcal{A}}$, $g \not\equiv 0$, be weakly feasible and $t_1 = t_1(g)$. Let $\kappa_0 := \frac{8}{9}\sqrt{2\pi} = 2.228\ldots$ be the constant of (C.17) and $\lambda_0 := 3.6$, so that $\kappa_0\lambda_0 > 8$, and let

$$\delta := \Big(\frac{\lambda_0 \log c'}{c'}\Big)^{2/3}, \qquad \text{so that} \qquad \kappa(\delta)\,c' \ge \kappa_0\,\delta^{3/2}c' = \kappa_0\lambda_0 \log c' > 8\log c' \tag{6.26}$$

by Lemma 6.7, provided $\delta < x_1^*$; this holds for $c' \ge 115$. As before let $t_\delta = c'(x_1^* - \delta)^2/3$, and suppose that $t_1 \le t_\delta$. The half-mass condition (2.16) and Theorem 3 with $C_\delta \le C_{\mathrm{conc}}\,\delta^{-5}$ give

$$\tfrac{1}{2} \le C_{\mathrm{conc}}\,\delta^{-5}c'^4 e^{-\kappa(\delta)c'} < C_{\mathrm{conc}}\,\delta^{-5}c'^{-4} \le C_{\mathrm{conc}}\,c'^{10/3-4} = C_{\mathrm{conc}}\,c'^{-2/3},$$

where we used $\delta^{-5} = (c'/\lambda_0\log c')^{10/3} \le c'^{10/3}$, valid because $\lambda_0\log c' \ge 1$. This is false for $c' \ge (2C_{\mathrm{conc}})^{3/2}$. Hence for $c \ge c_0^{\mathrm{opt}} := \max\{116,\, 1 + (2C_{\mathrm{conc}})^{3/2}\}$ we have $t_1 > t_\delta$, and

$$t_1 > \frac{c'}{3}(x_1^* - \delta)^2 \ge \xi_1^* c' - \frac{2}{3}\,x_1^*\,\delta\,c' = \xi_1^* c' - \frac{2}{3}\,x_1^*\lambda_0^{2/3}\,c'^{1/3}\log^{2/3} c', \qquad \frac{2}{3}\,x_1^*\lambda_0^{2/3} = 0.4393 \le 0.44.$$

□

The constant C_{conc}, and with it c_0^{opt}, is a product of the absolute constants of appendices B and C; it is explicit in principle, and we have not computed it. The theorem says that no weakly feasible functional undercuts $\xi_1^* c'$ by more than $O(c'^{1/3}\log^{2/3} c')$, while Conjecture 1(a) says that the best functional overshoots it by an amount of order $c^{1/3}$. The logarithm comes from the polynomial prefactor in (6.1) and is presumably not sharp.

Part IV Attainment

Section 7 is proved with computer assistance, and sections 8 and 10 are proved. Sections 7 and 8 use section 2 and, from section 6, in the proofs only Lemma 6.5 and Definition 6.6, the closed form of U and the zero law; section 10 uses in addition Proposition 6.4 and Lemma 6.7. Section 7 builds a feasible $g \in \bar{\mathcal{A}}$ at $\xi_1^* c' + O(c'^{1/3})$; section 8 shows that any feasible $g \in \bar{\mathcal{A}}$ bounds every CFT. Section 9 describes a second functional that attains the slope, at a physicist's level of rigor; nothing else depends on it. Section 10 shows that a functional that comes close to the bound has no choice: its zeros follow the zero law on which the functional of section 7 is built.

7 Attainment: an explicit functional reaching Λ_V

We construct, for every large central charge, one explicit function $g \in \bar{\mathcal{A}}$ that is feasible at $\xi_1^* c' + O(c'^{1/3})$. With Theorem 4 this proves the slope, Theorem 1. The function is an infinite product of elementary factors, and its zeros are placed according to the zero law of Definition 6.6. The construction is short (sections 7.1 and 7.2). The work is to prove that the product and its Fourier transform combine to a function that is positive on the band and has a positive vacuum value. Section 7.3 explains how this is done, without proofs. The proofs are in sections 7.4 to 7.10, and the long ones in appendices D to G, which may be skipped at first. The inequalities verified by computer are marked ⟨cert⟩ and listed in table 4 of appendix H.

7.1 Image charges on the strip, and the zero law as a blueprint

The idea is electrostatic. A zero of a holomorphic function is a unit charge for the logarithm of its modulus, and by Proposition 6.4 the profile u_g of every functional, (6.13), lies below the potential U of a definite charge distribution on the strip $\mathbb{S}$, up to $O(\log c'/c')$. To certify the gap bound x_1^*, the profile must touch the Cardy line $-L$ where U does. This suggests building a functional whose profile *is* U: charges on the slits at density ρ_U, and on the edges a modulus no larger than Lemma 6.1 allows. (Theorem 7 shows that the profile of every attaining sequence is U.) So we want zeros at density $c'\rho_U$ on the band and modulus one on the edges, and we build them out of the potential of one point charge between two grounded plates.

Glossary. A *site* χ_n is a point of the real b-axis at which a zero, or a conjugate pair of zeros, is placed, and *cell* n is the interval (χ_n, χ_{n+1}). The *comb* is the product B of image-charge factors over the sites. *Detuning* means moving a real double zero to a conjugate pair $\chi_n \pm i\varepsilon_n$. The *onset* is the neighborhood of the first kept site χ_2; the comb omits the first site of the law (section 7.2). The *Airy length* $\ell_c = (\kappa_{\text{tip}}c')^{-2/3}$ is the scale of the spacing of the first sites, and the *hand-off point* $x_I = x_1^* + c'^{-\theta_{\text{on}}}$, with $\theta_{\text{on}} = 0.2$, is where the onset (Region I) ends and steepest descent takes over (Region II). Four functions that are defined in sections 7.5 and 7.6 appear already in section 7.3: the *site index* $\nu(x)$, which equals $k-2$ at the site χ_k, with the comb phase $\Psi = 2\pi\nu - \pi$; the *envelope* Env of the undetuned comb; the *level* Lev, the explicit unit of all ratios; and the *amplitude* Amp of the transform.

Toolkit: image charges on the strip

One factor. For ζ with $|\operatorname{Im}\zeta| < \frac{1}{2}$ let

$$T_\zeta(b) := \tanh\frac{\pi(b-\zeta)}{2}\,\tanh\frac{\pi(b+\zeta)}{2} = \frac{\cosh\pi b - \cosh\pi\zeta}{\cosh\pi b + \cosh\pi\zeta}. \tag{7.1}$$

For real ζ, $-\log|T_\zeta(b)|$ is the Green's function of the strip with poles at $\pm\zeta$: the potential at b of unit charges at $\pm\zeta$ between the two grounded plates $E_\pm$. The zeros and poles of T_ζ are the successive mirror images of $\pm\zeta$ in the plates (figure 7a). The map $w = \tanh\frac{\pi b}{2}$ takes $\mathbb{S}$ onto the unit disk and turns T_ζ into a product of two Blaschke factors [64]; T_ζ is the *Blaschke factor of the strip*. We use four facts.

(T1) *Modulus.* For real ζ, $|T_\zeta| = 1$ on both edges and $|T_\zeta| < 1$ in $\mathbb{S}$. The same holds for the product $T_\zeta T_{\bar\zeta}$ of a conjugate pair, $\zeta = \chi + i\varepsilon$ with $0 < \varepsilon < \frac{1}{2}$. A bounded holomorphic function on $\mathbb{S}$ whose modulus is one on the edges is called *inner*; a zero-free factor such as $\operatorname{sech}^2\frac{\pi b}{2}$, which is determined by its modulus on the edges, is *outer*.

(T2) *Pairs on the real axis.* For real χ, $0 \le \varepsilon < \frac{1}{2}$ and real x,

$$T_{\chi+i\varepsilon}(x)\,T_{\chi-i\varepsilon}(x) = \prod_{\pm}\frac{\cosh\pi(x\mp\chi) - \cos\pi\varepsilon}{\cosh\pi(x\mp\chi) + \cos\pi\varepsilon} \;\ge\; T_\chi(x)^2,$$

and the left side is positive if $\varepsilon > 0$: lifting a double zero off the axis raises the modulus on the axis.

(T3) *Reflection.* $T_\zeta(b+i) = 1/T_\zeta(b)$, and $T_\zeta(\frac{i}{2}) = -1$ for every ζ.

(T4) *Zeros and poles.* For $\operatorname{Re}\zeta \neq 0$, T_ζ has simple zeros at $\{\pm\zeta\} + 2i\mathbb{Z}$, simple poles at $\{\pm\zeta\} + i(2\mathbb{Z}+1)$, and no others.

All four follow from (7.1). For (T1) note that $\cosh\pi b$ is imaginary on $E_\pm$, so that numerator and denominator have the same modulus when $\cosh\pi\zeta$ is real, and numerator and denominator of the pair are conjugate to each other in general; the maximum principle gives the inequality inside.

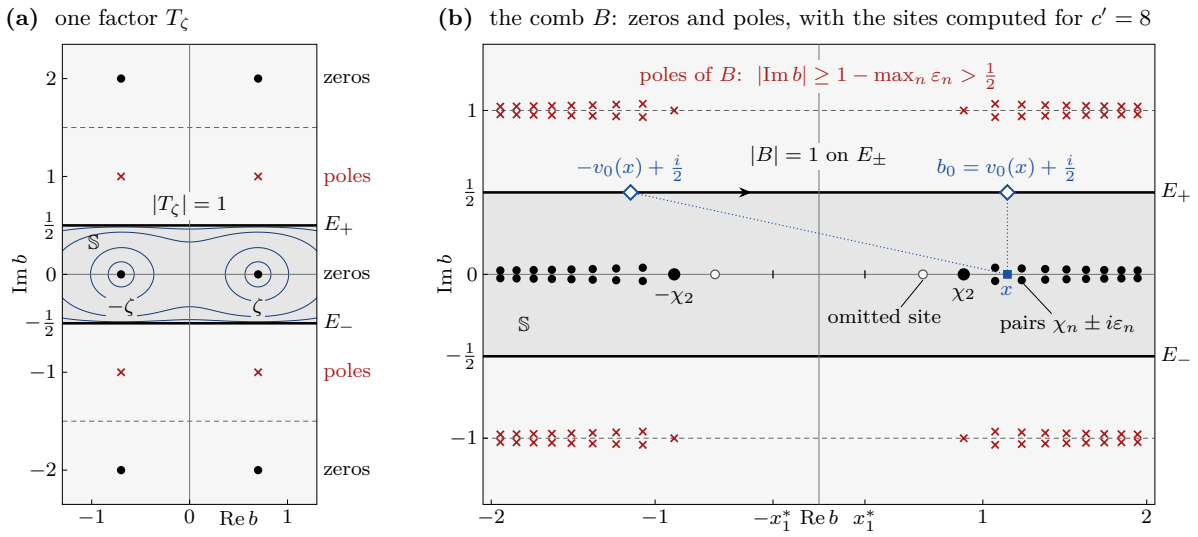


Figure 7: Image charges on the strip. (a) One factor $T_\zeta(b) = \tanh\frac{\pi(b-\zeta)}{2}\tanh\frac{\pi(b+\zeta)}{2}$, here with $\zeta = 0.70$: zeros at $\pm\zeta + 2i\mathbb{Z}$ (dots) and poles at $\pm\zeta + i(2\mathbb{Z}+1)$ (crosses), which are the successive images of $\pm\zeta$ in the edges $E_\pm$ (dashed lines: the image edges $\mathrm{Im}\, b = \pm\frac{3}{2}$), so that $|T_\zeta| = 1$ on $E_\pm$; the curves inside $\mathbb{S}$ are the level curves $|T_\zeta| = 0.2, 0.45, 0.8, 0.95$. (b) The zeros and poles of the comb B of section 7.2. The sites χ_n, $c'N(\chi_n) = n - \frac{1}{4}$, are computed for $c' = 8$, a value chosen only to make the pairs visible: the simple zero at $\pm\chi_2$, the pairs $\pm\chi_n \pm i\varepsilon_n$ ($n \geq 3$) with $\varepsilon_n = \frac{1}{4}(\chi_{n+1} - \chi_n)$, and the omitted first site of the law (open circle). All poles lie in $|\mathrm{Im}\, b| \geq 1 - \max_n \varepsilon_n > \frac{1}{2}$, and $|B| = 1$ on $E_\pm$. Diamonds mark the saddle points $b_0 = \pm v_0(x) + \frac{i}{2}$ of the edge integral for the band point x (square), as in figure 2.

The next lemma says that the zero law is the right density for these factors. It is the continuum limit of every sum over sites in this section.

Lemma 7.1 (Riesz representation of U; proved)**.** *For every b in the closed strip $\bar{\mathbb{S}}$,*

$$\int_{x_1^*}^{\infty} \rho_U(x')\, \log|T_{x'}(b)|\, \mathrm{d}x' = U(b), \tag{7.2}$$

and the integral converges absolutely. In particular the left side vanishes on $E_\pm$ and equals $-L(x)$ at real $b = x$ with $|x| \geq x_1^*$.

The proof is in appendix D.1: both sides have the same charge on $\mathbb{S}$, both vanish on the edges, and both grow at most linearly; a potential with these three properties is unique. In words: a continuum of factors $T_{x'}$ at the density of the law reproduces the Cardy decay $e^{-c'L}$ on the band exactly, and is invisible in modulus on the edges.

Notation for the edge. On the edge E_+ we write $b = v + \frac{i}{2}$ with v real. The function p of Lemma 6.5 is real there, and we call

$$F(v) := p(v + \tfrac{i}{2}) = \frac{1}{\pi}\,\mathrm{arcsinh}(\cosh \pi v), \qquad \cosh \pi v_0(x) = \sinh \pi x, \qquad \rho_U(x) = \tfrac{4}{3}\, v_0(x), \tag{7.3}$$

the *edge function*. It is even, convex, and increasing on $[0, \infty)$, with $F(0) = x_1^*$ and $0 < F' < 1$ on $(0, \infty)$. Its inverse $v_0 \colon [x_1^*, \infty) \to [0, \infty)$, $F(v_0(x)) = x$, is given by the second formula, and the third is (6.21): up to the factor $\frac{4}{3}$, the zero law is the inverse of the edge function. We write $b_0(x) := v_0(x) + \frac{i}{2}$ for the point of the edge that corresponds to the band point x.

7.2 The functional and the theorem

The functional is the zero law made discrete. The sites are the quantiles of the counting function N: the points $\chi_n > x_1^*$ with $c'N(\chi_n) = n - \frac{1}{4}$, for $n = 2, 3, \ldots$; the site $n = 1$ of the law is

omitted. At χ_2 we place a simple real zero. Every later site is lifted into a conjugate pair $\chi_n \pm i\varepsilon_n$ with $\varepsilon_n := \eta_0(\chi_{n+1} - \chi_n)$ and $\eta_0 = \frac{1}{4}$. We multiply by an outer factor, which makes the product integrable, and antisymmetrize under the Fourier transform:

$$h_0(b) := \operatorname{sech}^2 \frac{\pi b}{2}\, B(b), \qquad B := T_{\chi_2} \prod_{n\geq 3} T_{\chi_n + i\varepsilon_n}\, T_{\chi_n - i\varepsilon_n}, \qquad g := \tfrac{1}{2}(h_0 - \hat{h}_0). \tag{7.4}$$

Here h_0 is even in b and is read as a function of $t = c'b^2/3$; for $-a \leq t < 0$ the point b lies on the imaginary axis. The hat is the transform (2.9). We also need the *undetuned comb* $B^0 := T_{\chi_2} \prod_{n\geq 3} T_{\chi_n}^2$, which has double zeros at the sites $n \geq 3$, and $h_0^0 := \operatorname{sech}^2 \frac{\pi b}{2}\, B^0$. The zeros and poles of B are drawn in figure 7(b).

Theorem 5 (Attainment; proved, computer-assisted)**.** *There is a central charge $c_0^{\mathrm{att}} \geq 40$, explicit in principle but not computed, such that for every $c \geq c_0^{\mathrm{att}}$ the function g of (7.4) has the following properties.*

(i) $g \in \bar{\mathcal{A}}$.

(ii) $g(t) > 0$ *for all* $t \geq t_\star + 1$, *where*

$$t_\star := \frac{c'\chi_2^2}{3} = \xi_1^* c' + A_1\, c'^{1/3}(1 + O(c'^{-2/3})), \qquad A_1 = \tfrac{2}{3}\, x_1^*\, \kappa_{\mathrm{tip}}^{-2/3} \big(\tfrac{7}{4}\big)^{2/3} = 0.483. \tag{7.5}$$

(iii) $g_{\mathrm{vac}} > 0$.

Hence g is feasible at $t_\star + 1$ in the sense of Definition 2.3, so that $T_V(c) \leq \xi_1^* c' + A_1\, c'^{1/3} + O(1)$; with Theorem 4 this proves Theorem 1. Moreover $|g(t)| \leq C(c)\, e^{-c'L(x)} e^{-\pi x}$ for $t = c'x^2/3 \geq 0$: both h_0 and $\hat{h}_0$ decay faster than the inverse of the Cardy weight.

In words: a product of image-charge factors at the quantiles of the zero law, minus its own Fourier transform, is a functional that certifies a gap within $O(c^{1/3})$ of c/Λ_V. The offset $+1$ is cosmetic: the proof gives $g > 0$ already from $t_\star + o(1/c')$ on (section 7.8). The next proposition collects what is elementary about h_0.

Proposition 7.2 (Elementary properties; proved)**.** *Let $c \geq 40$, the standing assumption of section 2.6. Then $\max_n \varepsilon_n < \frac{1}{2}$, the product B converges locally uniformly on $|\operatorname{Im} b| < 1 - \max_n \varepsilon_n$, and:*

(a) $|B| \leq 1$ *on* $\bar{\mathbb{S}}$ *and* $|B| = 1$ *on* $E_\pm$.

(b) $B(\frac{i}{2}) = -1$. *Hence $h_0(t_0) = -2$ at the vacuum, and the second difference $h_{0,\mathrm{vac}} := h_0(t_0) - 2h_0(t_0+1) + h_0(t_0+2)$ satisfies $|h_{0,\mathrm{vac}}| \leq 8$.*

(c) *On the physical axis, $h_0 < 0$ on the lobe interval $[0, t_\star)$, h_0 has a simple zero at $t_\star$, and $h_0 > 0$ for $t > t_\star$.*

(d) *On the edge, $|h_0(v + \frac{i}{2})| = 2/\cosh \pi v$ exactly.*

On the edge through the vacuum the comb is invisible in modulus, and all the information that it carries is a phase.

Proof. First, $\max_n \varepsilon_n < \frac{1}{2}$; this places every pair under (T1) and keeps the poles of B out of $\bar{\mathbb{S}}$. By (7.3), $\rho_U' = \frac{4}{3}/F'(v_0) \geq \frac{4}{3}$ on (x_1^*, ∞), so that $\rho_U(y) \geq \frac{4}{3}(y - \chi_n)$ for $y \geq \chi_n$. One cell carries the charge $1 = c'N(\chi_{n+1}) - c'N(\chi_n) = \frac{c'}{2}\int_{\chi_n}^{\chi_{n+1}} \rho_U \geq \frac{c'}{3}(\chi_{n+1} - \chi_n)^2$. Hence $\chi_{n+1} - \chi_n \leq (3/c')^{1/2} \leq 0.28$ and $\varepsilon_n \leq 0.07$ for $c' \geq 39$.

Everything else follows from (T1)–(T3) once the product converges. By (7.1), $-T_\zeta = 1 - 2\cosh \pi b/(\cosh \pi b + \cosh \pi \zeta)$, so a pair differs from 1 by $O(e^{\pi|\operatorname{Re} b|} e^{-\pi\chi_n})$ away from its poles, and $\sum_n e^{-\pi\chi_n} < \infty$ because the number of sites below x is at most $c'N(x) = O(c'x^2)$; by (T4) the poles lie at $|\operatorname{Im} b| \geq 1 - \max_n \varepsilon_n$. This gives the convergence. Part (a) is (T1) for each factor. For (b), (T3) gives $T_{\chi_2}(\frac{i}{2}) = -1$ and the value $(-1)^2$ for each pair, and $\operatorname{sech}^2 \frac{\pi i}{4} = 2$; on the segment

from the vacuum to the threshold $|\mathrm{sech}^2 \frac{\pi b}{2}| \le 2$ and $|B| \le 1$, so each of the three values in $h_{0,\mathrm{vac}}$ is at most 2 in modulus ($t_0 + 2 \le 0$ because $a \ge 2$). For (c), the pairs are positive on the real axis by (T2), and $T_{\chi_2}(x)$ is negative for $0 \le x < \chi_2$, vanishes to first order at χ_2 and is positive beyond. For (d), $|B| = 1$ on the edge and $\left|\cosh \frac{\pi}{2}(v + \frac{i}{2})\right|^2 = \frac{1}{2}(\cosh \pi v + \cos \frac{\pi}{2}) = \frac{1}{2} \cosh \pi v$. □

What is fixed. The construction has free parameters: the number $m \ge 1$ of omitted sites, the node phase k_∞ in $c' N(\chi_n) = n - k_\infty$, and the detuning η_0. Only the onset index $n_1 = m + 1 - k_\infty$ enters the coefficient of $c'^{1/3}$, which is $A_m = 0.3326\, n_1^{2/3}$. Indeed $N(x) \simeq \kappa_{\mathrm{tip}}(x - x_1^*)^{3/2}$ by (6.22), and $c' N(\chi_2) = n_1$, so that

$$\chi_2 - x_1^* \simeq \Big(\frac{n_1}{\kappa_{\mathrm{tip}} c'}\Big)^{2/3}, \qquad t_\star - \xi_1^* c' \simeq \tfrac{2}{3}\, x_1^*\, c'\, (\chi_2 - x_1^*), \qquad A_m = \tfrac{2}{3}\, x_1^*\, \kappa_{\mathrm{tip}}^{-2/3}\, n_1^{2/3}. \tag{7.6}$$

In this paper $(m, k_\infty, \eta_0) = (1, \frac{1}{4}, \frac{1}{4})$, so $n_1 = \frac{7}{4}$, and the outer factor is sech^2. Neither the constant 0.483 nor c_0^{att} is optimized, and nothing is claimed at finite c.

The remainder in (7.5) is obtained in the same way. Write $\chi_2 = x_1^* + \ell_c \varsigma_2$ with the Airy length ℓ_c, as in Lemma F.2(c). Then $t_\star = \xi_1^* c' + \frac{2}{3}\, x_1^*\, c' \ell_c\, \varsigma_2 + \frac{1}{3}\, c' \ell_c^2 \varsigma_2^2$. Here $c' \ell_c = \kappa_{\mathrm{tip}}^{-2/3} c'^{1/3}$, and $\varsigma_2 = (\frac{7}{4})^{2/3}(1 + O(\ell_c))$ by (F.12), and the last term is $O(c'^{-1/3})$. Since $\ell_c = O(c'^{-2/3})$, this is (7.5) with $A_1 = \frac{2}{3}\, x_1^*\, \kappa_{\mathrm{tip}}^{-2/3} (\frac{7}{4})^{2/3}$.

The threshold c_0^{att} is named before it is fixed. Throughout this section and appendices D to G, a statement made for $c \ge c_0^{\mathrm{att}}$, or for c large, holds for c above a threshold of its own, which may depend on a parameter that is named there (r in Lemma 7.5, ϵ in Proposition 7.4). The proof of Theorem 5 meets finitely many of these thresholds, each at a fixed value of its parameter; none of them depends on a later one, and c_0^{att} is the largest of them. It is fixed at the end of that proof, in section 7.10.

7.3 Idea of the proof

There are three things to prove: (i) $g > 0$ on the band $t \ge t_\star + 1$; (ii) $g_{\mathrm{vac}} > 0$; (iii) $g \in \bar{\mathcal{A}}$. The relation $\hat{g} = -g$ is automatic. Since $h_0 \ge 0$ on the band, everything in (i) reduces to one statement: $\hat{h}_0$ *is smaller than* h_0 *there*. Figure 8 shows this at $c = 256$. The function h_0 is a train of positive bumps, one per cell. Its transform oscillates in lock-step with it, with an amplitude of about $\frac{1}{2}$ in units of the level Lev; this amplitude is about 0.29 of the height of the bumps. The difference $2g = h_0 - \hat{h}_0$ stays positive.

How $\hat{h}_0$ is computed. The transform at a band point x is an integral of h_0 times a Hankel kernel along the *edge* E_+ of the strip (section 7.4; figure 2). On the edge $|h_0|$ is explicit and does not depend on the comb (Proposition 7.2(d)), and the kernel has modulus $e^{-c' L(x)}$. So the size of the integrand is pinned at the Cardy level, and the comb enters through a phase only. The phase has two stationary points $\pm v_0(x)$ on the edge, and they exist exactly when $x \ge x_1^*$: this is how the band appears in the transform.

Three regimes. Three scales organize the proof, $\ell_c \ll c'^{-\theta_{\mathrm{on}}} \ll c'^{-1/(4n_1)}$; they are drawn at the bottom of figure 8. In *Region II*, $x \ge x_I$ (sections 7.6 and 7.7), steepest descent gives $|\hat{h}_0| \le \mathrm{Amp}\,(1 + o(1))$ with an explicit amplitude $\mathrm{Amp} \le 0.504\,\mathrm{Lev}$, and the detuning gives a floor $h_0 \ge \mu\,\mathrm{Lev}$ with $\mu > 0.504$. Positivity is one inequality between explicit functions that does not involve c, and no information on the phase of $\hat{h}_0$ is used. In *Region I*, $\chi_2 \le x \le x_I$ (section 7.8), the two saddles coalesce and the asymptotics is not uniform. There we use only the crude bound $|\hat{h}_0| \le C\sqrt{c'}\, e^{-c' L}$, and the fact that near the onset the comb stands above the Cardy level by a power of c'. We call this the *overshoot*. It is there because the charge of the omitted site is missing from the comb. The two regions overlap, because the overshoot beats the

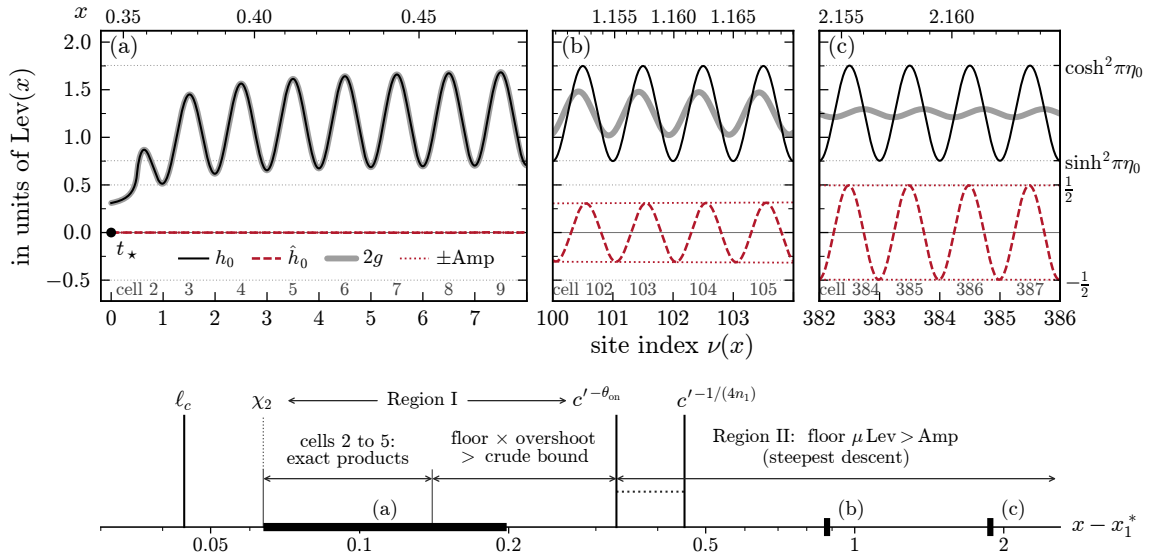


Figure 8: The functional of Theorem 5 at $c = 256$, with $(m, k_\infty, n_1, \eta_0) = (1, \frac{1}{4}, \frac{7}{4}, \frac{1}{4})$ and outer factor sech^2: the comb h_0 (thin), its transform $\hat{h}_0$ (dashed), and $2g = h_0 - \hat{h}_0$ (thick gray), all divided by the level $\mathrm{Lev}(x)$ and plotted against the site index $\nu(x)$, which is an integer at every site (top axes: x); dotted: $\pm\mathrm{Amp}/\mathrm{Lev}$. (a) The onset, cells 2–9, beginning at the simple zero χ_2 ($t = t_\star = 10.084$): the transform is below 0.4% of the level, so that $2g$ and h_0 coincide to the width of the line. (b) Cells 102–105. (c) Cells 384–387, deep in the band: h_0 oscillates between the floor $\sinh^2 \pi\eta_0$ and $\cosh^2 \pi\eta_0$, $\hat{h}_0$ between $\mp\frac{1}{2}$, in lock-step, one period per cell and maxima on maxima, so that $2g$ stays near $\frac{5}{4}$. Bottom: the three scales $\ell_c \ll c'^{-\theta_{\rm on}} \ll c'^{-1/(4n_1)}$ of the onset, at their values 0.044, 0.33, 0.45 for $c = 256$, on a logarithmic axis of $x - x_1^*$, with the inequality used on each stretch (the dotted segment continues the range on which the overshoot beats the crude bound) and the positions of the three panels.

crude bound up to $x - x_1^* \approx c'^{-1/(4n_1)}$, which is beyond x_I. For the *vacuum* (section 7.9), $g_{\rm vac}$ is the mass of the lobe minus the mass of the band, up to $O(1)$. Both are dominated by a window of width ℓ_c around the onset, and the band is at most a fixed fraction $R_{\rm vac} < 1$ of the lobe (Proposition 7.13). The computer enters as follows. Once the factors that tend to one as $c \to \infty$ are bounded by hand, each regime leaves inequalities that do not involve c, for explicit functions of one real variable: for the amplitude and the floor in Region II, for finite products over the first cells in Region I, and for a ratio of two integrals at the vacuum. These inequalities, marked $\langle$cert$\rangle$, are proved in interval arithmetic (appendix H.1); nothing that depends on c is computed.

Why each ingredient is there. *Sites at the quantiles of the law.* Besides the Cardy decay $|B| \approx e^{-c'L}$ on the band (Lemma 7.1), this makes the phase of the integrand on the edge stationary exactly at the points $\pm v_0(x)$ that correspond to band points x, where the phase of B advances by 2π per site (D.13).

Detuning by $\eta_0 = \frac{1}{4}$. The undetuned comb is $|h_0^0| = \mathrm{Env} \sin^2 \pi\nu$. It returns to zero in every cell, while its transform does not, so g would be negative near every site. Lifting the zeros off the axis creates a floor above $\frac{1}{2}\mathrm{Lev}$. It changes nothing on the edge, where a conjugate pair is still unimodular, so the amplitude of the transform is untouched. The value matters: for $\eta_0 = 0.2$ the floor of Lemma 7.9 is below 0.45, which is not enough.

Why the amplitude is $\frac{1}{2}$. Write $h_0^0 = \frac{1}{2}\mathrm{Env}\,(1 + \cos\Psi)$. The transform reproduces the oscillating part $\frac{1}{2}\mathrm{Env}\cos\Psi$. It cannot see the mean, which has no stationary phase.

The omitted site, $m = 1$. It makes the first zero simple. It produces the overshoot at the onset. And it makes the vacuum lopsided in favor of the lobe. It costs $A_1 c^{1/3}$ in the bound, and nothing at the order of the slope. With no site omitted and the same node phase one finds

numerically |Lobe|/Band ≈ 0.8 [NUMERICAL], and that comb is not feasible.

The node phase $\frac{1}{4}$. This is a convention and is not tuned. Placing nodes at the quantiles of an equilibrium density is a Bohr–Sommerfeld rule, familiar from the choice of interpolation nodes in the numerical bootstrap [66, Sec. 3.3]. Only $n_1 = \frac{7}{4}$ enters the certified constants. With $\frac{1}{4}$ the phase of the transform coincides with that of the comb deep in the band (figure 8c).

The outer factor sech^2 *and the simple zero at* χ_2. The outer factor gives integrability and membership in $\bar{\mathcal{A}}$, and it cancels from the ratio Amp/Lev up to the factor $\coth \frac{\pi x}{2}$. The zero is simple because a feasible g must change sign once, at t_1.

7.4 Three exact identities

Three identities turn the three claims into statements about h_0 alone.

Lemma 7.3 (Three identities; proved)**.** *Let* $\max_n \varepsilon_n < \frac{1}{2}$. *For* (a) *and* (b) *suppose in addition that* $\hat{h}_0$ *is continuous and that* $|h_0(t)| + |\hat{h}_0(t)| \le C(c)\, e^{-c'L(x)-\pi x}$ *for* $t = c'x^2/3 \ge 0$*; this is proved in section 7.10, from Lemma 7.5*(c)*, Lemma 7.10 and the bound* (7.25)*, which uses* (c) *but neither* (a) *nor* (b).

(a) $\hat{g} = -g$.

(b) *With the second difference* $h_{0,\mathrm{vac}}$ *of Proposition 7.2*(b)*,*

$$g_{\mathrm{vac}} = \frac{1}{2}\Big[h_{0,\mathrm{vac}} - 2\pi \int_0^\infty h_0\, V\, \mathrm{d}t\Big]. \tag{7.7}$$

(c) *For every* $x > 0$*, with* $k_x := \frac{4\pi}{3}c'x$*,*

$$\hat{h}_0(c'x^2/3) = \frac{2\pi c'}{3} \int_{E_+} h_0(b)\, H_0^{(1)}(k_x b)\, b\, \mathrm{d}b. \tag{7.8}$$

On the edge the Hankel function is, by (E.3) [67, (10.17.13)–(10.17.15)],

$$|H_0^{(1)}(k_x b)| = \Big(\frac{2}{\pi k_x |b|}\Big)^{1/2} e^{-c'L(x)}\, |1 + \varepsilon_H(k_x b)|, \qquad |\varepsilon_H(z)| \le \frac{0.33}{|z|} \quad (|z| \ge 1), \tag{7.9}$$

because $k_x \operatorname{Im} b = \frac{1}{2}k_x = c'L(x)$ there.

Proof. We prove (c) first; it uses only Proposition 7.2 and (T4).

(c). By (2.9), with $t = c'b^2/3$ and $s = c'x^2/3$ we have $4\pi\sqrt{st} = k_x b$ and $\mathrm{d}t = \frac{2c'}{3} b\, \mathrm{d}b$, so $\hat{h}_0(s) = \frac{4\pi c'}{3}\int_0^\infty h_0(b) J_0(k_x b)\, b\, \mathrm{d}b$. On the positive axis $J_0 = \frac{1}{2}(H_0^{(1)} + H_0^{(2)})$, and $H_0^{(2)}(z) = -H_0^{(1)}(ze^{i\pi})$ [67, (10.11.5)]. Since h_0 is even, the substitution $b \to -b$ in the term with $H_0^{(2)}$ gives $\hat{h}_0(s) = \frac{2\pi c'}{3}\int_{-\infty}^\infty \mathcal{I}(b)\, \mathrm{d}b$ with $\mathcal{I}(b) := h_0(b) H_0^{(1)}(k_x b)\, b$, the real axis being approached from above at $b = 0$, where $\mathcal{I} = O(|b| \log |b|)$. By (T4) the poles of B lie at $|\operatorname{Im} b| \ge 1 - \max_n \varepsilon_n > \frac{1}{2}$, and those of $\operatorname{sech}^2 \frac{\pi b}{2}$ at $|\operatorname{Im} b| = 1$, so $\mathcal{I}$ is analytic in $0 < \operatorname{Im} b < 1 - \max_n \varepsilon_n$. On $0 \le \operatorname{Im} b \le \frac{1}{2}$ we have $|B| \le 1$, $|\operatorname{sech}^2 \frac{\pi b}{2}| \le 4e^{-\pi|\operatorname{Re} b|}$ and $|H_0^{(1)}(k_x b)| \le C|k_x b|^{-1/2}$ for $|b| \ge 1$, so $\mathcal{I}$ decays exponentially as $|\operatorname{Re} b| \to \infty$, uniformly in the height. Cauchy's theorem moves the contour from $\mathbb{R}$ to E_+.

(a). By hypothesis h_0 and $\hat{h}_0$ are continuous and integrable on $[0, \infty)$, so Fourier inversion for radial functions on $\mathbb{R}^2$ gives $\hat{\hat{h}}_0 = h_0$, and $\hat{g} = \frac{1}{2}(\hat{h}_0 - h_0) = -g$.

(b). The idea is to continue Fourier inversion analytically in α, from $\alpha \le 0$ to $0 \le \alpha \le a$. By Lemma B.2(e), $K_a \le e^{c'L}$, so $\int_0^\infty (|h_0| + |\hat{h}_0|) K_a\, \mathrm{d}t < \infty$ by the hypothesis. As in the proof of Lemma B.1, the kernel bound (B.1) and dominated convergence then show that $\alpha \mapsto 2\pi \int_0^\infty \hat{h}_0 K_\alpha\, \mathrm{d}t$ is continuous on the parabolic region $\mathcal{D}_a$ of that lemma and holomorphic in its interior. For $\alpha = -s \le 0$ it equals $\hat{\hat{h}}_0(s) = h_0(s)$. The function $\alpha \mapsto h_0|_{t=-\alpha}$ has the same

regularity on $\mathcal{D}_a$, which is the image of $\bar{\mathbb{S}}$ under $\alpha = -c'b^2/3$. Two such functions that agree on $\alpha \le 0$ agree on $\mathcal{D}_a$. Since the values of g below the threshold are defined by the eigen-identity (2.14) (Definition 2.5), for $0 \le \alpha \le a$ we get $g(-\alpha) = -2\pi \int_0^\infty g K_\alpha \, \mathrm{d}t = \frac{1}{2}\big[h_0|_{t=-\alpha} - 2\pi \int_0^\infty h_0 K_\alpha \, \mathrm{d}t\big]$. The second difference in α at $a, a-1, a-2$, with $V = K_a - 2K_{a-1} + K_{a-2}$, is (7.7). □

7.5 The comb on the real axis: site index, envelope, level

On the band, $\log|B(x)|$ is a sum over the sites of the potentials $\log|T_{\chi_k}(x)|$. By Lemma 7.1 the integral which this sum approximates is $-c'L(x)$, corrected for the omitted charge. So h_0 is the Cardy decay, times the effect of the omitted charge, times a bounded function of the position of x in its cell. This subsection names these pieces and states two-sided bounds for them. The proofs are in appendix F. They use nothing about $\hat{h}_0$.

Site index and envelope. For real $a > \frac{1}{4}$ (as the index of a site, here and in appendices F and G, the letter a is a real number and not $c'/12$) let χ_a be the point with $c'N(\chi_a) = a - \frac{1}{4}$; the sites are the integer values of a. Let $\ell_n := \chi_{n+1} - \chi_n$ be the length of cell n, and for x in cell n let $u := (x - \chi_n)/\ell_n \in (0,1)$ be the position in the cell. The site index and the comb phase are

$$\nu(x) := c'N(x) + \tfrac{1}{4} - 2, \qquad \nu(\chi_a) = a - 2, \qquad \Psi(x) := 2\pi\nu(x) - \pi, \tag{7.10}$$

so that ν runs over $(n-2, n-1)$ on cell n. Beyond χ_2 the undetuned comb has its double zeros exactly where $\sin^2 \pi\nu$ has them. The envelope is therefore defined, for $x > \chi_2$, by

$$|h_0^0(x)| = \mathrm{Env}(x)\, \sin^2 \pi\nu(x) = \tfrac{1}{2}\,\mathrm{Env}(x)\,(1 + \cos\Psi(x)), \tag{7.11}$$

and is positive and smooth there. Off the sites, $h_0 = h_0^0\,\Pi$ with $\Pi := |B|/|B^0| \ge 1$ by (T2).

The absent charge, the end correction and the level. The comb lacks the charge which the law places on $[x_1^*, \chi_2]$. Its total weight is $c' \int_{x_1^*}^{\chi_2} \rho_U = 2n_1$, and its potential is

$$c'\mathcal{P}(x) := -c' \int_{x_1^*}^{\chi_2} \rho_U(x')\, \log|T_{x'}(x)|\, \mathrm{d}x' \;\ge 0. \tag{7.12}$$

By Lemma 7.1 the continuum over the range that is kept is $c' \int_{\chi_2}^\infty \rho_U \log|T_{x'}(x)|\, \mathrm{d}x' = -c'L(x) + c'\mathcal{P}(x)$ for $x \ge x_1^*$. The factor $e^{c'\mathcal{P}}$ is the overshoot of section 7.3. We write $\mathcal{P}_Y$ for (7.12) with χ_2 replaced by Y. The simple zero at χ_2 stands for the half cell of continuum between χ_2 and $\chi_{5/2}$. The difference is the *end correction*

$$\mathcal{J}_{\mathrm{end}}(x) := \log|T_{\chi_2}(x)| - 2\int_2^{5/2} \log|T_{\chi_a}(x)|\, \mathrm{d}a, \qquad 0 \le \mathcal{J}_{\mathrm{end}}(x) \le C_J \quad (x \ge \chi_3), \tag{7.13}$$

with an absolute constant $C_J \le 0.65$ (Lemma F.8). The *level* is

$$\mathrm{Lev}(x) := 4\,\mathrm{sech}^2\,\frac{\pi x}{2}\; e^{-c'L(x)}\, e^{c'\mathcal{P}(x) + \mathcal{J}_{\mathrm{end}}(x)}, \qquad \frac{h_0}{\mathrm{Lev}} = \tfrac{1}{4}\,|B|\, e^{c'L - c'\mathcal{P} - \mathcal{J}_{\mathrm{end}}} \quad (x > \chi_2). \tag{7.14}$$

The level is explicit, it is smooth on the cells $n \ge 3$, and it does not oscillate. The factor 4 makes Env/Lev close to one. The end correction is put inside the level because it enters the upper and the lower bounds below in the same way, so that it cancels from h_0/Lev and from Env/Lev. It does not cancel from Amp/Lev, and there its sign is used (section 7.7).

Hole functions. A *hole function* is the potential at x of the sites nearest to x, kept exactly, minus that of the piece of continuum of the same charge which they replace. All other sites are replaced by the continuum, by an inequality with a definite sign and no remainder: apart from the sites far to the left of x, the summand $a \mapsto \log|T_{\chi_a}(x)|$ is concave on either side of x, and for a concave function the trapezoid rule lies below the integral and the midpoint rule above it (appendix F.2). For x in cell n and $j \geq 1$, the upper bound (for B^0) keeps the $2j+2$ nearest sites with the weights $1, 2, \dots, 2, 1$ and leaves $\mathcal{H}^+_{n,j}(x)$; the lower bound (for B) keeps the $2j$ nearest pairs with their exact moduli and leaves $\mathcal{H}^-_{n,j}(x)$ ((F.39), (F.40); $\mathcal{H}^\pm_n := \mathcal{H}^\pm_{n,1}$). The two charges are equal, so the length of the cell cancels: as $n \to \infty$ the hole functions tend to explicit functions $h^\pm_j$ of the position u in the cell alone, (F.41) and (F.42). For $j = 1$ we write $h^\pm_\infty := h^\pm_1$:

$$\begin{aligned} h^+_\infty(u) &= \log(1+u) + 2\log u + 2\log(1-u) + \log(2-u) - 2\int_{-1}^{2} \log|u-v|\,\mathrm{d}v, \\ h^-_\infty(u;\eta_0) &= \log(u^2+\eta_0^2) + \log((1-u)^2+\eta_0^2) - 2\int_{-1/2}^{3/2} \log|u-v|\,\mathrm{d}v. \end{aligned} \tag{7.15}$$

The rate is $|\mathcal{H}^\pm_{n,j} - h^\pm_j| \leq C_j(\frac{1}{n} + \ell_n)$ on the cells $n \geq 2j+4$, where $C_j = C\,j^2\log(2j+2)$ with C absolute (F.45). Both $e^{\mathcal{H}^\pm}$ contain the factor 4 of the level: as $j \to \infty$, $e^{h^-_j(u;\eta_0)} \to 4(\sin^2\pi u + \sinh^2\pi\eta_0)$. The extrema of $h^\pm_j$ are rows 3, 6, 7 and 8 of table 4. The sites far to the left of x are not concave summands; for them the midpoint rule has an ordinary remainder $e_L(x) \geq 0$ (F.23), whose supremum over the cells $n \geq 6$ and $c \geq c_0^{\mathrm{att}}$ is $C_L \leq 0.006$ (Lemma F.6(d); row 5).
Proposition 7.4 says what the unit means, Env $\approx$ Lev; the proofs of positivity do not use it.

Proposition 7.4 (Envelope and level; proved, computer-assisted)**.** *Let $c \geq c_0^{\mathrm{att}}$ and $\lambda :=$* Env/Lev. *On the cells $n \geq 6$,*

$$0.819\; e^{-2C_L - C_1(\frac{1}{n}+\ell_n)} \;\leq\; \lambda(x) \;\leq\; 1.278\; e^{2C_L + C_1(\frac{1}{n}+\ell_n)}. \tag{7.16}$$

Here $[0.819, 1.278]$ $\langle$cert$\rangle$ (row 6 of table 4) is the bracket that the limits $h^\pm_1$ give, $e^{\pm 2C_L}$ is the loss from the sites far to the left, and $e^{\pm C_1(\frac{1}{n}+\ell_n)} \to 1$ accounts for the displacement of the sites. With $h^\pm_4$ the bracket is $[e^{-0.0422}, e^{0.0749}]$ $\langle$cert$\rangle$; hence, for fixed $\epsilon > 0$ and c large depending on ϵ, on the cells $n \geq \epsilon c'$ we have $\lambda \in [0.949, 1.089]$, where a factor 1 ± 0.01 absorbs all corrections.

The next lemma lists everything else that is used about the comb on the real axis. Item (a) is the main statement; (b) and (d1) control the overshoot; (c) and (e) are upper bounds, for integrability and for the vacuum; (d2) and (f) concern the vacuum only.

Lemma 7.5 (The comb on the band; proved, computer-assisted)**.** *Let $c \geq c_0^{\mathrm{att}}$. Let $r > 0$ be fixed, and let C_r denote constants which depend on r only; the statements on the far band $x \geq x_1^* + r$ are made for $c \geq c_0(r)$, so large that $\chi_6 \leq x_1^* + r/2$.*

(a) Two-sided bounds. *For x in a cell $n \geq 6$, with all functions evaluated at x,*

$$c'\mathcal{P} + \mathcal{J}_{\mathrm{end}} + \mathcal{H}^-_n - 2C_L \;\leq\; \log|B| + c'L, \qquad \log|B^0| + c'L \;\leq\; c'\mathcal{P} + \mathcal{J}_{\mathrm{end}} + \mathcal{H}^+_n + 2C_L. \tag{7.17}$$

An upper bound for B costs in addition the detuning factor of (e).

(b) The overshoot. *For $x > \chi_2$,*

$$2n_1\,|\log|T_{x_1^*}(x)|| \;\leq\; c'\mathcal{P}(x) \;\leq\; 2n_1\,|\log|T_{\chi_2}(x)||. \tag{7.18}$$

Consequently $e^{c'\mathcal{P}} \leq C_r$ on $x \geq x_1^* + r$; $e^{c'\mathcal{P}} \to 1$ exponentially deep in the band; and $e^{c'\mathcal{P}(x)} \geq (2/(\pi(x - x_1^*)))^{2n_1}$, which is a power of c' near the onset.

(c) Sup bound.

$$\sup_{x\ge\chi_2}\big[\log|B|+c'L\big]\le\tfrac{4}{3}n_1\log c'+C,\qquad \sup_{x\ge x_1^*+r}\big[\log|B|+c'L\big]\le C_r. \tag{7.19}$$

(d1) The Airy window. *For $x=x_1^*+\ell_c\varsigma$ with ς in a bounded set, $e^{c'\mathcal{P}(x)}=\ell_c^{-2n_1}e^{p_2(\varsigma)}(1+O(\ell_c\log\frac{1}{\ell_c}))$, with an explicit continuous function p_2 that does not depend on c (F.19). Hence $\operatorname{Lev}e^{c'L}\asymp\ell_c^{-2n_1}\asymp c'^{\frac{4}{3}n_1}$ on the part $x\ge\chi_3$ of the window, and $\operatorname{Lev}e^{c'L}\asymp(x-x_1^*)^{-2n_1}$ for $\ell_c\ll x-x_1^*\ll 1$.*

(d2) Lobe and band in the window. *In the variable ς the integrands of the lobe and of the first cells of the band have one common factor, proportional to $c'^{\frac{4}{3}n_1-\frac{1}{6}}$: on the part $x_1^*\le x<\chi_2$ of the lobe $|h_0|V\,\mathrm{d}t$ is at least this factor times a function of ς, and on each of the first N_1 cells of the band, for any fixed N_1, $h_0V\,\mathrm{d}t$ is at most this factor times another. The integrals of these functions differ by $O(\ell_c)$ from those of explicit functions that do not depend on c. The precise statement is Lemma G.2. It is used in section 7.9 only.*

(e) Upper bound with detuning. *Since $\sup_u h_\infty^+(u)=6-4\log 3\le 1.606$ ⟨cert⟩ (row 7), on the cells $n\ge 6$ we have $\sup_{\text{cell}}e^{\mathcal{H}_n^+}\le 5.0\,e^{94/n+C\ell_n}$, and*

$$|B(x)|\,e^{c'L(x)}\ \le\ 5.0\,(1+4\eta_0^2)^2\,e^{C_{\det}\eta_0^2}\,e^{2C_L+94/n+C\ell_n}\,e^{c'\mathcal{P}(x)+\mathcal{J}_{\text{end}}(x)}, \tag{7.20}$$

with an absolute constant $C_{\det}\le 16.6$ (Lemma F.7). In particular $|B|\,e^{c'L}\le C_r$ on $x\ge x_1^*+r$.

(f) The lobe. *For $0\le x<\chi_2$, with all functions evaluated at x,*

$$\log|T_{\chi_2}|+c'U+c'\mathcal{P}_{\chi_{5/2}}\ \le\ \log|B|\ \le\ \log|T_{\chi_2}T_{\chi_3}|+c'U+c'\mathcal{P}_{\chi_3}+4\zeta(2)\,\eta_0^2. \tag{7.21}$$

Here $\zeta(2)=\pi^2/6$ is the value of Riemann's zeta function, $U=-L$ on $[x_1^*,\chi_2)$, and no certified constant enters.

Proofs. Item (a) and Proposition 7.4 are proved in appendix F.5; (b) and (d1) in appendix F.1; (c), (e) and (f) in appendix F.4, with the detuning estimate of appendix F.3; and (d2) in appendix G.2. The proof of (b) takes one line: for $x>\chi_2$ the function $x'\mapsto|\log|T_{x'}(x)||$ increases on $[x_1^*,\chi_2]$, and $c'\mathcal{P}(x)$ is $2n_1$ times an average of it over this interval. The last consequence in (b) then follows from $\tanh z\le z$.

7.6 The transform by steepest descent

We compute $\hat{h}_0$ on the band by stationary phase in the edge representation (7.8). This needs the phase of B on the edge (Lemma 7.6) and a saddle-point lemma with explicit remainders (Lemma 7.7). The comb drops out of the amplitude Amp, which depends only on the outer factor and on F.

Lemma 7.6 (Edge phase; proved)**.** *Let c be so large that $\max_n\varepsilon_n\le\frac{1}{8}$. On the strip $\frac{1}{4}\le\operatorname{Im}b\le\frac{3}{4}$, and for $\operatorname{Re}\zeta\ge x_1^*$, $|\operatorname{Im}\zeta|\le\frac{1}{8}$, let $\varphi_\zeta(b):=\log\big(-T_\zeta(b)\big)$ be the normalized branch of (D.4): it is continuous in (b,ζ), it tends to 0 as $\operatorname{Re}\zeta\to\infty$, and $\varphi_\zeta(\frac{i}{2})=0$. Let $\Phi_0(b):=\int_{x_1^*}^\infty\rho_U(x')\,\varphi_{x'}(b)\,\mathrm{d}x'$ as in (D.7), and let $\log B$ be the branch with $\log B(\frac{i}{2})=i\pi$. Then, on E_+,*

$$\log B=c'\Phi_0+\Phi_1,\qquad \operatorname{Re}\Phi_0=0,\qquad \Phi_0(\tfrac{i}{2})=0,\qquad \partial_v\operatorname{Im}\Phi_0(v+\tfrac{i}{2})=-\frac{4\pi}{3}F(v), \tag{7.22}$$

where F is the edge function (7.3). Moreover $\Phi_1=i\pi-2n_1\bar{\varphi}+O(c'^{-2/3})$, where $\bar{\varphi}$ is the average of $\varphi_{x'}$ over the absent charge on $[x_1^*,\chi_2]$; $\operatorname{Re}\Phi_1=0$ on E_+; and Φ_1, Φ_1', Φ_1'' are bounded on the whole strip $\frac{1}{4}\le\operatorname{Im}b\le\frac{3}{4}$, uniformly in c' and in $\operatorname{Re}b$.

The proof is in appendix D.3 (Lemma D.2). The term $c'\Phi_0$ is the continuum of Lemma 7.1, continued across the edge. The three parts of Φ_1 are the sign of the simple zero, the absent charge, and the $O(c'^{-2/3})$ from the detuning and the discreteness of the sites. In words: on the edge the comb is a pure phase $e^{ic'\,\mathrm{Im}\,\Phi_0}$, up to a slowly varying factor, and the derivative of this phase is the edge function.

The saddles. By (7.9) the phase of the kernel $H_0^{(1)}(k_x b)$ along $b = v + \frac{i}{2}$ is $k_x v$ plus slowly varying terms. The phase of the integrand of (7.8) is therefore $c'\big[\mathrm{Im}\,\Phi_0(v+\frac{i}{2}) + \frac{4\pi}{3}xv\big]$ at leading order, and by (7.22) it is stationary where $F(v) = x$. Since F is even and increases from $F(0) = x_1^*$, there are two saddles $v = \pm v_0(x)$ when $x > x_1^*$, which coalesce at $v = 0$ as $x \downarrow x_1^*$, and none when $x < x_1^*$. The curvature there is $-\frac{4\pi}{3}c'F'(v_0)$, with $F'(v_0) = (\sinh^2\pi x - 1)^{1/2}/\cosh\pi x$; it vanishes like $(x - x_1^*)^{1/2}$ at the tip, so the next lemma stops at x_I.

Lemma 7.7 (The transform on the band; proved)**.** *Let $\theta_{\mathrm{on}} = 0.2$ and $x_I = x_1^* + c'^{-\theta_{\mathrm{on}}}$; any $\theta_{\mathrm{on}} \in (\frac{1}{4n_1}, \frac{2}{3})$ would do. For c large and every $x \ge x_I$,*

$$\hat{h}_0(c'x^2/3) = \mathrm{Amp}(x)\,\big[\cos\hat{\Psi}(x) + \varepsilon_{\mathrm{sd}}(x)\big], \tag{7.23}$$

with a real phase $\hat{\Psi}$, given in (E.11), and

$$\mathrm{Amp}(x)\,e^{c'L(x)} = \frac{4}{\sinh\pi x}\Big(\frac{|b_0|}{x\,F'(v_0)}\Big)^{1/2}(1 + O(1/c')), \qquad |\varepsilon_{\mathrm{sd}}(x)| \le \frac{C}{c'\min\{1, v_0(x)\}^3}. \tag{7.24}$$

Here $b_0 = v_0(x) + \frac{i}{2}$, and $4/\sinh\pi x = 2|\mathrm{sech}^2\,\frac{\pi b_0}{2}|$ by Proposition 7.2(d): the comb does not appear in the amplitude. Moreover

$$|\hat{h}_0(c'x^2/3)| \le C_{\mathrm{glob}}\,F'(v_0)^{-1/2}\,e^{-\pi v_0(x)}\,e^{-c'L(x)} \qquad (x \ge x_I), \qquad C_{\mathrm{glob}} = 2^5. \tag{7.25}$$

The first formula of (7.24) is (E.14) with the outer factor sech^2, and its $O(1/c')$ is at most $0.33/|k_x b_0|$. The second is (E.31); it is $O(1/c')$ deep in the band and at most $Cc'^{-(1-3\theta_{\mathrm{on}}/2)} = Cc'^{-0.7}$ at x_I. The bound (7.25) is Corollary E.3. The general statement is Lemma E.1, which deforms the edge into the two steepest-descent paths through $\pm b_0$; its hypotheses (SD1)–(SD4) are verified for the comb in appendix E.4, where the condition $\theta_{\mathrm{on}} < \frac{2}{3}$ enters.

[ORIENTATION] At leading order $\hat{\Psi}' = \Psi'$, by the eikonal identity (D.13), so $\hat{h}_0$ oscillates once per cell, in step with h_0 (figure 8); this is not used, since section 7.7 uses $|\cos\hat{\Psi}| \le 1$ only.

7.7 Positivity on the band beyond the onset (Region II)

In Region II, $x \ge x_I$, both sides of $\hat{h}_0 < h_0$ are known in units of the level: $|\hat{h}_0| \le \mathrm{Amp}\,(1 + |\varepsilon_{\mathrm{sd}}|)$ by Lemma 7.7, and by the detuning h_0 stays above a multiple of Lev that is fixed up to factors which tend to one. The first lemma computes Amp/Lev, the second gives the floor, and the criterion compares them.

Lemma 7.8 (The amplitude in units of the level; proved, computer-assisted)**.** *For c large and every $x \ge x_I$,*

$$\varrho := \frac{\mathrm{Amp}}{\mathrm{Lev}} \;\le\; \varrho_\infty\,(1 + O(1/c')), \qquad \varrho_\infty(x) := \frac{1}{2}\Big(\frac{|b_0|}{x\,F'(v_0)}\Big)^{1/2}\coth\frac{\pi x}{2}\;e^{-2n_1|\log|T_{x_1^*}(x)||}. \tag{7.26}$$

The function ϱ_∞ is explicit and does not depend on c. It vanishes like $(x - x_1^*)^{2n_1 - \frac{1}{4}}$ at the tip, it tends to $\frac{1}{2}$ as $x \to \infty$, and

$$\varrho_\infty \le 0.5029 \;\langle\mathrm{cert}\rangle\; \textit{on}\; (x_1^*, 3], \qquad \varrho_\infty \le 0.504 \;\textit{on}\; [3, \infty), \qquad \varrho_\infty \le 0.41 \;\langle\mathrm{cert}\rangle\; \textit{on}\; (x_1^*, 1.33].$$

Proof. We divide (7.24) by (7.14). Since $(\sinh \pi x)^{-1} \cosh^2 \frac{\pi x}{2} = \frac{1}{2} \coth \frac{\pi x}{2}$,

$$\varrho(x) = \frac{1}{2} \Big(\frac{|b_0|}{x\, F'(v_0)} \Big)^{1/2} \coth \frac{\pi x}{2}\; e^{-c' \mathcal{P}(x) - \mathcal{J}_{\mathrm{end}}(x)} \, (1 + O(1/c')) :$$

the outer factor has canceled up to the factor coth. For c large $x_I > \chi_3$, because $\chi_3 - x_1^* \asymp \ell_c \ll c'^{-\theta_{\mathrm{on}}}$. So $\mathcal{J}_{\mathrm{end}} \geq 0$ by (7.13), and $c'\mathcal{P} \geq 2n_1 |\log |T_{x_1^*}(x)||$ by Lemma 7.5(b). This is (7.26). At the tip $F'(v_0) \asymp (x - x_1^*)^{1/2}$ and $|T_{x_1^*}(x)| \asymp x - x_1^*$, which gives the power; as $x \to \infty$ every factor except $\frac{1}{2}$ tends to one. The bounds 0.5029 and 0.41 are rows 1 and 2 of table 4. Row 1 is verified in interval arithmetic on $[x_1^* + 10^{-3}, 3]$, where ϱ_∞ is largest at the right end, $\varrho_\infty(3) = 0.50271$, and row 2 on the part $x \leq 1.33$ of the same covering. On $(x_1^*, x_1^* + 10^{-3}]$ we have $|T_{x_1^*}(x)| \leq \frac{\pi}{2}(x - x_1^*)$, $F'(v_0) = \sinh \pi v_0 / \cosh \pi x \geq 2(x - x_1^*)^{1/2}$ (as $\sinh^2 \pi v_0 = \sinh^2 \pi x - 1 \geq 2\sqrt{2}\, \pi (x - x_1^*)$ by convexity), $(|b_0|/x)^{1/2} \leq 1.34$ and $\coth \frac{\pi x}{2} \leq \coth \frac{\pi x_1^*}{2} = 1 + \sqrt{2}$, which give $\varrho_\infty \leq 6\,(x - x_1^*)^{13/4} < 10^{-8}$. For $x \geq 3$ the bound is by hand: $F'(v_0) \geq 0.9999$; $v_0 < x$, so $(|b_0|/x)^{1/2} \leq (1 + \frac{1}{4x^2})^{1/4} \leq (1 + \frac{1}{36})^{1/4} \leq 1.0069$; $\coth \frac{\pi x}{2} \leq 1.0002$; and the exponential is at most one. Then $\frac{1}{2} \cdot 1.0069 \cdot 1.0002 \cdot 0.9999^{-1/2} \leq 0.5036 < 0.504$. □

Lemma 7.9 (The detuned floor; proved, computer-assisted)**.** *Let $c \geq c_0^{\mathrm{att}}$, let $j \in \{1, 4\}$ and let x lie in a cell $n \geq 2j + 4$. Then*

$$\frac{h_0(x)}{\mathrm{Lev}(x)} \;\geq\; \tfrac{1}{4}\, e^{\mathcal{H}^-_{n,j}(x) - 2e_L(x)} \;\geq\; \mu_j \Big[1 - C_j \big(\tfrac{1}{n} + \ell_n\big)\Big] e^{-2C_L}, \qquad \mu_j := \min_{0 \leq u \leq 1} \tfrac{1}{4}\, e^{h_j^-(u;\eta_0)}, \quad (7.27)$$

with C_j as in section 7.5, and for $\eta_0 = \frac{1}{4}$

$$\mu_1 \geq 0.536 \;\; \langle \mathrm{cert} \rangle, \qquad \mu_4 \geq 0.699 \;\; \langle \mathrm{cert} \rangle.$$

The factor in brackets tends to 1 as $n \to \infty$. On a cell where it is not positive only the first inequality has content.

This is (F.53); the proof is in appendix F.6, and the two numbers are row 3 of table 4. Every pair beyond the $2j$ nearest is bounded below by its undetuned value, by (T2), and then by the continuum. The minimum over the cell is attained at the sites, $u \in \{0, 1\}$, where one pair is at its least value. Keeping more pairs exactly removes more of the loss in the midpoint rule, which is why $\mu_4 > \mu_1$; as $j \to \infty$, $\mu_j \to \sinh^2 \pi\eta_0 = 0.7546$, the floor seen in figure 8(c).

The criterion. Let $x \geq x_I$ lie in cell n, and let $j \in \{1, 4\}$. Since $2g = h_0 - \hat{h}_0$, Lemmas 7.7 to 7.9 give

$$\frac{2g(t)}{\mathrm{Lev}(x)} \;\geq\; \mu_j \Big[1 - C_j \big(\tfrac{1}{n} + \ell_n\big)\Big] e^{-2C_L} \;-\; \varrho_\infty(x)\, (1 + |\varepsilon_{\mathrm{sd}}(x)|)(1 + O(1/c')). \quad (7.28)$$

No information on the phase $\hat{\Psi}$ has been used. The factors that tend to one are controlled as follows. In Region II the cell index is $\gtrsim c'^{1 - 3\theta_{\mathrm{on}}/2}$, because $c' N(x_I) \simeq \kappa_{\mathrm{tip}} c'\, c'^{-3\theta_{\mathrm{on}}/2}$ by (6.22), and $\ell_n \leq \ell_c$; so the factor in brackets tends to 1 uniformly on Region II, and $n \geq 2j + 4$ holds there. The factor $1 + |\varepsilon_{\mathrm{sd}}|$ tends to 1 uniformly by (7.24). We take c_0^{att} so large that, for $c \geq c_0^{\mathrm{att}}$ and all $x \geq x_I$, the bracket is at least 0.995 and $(1 + |\varepsilon_{\mathrm{sd}}|)(1 + O(1/c')) \leq 1.1$. Also $e^{-2C_L} \geq 0.988$, by Lemma F.6(d). We use $j = 1$ where $x \leq 1.33$, and $j = 4$ where $x \geq 1.33$:

$$\begin{aligned} \frac{2g}{\mathrm{Lev}} \;&\geq\; 0.995 \cdot 0.536 \cdot 0.988 - 0.41 \cdot 1.1 \;\geq\; 0.07 \quad (x_I \leq x \leq 1.33), \\ \frac{2g}{\mathrm{Lev}} \;&\geq\; 0.995 \cdot 0.699 \cdot 0.988 - 0.504 \cdot 1.1 \;\geq\; 0.13 \quad (x \geq 1.33). \end{aligned} \quad (7.29)$$

The second line uses 0.504, which covers both the certified 0.5029 on $(x_1^*, 3]$ and the bound by hand beyond 3. With $j = 4$ the second line alone holds on all of Region II, because its bracket also tends to one there; the first line is kept to show the margin with the smaller hole. The cells are open intervals; since g is continuous (section 7.10) and Lev is continuous and positive on (χ_2, ∞), the inequalities (7.29) hold at the sites as well. Hence $g > 0$ on Region II for $c \geq c_0^{\mathrm{att}}$.

7.8 The onset (Region I)

In Region I, $\chi_2 \le x \le x_I$, the two saddles are too close for Lemma 7.7. Instead we compare a crude upper bound for $\hat{h}_0$, which exceeds the Cardy level by $\sqrt{c'}$, with lower bounds for h_0 that contain the overshoot, a larger power of c'.

The cells $2, \dots, 5$ lie in Region I for c large, because $\chi_6 - x_1^* \asymp \ell_c \asymp c'^{-2/3} \ll c'^{-\theta_{\mathrm{on}}}$. On them nothing is replaced by a continuum to the left of x, and h_0 is bounded below by an exact finite product (Lemma 7.12). On the cells $n \ge 6$ that meet Region I the floor times the overshoot (Lemma 7.11) exceeds the crude bound (Lemma 7.10).

Lemma 7.10 (Crude bound; proved)**.** *For every $x > 0$ with $c'L(x) \ge 1$,*

$$|\hat{h}_0(c'x^2/3)|\, e^{c'L(x)} \le C\sqrt{c'/x}, \qquad \text{and} \qquad |\hat{h}_0(t)| \le Cc' \quad \text{for all } t \ge 0. \tag{7.30}$$

Proof. We take absolute values in (7.8). On E_+, $|h_0| = 2/\cosh \pi v$ by Proposition 7.2(d), and $k_x|b| \ge \frac{1}{2}k_x = c'L(x) \ge 1$, so (7.9) applies with $|1 + \varepsilon_H| \le 1.33$. Hence

$$|\hat{h}_0| \le \frac{2\pi c'}{3} \int_{-\infty}^{\infty} \frac{2}{\cosh \pi v} \Big(\frac{2}{\pi k_x |b|}\Big)^{1/2} 1.33\, e^{-c'L(x)}\, |b|\, \mathrm{d}v \le C\, c'\, (c'x)^{-1/2}\, e^{-c'L(x)} \int_{-\infty}^{\infty} \frac{|b|^{1/2}}{\cosh \pi v}\, \mathrm{d}v,$$

and the last integral is a number. For the second bound we use $|J_0| \le 1$ on the real axis in (2.9): $|\hat{h}_0| \le 2\pi \int_0^\infty |h_0|\, \mathrm{d}t = \frac{4\pi c'}{3} \int_0^\infty |h_0(x)|\, x\, \mathrm{d}x \le Cc'$, because $|h_0(x)| \le 4e^{-\pi x}$. □

Lemma 7.11 (Overshoot; proved, computer-assisted)**.** *Let $c \ge c_0^{\mathrm{att}}$. On the cells $n \ge 6$,*

$$|B(x)|\, e^{c'L(x)} \;\ge\; 32\, \eta_0^2\, e^{-C(\frac{1}{n} + \ell_n) - 2C_L} \Big(\frac{2}{\pi(x - x_1^*)}\Big)^{2n_1} \;\ge\; c_T\, \eta_0^2 \Big(\frac{2}{\pi(x - x_1^*)}\Big)^{2n_1}, \tag{7.31}$$

with an absolute constant $c_T > 0$. Only the positivity of c_T is used.

This is (F.38), proved in appendix F.4. It follows from the lower bound of Lemma 7.5(a) with $\mathcal{J}_{\mathrm{end}} \ge 0$, from the last consequence in Lemma 7.5(b), and from $\min_u e^{h_\infty^-(u;\eta_0)} \ge 32\eta_0^2$ ⟨cert⟩ (row 8 of table 4). The exponent in the middle is bounded because $\frac{1}{n} \le \frac{1}{6}$ and $\ell_n \le \ell_c$.

Now let $x \le x_I$ lie in a cell $n \ge 6$. Then $x - x_1^* \le c'^{-\theta_{\mathrm{on}}}$, and $\operatorname{sech}^2 \frac{\pi x}{2}$ is bounded below, so Lemma 7.11 and Lemma 7.10 give

$$h_0\, e^{c'L} \;\ge\; C^{-1}(x - x_1^*)^{-2n_1} \;\ge\; C^{-1} c'^{\,2n_1\theta_{\mathrm{on}}} = C^{-1} c'^{\,0.7}, \qquad |\hat{h}_0|\, e^{c'L} \le C\, c'^{\,1/2},$$

and $g > 0$ for c large, because $2n_1\theta_{\mathrm{on}} > \frac{1}{2}$, that is, $\theta_{\mathrm{on}} > \frac{1}{4n_1}$ (figure 8).

Lemma 7.12 (First cells; proved, computer-assisted)**.** *Let $c \ge c_0^{\mathrm{att}}$. On the cells $n = 3, 4, 5$,*

$$h_0 \;\ge\; \mathrm{Lev}\, e^{-\mathcal{J}_{\mathrm{end}}}\, \mu_n^{\mathrm{I}}\, (1 - C\ell_c \log \tfrac{1}{\ell_c}), \qquad \mu_3^{\mathrm{I}} \ge 0.679, \quad \mu_4^{\mathrm{I}} \ge 0.683, \quad \mu_5^{\mathrm{I}} \ge 0.686 \;\; ⟨\mathrm{cert}⟩, \tag{7.32}$$

and on the whole of cell 2,

$$h_0(x) \;\ge\; \mathrm{Lev}\, e^{-\mathcal{J}_{\mathrm{end}}}\, \mu_{\mathrm{slope}}\, \frac{x - \chi_2}{\chi_3 - \chi_2}\, (1 - C\ell_c \log \tfrac{1}{\ell_c}), \qquad \mu_{\mathrm{slope}} = 0.686 \quad ⟨\mathrm{cert}⟩. \tag{7.33}$$

On these cells $\mathrm{Lev}\, e^{-\mathcal{J}_{\mathrm{end}}} e^{c'L} \asymp \ell_c^{-2n_1} \asymp c'^{\frac{4}{3}n_1} \gg \sqrt{c'}$.

The proof is in appendix F.7 (Lemma F.12), and the numbers are row 4 of table 4. Here all the sites up to χ_{n+4} are kept exactly, and the midpoint rule is used only beyond them. In the Airy variable $\varsigma = (x - x_1^*)/\ell_c$ the finite product becomes a function on each cell that does not depend on c, and μ_n^{I} is its minimum (F.57). The unit is $\mathrm{Lev}\, e^{-\mathcal{J}_{\mathrm{end}}}$ and not Lev because the exact block reaches the end of the comb: there is no end term, and there is no loss $e^{\pm 2C_L}$. Its size is Lemma 7.5(d1). On cell 2 the function h_0 vanishes at the left end, so the bound is a multiple of the distance to the zero.

Conclusion for Region I. On the cells $3, 4, 5$ we have $h_0\, e^{c'L} \geq C^{-1} c'^{\frac{4}{3}n_1}$ against $|\hat{h}_0|\, e^{c'L} \leq C\sqrt{c'}$, so $g > 0$ for c large. On cell 2,

$$2g\, e^{c'L} \;\geq\; C^{-1} c'^{\frac{4}{3}n_1}\, \frac{x - \chi_2}{\ell_c} - C\, c'^{1/2},$$

which is positive as soon as $x - \chi_2 \geq C\ell_c\, c'^{\frac{1}{2}-\frac{4}{3}n_1} = C\, c'^{-5/2}$, that is, $t - t_\star \geq C c'^{-3/2}$. There is no uniform margin at the simple zero; hence the offset in Theorem 5(ii), which is far larger than needed. The bounds of Lemmas 7.11 and 7.12 are inequalities between continuous functions of x; proved on the open cells, they hold at the sites χ_n, $n \geq 3$, as well. With the cells $n \geq 6$ treated above, $g > 0$ on $t_\star + o(1/c') \leq t \leq c' x_I^2/3$.

7.9 The vacuum inequality

The vacuum value is a competition between the negative lobe of h_0 below $t_\star$ and the positive band beyond it, both weighted with the Cardy weight V. The lobe wins: the proof gives the factor $1/R_{\rm vac} \geq 8$. The omitted site is what makes it so: the stretch from the first site of the law to χ_2, which would otherwise be the first cell of the band, belongs to the lobe.

By Lemma 7.3(b) and Proposition 7.2(b),(c),

$$g_{\rm vac} = \tfrac{1}{2}\, h_{0,\rm vac} + \pi(|\text{Lobe}| - \text{Band}), \qquad \text{Lobe} := \int_0^{t_\star} h_0\, V\, \mathrm{d}t, \qquad \text{Band} := \int_{t_\star}^{\infty} h_0\, V\, \mathrm{d}t, \quad (7.34)$$

with Lobe $< 0 <$ Band and $|h_{0,\rm vac}| \leq 8$. The transform $\hat{h}_0$ enters only through the hypothesis of Lemma 7.3(b), which is verified in section 7.10. By Lemma 7.5(d1) both integrals are dominated by a window of width $O(\ell_c)$ around x_1^*, where $|B|\, e^{c'L}$ is of order $\ell_c^{-2n_1}$. In the variable $\varsigma = (x - x_1^*)/\ell_c$ the lobe and the first N_1 cells of the band are one common factor, proportional to $c'^{\frac{4}{3}n_1 - \frac{1}{6}} = c'^{13/6}$, times integrals that do not depend on c (Lemma 7.5(d2)). The later cells, up to a fixed distance from the tip, carry the same factor times a small number, because the overshoot decays like ς^{-2n_1}, and the rest of the band contributes $O(\sqrt{c'})$, by Lemma 7.5(e). The common factor cancels from the ratio.

Proposition 7.13 (Vacuum inequality; proved, computer-assisted)**.** *There is a number $R_{\rm vac} < 1$, which does not depend on c, such that for $c \geq c_0^{\rm att}$*

$$\text{Band} \;\leq\; R_{\rm vac}\, |\text{Lobe}|, \qquad R_{\rm vac} := \hat{R}_{\rm vac}(N_1) + \delta_{\rm tail} + 0.01 \;\leq\; 0.1021 + 0.02, \qquad N_1 = 100, \quad (7.35)$$

and $|\text{Lobe}| \to \infty$ as $c \to \infty$, at least like $c'^{13/6}$. Hence $g_{\rm vac} \geq \pi(1 - R_{\rm vac})|\text{Lobe}| - 4 > 0$. Here $\hat{R}_{\rm vac}(N_1)$ is the scaled vacuum ratio (G.15)*, the ratio of the c-independent integrals of Lemma 7.5*(d2)* over the first N_1 cells of the band and over the lobe, and $\hat{R}_{\rm vac}(100) \leq 0.1021$ ⟨cert⟩ (row 11 of table 4); the term $\delta_{\rm tail} := \frac{C_{\rm tail}}{I_{\rm Lobe}} \frac{(N_1 - \frac{1}{4})^{-5/3}}{2.5} \leq 0.01$ bounds the cells beyond them, by hand, with the explicit constant $C_{\rm tail}$ of Lemma G.5 and the scaled integral $I_{\rm Lobe}$ over the lobe; and 0.01 covers the corrections at finite c.*

The proof is in appendix G, and the assembly is in appendix G.5. Besides Lemma 7.5(d2),(e),(f), it uses the two-sided asymptote $V = \text{as}(c'L)\,[(1 - e^{-4\pi x})^2 + O(1/c')]$ of the Cardy weight (Lemma B.4, (B.7)). It matters that the asymptote is two-sided: the lobe is bounded below and the band above, and both must be measured with the same weight; with the one-sided bound $V \leq e^{c'L}$ on the band the estimate of the ratio would be larger by the factor $1.92\sqrt{c'}$, and would exceed one (appendix G.5). Only $R_{\rm vac} < 1$ is needed, so the margin is wide.

7.10 Membership, end of the proof, and a numerical illustration

It remains to check that g belongs to $\bar{\mathcal{A}}$, which also supplies the hypothesis of Lemma 7.3.

Membership. On the real axis $|h_0| \le 4e^{-\pi x}|B|$. By Lemma 7.5(c), $|B| \le C(c)\, e^{-c'L}$ for $x \ge \chi_2$, and $|B| \le 1$ below χ_2, where $e^{-c'L}$ is bounded below. So h_0 is continuous and $|h_0(t)| \le C(c)\, e^{-c'L(x)-\pi x}$ for $t \ge 0$. In particular h_0 is integrable, so $\hat h_0$ is continuous. Both are real for $t \ge 0$: T_{χ_2} is real on the real axis and the other factors of B come in conjugate pairs, and the kernel of (2.9) is real. For $x \ge x_I$ the bound (7.25) gives $|\hat h_0| \le C(c)\, e^{-c'L-\pi x}$: indeed $e^{\pi v_0} \ge \cosh \pi v_0 = \sinh \pi x$, so $e^{-\pi v_0} \le Ce^{-\pi x}$, and $F'(v_0)^{-1/2} \le Cc'^{\theta_{\mathrm{on}}/4}$ there. For $x \le x_I$ we have $|\hat h_0| \le Cc'$ by Lemma 7.10, and $e^{-c'L-\pi x}$ is bounded below. This is the hypothesis of Lemma 7.3(a),(b), and with it the decay stated in Theorem 5. Thus $g = \frac12(h_0 - \hat h_0)$ is real and continuous on $[0,\infty)$. The three conditions of Definition 2.5 follow. Condition (i) is the integrability just shown. Condition (ii) is Lemma 7.3(a). For (iii), $V \le (4\pi^2 t/a)\, e^{c'L}$ by Lemma B.2(d), so $|g|\, V \le C(c)\, t\, e^{-\pi x}$, which is integrable.

End of the proof of Theorem 5. Part (i) is the preceding paragraph. For (ii), section 7.7 gives $g > 0$ for $x \ge x_I$, and section 7.8 gives $g > 0$ for $t_\star + o(1/c') \le t \le c'x_I^2/3$; these cover $t \ge t_\star + 1$. Part (iii) is Proposition 7.13. Let c_0^{att} be the largest of the finitely many thresholds met on the way. Each of them is explicit in principle, and none has been computed. □

A numerical illustration [NUMERICAL]**.** At $c = 128$, 256, 512, 1024 the smallest sampled value of g, in units of h_0 at the middle of the same cell, lies between $+0.065$ and $+0.080$; it is attained at the first pair of detuned sites, and deep in the band the same ratio is about 0.35. Also Band/|Lobe| $\in [0.074, 0.081]$. The proof uses none of these numbers. At $c = 256$ the functional would give $\Delta_1 \le a + t_\star + 1 = 32.3$, against the numerical optimum 29.72 of table 2.

Three things are *not* claimed: that the optimal functional has this form; that 0.483 is the best constant in (7.5); and anything at a specific finite c.

8 From functionals to CFT spectra

Theorem 5 supplies a feasible function in $\bar{\mathcal{A}}$. That such a function constrains every conformal field theory is Theorem 2, which we prove in this section, without a computer; Corollary 6 then follows at once.

8.1 The issue, the idea, and the statement

The sum rule (2.5) came from applying a functional to the crossing equation term by term. For a functional of finite order with compact support in β this is termwise differentiation of a series of exponentials that converges uniformly with all its derivatives. A function $g \in \bar{\mathcal{A}}$ is only continuous and integrable against the Cardy weight. If it comes from a functional ω at all, the support of ω may reach the boundary of moduli space, $\beta \to 0$ and $\beta \to \infty$, and exchanging ω with the sum over primaries is then a genuine condition, the analogue of the swapping conditions for four-point functions [35, 36, 68]. Two things can go wrong. First, $\sum_n d_n\, g(t_n)$ need not converge absolutely: the primaries can sit anywhere, their number grows like the Cardy density, and $M[g] < \infty$ controls $|g|$ only in the mean. Second, the vacuum sits at $t = -a$, that is, at $b = \pm i/2$ in the variable of section 2.5, off the real axis, where g is not given but *defined* by the eigen-identity (Definition 2.5); one must show that $g_{\mathrm{vac}} = -\int g\, \rho_C$ so defined is what crossing assigns to the vacuum.

The idea. We never construct ω. We expand g in the Laguerre functions ψ_k of (2.10). Because $\hat g = -g$ only odd k occur, and each odd ψ_k is a derivative functional of finite order at $\beta = 1$, which annihilates the crossing equation. The Laguerre series of g cannot be summed against the spectrum term by term, because its partial sums need not converge there. We therefore insert a factor r^k with $0 < r < 1$ and consider the *Abel mean* $\mathrm{Ab}_r g = \sum_k r^k g_k \psi_k$, where g_k are the

Laguerre coefficients of g. On the crossing kernel this regulator is a contraction of the modulus toward the self-dual point: $\mathrm{Ab}_r\Xi_\beta$ is a multiple of Ξ_{β_r}, where $\varpi(\beta_r) = r\,\varpi(\beta)$ in the variable $\varpi := (\beta-1)/(\beta+1)$, so that β_r stays in the compact interval $[\frac{1-r}{1+r}, \frac{1+r}{1-r}]$. Each Abel mean thus behaves as a functional supported strictly inside moduli space, and the sum rule holds for $\mathrm{Ab}_r g$ at every $r < 1$ at no cost beyond $\hat{Z}(\beta) < \infty$.

The content of the theorem is the removal of the regulator, $r \uparrow 1$, which lets the support reach the cusps where the Cardy growth lives. The Abel mean is an integral operator with a positive, symmetric kernel, known in closed form, which concentrates on the diagonal as $r \uparrow 1$. The vacuum enters through its S-image, the Cardy continuum on $t \geq 0$, and symmetry moves Ab_r from g onto ρ_C. The kernel preserves the Cardy growth of ρ_C up to a constant factor, uniformly in r (Lemma 8.1), so $M[g] < \infty$ is exactly the domination that dominated convergence requires, and the vacuum side tends to $\int g\,\rho_C = -g_{\mathrm{vac}}$. On the primary side no domination is available. Feasibility supplies a sign instead, and for non-negative terms Fatou's lemma needs none: the sum of the lower limits is at most the lower limit of the sum, $\sum_n \liminf_r \leq \liminf_r \sum_n$. It applies to the positive part g_+. The negative part g_-, the lobe, lives on $[0, T]$, below every primary by hypothesis, and its leakage onto the primaries, a Gaussian tail of the kernel, vanishes against the Cardy growth of their number. The outcome is $0 \leq \sum_n d_n\, g(t_n) \leq -g_{\mathrm{vac}} < 0$.

The statement. This proves Theorem 2: for $c \geq 40$, if $g \in \bar{\mathcal{A}}$ is feasible at some $T > 0$, then no admissible spectrum (Definition 2.1) has all its primaries at $t_n \geq T$. The argument is by contradiction from $t_n \geq T > 0$ for all n, so light primaries never enter it, while in the conclusion the primary with $t_n < T$ may be a light one. The hypothesis that there are no conserved currents beyond Virasoro (section 2.1) cannot be dropped within this framework: a current J enters every sum rule as $d_J[g(t_J) - g(t_J+1)]$, a difference whose sign feasibility does not control.

8.2 Set-up

We list what section 8.3 uses, so that the proof can be checked line by line. Classical facts about Laguerre polynomials are quoted from [69]; everything else is proved.

Conventions. Throughout this section $u := 4\pi t$ and $\sigma := \sqrt{u}$ and likewise for u'; a function of $t \geq 0$ is regarded as a function of u without change of name, and $L^p(\mathrm{d}u)$ refers to $[0, \infty)$. Thus $\psi_k = L_k(u)e^{-u/2}$. We write $e_\beta(t) := e^{-2\pi\beta t} = e^{-\beta u/2}$, so that $\Xi_\beta = e_\beta - \beta^{-1}e_{1/\beta}$ by (2.4); $r \in (0,1)$ is the Abel ratio. For a spectrum $\{(t_n, d_n)\}$ with all $t_n \geq 0$ the *signed spectral measure* and its pairing with a function f on $[0,\infty)$ are

$$\mathfrak{m} := \sum_n d_n\,\delta_{t_n} - \rho_C(t)\,\mathrm{d}t, \qquad \langle \mathfrak{m}, f\rangle := \sum_n d_n\, f(t_n) - \int_0^\infty \rho_C\, f\,\mathrm{d}t, \tag{8.1}$$

and $|\mathfrak{m}|$ is the same measure with a plus sign. By (2.12) the vacuum term of $\hat{Z}(\beta)$ equals $\beta^{-1}\int_0^\infty \rho_C\, e_{1/\beta}\,\mathrm{d}t$, so the crossing equation (2.3) reads $\langle \mathfrak{m}, \Xi_\beta\rangle = 0$: the vacuum has been traded for its S-image, and only $t \geq 0$ occurs. Growth and decay are measured by the weights

$$W_{q,\ell}(t) := (1+u)^q\, e^{\ell\sigma} \quad (q, \ell \in \mathbb{R}), \qquad \ell_a := 2\sqrt{\pi a}, \qquad 0 \leq \rho_C \leq C_\rho\, W_{-1/4,\ell_a}. \tag{8.2}$$

Here $e^{\ell_a\sigma} = e^{4\pi\sqrt{at}} = e^{c'L(x)}$ is the Cardy factor. The upper bound on ρ_C, with $C_\rho = C_\rho(a)$, follows from $\rho_C = 2\pi V \leq 4\pi K_a$ and $K_a = I_0(\ell_a\sigma) \leq 1.18\, e^{\ell_a\sigma}/\sqrt{1+\ell_a\sigma}$ (Lemma B.4(c)); $\rho_C \geq 0$ by Lemma B.2(a). Since c is fixed, constants may depend on a; what matters is uniformity in r.

Five facts about the spectrum. Let $\{(t_n, d_n)\}$ be an admissible spectrum with all $t_n \geq 0$, and $\mathcal{N}_Z(R) := \sum_{t_n \leq R} d_n$ its counting function.

(Z1) $\int e^{-2\pi\beta t}\,\mathrm{d}|\mathfrak{m}|(t) < \infty$ for every $\beta > 0$: the sum over primaries is at most $\hat{Z}(\beta)$, and the integral is the right side of (2.12).

(Z2) $\langle \mathfrak{m}, \Xi_\beta \rangle = 0$ for every $\beta > 0$, with absolute convergence. (Z1) and (Z2) restate the definition of an admissible spectrum.

(Z3) *Cardy counting bound.* $\mathcal{N}_Z(R) \le C_Z\sqrt{R/a}\; e^{4\pi\sqrt{aR}}$ for all $R \ge a$, where $C_Z := 1 + \hat{Z}(1)$. Consequently $\mathcal{N}_Z(t) \le C_N\,(1+\sigma)\,e^{\ell_a\sigma}$ for all $t \ge 0$, where $C_N := C_Z\,e^{4\pi a}\max(1, a^{-1/2})$.

(Z4) For every odd k, $\sum_n d_n|\psi_k(t_n)| < \infty$ and $\langle \mathfrak{m}, \psi_k\rangle = 0$.

(St) *Stieltjes summation.* If $\phi \ge 0$ is C^1 and non-increasing on $[T_0, \infty)$, then $\sum_{t_n \ge T_0} d_n\,\phi(t_n) \le \limsup_{R\to\infty} \phi(R)\mathcal{N}_Z(R) + \int_{T_0}^\infty \mathcal{N}_Z\,|\phi'|\,\mathrm{d}t$. This is integration by parts in $\int_{[T_0,R]} \phi\,\mathrm{d}\mathcal{N}_Z$, with the boundary term $-\phi(T_0)\mathcal{N}_Z(T_0^-) \le 0$ dropped.

Proof of (Z3). This is Chebyshev's inequality (a sum of positive terms bounds each of its parts) for $\hat{Z}(\beta)$ at small β, after crossing. For $\beta' \ge 1$, with $\Delta_n = t_n + a > 0$, $\hat{Z}(\beta')\,e^{-2\pi a\beta'} = (1-e^{-2\pi\beta'})^2 + \sum_n d_n e^{-2\pi\beta'\Delta_n} \le 1 + \sum_n d_n e^{-2\pi\Delta_n} \le C_Z$. For $R \ge a$ put $\beta := \sqrt{a/R} \le 1$. Every term with $t_n \le R$ has $e^{-2\pi\beta t_n} \ge e^{-2\pi\beta R}$, so by (2.3)

$$\mathcal{N}_Z(R)\,e^{-2\pi\beta R} \le \sum_n d_n\,e^{-2\pi\beta t_n} \le \hat{Z}(\beta) = \beta^{-1}\hat{Z}(1/\beta) \le \beta^{-1}C_Z\,e^{2\pi a/\beta} = C_Z\sqrt{R/a}\;e^{2\pi\sqrt{aR}},$$

and multiplying by $e^{2\pi\beta R} = e^{2\pi\sqrt{aR}}$ gives the first claim. It implies the second for $t \ge a$, because $\sqrt{t/a} \le a^{-1/2}\sigma$ and $4\pi\sqrt{at} = \ell_a\sigma$; for $t \le a$ use $\mathcal{N}_Z(t) \le \mathcal{N}_Z(a) \le C_Z\,e^{4\pi a}$. □

Laguerre functions. The generating function of the Laguerre polynomials [69, (5.1.9)] is $\sum_{k\ge0} L_k(u)\,w^k = (1-w)^{-1}e^{-uw/(1-w)}$ for $|w| < 1$. Multiply it by $e^{-u/2}$ and put $w = \varpi := \frac{\beta-1}{\beta+1}$, so that $\frac12 + \frac{w}{1-w} = \frac{\beta}{2}$ and $1 - \varpi = \frac{2}{\beta+1}$; the map $\beta \mapsto \varpi$ takes $(0,\infty)$ onto $(-1,1)$ and $1/\beta$ to $-\varpi$. Then

$$e_\beta = (1-\varpi)\sum_{k\ge0} \varpi^k\,\psi_k. \tag{8.3}$$

The Laguerre functions are orthonormal [69, (5.1.1)], $\int_0^\infty \psi_j\psi_k\,\mathrm{d}u = \delta_{jk}$, so the coefficients $g_k := \int_0^\infty g\,\psi_k\,\mathrm{d}u$ of $g \in L^2(\mathrm{d}u)$ obey Bessel's inequality $\sum_k |g_k|^2 \le \|g\|^2_{L^2(\mathrm{d}u)}$. Cauchy's estimate for the coefficient of w^k in the generating function on the circle $|w| = \theta$, where $|1-w| \ge 1-\theta$ and $\mathrm{Re}\,\frac{w}{1-w} \ge -\frac{\theta}{1+\theta}$, gives after multiplication by $e^{-u/2}$ the *Cauchy bound*

$$|\psi_k(u)| \le \frac{\theta^{-k}}{1-\theta}\,e^{-\epsilon_\theta u}, \qquad \epsilon_\theta := \frac{1-\theta}{2(1+\theta)} > 0, \qquad 0 < \theta < 1,\ k \ge 0,\ u \ge 0. \tag{8.4}$$

The Fourier parity $\hat{\psi}_k = (-1)^k\psi_k$ of (2.10) follows from (8.3). By (2.8) the transform of e_β is $\beta^{-1}e_{1/\beta}$, and $\beta^{-1}(1+\varpi) = 1-\varpi$. The series (8.3) converges in $L^1(\mathbb{R}^2)$ by (8.4) and may be transformed term by term: $\sum_k \varpi^k\hat{\psi}_k = (1-\varpi)^{-1}\beta^{-1}e_{1/\beta} = \sum_k(-\varpi)^k\psi_k$, the last step being (8.3) at $1/\beta$; now compare coefficients. The same computation expands the crossing kernel:

$$\Xi_\beta = e_\beta - \beta^{-1}e_{1/\beta} = (1-\varpi)\sum_{k\ge0}\bigl[1-(-1)^k\bigr]\varpi^k\psi_k = \frac{4}{\beta+1}\sum_{k\ \text{odd}} \varpi^k\,\psi_k. \tag{8.5}$$

In particular an odd ψ_k is the coefficient of ϖ^k in $\frac{\beta+1}{4}\Xi_\beta$, a combination of the derivatives $\partial_\beta^j\Xi_\beta\big|_{\beta=1}$ with $1 \le j \le k$: it is a derivative functional (2.6).

Proof of (Z4). Let $\Upsilon_\varpi := \sum_{k\ \text{odd}} \varpi^k\psi_k$. Multiplying (Z2) by $\frac{\beta+1}{4}$ and using (8.5) gives $\sum_n d_n\Upsilon_\varpi(t_n) = \int_0^\infty \rho_C\Upsilon_\varpi\,\mathrm{d}t$ for every $\varpi \in (-1,1)$. Fix $\theta \in (0,1)$. By (8.4), $\sum_k|\varpi|^k|\psi_k(u)| \le (1-\theta)^{-1}(1-|\varpi|/\theta)^{-1}e^{-\epsilon_\theta u}$ for $|\varpi| < \theta$, and $e^{-\epsilon_\theta u} = e^{-4\pi\epsilon_\theta t}$ is $|\mathfrak{m}|$-integrable by (Z1). Hence for $|\varpi| < \theta$ both sides converge absolutely as double series and can be rearranged into power series in ϖ, whose coefficients $\sum_n d_n\psi_k(t_n)$ and $\int_0^\infty \rho_C\,\psi_k\,\mathrm{d}t$, with k odd, converge absolutely. Two power series that agree on an interval have equal coefficients. □

The Abel mean. The Hille–Hardy formula [69, Theorem 5.1], [67, (18.18.27)] sums products of Laguerre functions against a geometric weight: for $0 < r < 1$ and $u, u' \ge 0$,

$$\sum_{k\ge 0} r^k\, \psi_k(u)\, \psi_k(u') = \mathcal{K}_r(u,u') := \frac{1}{1-r}\exp\Big(-\frac{1+r}{2(1-r)}\,(u+u')\Big)\, I_0\Big(\frac{2\sqrt{r\,uu'}}{1-r}\Big), \tag{8.6}$$

the series converging absolutely by (8.4) with $\theta = r^{1/4}$. The *Abel kernel* $\mathcal{K}_r$ is positive and symmetric. By the Laplace formula (2.11) its total mass is $m_r(u) := \int_0^\infty \mathcal{K}_r(u,u')\,\mathrm{d}u' = \frac{2}{1+r}\exp(-\frac{1-r}{2(1+r)}u)$; thus $0 < m_r < 2$, and $m_r(u) \to 1$ as $r \uparrow 1$. For measurable f with $\int_0^\infty \mathcal{K}_r(u,u')|f(u')|\,\mathrm{d}u' < \infty$ the *Abel mean* is $\mathrm{Ab}_r f(u) := \int_0^\infty \mathcal{K}_r(u,u') f(u')\,\mathrm{d}u'$. It is linear and positive, so $|\mathrm{Ab}_r f| \le \mathrm{Ab}_r|f|$. For $g \in L^1(\mathrm{d}u) \cap L^2(\mathrm{d}u)$ it is the Abel-summed Laguerre series, and it decays exponentially in u, whatever the decay of g:

$$\mathrm{Ab}_r g = \sum_{k\ge 0} r^k\, g_k\, \psi_k, \qquad |\mathrm{Ab}_r g(u)| \le \frac{\|g\|_{L^2(\mathrm{d}u)}}{(1-\sqrt{r})\sqrt{1-r}}\; e^{-\epsilon_{\sqrt{r}}\,u}. \tag{8.7}$$

For the first statement insert $g_k = \int g\,\psi_k\,\mathrm{d}u'$ and sum under the integral by (8.6); this is permitted because (8.4) with $\theta = r^{1/4}$ bounds $r^k|\psi_k(u)\psi_k(u')|$ by $(1-r^{1/4})^{-2}r^{k/2}$, and $g \in L^1(\mathrm{d}u)$. For the second, bound $|\mathrm{Ab}_r g(u)|$ by $\sum_k r^k|g_k||\psi_k(u)|$ and use (8.4) with $\theta = \sqrt{r}$, then the Cauchy–Schwarz and Bessel inequalities. Finally, by (8.5) and orthonormality the coefficients of Ξ_β are $\frac{4}{\beta+1}\varpi^k$ for odd k and zero for even k, so $\mathrm{Ab}_r\Xi_\beta = \frac{4}{\beta+1}\sum_{k\ \mathrm{odd}}(r\varpi)^k\psi_k$, which is (8.5) at the modulus β_r where ϖ takes the value $r\,\varpi(\beta)$:

$$\mathrm{Ab}_r\,\Xi_\beta = \frac{1+\beta_r}{1+\beta}\,\Xi_{\beta_r}, \qquad \beta_r := \frac{1+r\varpi}{1-r\varpi}, \qquad \varpi(\beta_r) = r\,\varpi(\beta), \qquad \beta_r \in \Big[\frac{1-r}{1+r}, \frac{1+r}{1-r}\Big]. \tag{8.8}$$

The kernel on weighted spaces. The proof needs Ab_r to be bounded uniformly in r, and to tend to the identity, on functions that grow or decay like the Cardy factor. These are (K1) and (K3) of the next lemma; (K2) serves only to prove (K3). The proof is a Gaussian estimate and can be skipped at first reading.

Lemma 8.1 (Abel kernel on Cardy weights; proved)**.** *Fix $q, \ell \in \mathbb{R}$. There is a constant $C_K = C_K(|q|,|\ell|)$ such that for all $r \in [\frac14, 1)$ and all $u \ge 0$:*

(K1) $\mathrm{Ab}_r W_{q,\ell}(u) \le C_K\, W_{q,\ell}(u)$;

(K2) *for every $\epsilon > 0$,*

$$\int_{|\sigma'-\sigma|\ge\epsilon} \mathcal{K}_r(u,u')\, W_{q,\ell}(u')\,\mathrm{d}u' \le C_K\Big[W_{q,\ell}(u)\, e^{-\frac{\epsilon^2}{4(1-r)}} + \frac{W_{|q|+\frac12,|\ell|}(u)}{1-r}\, e^{-\frac{\max(u/4,\,1)}{4(1-r)}}\Big], \tag{8.9}$$

which tends to 0 as $r \uparrow 1$ at fixed u;

(K3) *if f is continuous on $[0,\infty)$ and $|f| \le C_f\, W_{q,\ell}$, then $\mathrm{Ab}_r f(u) \to f(u)$ as $r \uparrow 1$, for every $u \ge 0$.*

Proof. We bound the kernel by a Gaussian in $\sigma' - \sigma$ of width of order $(1-r)^{1/2}$ and split the integral into a near part, where the weight is comparable to its value at u, and a far part, where the Gaussian wins. Let $\gamma_r := 2\sqrt{r}/(1-r)$, so that the argument of I_0 in (8.6) is $\gamma_r\sigma\sigma'$. Since $\frac{1+r}{2(1-r)} = \frac{\gamma_r}{2} + \frac{(1-\sqrt{r})^2}{2(1-r)} \ge \frac{\gamma_r}{2}$ and $I_0(z) \le 1.18\, e^z/\sqrt{1+z}$ (Lemma B.4(c)),

$$\mathcal{K}_r(u,u') \le \frac{1.18}{1-r}\,\big(1+\gamma_r\sigma\sigma'\big)^{-1/2}\, e^{-\frac{\gamma_r}{2}(\sigma-\sigma')^2}. \tag{8.10}$$

For $r \ge \frac14$ we have $\gamma_r(1-r) = 2\sqrt{r} \in [1,2]$, hence $\gamma_r \ge (1-r)^{-1} \ge 1$. Let $s := \sigma' - \sigma$, so that $\mathrm{d}u' = 2\sigma'\,\mathrm{d}s$, and $\sigma_* := \max(\sigma/2, 1)$; the near set is $\{|s| \le \sigma_*\}$, the far set its complement. In this proof C denotes constants that depend only on $|q|$ and $|\ell|$.

Near set. If $\sigma \ge 2$ then $\sigma' \in [\sigma/2, 3\sigma/2]$ and $(1+u')/(1+u) \in [\frac14, \frac94]$; if $\sigma \le 2$ then $\sigma' \in [0,3]$ and $(1+u')/(1+u) \in [\frac15, 10]$. Thus $(1+u')^q \le 10^{|q|}(1+u)^q$, while $e^{\ell\sigma'} \le e^{\ell\sigma} e^{|\ell||s|}$, and by (8.10)

$$\int_{\text{near}} \mathcal{K}_r\, W_{q,\ell}\, \mathrm{d}u' \le \frac{C\, W_{q,\ell}(u)}{1-r} \int_{\text{near}} 2\sigma' (1+\gamma_r \sigma\sigma')^{-1/2} e^{-\frac{\gamma_r}{2}s^2 + |\ell||s|}\, \mathrm{d}s. \tag{8.11}$$

If $\gamma_r\sigma^2 \ge 1$, then $2\sigma'(1+\gamma_r\sigma\sigma')^{-1/2} \le 2\sqrt{\sigma'/(\gamma_r\sigma)} \le 2\gamma_r^{-1/2}(1+\sqrt{|s|/\sigma}) \le 2\gamma_r^{-1/2}(1+\gamma_r^{1/4}|s|^{1/2})$, and the substitution $s = z/\sqrt{\gamma_r}$ bounds the last integral by $2\gamma_r^{-1}\int_{\mathbb{R}}(1+|z|^{1/2})\, e^{-z^2/2+|\ell||z|}\, \mathrm{d}z$. If $\gamma_r\sigma^2 < 1$, then $(1+\gamma_r\sigma\sigma')^{-1/2} \le 1$ and $2\sigma' \le 2(\gamma_r^{-1/2} + |s|)$, and the same substitution gives $2\gamma_r^{-1}\int_{\mathbb{R}}(1+|z|)\, e^{-z^2/2+|\ell||z|}\, \mathrm{d}z$. Either way the right side of (8.11) is at most $C\, W_{q,\ell}(u)/(\gamma_r(1-r)) \le C\, W_{q,\ell}(u)$.

Far set. There $\frac{\gamma_r}{2}s^2 \ge \frac{\gamma_r}{4}s^2 + \frac{\gamma_r}{4}\sigma_*^2$, and $1+\sigma'^2 \le 2(1+\sigma^2)(1+s^2)$ gives $2\sigma'\, W_{q,\ell}(u') \le C\, W_{|q|+\frac12,|\ell|}(u)\,(1+s^2)^{|q|+\frac12} e^{|\ell||s|}$. Since $\gamma_r \ge 1$, the integral of the last two factors against $e^{-\gamma_r s^2/4}$ is bounded uniformly in r; with $(1+\gamma_r\sigma\sigma')^{-1/2} \le 1$ in (8.10),

$$\int_{\text{far}} \mathcal{K}_r\, W_{q,\ell}\, \mathrm{d}u' \le C\, W_{|q|+\frac12,|\ell|}(u)\, \frac{e^{-\gamma_r\sigma_*^2/4}}{1-r}. \tag{8.12}$$

Now $\gamma_r\sigma_*^2/4 \ge \lambda/(1-r)$ with $\lambda := \max(\sigma^2, 4)/16 \ge \frac14$, and $(1-r)^{-1}e^{-\lambda/(1-r)} = e^{-\lambda}\,(1-r)^{-1}e^{-\lambda r/(1-r)} \le e^{-\lambda}\sup_{x\ge0}(1+x)e^{-x/4}$. Since $W_{|q|+\frac12,|\ell|}(u)\, e^{-\lambda} \le C\, W_{q,\ell}(u)$, a Gaussian in σ beating every weight, the far part is at most $C\, W_{q,\ell}(u)$ as well. This proves (K1).

(K2). On the part of the near set with $|s| \ge \epsilon$ we write $e^{-\frac{\gamma_r}{2}s^2} \le e^{-\gamma_r\epsilon^2/4}\, e^{-\frac{\gamma_r}{4}s^2}$ and repeat the near estimate with $\gamma_r/4$ in place of $\gamma_r/2$; this changes only the constants and produces the factor $e^{-\gamma_r\epsilon^2/4} \le e^{-\epsilon^2/4(1-r)}$. On the far set, (8.12) already carries $(1-r)^{-1}e^{-\gamma_r\sigma_*^2/4} \le (1-r)^{-1}e^{-\sigma_*^2/4(1-r)}$ with $\sigma_*^2 = \max(u/4, 1)$.

(K3). Fix u and $\epsilon > 0$, and let $\mathrm{osc}_\epsilon := \sup\{|f(u') - f(u)| : |\sigma' - \sigma| \le \epsilon\}$. Then $|\mathrm{Ab}_r f(u) - m_r(u) f(u)| \le \mathrm{osc}_\epsilon\, m_r(u) + \int_{|\sigma'-\sigma|\ge\epsilon} \mathcal{K}_r(u,u')(C_f\, W_{q,\ell}(u') + |f(u)|)\, \mathrm{d}u'$. As $r \uparrow 1$ the integral tends to 0 by (K2), applied to $W_{q,\ell}$ and to $W_{0,0}$, and $m_r(u) \to 1$; hence $\limsup_{r\uparrow1}|\mathrm{Ab}_r f(u) - f(u)| \le \mathrm{osc}_\epsilon$, which tends to 0 with ϵ because f is continuous at u. □

8.3 Proof of Theorem 2

Proof of Theorem 2. Let $c \ge 40$, let $g \in \bar{\mathcal{A}}$ be feasible at $T > 0$, and suppose that an admissible spectrum has $t_n \ge T$ for all n; it has no light primaries, so (Z1)–(Z4) and (St) apply. We derive a contradiction in four steps: (i) the sum rule for the Abel means $\mathrm{Ab}_r g$; (ii) the limit $r \uparrow 1$ on the continuum side, by dominated convergence; (iii) the vanishing of the leakage of the lobe; (iv) Fatou's lemma on the primaries.

Step (i)*: the sum rule for Abel means.* By Definition 2.5, $\int_0^\infty |g|\, \mathrm{d}t < \infty$, and $\|g\|_\infty \le 2\pi\int_0^\infty |g|\, \mathrm{d}t$ by $g = -\hat{g}$ and $|J_0| \le 1$ in (2.9); so $g \in L^1(\mathrm{d}u) \cap L^2(\mathrm{d}u)$. Its Laguerre coefficients vanish for even k: by $\hat{\psi}_k = (-1)^k\psi_k$, by $\int_{\mathbb{R}^2}\hat{g}\,\psi_k = \int_{\mathbb{R}^2} g\,\hat{\psi}_k$ (Fubini's theorem) and by $\hat{g} = -g$, we have $g_k = (-1)^k\int_0^\infty \hat{g}\,\psi_k\,\mathrm{d}u = -(-1)^k g_k$. Let $0 < r < 1$. The function $\mathrm{Ab}_r g$ obeys (8.7), so $\langle \mathfrak{m}, \mathrm{Ab}_r g\rangle$ converges absolutely by (Z1). Moreover, by (8.4) with $\theta = \sqrt{r}$, $\sum_k r^k|g_k|\int|\psi_k|\,\mathrm{d}|\mathfrak{m}| \le (1-\sqrt{r})^{-1}\big(\sum_k r^{k/2}|g_k|\big)\int e^{-\epsilon\sqrt{r}u}\,\mathrm{d}|\mathfrak{m}| < \infty$, so the series in (8.7) may be paired with $\mathfrak{m}$ term by term: $\langle \mathfrak{m}, \mathrm{Ab}_r g\rangle = \sum_{k\ \text{odd}} r^k g_k \langle \mathfrak{m}, \psi_k\rangle = 0$ by (Z4). Thus, with both sides absolutely convergent,

$$\sum_n d_n\, \mathrm{Ab}_r g(t_n) = \int_0^\infty \rho_C\, \mathrm{Ab}_r g\, \mathrm{d}t \qquad \text{for every } r \in (0,1). \tag{8.13}$$

Step (ii)*: the continuum side.* By the symmetry of $\mathcal{K}_r$, Tonelli's theorem, (8.2) and (K1), $\int_0^\infty\int_0^\infty \rho_C(u)\,\mathcal{K}_r(u,u')|g(u')|\,\mathrm{d}u\,\mathrm{d}u' = \int_0^\infty |g|\,\mathrm{Ab}_r\rho_C\,\mathrm{d}u' \le C_\rho C_K\int_0^\infty |g|\, W_{-1/4,\ell_a}\,\mathrm{d}u'$. The right side is finite. Indeed, by Lemma B.2(c) and (e), for $t \ge \xi_1^* c'$ we have $V \ge 0.9\, K_a \ge 0.9\, e^{-2}e^{\ell_a\sigma}/\sqrt{\ell_a\sigma} \ge c_* W_{-1/4,\ell_a}$ with a constant $c_* = c_*(a) > 0$, so that $\int_{t\ge\xi_1^*c'}|g|\, W_{-1/4,\ell_a}\,\mathrm{d}t \le$

$c_*^{-1} M[g] < \infty$, while on $[0, \xi_1^* c']$ the weight is bounded and g is integrable. Hence Fubini's theorem gives $\int \rho_C \operatorname{Ab}_r g \, \mathrm{d}t = \int g \operatorname{Ab}_r \rho_C \, \mathrm{d}t$. As $r \uparrow 1$, $\operatorname{Ab}_r \rho_C \to \rho_C$ pointwise by (K3), since ρ_C is continuous and bounded by $C_\rho W_{-1/4,\ell_a}$, and $|g \operatorname{Ab}_r \rho_C| \le C_\rho C_K |g| \, W_{-1/4,\ell_a}$, an integrable function that does not depend on $r \in [\frac{1}{4}, 1)$. By dominated convergence, $\int_0^\infty \rho_C \operatorname{Ab}_r g \, \mathrm{d}t \to \int_0^\infty \rho_C \, g \, \mathrm{d}t = -g_{\mathrm{vac}}$ as $r \uparrow 1$.

Step (iii)*: the leakage of the lobe.* The lobe lives on $[0, T]$, the primaries on $[T, \infty)$, and what the kernel carries from the one to the others vanishes as $r \uparrow 1$: below $T+1$ by (K3), and beyond $T+1$ because across the gap the Gaussian tail of the kernel beats the Cardy growth of $\mathcal{N}_Z$. Let $g_\pm := \max(\pm g, 0)$, so that $g_+ = g + g_-$. Both are continuous with $0 \le g_\pm \le \|g\|_\infty$, and $\operatorname{supp} g_- \subset [0, T]$ because $g \ge 0$ on $[T, \infty)$. Let $u_T := 4\pi T$, $\sigma_T := \sqrt{u_T}$, $\epsilon := \sqrt{4\pi(T+1)} - \sigma_T > 0$ and $C_g := 1.18 \, u_T \|g\|_\infty$. For $t \ge T$ and $u' \le u_T$ we have $(\sigma - \sigma')^2 \ge (\sigma - \sigma_T)^2$, so (8.10) gives $\operatorname{Ab}_r g_-(t) \le \|g\|_\infty \int_0^{u_T} \mathcal{K}_r(u, u') \, \mathrm{d}u' \le \phi_r(t) := C_g (1-r)^{-1} e^{-\frac{\gamma_r}{2}(\sigma - \sigma_T)^2}$, and ϕ_r is C^1 and non-increasing on $[T, \infty)$. The primaries in $[T, T+1)$ carry total degeneracy at most $\mathcal{N}_Z(T+1) < \infty$; at each of them $0 \le \operatorname{Ab}_r g_-(t_n) \le \|g\|_\infty m_r \le 2\|g\|_\infty$ and $\operatorname{Ab}_r g_-(t_n) \to g_-(t_n) = 0$ by (K3) with $q = \ell = 0$, so $\sum_{t_n < T+1} d_n \operatorname{Ab}_r g_-(t_n) \to 0$ by dominated convergence. For those in $[T+1, \infty)$ we use (St) and (Z3): $\sum_{t_n \ge T+1} d_n \operatorname{Ab}_r g_-(t_n) \le \limsup_R \phi_r(R) \mathcal{N}_Z(R) + \int_{T+1}^\infty \mathcal{N}_Z \, |\phi_r'| \, \mathrm{d}t$. The first term vanishes: ϕ_r is a Gaussian in σ and $\mathcal{N}_Z$ at most exponential in σ. In the second, $|\phi_r'| \, \mathrm{d}t = C_g (1-r)^{-1} \gamma_r \, (\sigma - \sigma_T) \, e^{-\frac{\gamma_r}{2}(\sigma - \sigma_T)^2} \mathrm{d}\sigma$. With $s := \sigma - \sigma_T \ge \epsilon$ and $e^{-\frac{\gamma_r}{2} s^2} \le e^{-\gamma_r \epsilon^2/4} e^{-s^2/4}$, which holds because $\gamma_r \ge 1$ for $r \ge \frac{1}{4}$,

$$\int_{T+1}^\infty \mathcal{N}_Z \, |\phi_r'| \, \mathrm{d}t \le C' \, \frac{\gamma_r}{1-r} \, e^{-\gamma_r \epsilon^2/4}, \qquad C' := C_g C_N \int_0^\infty (1 + \sigma_T + s) \, s \, e^{\ell_a(\sigma_T + s) - s^2/4} \, \mathrm{d}s, \tag{8.14}$$

and C' does not depend on r. Since $(1-r)^{-1} \le \gamma_r \to \infty$, this tends to 0 as $r \uparrow 1$. Hence $\sum_n d_n \operatorname{Ab}_r g_-(t_n) \to 0$ as $r \uparrow 1$, and the sum is finite for each $r \in [\frac{1}{4}, 1)$.

Step (iv)*: Fatou's lemma on the primaries.* Since $\mathcal{K}_r > 0$, the function $\operatorname{Ab}_r g_+ = \operatorname{Ab}_r g + \operatorname{Ab}_r g_-$ is non-negative, and at every primary $\operatorname{Ab}_r g_+(t_n) \to g_+(t_n) = g(t_n)$ by (K3). By (8.13) and steps (ii) and (iii), $\sum_n d_n \operatorname{Ab}_r g_+(t_n) = \int_0^\infty \rho_C \operatorname{Ab}_r g \, \mathrm{d}t + \sum_n d_n \operatorname{Ab}_r g_-(t_n) \to -g_{\mathrm{vac}}$. Fatou's lemma [65, 1.28] for the positive measure $\sum_n d_n \delta_{t_n}$, along any sequence $r_j \uparrow 1$, now gives

$$0 \le \sum_n d_n \, g(t_n) = \sum_n d_n \lim_{j \to \infty} \operatorname{Ab}_{r_j} g_+(t_n) \le \liminf_{j \to \infty} \sum_n d_n \operatorname{Ab}_{r_j} g_+(t_n) = -g_{\mathrm{vac}} < 0, \tag{8.15}$$

a contradiction. Hence some primary has $t_n < T$. For the last assertion of Theorem 2, given $\varepsilon > 0$ choose $g \in \bar{\mathcal{A}}$ feasible at some $T \le T_V(c) + \varepsilon$; then $T > 0$ by section 2.4, so $\Delta_1 < T + a \le T_V(c) + a + \varepsilon$ for every admissible CFT, and ε is arbitrary. □

[ORIENTATION] If $g \in \bar{\mathcal{A}}$ obeys $|g(t)| \le C(1+t)^{-q} e^{-4\pi\sqrt{at}}$ for some $q > 1$, the same steps give a two-sided statement, whether or not g is feasible: on every admissible spectrum without light primaries, $\sum_n d_n |g(t_n)| < \infty$ and $g_{\mathrm{vac}} + \sum_n d_n \, g(t_n) = 0$. Indeed (St) and (Z3) then make $W_{-q,-\ell_a}$ integrable against $|\mathfrak{m}|$, and (K1), (K3) allow dominated convergence on both sides of $\langle \mathfrak{m}, \operatorname{Ab}_r g \rangle = 0$. The function of Theorem 5 decays in this way, for every q; Theorem 2 does not need it.

8.4 Consequences

By Theorem 2, $\Delta_1 \le T_V(c) + a$ for every admissible CFT with $c \ge 40$: the quantity that Theorem 4 bounds from below is a bound on theories, not only the value of a linear program. The two halves of Theorem 1 still say different things: attainment, with Theorem 2, is a statement about the spectra of actual theories, while optimality is a statement about the reach of the method—no functional in $\bar{\mathcal{A}}$ does better—and says nothing about the existence of theories with a gap near Δ_1^{best}.

Corollary 6 (proved, computer-assisted)**.** *For $c \geq c_0^{\mathrm{att}}$ the function $g = \frac{1}{2}(h_0 - \hat{h}_0)$ of Theorem 5 is feasible at $t_\star + 1$. Hence every admissible CFT with central charge $c \geq c_0^{\mathrm{att}}$ has*

$$\Delta_1 \;<\; a + t_\star + 1 \;=\; \frac{c}{\Lambda_V} + A_1\, c^{1/3} + O(1), \qquad A_1 = 0.483. \tag{8.16}$$

Proof. Theorem 5 states that $g \in \bar{\mathcal{A}}$ and that g is feasible at $t_\star + 1$; Theorem 2, which applies because $c_0^{\mathrm{att}} \geq 40$, then gives a primary with $t_n < t_\star + 1$. By Theorem 5, $t_\star = \xi_1^* c' + A_1 c'^{1/3}(1 + O(c'^{-2/3}))$, and $a + \xi_1^* c' = c'/\Lambda_V$ by the definition of Λ_V in Theorem 1; replacing $c' = c - 1$ by c changes the right side by $O(1)$. □

The tag is inherited from Theorem 5; the step from the functional to theories is by hand. The coefficient 0.483 belongs to one explicit construction and is not claimed to be the best; Conjecture 1 predicts $A_{\mathrm{opt}} = 0.27666$ for Δ_1^{best}. Nothing is said about the size of c_0^{att} or about finite c: at every central charge accessible to numerical work (8.16) is weaker than the numerical bounds (section 7.10). What Corollary 6 adds is that the slope Λ_V is reached by a bound on actual theories.

Remark (the case $g_{\mathrm{vac}} = 0$; proved)**.** Only the last step of (8.15) used $g_{\mathrm{vac}} > 0$. If $g \in \bar{\mathcal{A}}$ is weakly feasible at $T > 0$ with $g_{\mathrm{vac}} = 0$, steps (i)–(iv) give $\sum_n d_n\, g(t_n) \leq 0$ for every admissible spectrum with all $t_n \geq T$; since each term is non-negative, such a spectrum is supported on the zeros of g in $[T, \infty)$. This is the extremality statement of section 2.2, and by itself it bounds nothing.

9 A second route to attainment: one transform of one real function

Theorem 5 attains the slope with a functional $g = \frac{1}{2}(h_0 - \hat{h}_0)$, where h_0 is a product whose zeros sit at the quantiles of the zero law ρ_U. It is positive on the band because $\hat{h}_0$ is smaller there than h_0 itself; this, with a similar inequality for the vacuum value, is where a computer certifies finitely many inequalities. That proof gives a rate, $T_V(c) \leq \xi_1^* c' + 0.483\, c'^{1/3} + O(1)$, and it shows how the extremal potential U is a blueprint for a functional.

This section describes a second, quite different way to build a functional that certifies $\Delta_1 \leq c/\Lambda_V + o(c)$. It gives less and costs much less. Its building block is minus the imaginary part of a rotation of phase space by 45° applied to one real, positive function: $|\mathbf{r}'|^2$ times a bell that is a product of two double sine functions. The functional itself is the same transform of one real function, a combination of a few such blocks and of Gaussians. Its construction needs no positivity on an oscillating band and no computer. It gives the slope Λ_V but no rate, and it is far from the optimal functional. Nothing outside this section depends on it.

Result S1

For every $x_g > x_1^*$ there is $c_0(x_g) \geq 40$ such that for every $c \geq c_0(x_g)$ there is a functional $g \in \bar{\mathcal{A}}$ that is feasible at $T = c' x_g^2/3$. By Theorem 2 every admissible CFT with $c \geq c_0(x_g)$ then has $\Delta_1 < a + c' x_g^2/3$. Hence $\limsup_{c\to\infty} T_V(c)/c' \leq \xi_1^*$, and with Theorem 4, $\lim_{c\to\infty} c/\Delta_1^{\mathrm{best}}(c) = \Lambda_V$. No computer is used.

What is not obtained: a rate (the statement is $o(c)$ only), a value of $c_0(x_g)$, and any information about the optimal functional. The strategy has three steps.

(i) *Every real function gives a functional* (section 9.1). The Fourier transform is a quarter-turn of phase space (section 2.3). Let $\mathcal{R}$ be the eighth-turn, its square root. For every real radial function ϕ the imaginary part of $\mathcal{R}[\phi]$ is mapped to minus itself by the Fourier transform. So there is no constraint left to solve, and all the content is in the choice of ϕ.

(ii) *A seed whose image is a bump* (sections 9.2 and 9.3). We choose for ϕ the factor $|\mathbf{r}'|^2$ times a positive bell with a Gaussian core and exponential tails. At large c its image g_γ is a *bump*: it is negative on a window that contains its peak, its Cardy-weighted size $|g_\gamma|V$ is concentrated at exponential order around one point x_γ, its vacuum value is positive and of the same exponential order as the peak, and beyond the peak it decays faster than the Cardy weight grows. A parameter $\gamma \in (0,\pi)$ moves the peak over the whole interval $x_1^* < x_\gamma < \frac{1}{2}$ between the optimal gap bound and Hellerman's point. In terms of t the bump at central charge c is the *critical* member $\gamma = \pi$ of the family at the larger central charge $c'_\gamma = (\pi/\gamma)^2 c'$; read against the weaker Cardy growth of the lighter theory, it acquires a margin.

(iii) *From bumps to a feasible functional* (section 9.4). One bump with its peak just above x_1^* already has the right vacuum value and a negative lobe in the right place. Beyond x_g it is exponentially small compared with the inverse Cardy weight, but its sign is not known. We add, with an exponentially small coefficient, the negatives of bumps whose peaks cover $[x_g, \frac{1}{2}]$: they form a positive plateau that lies just below the Cardy line and dominates everything of unknown sign. Beyond $x = \frac{1}{2}$ the crossing kernels Ξ_β with $\beta < 1$ do the same job.

Level of rigor. The aim is to explain the strategy and the functional. Exact statements are marked as such. The large-c statements are leading-order saddle-point estimates; we state what they give and why, without uniform bounds on the remainders. For this reason Result S1 and Result S2 do not carry the tag [PROVED] of section 1.3, and the status of Theorem 1, Theorem 5 and Corollary 6 does not rest on this section.

Notation. It is that of section 2: $t = |\mathbf{r}|^2/2$ and $b = x + iy = \sqrt{3t/c'}$ (2.17); a functional is a real radial function g of $\mathbf{r} \in \mathbb{R}^2$, written as a function of t, with $\hat{g} = -g$ for the transform (2.9); ψ_k are the Laguerre functions (2.10); the Cardy weight V grows like $e^{c'L(x)}$ (2.18), and $\rho_C = 2\pi V$; for $g \in \bar{\mathcal{A}}$ the vacuum value is $g_{\mathrm{vac}} = -\int_0^\infty g\,\rho_C\,\mathrm{d}t$ (Definition 2.5), and feasibility is as in Definition 2.3; Ξ_β is the crossing kernel (2.4). The extremal potential U and $U_0 = U(0) = -0.388748$ are those of Lemma 6.5, with $U'(x) = -\frac{4}{3}\operatorname{arcsin}\sinh \pi x$ on $|x| < x_1^*$. The letters γ, b, Q, $\mathcal{G}$, s, w, σ, η, K are local to this section.

9.1 Every real function gives a functional: the eighth-turn

For a radial function ϕ on $\mathbb{R}^2$ let

$$\mathcal{R}[\phi](\mathbf{r}) := \sqrt{2}\, e^{i\pi/4}\, e^{-i\pi|\mathbf{r}|^2} \int_{\mathbb{R}^2} \phi(\mathbf{r}')\, e^{-i\pi|\mathbf{r}'|^2}\, e^{2\pi i\sqrt{2}\,\mathbf{r}\cdot\mathbf{r}'}\, \mathrm{d}^2\mathbf{r}', \tag{9.1}$$

a chirp, a Fourier transform dilated by $\sqrt{2}$, and a chirp. In the variables $t = |\mathbf{r}|^2/2$, $t' = |\mathbf{r}'|^2/2$,

$$\mathcal{R}[\phi](t) = 2\sqrt{2}\,\pi\, e^{i\pi/4} \int_0^\infty \phi(t')\, e^{-2\pi i(t+t')}\, J_0\big(4\pi\sqrt{2tt'}\big)\, \mathrm{d}t'. \tag{9.2}$$

Three exact properties are all that we need.

Gaussians. For $\operatorname{Re}\tau > 0$, a Fresnel integral gives

$$\mathcal{R}\big[e^{-2\pi\tau t'}\big](t) = \frac{\sqrt{2}\, e^{i\pi/4}}{\tau + i}\, e^{-2\pi\beta(\tau)\, t}, \qquad \beta(\tau) := \frac{1+i\tau}{\tau+i} = \frac{2\tau + i(\tau^2-1)}{1+\tau^2}. \tag{9.3}$$

For real $\tau > 0$ the image is a Gaussian at a complex inverse temperature on the unit circle, $|\beta| = 1$, $\operatorname{Re}\beta > 0$: it is a Gaussian times a chirp. As τ runs from 0 to ∞, $\beta(\tau)$ runs from $-i$ through 1 to $+i$.

Laguerre functions. Inserting $\tau = (1+z)/(1-z)$ in (9.3) and using the generating function $\sum_k \psi_k(t) z^k = (1-z)^{-1} e^{-2\pi t(1+z)/(1-z)}$, one finds that $\mathcal{R}$ maps the generating function at z to the one at iz. Hence

$$\mathcal{R}\,\psi_k = i^k\,\psi_k, \qquad \text{so that} \qquad \mathcal{R}^2\phi = \hat{\phi} \tag{9.4}$$

on radial functions. In the language of section 2.3, ψ_k is a state of the planar oscillator with $2k$ quanta, the Fourier transform is the evolution through a quarter period, and $\mathcal{R}$ is the evolution through one eighth of a period (in the opposite sense; on radial functions either sense squares to the Fourier transform). On WKB data the Fourier transform is the quarter-turn R of phase space (4.4), and $\mathcal{R}$ is a rotation by 45°.

Real seeds. Let $\phi = \sum_k c_k \psi_k$ with real c_k. By (9.4) and (2.10), $\widehat{\mathcal{R}[\phi]} = \sum_k c_k (-1)^k i^k \psi_k = \overline{\mathcal{R}[\phi]}$. Therefore

$$\Omega[\phi] := \operatorname{Im}\mathcal{R}[\phi] = \sum_{j\geq 0} (-1)^j\, c_{2j+1}\,\psi_{2j+1} \qquad \text{is real, radial, and} \qquad \widehat{\Omega[\phi]} = -\Omega[\phi]. \tag{9.5}$$

Every real radial function ϕ gives a functional $\Omega[\phi]$. In words, Ω discards the even Laguerre components of the seed, which the Fourier transform leaves alone, and keeps the odd ones with alternating signs. Only the part $\frac{1}{2}(\phi - \hat{\phi})$ of the seed matters, and a seed with $\hat{\phi} = \phi$, for instance $e^{-2\pi t}$, gives zero.

The sum rule, seen directly. Apply (9.3) to the reduced partition function (2.2) term by term. The Gaussian seed $e^{-2\pi\tau\tau'}$ produces $\frac{\sqrt{2}e^{i\pi/4}}{\tau+i}\hat{Z}(\beta)$ with $\beta = \beta(\tau)$ on the unit circle, where $1/\beta = \bar{\beta}$. There the crossing equation (2.3), $\hat{Z}(\beta) = \beta^{-1}\hat{Z}(1/\beta)$, continued to $\operatorname{Re}\beta > 0$, reads $\hat{Z}(\beta) = \beta^{-1}\overline{\hat{Z}(\beta)}$: it says that $\beta^{1/2}\hat{Z}(\beta)$ is real. Since $\beta(\tau) = i(\tau-i)/(\tau+i)$, the coefficient in (9.3) is $\sqrt{2/(1+\tau^2)}\;\beta^{1/2}$, a positive multiple of the principal square root of β. So $\mathcal{R}$ of a real superposition of Gaussians, applied to $\hat{Z}$, is real provided the superposition converges on $\hat{Z}$, and its imaginary part vanishes: this is the sum rule for $\Omega[\phi]$. The bell $\mathcal{G}$ of section 9.2 is a superposition of Gaussians $e^{-2\pi\tau\tau'}$, $\tau > 0$, with positive weights (the product over its zeros and poles shows that $\mathcal{G}$ is a completely monotone function of r^2), and the factor $|\mathbf{r}'|^2 = 2t'$ of the seed is $-\pi^{-1}\partial_\tau$ acting on them. So the seed is a real superposition, which converges on $\hat{Z}$ for $\gamma < \pi$, and its functional acts on $\hat{Z}$ along the unit semicircle in the β-plane, which is the set fixed by S followed by complex conjugation. The crossing kernels are of this form too: for $0 < \beta < 1$, Ξ_β is a multiple of Ω applied to the real part of a complex Gaussian. In the proof of Result S1 we do not use this paragraph; Theorem 2 handles the sum rule for every feasible $g \in \bar{\mathcal{A}}$.

9.2 The seed and the functional

Fix a *deformation parameter* $\gamma \in (0, \pi)$. Let

$$\mathsf{b} := \frac{\gamma}{2\pi}\sqrt{\frac{3}{c'}}, \qquad Q := \mathsf{b} + \frac{1}{\mathsf{b}}, \qquad \mathcal{G}(r) := S_{\mathsf{b}}(\tfrac{Q}{4} + ir)\, S_{\mathsf{b}}(\tfrac{Q}{4} - ir) = \left|S_{\mathsf{b}}(\tfrac{Q}{4} + ir)\right|^2, \tag{9.6}$$

where $S_{\mathsf{b}}(z) = \Gamma_{\mathsf{b}}(z)/\Gamma_{\mathsf{b}}(Q-z)$ is the double sine function familiar from Liouville theory [70, 71]; the letter b is its parameter and has nothing to do with the variable b of (2.17). All that is needed about it follows from the integral representation

$$\log\mathcal{G}(r) = \int_0^\infty \frac{\mathrm{d}v}{v}\left[\frac{\sinh(Qv/2)}{\sinh(\mathsf{b}v)\,\sinh(v/\mathsf{b})}\,\cos(2rv) - \frac{Q}{2v}\right], \qquad |\operatorname{Im} r| < \frac{Q}{4}. \tag{9.7}$$

The seed and the functional are

$$\boxed{\phi_\gamma(\mathbf{r}') := |\mathbf{r}'|^2\,\frac{\mathcal{G}(|\mathbf{r}'|)}{\mathcal{G}(0)}, \qquad g_\gamma := -\,\Omega[\phi_\gamma] = -\operatorname{Im}\mathcal{R}[\phi_\gamma].} \tag{9.8}$$

The argument of $\mathcal{G}$ is the radius in the plane, and c enters only through b. By (9.5), $\hat{g}_\gamma = -g_\gamma$ exactly, for every c and every γ. As $\gamma \to 0$ the seed becomes $|\mathbf{r}'|^2 e^{-\pi|\mathbf{r}'|^2} = \frac{1}{2\pi}(\psi_0 - \psi_1)$ and $g_\gamma \to \frac{1}{2\pi}\psi_1$, the lowest derivative functional of section 2.2.

The seed at large c. Let $s := \sqrt{3t'/c'}$ be the rescaled radius of the seed, so that s is to $\mathbf{r}'$ what x is to $\mathbf{r}$, and let $w := \sqrt{2}\,\gamma s = 2\pi\mathsf{b}|\mathbf{r}'|$. Expanding (9.7) at small b,

$$\log \frac{\mathcal{G}}{\mathcal{G}(0)} = c'\, h_\gamma(s) - \tfrac{1}{4}\log\cosh w + O(1/c'), \qquad h_\gamma(s) := -\frac{2\pi}{3\gamma^2}\int_0^{\sqrt{2}\gamma s} \mathrm{gd}(w')\,\mathrm{d}w', \tag{9.9}$$

uniformly on $|\mathrm{Im}\, w| \le \frac{\pi}{2} - \epsilon$, where $\mathrm{gd}\, w = \arctan\sinh w = \int_0^w \mathrm{sech}$ is the Gudermannian. Thus $\mathcal{G}$ is a positive bell. For $w \ll 1$ it is the Gaussian $e^{-2\pi t'}$, because $h_\gamma \simeq -\frac{2\pi}{3}s^2$. For $w \gg 1$ it has the exponential tail $e^{-c'(\sqrt{2}\pi^2/3\gamma)\,s}$, because $\mathrm{gd} \to \frac{\pi}{2}$. It is analytic in the strip $|\mathrm{Im}\, s| < \pi/(2\sqrt{2}\gamma)$; the first pole of $\mathcal{G}$, at $r = iQ/4$, lies on the imaginary axis just outside it, at $\mathrm{Im}\, s = (1+\mathsf{b}^2)\,\pi/(2\sqrt{2}\gamma)$. Nothing else about S_b is used. In particular the elementary function $|\mathbf{r}'|^2(\cosh w)^{-1/4}e^{c'h_\gamma(s)}$ could serve as the seed as well, since exactness comes from (9.5) and not from the seed; $\mathcal{G}$ is the completion of this expression to all orders in $1/c'$ (section 9.5). The factor $|\mathbf{r}'|^2$ is there to make the imaginary part the larger part of $\mathcal{R}[\phi_\gamma]$.

9.3 At large c the functional is a bump

Classical data. For $0 < \gamma \le \pi$ and $0 \le x \le x_\mathrm{t}$ let

$$q_\gamma(x) := \frac{\mathrm{arcsin}\sinh(\gamma x)}{\gamma}, \qquad x_\mathrm{t} := \frac{\mathrm{arcsinh}\,1}{\gamma} = \frac{\pi}{\gamma}\,x_1^*, \qquad x_\gamma := \frac{1}{\gamma}\,\mathrm{arcsinh}\sin\frac{\gamma}{2}. \tag{9.10}$$

The function q_γ increases from 0 to $\pi/2\gamma$ at the *turning point* x_t, and $q_\gamma(x_\gamma) = \frac{1}{2}$. The *profile* of the bump is

$$U_\gamma(x) := -m_\gamma - \frac{4\pi}{3}\int_0^x q_\gamma(x')\,\mathrm{d}x', \qquad m_\gamma := \frac{4\pi}{3}\int_0^{x_\gamma}(\tfrac{1}{2} - q_\gamma)\,\mathrm{d}x, \tag{9.11}$$

where the constant m_γ is chosen so that $U_\gamma + L$ has the maximum 0; the maximum is at x_γ, because $U_\gamma' = -\frac{4\pi}{3}q_\gamma$ equals $-L' = -\frac{2\pi}{3}$ there. In the language of section 4.1, $p = -iq_\gamma$ is the imaginary momentum (4.3) of a wave function under a barrier, $q_\gamma(x)/x$ is its local inverse temperature (the $\mathrm{Im}\,\tau$ of section 4.1), and (b, p) lies on the curve $\sinh\gamma b = i\sinh\gamma p$, which is the spectral curve (4.13) with π replaced by γ. Since $(U_\gamma + L)'' = -\frac{4\pi}{3}\cosh\gamma x\,(1 - \sinh^2\gamma x)^{-1/2} \le -\frac{4\pi}{3}$,

$$U_\gamma(x) + L(x) \le -\tfrac{2\pi}{3}\,(x - x_\gamma)^2 \qquad (0 \le x \le x_\mathrm{t}). \tag{9.12}$$

At $\gamma = \pi$ one has $x_\gamma = x_\mathrm{t} = x_1^*$, $m_\pi = -U_0 = 0.388748$ and $U_\pi = U$ on $[0, x_1^*]$ (6.18). For general γ,

$$U_\gamma(x) + m_\gamma = \Big(\frac{\pi}{\gamma}\Big)^2\Big[U\Big(\frac{\gamma x}{\pi}\Big) - U_0\Big], \qquad \text{that is,} \qquad c'\,[U_\gamma(x) + m_\gamma] = c'_\gamma\,[U(\tilde{x}) - U_0] \tag{9.13}$$

with $c'_\gamma = (\pi/\gamma)^2 c'$ and $\tilde{x} = \sqrt{3t/c'_\gamma} = \gamma x/\pi$: at a given t, the profile is the critical one of the heavier theory. This is exact for the functional itself: b depends on γ^2/c' only, so g_γ at c' and g_π at c'_γ are the same function of t. As γ decreases from π to 0, the peak x_γ increases from x_1^* to $\frac{1}{2}$, the distance $x_\mathrm{t} - x_\gamma$ from the peak to the turning point increases from 0 to ∞, and m_γ increases from 0.3887 to $\pi/6$. Figure 9(a) shows $U_\gamma + L$.

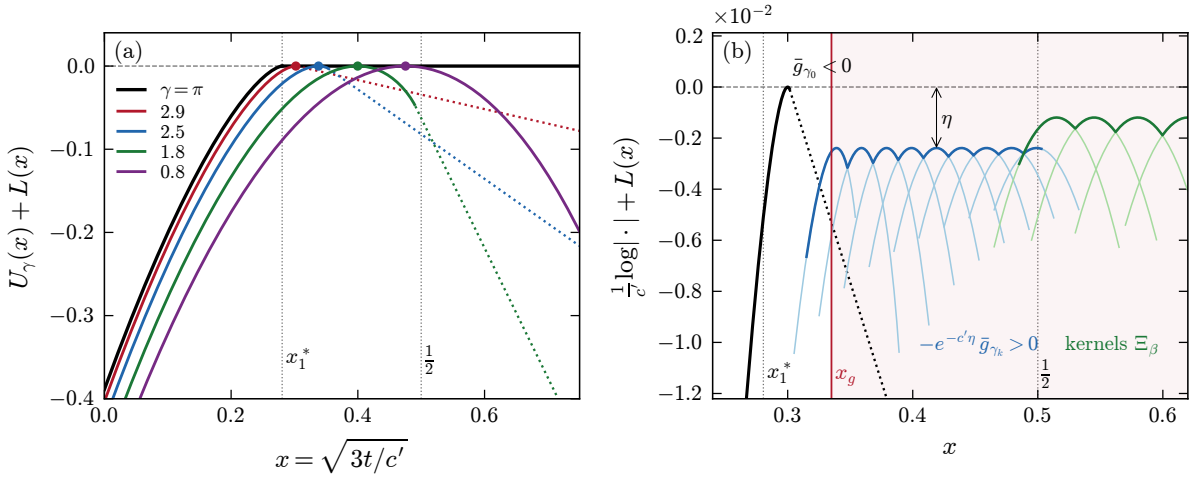


Figure 9: Drawn from the leading-order formulas of sections 9.3 and 9.4, not from data. (a) The Cardy-weighted profile $U_\gamma + L$ of the bump g_γ, that is, the large-c limit of $\frac{1}{c'}\log\big(|\bar g_\gamma| V\big)$. It has its maximum 0 at the peak x_γ (dots), which moves from x_1^* to $\frac12$ as γ decreases from π to 0. Solid: up to the turning point x_t; dotted: beyond it, where by (B2) $|g_\gamma|$ falls at least with the slope $-2\pi^2/3\gamma$, steeper than the Cardy line. The critical member $\gamma=\pi$ is the extremal potential U of section 6; beyond x_1^* it runs along the Cardy line. (b) The assembly of section 9.4; margins and heights are schematic, chosen for visibility. Black: the main bump $\bar g_{\gamma_0}$, negative near its peak; its tail (dotted) has unknown sign but lies below the Cardy line by η_1 or more beyond x_g. Blue: the negated bumps $-e^{-c'\eta}\bar g_{\gamma_k}$ (light blue, drawn near their peaks), positive on their windows, whose upper envelope is a plateau at height $-\eta$ over $[x_g, \frac12]$. Green: crossing kernels Ξ_β with $\beta<1$, which take over beyond $x=\frac12$. The sum is non-negative on the shaded region $x \ge x_g$.

The saddle point. Put $t = c'x^2/3$ and $t' = c's^2/3$ in (9.2). For $x \ge x_\mathrm{min} > 0$ the argument of the Bessel function is large except near $s=0$. Since the seed is even and analytic in s, one may replace J_0 on the half line by $\frac12 H_0^{(1)}$ on a line just above the real axis, and $H_0^{(1)}(z) \simeq \sqrt{2/\pi z}\, e^{i(z-\pi/4)}$. With (9.9) the integrand becomes a slowly varying amplitude times $e^{c'\Theta}$, where

$$\Theta(s;x) := -\frac{2\pi i}{3}\,(x^2 - 2\sqrt2\, xs + s^2) + h_\gamma(s). \tag{9.14}$$

The first term is the generating function of the rotation by 45°, and the second is the WKB exponent of the seed. The saddle-point equation $\partial_s\Theta = 0$ reads $\mathrm{gd}(\sqrt2\gamma s) = i\gamma\,(2x - \sqrt2 s)$. It is solved with the identity $\mathrm{gd}(A+iB) = B + iA$, valid whenever $\sinh A = \sin B$ with $|B| < \frac\pi2$: take $A = \gamma x$ and $B = \gamma q_\gamma(x)$. The saddle is at

$$s_*(x) = \frac{x + i\,q_\gamma(x)}{\sqrt2}, \qquad \text{where} \qquad \Theta\big(s_*(x);x\big) = U_\gamma(x) + m_\gamma \tag{9.15}$$

and $\partial_s^2\Theta = -\frac{4\pi}{3}\big(i + \mathrm{sech}\,\gamma(x+iq_\gamma)\big)$, whose real part is negative. The value at the saddle holds because both sides vanish at $x=0$ and $\frac{\mathrm d}{\mathrm dx}\Theta(s_*(x);x) = \partial_x\Theta\big|_{s_*} = -\frac{4\pi i}{3}(x - \sqrt2 s_*) = -\frac{4\pi}{3}q_\gamma(x)$. The transform samples the real, positive seed at a *complex* radius, and the rotation turns its bell into a tunnelling profile. The saddle lies inside the strip of analyticity of the seed as long as $q_\gamma(x) < \pi/2\gamma$, that is, $x < x_\mathrm{t}$: it reaches the edge of the strip, which to leading order is the height of the first pole of the seed, exactly at the turning point. There also $\partial_s^2\Theta = 0$: two saddles coalesce. On a horizontal line $\mathrm{Re}\,\Theta$ is concave in $\mathrm{Re}\,s$, because $\mathrm{Re}\,\mathrm{sech}\,w > 0$ for $|\mathrm{Im}\,w| < \frac\pi2$; so on the line through s_* the maximum of $|e^{c'\Theta}|$ is at s_*. Laplace's method gives the first of the following three properties.

Result S2 (the bump)

Fix $\gamma \in (0,\pi)$, $0 < x_{\min} < 0.18$, $0 < \delta \le \frac{1}{3}(x_{\mathrm{t}} - x_\gamma)$ and $\bar{x} \in (x_\gamma, x_{\mathrm{t}} - \delta]$. As $c \to \infty$:

(B1) *Window.* Uniformly for $x_{\min} \le x \le x_{\mathrm{t}} - \delta$,

$$\mathcal{R}[\phi_\gamma](c'x^2/3) = c' A_\gamma(x)\, e^{c'[U_\gamma(x)+m_\gamma]}\, e^{i\varphi_\gamma(x)}(1 + O(c'^{-1/2})), \tag{9.16}$$

with the phase $\varphi_\gamma = \frac{5}{2}\arctan(q_\gamma/x) - \frac{\pi}{8}$ and the amplitude $A_\gamma = \frac{2^{3/4}}{6}(x^2 + q_\gamma^2)^{5/4} x^{-1/2}(1-\sinh^2\gamma x)^{-1/4} > 0$. Since $1 \le q_\gamma/x \le 1/(2x_1^*) = 1.782$, the phase lies in $[\frac{\pi}{2}, 2.26]$ and $\sin\varphi_\gamma \ge 0.77$. Hence $g_\gamma < 0$ on the window, and $-g_\gamma = e^{c'[U_\gamma(x)+m_\gamma+o(1)]}$.

(B2) *Tail.* For $x \ge \bar{x}$, $|g_\gamma(c'x^2/3)| \le e^{c'[U_\gamma(\bar{x})+m_\gamma - \frac{4\pi}{3}q_\gamma(\bar{x})(x-\bar{x})+o(1)]}$: the slope is steeper than that of the Cardy line, since $q_\gamma(\bar{x}) > \frac{1}{2}$. Also $|g_\gamma| \le C$ for all $t \ge 0$.

(B3) *Vacuum.* $g_{\gamma,\mathrm{vac}} = -\int_0^\infty g_\gamma\, \rho_C\, \mathrm{d}t = e^{c'[m_\gamma+o(1)]} > 0$.

For (B2) one keeps the contour at the height $\operatorname{Im} s = q_\gamma(\bar{x})/\sqrt{2}$ for all $x \ge \bar{x}$; on that line $\operatorname{Re}\Theta(\cdot\,;x) = \operatorname{Re}\Theta(\cdot\,;\bar{x}) - \frac{4\pi}{3}q_\gamma(\bar{x})(x-\bar{x})$ exactly, by (9.14). The bound $|g_\gamma| \le C$ is $|J_0| \le 1$ in (9.2). For (B3), by (B1) the integrand $-g_\gamma\rho_C$ is positive on the window and equals $e^{c'[U_\gamma+L+m_\gamma+o(1)]}$, which is $e^{c'[m_\gamma+o(1)]}$ at the peak; the rest of the window is smaller by (9.12), the tail by (B2), and the region $x \le x_{\min}$ contributes at most $Cc'e^{c'L(x_{\min})}$, which is negligible because $L(x_{\min}) < 0.38 < m_\gamma$. By (B2), $M[g_\gamma] < \infty$, so $g_\gamma \in \bar{\mathcal{A}}$.

In what follows we use the *normalized bump* $\bar{g}_\gamma := g_\gamma/g_{\gamma,\mathrm{vac}}$. It has vacuum value 1. On the window, $-\bar{g}_\gamma = e^{c'[U_\gamma(x)+o(1)]}$, which touches the inverse Cardy weight $e^{-c'L}$ at x_γ and lies below it elsewhere. With $\bar{x} := x_\gamma + 2\delta \le x_{\mathrm{t}} - \delta$, (B1), (9.12) and (B2) give

$$|\bar{g}_\gamma(c'x^2/3)| \le e^{-c'[L(x)+\eta_\delta-o(1)]} \qquad (x \ge x_\gamma + \delta), \qquad \eta_\delta := \tfrac{2\pi}{3}\delta^2. \tag{9.17}$$

Beyond $\bar{x}$ the bump carries in addition the factor $e^{-c'\sigma(x-\bar{x})}$ with $\sigma := \frac{4\pi}{3}(q_\gamma(\bar{x}) - \frac{1}{2}) > 0$, by (B2). A bump is thus a functional that, per unit of vacuum value, delivers the Cardy rate at one point $x_\gamma \in (x_1^*, \frac{1}{2})$ of our choice, with the negative sign, and is exponentially smaller than the Cardy rate beyond it.

9.4 From bumps to a feasible functional

Crossing kernels beyond Hellerman's point. Let $x' > \frac{1}{2}$ and $\beta = 1/(2x') < 1$. Then $\Xi_\beta(t) \ge \frac{1}{2}e^{-2\pi\beta t} > 0$ for $t \ge t_\beta := \log(2/\beta)/[2\pi(\beta^{-1} - \beta)]$, which does not depend on c, and the vacuum value of Ξ_β is negative with $-\Xi_{\beta,\mathrm{vac}} \le \beta^{-1}e^{2\pi a/\beta} = 2x'e^{\frac{1}{2}c'L(x')}$. Since $2\pi\beta t = \pi c'x^2/3x'$ and $x' + x^2/x' = 2x + (x-x')^2/x'$, for $t = c'x^2/3 \ge t_\beta$

$$\frac{\Xi_\beta(c'x^2/3)}{-\Xi_{\beta,\mathrm{vac}}} \;\ge\; \frac{1}{4x'}\,\exp\Big\{-c'\Big[L(x) + \frac{\pi(x-x')^2}{3x'}\Big]\Big\}. \tag{9.18}$$

Per unit of vacuum cost, the kernel $\Xi_{1/2x'}$ delivers the Cardy rate at $x = x'$, with the positive sign. But it does so only for $x' > \frac{1}{2}$, because Ξ_β with $\beta > 1$ is negative at large t. This is why a positive plateau at the Cardy rate can be made of crossing kernels with real β only beyond Hellerman's point $x = \frac{1}{2}$, that is, $\Delta \approx c/6$; the bumps reach the Cardy rate on the remaining interval $(x_1^*, \frac{1}{2})$.

Consequently, let $|f(c'x^2/3)| \le e^{-c'[L(x)+\eta']}$ for $x \ge x_a \ge \frac{1}{2}$, with the extra factor $e^{-c'\sigma(x-x_b)}$, $\sigma > 0$, for $x \ge x_b$. Then, for all sufficiently large c, f is dominated there by a combination $R = \sum_j \alpha_j \Xi_{\beta_j}$ with $\alpha_j \ge 0$ and $\beta_j < 1$: $R \ge |f|$ for $x \ge x_a$, $R \ge 0$ for $t \ge t_R$ with t_R independent of c, and $-R_{\mathrm{vac}} \le e^{-c'\eta'/4}$. On the compact range $[x_a, x_b]$ one takes finitely many nodes $x_j' > \frac{1}{2}$, bounded away from $\frac{1}{2}$, at a spacing small compared with $\sqrt{\eta'}$, with the coefficients

$\alpha_j = e^{-c'\eta'/2}/(-\Xi_{\beta_j,\mathrm{vac}})$: by (9.18) the node next to x gives more than $e^{-c'[L(x)+\eta']}$, and each node costs $e^{-c'\eta'/2}$ of vacuum value. On the tail $x \geq x_b$ one takes equally spaced nodes whose coefficients decrease from node to node by the factor that f loses, so that their costs form a geometric series. We call R a *repair* of f.

The functional. Fix $x_g \in (x_1^*, \frac{1}{2})$. The map $\gamma \mapsto x_\gamma$ is a decreasing bijection of $(0,\pi)$ onto $(x_1^*, \frac{1}{2})$.

(1) *Main bump.* Choose γ_0 with $x_1^* < x_{\gamma_0} < x_g$. By (9.12) and (B2), used with $\bar{x}$ between x_{γ_0} and $\min(x_g, x_\mathrm{t})$, there is $\eta_1 > 0$ with $|\bar{g}_{\gamma_0}| \leq e^{-c'[L(x)+\eta_1-o(1)]}$ for $x \geq x_g$.

(2) *Margins.* Let γ_g be the value of γ with $x_\gamma = x_g$, and let δ be a third of the distance $x_\mathrm{t} - x_\gamma$ at γ_g. This distance grows as γ decreases, so $\delta \leq \frac{1}{3}(x_\mathrm{t} - x_\gamma)$ for every bump with its peak in $[x_g, \frac{1}{2})$. Let K bound $\frac{1}{2}|(U_\gamma + L)''|$ on the windows $[x_{\min}, x_\gamma + \delta]$ of all these bumps; it is finite because $(U_\gamma + L)''$ depends on γx only, and $\gamma x \leq \gamma_g(x_g + \delta) < \operatorname{arcsinh} 1$ there. Choose a mesh $\epsilon < \delta/2$ and $\eta > 0$ with $\eta + K\epsilon^2 < \min(\eta_1, \eta_\delta)$.

(3) *Plateau.* Choose $\gamma_1 > \cdots > \gamma_N$ whose peaks $x^{(k)} := x_{\gamma_k}$ form a grid of $[x_g, \frac{1}{2})$ of mesh at most ϵ, with $x^{(1)} \leq x_g + \epsilon$ and $x^{(N)} \geq \frac{1}{2} - \epsilon$.

(4) *Repairs.* Let R_0 be a repair of $\bar{g}_{\gamma_0}$ on $x \geq \frac{1}{2}$, and R_k a repair of $\bar{g}_{\gamma_k}$ on $x \geq \max(\frac{1}{2}, x^{(k)} + \delta)$; what a repair needs is supplied by step (1), by (9.17) and by the remark after it.

All these choices are made before $c \to \infty$; for the repairs this means their nodes, hence t_R, while their coefficients depend on c. The functional is the flat sum

$$\boxed{g := \bar{g}_{\gamma_0} + R_0 + e^{-c'\eta} \sum_{k=1}^{N} (-\bar{g}_{\gamma_k} + R_k).} \tag{9.19}$$

It is drawn in figure 9(b).

Why it is feasible at $T = c'x_g^2/3$. *On $x_g \leq x \leq \frac{1}{2}$.* The repairs are non-negative there, since $c'x_g^2/3 \geq t_R$ for large c. A bump with $x \leq x^{(k)} + \delta$ has x in its window, where $-\bar{g}_{\gamma_k} > 0$ by (B1); the one whose peak is within ϵ of x contributes at least $e^{-c'[L(x)+\eta+K\epsilon^2+o(1)]}$. A bump with $x > x^{(k)} + \delta$ contributes at most $e^{-c'[L(x)+\eta+\eta_\delta-o(1)]}$ in modulus, by (9.17). With step (1),

$$g(c'x^2/3) \;\geq\; e^{-c'L(x)}\Big[e^{-c'(\eta+K\epsilon^2+o(1))} - e^{-c'(\eta_1-o(1))} - N\,e^{-c'(\eta+\eta_\delta-o(1))}\Big] > 0 \tag{9.20}$$

for large c, by step (2). *On $x \geq \frac{1}{2}$.* Here $\bar{g}_{\gamma_0} + R_0 \geq 0$; and for each k either x is in the window of the k-th bump and $-\bar{g}_{\gamma_k} > 0$, or $x \geq x^{(k)} + \delta$ and $-\bar{g}_{\gamma_k} + R_k \geq 0$. *Vacuum.* By linearity $g_\mathrm{vac} \geq 1 - 2e^{-c'\eta_1/4} - N\,e^{-c'\eta}\,(1 + o(1)) > 0$. *Class.* Each term is in $\bar{\mathcal{A}}$. The tail repairs are infinite sums; they converge in L^1 and in the norm $M[\,\cdot\,]$, because $M[\Xi_\beta] \leq \frac{1}{\pi}\beta^{-1}e^{2\pi a/\beta}$, the quantity that bounds the vacuum cost. So $g \in \bar{\mathcal{A}}$.

Thus $g \in \bar{\mathcal{A}}$ is feasible at $c'x_g^2/3$ for all sufficiently large c, which is Result S1. Everything rests on one feature of the bumps: all windows begin at the same point $x_{\min} < x_1^*$. At any $x \geq x_g$ a negated bump is either inside its window, and then positive, or beyond it, and then exponentially below the Cardy line. So all the negated bumps can enter with the same coefficient $e^{-c'\eta}$, and no positivity of an oscillating function is ever needed.

By linearity, $g = \Omega[\phi]$ for a single real seed,

$$\phi = -\bar{\phi}_{\gamma_0} + e^{-c'\eta}\sum_{k=1}^{N}\bar{\phi}_{\gamma_k} + (\text{real parts of complex Gaussians}), \qquad \bar{\phi}_\gamma := \phi_\gamma/g_{\gamma,\mathrm{vac}}\,: \tag{9.21}$$

the functional is one transform of one real function. For x_g near x_1^* the corrections to $-\bar{\phi}_{\gamma_0}$ are exponentially small on the real axis; they matter only after continuation to the complex radius s_* at which the transform samples the seed.

9.5 Remarks

Comparison with the functional of Theorem 5. The functional of Theorem 5 is built to have the profile U: its zeros are placed by the zero law, it runs along the Cardy line on the band, and the difficulty is to show that the oscillating function $h_0 - \hat{h}_0$ stays positive there. The functional (9.19) avoids the band altogether. On $[x_g, \frac{1}{2}]$ it lies below the Cardy line by the fixed margin η (figure 9(b)), so it is positive for a crude reason, and it is far from extremal. The price is that the margins η_1, η_δ, η go to zero as $x_g \to x_1^*$, while the estimates hold for $c'\eta \gg 1$; this is why no rate comes out. The two constructions share the potential U and nothing else. A third construction, in Mellin space, is sketched in appendix A.

Consistency with the optimality theorem. Theorem 3 forbids a function in $\bar{\mathcal{A}}$ whose Cardy-weighted mass sits below x_1^*. Accordingly the peaks obey $x_\gamma > x_1^*$. At $\gamma = \pi$ the peak, the turning point and x_1^* coincide, and to leading order the tail falls at the Cardy rate: $|g_\pi|V$ is flat at exponential order along the whole band, and the critical member has no margin. (It is still in $\bar{\mathcal{A}}$: the first pole of $\mathcal{G}$ is at $\operatorname{Im} r = Q/4$ and not at $1/4\mathsf{b}$, so its tail beats the Cardy weight by the factor $e^{-\pi x/2}$, which does not depend on c; $M[g_\gamma] = \infty$ only for $\gamma > \pi(1+\mathsf{b}^2)$.) For fixed $\gamma > \pi$ the tail is slower than the Cardy rate. Taking $\gamma < \pi$ is what creates the margins, and by (9.13) it amounts to borrowing the critical function of a heavier theory.

Why this seed [HEURISTIC]**.** On WKB data a function that the Fourier transform maps to $\pm$ itself lives on a curve invariant under the quarter-turn, and the relevant one is $\sinh \gamma b = i \sinh \gamma p$. It is exponential in both b and p, and an exponential of a momentum is a finite shift, so its quantization is a difference equation rather than a differential one. In the rotated coordinates $s = (b-p)/\sqrt{2}$, $p_s = (b+p)/\sqrt{2}$ the curve is a graph, $p_s = -(i/\sqrt{2}\gamma)\ \mathrm{gd}(\sqrt{2}\gamma s)$, with the momentum normalized as in (4.3): this is the saddle-point relation (9.15) read backwards, and $c'h_\gamma$ is the corresponding WKB exponent. On a graph the quantized equation is of first order, and its normalizable solution is $\mathcal{G}$: a first-order difference equation with trigonometric coefficients is solved by double sine functions, as $f(z+1) = zf(z)$ is solved by the Gamma function. The expansion (9.9) is its WKB form to one loop. The function $\mathcal{G}$ is moreover equal to its own Fourier transform in one dimension, a special case of the Fourier transformation formula of [70, 71], which reflects the invariance of the curve; we do not use this. So the bell $\mathcal{G}$ is the wave function of the quantized, deformed spectral curve in the rotated polarization, and the bump is the same state in the polarization of section 4. The passage to the plane, with the radius as the argument and the factor $|\mathbf{r}'|^2$, is a recipe that works because the centrifugal term is invisible at leading order; we have not derived it. We know of no meaning in conformal field theory of the shift by $i\mathsf{b}$, and at $\gamma = \pi$ the parameter is not that of Liouville theory at the same central charge ($\mathsf{b}^2 = 3/4c'$, against $6/c$).

Zeros. The functional (9.19) is strictly positive on $[x_g, \frac{1}{2}]$; it has no band of double zeros. If $x_g \to x_1^*$ slowly as $c \to \infty$, it is a sequence that attains Λ_V. By Theorem 7 its profile then tends to U, and its zeros in the strip have the density $c'\rho_U$ within any fixed distance of the slits. These zeros lie off the real axis; we have not located them.

10 What near-optimal functionals must look like

This section is proved throughout, and no computer enters. It uses Proposition 6.4, Lemma 6.5, Definition 6.6 and Lemma 6.7 and, only to know that attaining sequences exist, Theorem 5. Nothing outside this section depends on it.

Theorems 3 and 4 are inequalities at finite c: they bound what a functional can certify. Here we ask the converse question: what must a functional look like that comes close to the bound?

The tool is a limit. Along a sequence $g_j \in \bar{\mathcal{A}}$ at central charges $c_j \to \infty$ the profiles u_{g_j} are functions on one and the same strip $\mathbb{S}$, which does not depend on c. If the sequence attains the slope Λ_V, the limit is the extremal potential U, and the zeros of g_j follow the zero law ρ_U (Theorem 7).

10.1 Limits of potentials

Let $g \in \bar{\mathcal{A}} \setminus \{0\}$. By section 6.3, $G(b) = g(c'b^2/3)$ is even and holomorphic on $\mathbb{S}$, and bounded and continuous on $\bar{\mathbb{S}}$; and the profile (6.13), with its Riesz measure (6.10),

$$u_g(b) = \frac{1}{c'} \log \frac{|G(b)|}{M[g]}, \qquad \mathfrak{n}_g = \frac{1}{2\pi} \nabla^2 u_g = \frac{1}{c'} \sum_{\zeta \in \mathbb{S}:\ G(\zeta)=0} m_\zeta \, \delta_\zeta, \tag{10.1}$$

is the potential of positive point charges m_ζ/c' at the zeros of G in the strip: $\mathfrak{n}_g$ is the zero-counting measure of G divided by c'. For a sequence we write $u_j := u_{g_j}$ and $c_j' := c_j - 1$. As in Theorem 4, g is called weakly feasible if it is weakly feasible at some T, hence at $T = t_1(g)$, and $x_1(g) = \sqrt{3\, t_1(g)/c'}$ as in (2.17). The idea is that the three facts on which section 6 rests pass to the limit: limits of subharmonic functions are subharmonic; the majorant of Proposition 6.4, whose error is $O(\log c'/c')$, becomes exact; and weak feasibility, which enters through the half-mass condition (2.16), becomes contact with the Cardy line. The notions needed to say this are in the box; the proofs are in appendices I.1 to I.3.

Toolkit: limits of potentials

Let u_j be potentials of positive charges $\mathfrak{n}_j = \frac{1}{2\pi}\nabla^2 u_j$ on $\mathbb{S}$ (subharmonic functions). *Convergence in* L^1_{loc} is convergence of the potentials in the mean on every compact set, $\int_K |u_j - u| \, \mathrm{d}A \to 0$; pointwise convergence is too much to ask, because a potential is $-\infty$ at its charges, but the logarithm is integrable in two dimensions. *Vague convergence* $\mathfrak{n}_j \to \mathfrak{n}$ is convergence of the charge distributions when tested against continuous functions of compact support; then $\mathfrak{n}_j(K) \to \mathfrak{n}(K)$ for every compact K whose boundary carries no charge of $\mathfrak{n}$. *Compactness* [72, Thms. 3.2.12–3.2.13]: potentials that are bounded above on compact sets, uniformly in j, and do not run off to $-\infty$ carry a bounded charge on every compact set, and along a subsequence potentials and charges both converge. *Upper semicontinuity:* at a point a limit potential can jump up, never down; the form that we use is (I.1). *Superharmonic, strong minimum principle, circle means:* θ is superharmonic if $-\theta$ is subharmonic; on a connected open set a non-negative superharmonic function is identically zero or strictly positive, and its mean over a circle is at most its value at the center [72, §3.2], [63, Thm. 2.3.1].

Lemma 10.1 (Compactness; proved)**.** *Let $c_j \to \infty$ and $g_j \in \bar{\mathcal{A}} \setminus \{0\}$. After passing to a subsequence, either* (i) *$u_{g_j} \to -\infty$ uniformly on every compact subset of $\mathbb{S}$, or* (ii) *$u_{g_j} \to u$ in $L^1_{\mathrm{loc}}(\mathbb{S})$ for a subharmonic function $u \not\equiv -\infty$ on $\mathbb{S}$, and $\mathfrak{n}_{g_j} \to \frac{1}{2\pi}\nabla^2 u$ vaguely on $\mathbb{S}$.*

A function u that arises in (ii) is called a *limit profile* of the sequence.

Lemma 10.2 (Majorant; proved)**.** *Every limit profile satisfies $u \le U$ on all of $\mathbb{S}$, where U is extended across the slits as in Definition 6.6: it is continuous, equal to $-L$ on the slits, and subharmonic with charge density $\rho_U(x)\,\mathrm{d}x$ there. In particular $u \le 0$ on $\mathbb{S}$, and $u \le -L$ on the real axis.*

Proposition 10.3 (Contact; proved)**.** *Let $c_j \to \infty$, and let $g_j \in \bar{\mathcal{A}} \setminus \{0\}$ be weakly feasible with $x_1(g_j) \to x_\infty < \infty$. Then alternative* (i) *of Lemma 10.1 does not occur, and every limit profile u has a* contact point *$x_0 \in [x_1^*, x_\infty]$, at which $u(x_0) = U(x_0) = -L(x_0)$. In particular $x_\infty \ge x_1^*$, which is the qualitative statement of Theorem 4 once more.*

In the dictionary of section 6.2: a limit profile lies below the extremal potential, and the last sign change of the functionals leaves a mark on it, a point not beyond x_∞ at which the profile touches the Cardy line; by Lemma 6.7 this point lies on a slit.

10.2 Rigidity of the zeros

Theorem 7 (Rigidity of the zero law; proved)**.** *Let $c_j \to \infty$, and let $g_j \in \bar{\mathcal{A}} \setminus \{0\}$ be weakly feasible and attain the slope Λ_V, that is, $x_1(g_j) \to x_1^*$. (By Proposition 10.3 it suffices that $\limsup_j x_1(g_j) \le x_1^*$; such sequences exist by Theorem 5.) Then:*

(a) *$u_{g_j} \to U$ in $L^1_{\mathrm{loc}}(\mathbb{S})$, along the whole sequence.*

(b) *The normalized zero-counting measures converge vaguely on $\mathbb{S}$ to the zero law $\rho_U(x) = \frac{4}{3\pi}\operatorname{arccosh}(\sinh \pi|x|)$ of Definition 6.6, carried by the slits:*

$$\mathfrak{n}_{g_j} = \frac{1}{c_j'} \sum_\zeta m_\zeta \, \delta_\zeta \;\longrightarrow\; \rho_U(x)\,\mathrm{d}x \otimes \delta_{y=0} \qquad \text{on } |x| \ge x_1^*. \tag{10.2}$$

Concretely, counting zeros with multiplicity: in every compact subset of $\mathbb{S}$ disjoint from the slits G_j has $o(c_j')$ zeros, and for $x_1^* < x_a < x_b$ and $0 < y_0 < \frac{1}{2}$

$$\#\{\text{zeros of } G_j \text{ in } [x_a, x_b] \times [-y_0, y_0]\} = c_j' \int_{x_a}^{x_b} \rho_U(x)\,\mathrm{d}x + o(c_j'). \tag{10.3}$$

(c) *In the variable t: the number of zeros of g_j, with multiplicity, in the image of that rectangle under $b \mapsto c_j' b^2/3$ (a lens $|\operatorname{Im} t| \le \frac{2}{3} c_j' x_b y_0$ around $[c_j' x_a^2/3,\, c_j' x_b^2/3]$) is $c_j' \int_{\xi_a}^{\xi_b} 2\rho_V(\xi)\,\mathrm{d}\xi + o(c_j')$, where $\xi = x^2/3$, $\xi_a = x_a^2/3$, $\xi_b = x_b^2/3$, and $\rho_V = 3\rho_U/(4x)$ is the band density of (4.16). In words, near $[t, t+\mathrm{d}t]$ there are $2\rho_V(t/c')\,\mathrm{d}t$ zeros.*

Item (c) reproduces, counted with multiplicity, the density of the band of double zeros of Conjecture 1(b), and item (a) is the profile stated there, in the mean. Of what section 4 derived from the hypotheses (W), (A), (B) and (Sel), the band density and the profile thus follow, at leading order and in the weak sense of (a) and (b), from attainment alone; the finer statements of Conjecture 1 are not obtained in this way. The hypotheses themselves, which concern the semiclassical sheets of the optimal functional, are not thereby derived. The theorem also turns the blueprint of section 7.1 into a necessity.

What the theorem does not say. It does not say that the zeros near the band are real, or that they come in pairs; whether an attaining functional must oscillate there, as the numerical optima do, is not decided. It says nothing about individual positions, the Airy layer at the tip, the boundary layer at the vacuum, the phase of the comb, zeros on the edges or outside the closed strip, or rates.

Idea of the proof (appendix I.4). Let u be a limit profile. By Lemma 10.2 the deficit $\theta := U - u$ is non-negative; it is superharmonic on the slit strip D, where U is harmonic; and by Proposition 10.3 with $x_\infty = x_1^*$ it vanishes at the tip x_1^*, a boundary point of D. By the strong minimum principle either $\theta \equiv 0$ on D, which is the claim, or $\theta > 0$ on D. Had the contact point been inside D, this would end the proof; at a point of the open slit it would not; the tip is the borderline case, and it is decided by a competition of exponents. If $\theta > 0$ on D, then near the tip θ dominates a multiple of the harmonic measure of an arc in a disk slit along a radius. The square-root map that opens the slit shows that this harmonic measure vanishes at the tip only like the square root of the distance, so the mean of θ over a circle of radius ϵ about the tip is $\gtrsim \epsilon^{1/2}$. On the other hand u is subharmonic across the slit and $u(x_1^*) = U(x_1^*)$, so the circle means of θ are at most those of $U - U(x_1^*)$, which the Poisson–Jensen formula expresses through the charge of U near the tip. Since $\rho_U \sim \sqrt{x - x_1^*}$, they are at most $C\epsilon^{3/2}$. For small ϵ the two bounds contradict each other: the tip decides.

Part V Outlook

11 Discussion

11.1 Theorem, conjecture, open

In terms of the legend of section 1.3, the results stand as follows. *Proved:* the slope Λ_V (Theorem 1), in its two halves, optimality with a rate (Theorems 3 and 4) and attainment (Theorem 5); and certification (Theorem 2), which turns attainment into a bound on conformal field theories (Corollary 6). Only attainment and what rests on it, that is, the second half of Theorem 1, Theorem 5 and Corollary 6, use computer assistance. Also proved, without a computer, is the rigidity of the zero law (Theorem 7). *Conjectured:* everything finer (Conjecture 1), in particular the coefficient $A_{\mathrm{opt}} = 0.27666$ of $c^{1/3}$, the profile of the optimal functional, and the offset $c/24$ in the positions of its zeros (seen numerically in [10, 11]; section 4.6). *Explained but not proved:* the origin of the earlier extrapolation to the slope 9.08 [11] (section 5.2).

11.2 Three-dimensional gravity; Virasoro versus $U(1)^c$

Invariance under S at zero angular potential, used through functionals in $\bar{\mathcal{A}}$, certifies $\Delta_1 \lesssim c/9.1266$ at large c and no more: the window (1.3) is closed to it. This is a statement about the method. It neither supports nor threatens pure gravity [3], and it does not say which spectra with Δ_1 in the window are realized. To reach the BTZ threshold one needs spin [8, 23, 24], integrality of the degeneracies [25, 26], or data from correlation functions. Arguments through the *elliptic point* of order three, $\tau = e^{2\pi i/3}$, which is fixed not by S but by ST and so involves spin [73–76], aim at the BTZ threshold itself; the present results neither use them nor bear on them. The same holds for the bound $\Delta_1 \le (c-1)/12 + 0.23$ on what [76] calls the spinless gap: it rests on the kernel of ST^1S, and so on T as well as S, and it concerns spectra in which every non-vacuum primary has spin zero, whereas here primaries of every spin are counted.

Virasoro versus $U(1)^c$. The two problems have the same architecture and different numbers, 9.1266 against π^2. The slope π^2 is proved in [13, Ch. 1]; we have read the statements and the structure of that argument but have not independently verified it; nothing in this paper depends on it logically. That proof works on a strip in the Mellin variable, in dimension $d = 2c \to \infty$. Here the dimension $d = 2$ is fixed, the strip is in the position-like variable b, and c enters through the position of the vacuum; the version in the Mellin variable, where the strip becomes a domain with a free boundary, is sketched in appendix A. There is no analogue here of the condition $f(0) = 0$ on the functional of section 2.3, which the $U(1)^c$ proof uses to cancel a pole of the Mellin transform on the edge of the strip and to make the integral of the functional vanish. Two different objects should be kept apart. The *exact optimizers* of both problems, as computed numerically, have a band of double zeros (sections 3.1 and 4.6), whereas the *asymptotically attaining* functions constructed in [13, Ch. 1, Thm. 4.1] are free of real zeros on the whole constrained region. For Virasoro a functional that attains Λ_V must carry zeros at density $c'\rho_U$ near the real axis, by Theorem 7, though not necessarily on it; this freedom is what the detuning of section 7 exploits.

Note added. After this paper was completed, Chang, Liu and Ma [77] constructed modular-invariant torus partition functions with a unique vacuum, integer spins and positive integer degeneracies whose gap is $\Delta_1 = (1+\kappa)(c-1)/12$, for small fixed $\kappa > 0$ at every sufficiently large c. These are partition functions, not full conformal field theories. We have not verified this construction; if it stands, the lower end of the window (1.3) passes every constraint of the torus partition function, spin and integrality included, so that $\Lambda < 12$ for every bound that uses this function alone, and reaching the BTZ threshold requires data beyond it. Perlmutter [78] has

shown, for theories whose spectral counting fluctuations are logarithmically rigid, that $\Delta_1 - (c-1)/12 \le o(c)$, apart from at most one exceptional value of the scalar gap at each sufficiently large c. Salmon [79] has determined the asymptotic rate of Delsarte's linear programming bound for binary and spherical codes, with lower bounds from potential theory through an obstacle problem solved in closed form, as in appendix A.

11.3 Open problems

Effective constants. More useful than the values of c_0^{opt} and c_0^{att}, which are explicit in principle and not computed, would be certificates in interval arithmetic of the explicit functional at fixed c.

The coefficient of $c^{1/3}$. A proof of A_{opt} needs the comb with no site omitted (the construction of section 7 omits the first site of the zero law), the Airy layer at the tips, and the balance between lobe and band in the vacuum inequality. Apply the edge representation of section 7.4 to a numerically optimal functional, whose transform is $\hat g = -g$. It suggests that on the band $\hat g$ is the sum of two parts. One oscillates, with relative amplitude $\frac{1}{2}$ and in antiphase with the oscillation of g, so that the zeros are doubled rather than lifted off the axis. The other is a mean, which is manufactured near the vacuum point of the edge; the construction of section 7 does not attempt this. A proof of A_{opt} would have to control both. We do not claim it.

Further problems. To remove the logarithm in Theorem 4, that is, to prove $t_1(g) \ge \xi_1^* c' - O(c^{1/3})$, the scale of Conjecture 1. To find a convex dual of the linear program of section 2.2 with the extremal potential U as its value function, which would explain why the potential of section 6 is the curve of section 4. To bound $T_V(c)$ from below at a given c: numerics bound it from above only (section 2.6), and Theorem 4 starts at c_0^{opt}. To derive from the linear program the selection rule (Sel) of section 4.4, on which Conjecture 1 rests. To find what replaces the extremal problem of section 6 in the bootstrap with spin [8, 23].

A Mellin space approach

The proofs of sections 6 and 7 work in the variable $b = \sqrt{3t/c'}$, in which a functional is holomorphic on a strip. This appendix sketches a second derivation of the slope, Theorem 1, in which a functional is studied through its Mellin transform. It gives both halves: no functional in $\bar{\mathcal{A}}$ certifies more than Λ_V, and functionals exist that come arbitrarily close. The Mellin transform is the tool of the proof for the $U(1)^c$ problem in [13, Ch. 1], where the transform of a functional is controlled on a strip. The attaining functions of [13, Ch. 1, Thm. 4.1] are likewise built in Mellin space, by multiplying the Mellin transform of a Gaussian by factors that respect the Fourier symmetry and reading the signs from saddle points, and the functional of appendix A.6 has this form, with a symbol whose zeros come from the solution of the free-boundary problem described below. (The Mellin transform of the auxiliary functions of the sphere-packing linear program, with its functional equation and its relation to their Taylor coefficients, appears in Cohn and Miller [80, §5], for smooth and rapidly decreasing radial functions in any dimension. Properties (i) and (ii) of (A.3) follow from their formulas in dimension two with $\hat f = -f$ when $f(x) = g(x^2/2)$ is smooth and rapidly decreasing: with $M_f(s) = \int_0^\infty f(x)\, x^{s-1}\, \mathrm{d}x$ one has $m_g(z) = 2\pi^z M_f(2z)/\Gamma(z)$.) What is new for Virasoro is that the vacuum sits at $t = -a < 0$, off the half line over which the transform is taken. It then enters through all the integer moments of g at once, and the problem on a strip becomes a free-boundary problem in the plane: an obstacle problem, which we solve in closed form. The curve $\sinh \pi b = i \sinh \pi p$ appears once more, now as the solution of the free-boundary condition, and the threshold x_1^* is fixed by the point of the contact set that is nearest to the axis of the reflection $z \to 1 - z$, which is what the Fourier transform becomes.

What this appendix has in common with the main text is not repeated. The problem, the class $\bar{\mathcal{A}}$ and the vacuum value are those of section 2, and a feasible $g \in \bar{\mathcal{A}}$ bounds every conformal

field theory by Theorem 2. The two results are the following.

Result M1 (optimality)

For every $\delta \in (0, x_1^*)$ there is $C_\delta < \infty$ such that for all $c \geq 40$ and every $g \in \bar{\mathcal{A}}$, with no condition on the sign of g,

$$\int_0^{c'(x_1^*-\delta)^2/3} |g|\, V \,\mathrm{d}t \;\leq\; C_\delta\, c'^4\, e^{-\kappa_M(\delta)\, c'}\, M[g], \qquad \kappa_M(\delta) := \mathcal{W}\big(\tfrac{\pi}{3}(x_1^*-\delta)\big) > 0, \tag{A.1}$$

where $\mathcal{W}$ is the explicit function of appendix A.3. Consequently, by the half-mass condition (2.16), for every $x_T < x_1^*$ there is $c_0(x_T)$ such that for $c \geq c_0(x_T)$ no $g \in \bar{\mathcal{A}}$ other than zero is weakly feasible at $T = c' x_T^2/3$. No computer is used.

Result M2 (attainability)

For every $x_g > x_1^*$ there is $c_0(x_g) \geq 40$ such that for every real $c \geq c_0(x_g)$ there is $g_c \in \bar{\mathcal{A}}$ with $g_c > 0$ on $[c' x_g^2/3, \infty)$ and $(g_c)_{\mathrm{vac}} > 0$; moreover g_c decays faster than $e^{-4\pi\sqrt{\alpha t}}$ for every $\alpha > 0$. So g_c is feasible at $T = c' x_g^2/3$, and by Theorem 2 every admissible CFT with $c \geq c_0(x_g)$ has $\Delta_1 < a + c' x_g^2/3$.

Together they give $\lim_{c\to\infty} T_V(c)/c' = \xi_1^*$, that is, Theorem 1, once more. Result M1 is Theorem 3 with a smaller exponent, $\kappa_M(\delta) \simeq 3.73\,\delta^2$ against $\kappa(\delta) \simeq 2.65\,\delta^{3/2}$ (appendix A.4), and it contains the first statement of Theorem 4. Result M2 is Result S1 of section 9, by a third construction. Neither gives a rate, and the central charges c_0 are not explicit.

The plan is as follows. Appendix A.1 recasts the constraints in Mellin space: the Fourier transform becomes a reflection, and the vacuum becomes a series over the integers with positive coefficients, each of which bounds the transform on a vertical line. Appendix A.2 takes the scaling limit of these bounds, the *obstacle*, and explains why the threshold is the *tip* of the set where the largest subharmonic function below the obstacle touches it. Appendix A.3 finds this set and this function in closed form, and appendix A.4 turns the heuristic argument into Result M1. Appendices A.5 to A.7 construct the functionals of Result M2: the zeros of the Mellin transform are placed along four arcs inside the contact set, the functional is recovered by Mellin inversion, and its signs come from a saddle-point analysis in which one real saddle point dominates. Appendix A.8 is a dictionary between the Mellin plane and the strip of section 6.

Level of rigor. The results of this appendix have been verified rigorously, but the write-up is informal: the steps are stated and the estimates behind them are omitted. For this reason Result M1, Result M2 and Result M3 carry no status tag. One step, the univalence of a conformal map (appendix A.5), uses five inequalities that were checked in interval arithmetic [61]; they are listed there and are not part of table 4. Nothing outside this appendix depends on it.

Notation. It is that of section 2: $c' = c - 1$, $a = c'/12$, $t = \Delta - a$, $b = x + iy = \sqrt{3t/c'}$; β is the inverse temperature; V is the Cardy weight (2.12), $\rho_C = 2\pi V$, $L(x) = \frac{2\pi}{3}|x|$, and $M[g] = \int_0^\infty |g|\, V \,\mathrm{d}t$; $g_{\mathrm{vac}} = -\int_0^\infty g\, \rho_C \,\mathrm{d}t$ and feasibility are as in Definitions 2.3 and 2.5. The extremal potential U, its value $U_0 = U(0) = -0.388748$, the momentum p and the zero law ρ_U are those of Lemma 6.5 and Definition 6.6. The Mellin variable is z, and $\omega = \mu + i\nu$ is the rescaled variable of (A.8); in this appendix ω is not the linear functional of section 2.2. The letters m_g, θ_n, σ, ϑ, τ, η, η_v, ι, λ and the calligraphic letters $\mathcal{B}$, $\mathcal{U}$, $\mathcal{W}$, $\mathcal{K}$, $\mathcal{N}$, $\mathcal{E}$, $\mathcal{C}$, $\mathcal{H}$ are local to this appendix. C stands for constants that do not depend on c, on t or on the point ω.

A.1 The Mellin symbol and the vacuum inequality

For $g \in \bar{\mathcal{A}}$ we call

$$m_g(z) := \frac{(2\pi)^z}{\Gamma(z)} \int_0^\infty g(t)\, t^{z-1}\, \mathrm{d}t \qquad (\mathrm{Re}\, z > 0) \tag{A.2}$$

the *Mellin symbol* of g. The integral converges because g is bounded (Lemma B.3) and all its moments are finite, by (A.6) below. Three properties are used.

$$\begin{aligned} &\text{(i)} \quad m_g \text{ extends to an entire function, and } m_g(1-z) = -m_g(z); \\ &\text{(ii)} \quad m_g(n+1) = \frac{(2\pi)^{n+1}}{n!} \int_0^\infty g\, t^n\, \mathrm{d}t, \qquad m_g(-n) = (-2\pi)^{-n} g^{(n)}(0) \qquad (n = 0, 1, 2, \dots); \\ &\text{(iii)} \quad |m_g(z)| = |m_g(1-z)| \le \frac{(2\pi)^{\mathrm{Re}\, z}}{|\Gamma(z)|} \int_0^\infty |g|\, t^{\mathrm{Re}\, z - 1}\, \mathrm{d}t \qquad (\mathrm{Re}\, z > 0). \end{aligned} \tag{A.3}$$

For (i), the Laplace transform $F(\beta) := \int_0^\infty g\, e^{-2\pi\beta t}\, \mathrm{d}t$ obeys $F(\beta) = -\beta^{-1} F(1/\beta)$, by $\hat{g} = -g$ and (2.8). For $0 < \mathrm{Re}\, z < 1$ its Mellin transform in β is $\int_0^\infty F(\beta)\beta^{z-1}\mathrm{d}\beta = m_g(1-z)/(2\sin \pi z)$, by the reflection formula for Γ, so the substitution $\beta \to 1/\beta$ turns the functional equation of F into $m_g(1-z) = -m_g(z)$ on the strip, and this relation continues m_g to the whole plane. The division by Γ is what makes the symbol entire: *in Mellin space the Fourier transform is the reflection* $z \to 1 - z$, and a functional is an entire function that is odd under it. The first formula in (ii) is the definition; the second is the Taylor series of g at $t = 0$, where g is analytic by Lemma B.1, read through (i). In particular $m_g(0) = g(0)$. Item (iii) is the trivial bound together with (i).

The vacuum. For $a \ge 2$ the Cardy weight has the power series (2.13) with positive coefficients,

$$V(t) = \sum_{n \ge 2} v_n\, t^n, \qquad v_n = \theta_n \frac{(4\pi^2 a)^n}{(n!)^2}, \qquad \theta_n := 1 - 2(1 - \tfrac{1}{a})^n + (1 - \tfrac{2}{a})^n, \qquad \frac{1}{2a^2} \le \theta_n \le 1, \tag{A.4}$$

so that v_n is $(4\pi^2 a)^n/(n!)^2$ up to a factor polynomial in a, which is invisible on the exponential scale. Integrating $g_{\mathrm{vac}} = -2\pi \int_0^\infty g\, V\, \mathrm{d}t$ term by term, which is allowed because $M[g] < \infty$, and using (ii),

$$g_{\mathrm{vac}} = -\sum_{n \ge 2} \theta_n \frac{(2\pi a)^n}{n!}\, m_g(n+1)\,: \tag{A.5}$$

the vacuum is a series over the integer points $z = n + 1$*, with positive weights.* Since every term of the series for V is positive, each absolute moment of g is bounded separately:

$$\begin{aligned} v_n \int_0^\infty |g|\, t^n\, \mathrm{d}t \;&\le\; M[g] \qquad (n \ge 2), \\ \text{and} \qquad M[g] &\le 2 \int_0^T |g|\, V\, \mathrm{d}t \qquad \text{if } g \text{ is weakly feasible at } T, \end{aligned} \tag{A.6}$$

the second being the half-mass condition (2.16). Inserting the first in (iii) at $\mathrm{Re}\, z = n + 1$ gives, for every integer $n \ge 2$,

$$|m_g(z)| = |m_g(1-z)| \le \frac{(2\pi)^{n+1}}{v_n\, |\Gamma(z)|}\, M[g] \qquad (\mathrm{Re}\, z = n + 1). \tag{A.7}$$

Positivity beyond T and the vacuum condition thus bound the symbol, on all the lines $\mathrm{Re}\, z = n+1$ and on their reflections, by the Cardy-weighted mass that g carries below T. This is the starting point. In the strip of section 6 the vacuum is one point on an edge; here it is a bound on every vertical line through an integer.

A.2 The obstacle

The coefficient in (A.7) has an exponential order when n and $\operatorname{Im} z$ are of order c. We write

$$z = \tfrac{1}{2} + c'\,\omega, \qquad \omega = \mu + i\nu, \tag{A.8}$$

so that $z \to 1 - z$ is $\omega \to -\omega$, and use Stirling's formula in a form that is uniform in the imaginary part: for $\operatorname{Re} w \geq 0$, $w \neq 0$, $\log|\Gamma(\frac{1}{2} + w)| = \operatorname{Re}[w \log w - w] + \frac{1}{2}\log 2\pi - \epsilon(w)$ with $0 \leq \epsilon(w) \leq \frac{1}{2}\log 2$. (The remainder is minus the real part of a function that is bounded and holomorphic in the half-plane, so it is the Poisson integral of its boundary values, which are explicit because $|\Gamma(\frac{1}{2} + is)|^2 = \pi/\cosh \pi s$.) The main term is elementary: for $w = \mu + i\nu$ with $\mu > 0$, $\operatorname{Re}[w \log w - w] = \mu \log \mu - \mu - \mathsf{D}_\mu(\nu)$, where

$$\mathsf{D}_\mu(\nu) := \nu \arctan \frac{\nu}{\mu} - \frac{\mu}{2} \log\Bigl(1 + \frac{\nu^2}{\mu^2}\Bigr) = \int_0^\infty (1 - \cos s\nu)\, e^{-\mu s}\, \frac{\mathrm{d}s}{s^2} \;\geq 0 \tag{A.9}$$

is the price, in the exponent, of moving off the real axis along the line $\operatorname{Re} w = \mu$. It is homogeneous of degree one in (μ, ν), and $\mathsf{D}_\mu(\nu) \to \frac{\pi}{2}|\nu|$ as $\mu \to 0^+$. On the line $\operatorname{Re} z = n{+}1$ we have $n + \frac{1}{2} = c'\mu$. The factor $(n!)^2$ of $1/v_n$, the factor $(2\pi)^n (4\pi^2 a)^{-n}$ and the factor $1/|\Gamma(n + 1 + ic'\nu)|$ contribute $2c'\mu \log \frac{c'\mu}{e} - c'\mu \log \frac{\pi c'}{6} - c'\mu \log \frac{c'\mu}{e} + c'\mathsf{D}_\mu(\nu)$ to the logarithm of the coefficient; the scale c' cancels from the logarithms because $2\pi a = \frac{\pi}{6} c'$ exactly, and what remains is c' times the *obstacle*

$$\mathcal{B}(\mu + i\nu) := |\mu| \log \frac{6|\mu|}{\pi e} + \mathsf{D}_{|\mu|}(\nu) \quad (\mu \neq 0), \qquad \mathcal{B}(i\nu) := \frac{\pi}{2}|\nu|, \tag{A.10}$$

extended to $\mu < 0$ by the reflection. It is continuous on $\mathbb{C}$ and even in μ and in ν. Hence, for every $g \in \bar{\mathcal{A}}$, $g \not\equiv 0$,

$$\frac{1}{c'} \log \frac{|m_g(\frac{1}{2} + c'\omega)|}{M[g]} \;\leq\; \mathcal{B}(\omega) + O\Bigl(\frac{\log c'}{c'}\Bigr) \qquad \text{for } c'|\mu| \geq \tfrac{5}{2}, \tag{A.11}$$

with an error that is uniform in ω and in g; between two consecutive lines one interpolates with Hölder's inequality, because the moments are log-convex in their order. In the central strip $c'|\mu| < \frac{5}{2}$, that is, $-2 < \operatorname{Re} z < 3$, no moment of g is controlled by $M[g]$, and all one has there is a bound $|m_g| \leq C_g\, e^{\pi c'|\nu|/2}$ with a constant that depends on g. In the variable ω this strip shrinks to the imaginary axis.

For $\mu > 0$,

$$\mathcal{B}(\omega) = \mu \log \frac{6\mu^2}{\pi e} - \operatorname{Re}\bigl[\omega \log \omega\bigr], \qquad 2\,\partial_\omega \mathcal{B} = \partial_\mu \mathcal{B} - i\,\partial_\nu \mathcal{B} = \log \frac{6\mu^2}{\pi\omega}, \qquad \nabla^2 \mathcal{B} = \frac{2}{\mu}. \tag{A.12}$$

Away from the imaginary axis $\mathcal{B}$ is smooth and strictly subharmonic. On it $\mathcal{B}$ is not smooth: $\partial_\mu \mathcal{B} \to \mp\infty$ as $\mu \to 0^\pm$ with $\nu \neq 0$ fixed, so the imaginary axis is a concave *ridge*. On the positive real axis $\mathcal{B}(\mu) = \mu \log \frac{6\mu}{\pi e}$. We shall also need the harmonic function in the right half-plane that is even in ν and agrees with $\mathcal{B}$ on the positive real axis,

$$\operatorname{Re} \Upsilon_R = \mathcal{B} - 2\,\mathsf{D}_\mu(\nu), \qquad \Upsilon_R(\omega) := \omega \log \frac{6\omega}{\pi} - \omega \qquad (\mu > 0). \tag{A.13}$$

The obstacle problem. The inequality (A.11) is not the best that one can say. Since m_g is entire, the left side is a subharmonic function of ω [63]. If $\mathcal{B}$ were itself subharmonic nothing would be gained. It is subharmonic on either side of the ridge, but not across it, and a subharmonic function cannot follow a concave ridge from below. At exponential order the left side of (A.11) therefore lies below

$$\mathcal{U} := \sup\{u :\ u \text{ subharmonic on } \mathbb{C},\ u \leq \mathcal{B}\}. \tag{A.14}$$

To find the largest subharmonic minorant of a given function is the obstacle problem [81]; in the plane it is the equilibrium problem of weighted potential theory [82]. We use (A.14) only as a guide to the formulas of appendix A.3: Result M3 does not assert that the function defined there is the largest minorant, and neither of the two main arguments needs it. The general theory says what to expect. The plane splits into the open *non-contact set* $\mathcal{N} = \{\mathcal{U} < \mathcal{B}\}$, where $\mathcal{U}$ is harmonic, since otherwise it could be increased locally, and the closed *contact set* $\mathcal{K} = \{\mathcal{U} = \mathcal{B}\}$. Where the obstacle is smooth, $\mathcal{U}$ is C^1 across the *free boundary* $\partial\mathcal{K}$, that is, $\nabla\mathcal{U} = \nabla\mathcal{B}$ there, and this is the equation that determines $\partial\mathcal{K}$. The solution is even in μ and in ν. The ridge belongs to $\mathcal{N}$, because the mean of $\mathcal{B}$ over a small circle centered on it is smaller than the value at the center. Hence $\mathcal{K} = \mathcal{K}_+ \cup (-\mathcal{K}_+)$ with $\mathcal{K}_+$ a closed subset of $\{\mu > 0\}$. Finally, on $\mathcal{K}$ the Riesz measure $\frac{1}{2\pi}\nabla^2\mathcal{U}$ is $\frac{1}{2\pi}\nabla^2\mathcal{B}\,\mathrm{d}A = \mathrm{d}A/(\pi|\mu|)$, an area measure; this will matter in appendix A.5.

Why the tip of the contact set is the threshold. Let $g \in \bar{\mathcal{A}}$ be weakly feasible at $T = c'x_T^2/3$, so that it carries at least half of its mass below T, (A.6). On the other hand g is recovered from its symbol by Mellin inversion along any line $\operatorname{Re} z = n+1$, $g(t) = \frac{1}{2\pi i}\int m_g(z)\Gamma(z)(2\pi t)^{-z}\mathrm{d}z$. Insert $|m_g| \le M[g]\,e^{c'\mathcal{U}+o(c')}$ and $(2\pi)^{-n-1}|\Gamma(z)| = e^{-c'\mathcal{B}+o(c')}/v_n$:

$$v_n\,t^n\,|g(t)| \;\le\; M[g]\,\frac{c'}{2\pi t}\int_{\mathbb{R}} \exp\{-c'\,\mathcal{W}(\mu+i\nu)+o(c')\}\,\mathrm{d}\nu, \qquad \mathcal{W} := \mathcal{B}-\mathcal{U} \ge 0, \qquad c'\mu = n+\tfrac{1}{2}. \tag{A.15}$$

The obstacle has reappeared with the opposite sign, and only the difference is left. For given t we choose for n the index of the largest term of the series $V(t) = \sum v_n t^n$; this puts the line through the real saddle point of the inversion integral. The largest term is at $n \approx 2\pi\sqrt{at}$, that is, on the line

$$\mu = \frac{\pi}{3}\,x, \qquad x = \sqrt{3t/c'}, \tag{A.16}$$

and $V(t) = e^{o(c')}v_n t^n$. For $t \le T$ the line lies in $|\mu| \le \frac{\pi}{3}x_T$, and integration over $[0,T]$ gives

$$\int_0^T |g|\,V\,\mathrm{d}t \;\le\; M[g]\,e^{-c'\kappa+o(c')} \;\le\; 2\,e^{-c'\kappa+o(c')}\int_0^T |g|\,V\,\mathrm{d}t, \qquad \kappa := \inf_{|\mu|\le\pi x_T/3}\mathcal{W}. \tag{A.17}$$

If the closed strip $|\mu| \le \frac{\pi}{3}x_T$ lies in $\mathcal{N}$, and $\kappa > 0$, this forces $g = 0$ for large c. If the strip meets $\mathcal{K}$ then $\kappa = 0$ and nothing follows. The threshold is where the strip first touches the contact set, $x_T = \frac{3}{\pi}\mu_*$ with $\mu_* := \min\{\mu : \mu + i\nu \in \mathcal{K}_+\}$. We call the points $\pm\mu_*$ of $\mathcal{K}$ the *tips*.

A.3 The free boundary and the solution in closed form

It remains to find $\mathcal{N}$ and $\mathcal{U}$. We expect $\mathcal{N}$ to be a simply connected neighborhood of the ridge and write $\mathcal{U} = \operatorname{Re}\Upsilon$ in $\mathcal{N}$ with Υ holomorphic. The symmetries make Υ' odd and real on $\mathcal{N}\cap\mathbb{R}$. Instead of Υ' we use the pair of variables

$$b\,q = \frac{3\omega}{2\pi}, \qquad \frac{b}{q} = e^{\Upsilon'(\omega)}, \qquad \text{that is,} \qquad b^2 = \frac{3\omega}{2\pi}\,e^{\Upsilon'(\omega)}, \quad q^2 = \frac{3\omega}{2\pi}\,e^{-\Upsilon'(\omega)}. \tag{A.18}$$

Here b^2 and q^2 are holomorphic in $\mathcal{N}$, and the common sign of (b,q) is fixed by $b,q>0$ on the real segment $(0,\mu_*)$. The first variable is an old one: for a symbol $m_g = e^{c'\Upsilon+o(c')}$ the integrand of the inversion integral is $\exp\{c'[\Upsilon(\omega)+\omega\log\frac{c'\omega}{2\pi e t}]\}$, and it is stationary at $2\pi t = c'\omega\,e^{\Upsilon'}$, that is, at $t = c'b^2/3$. So b is the variable b of (2.17), evaluated at the saddle point that belongs to ω. Its partner q will turn out to be ip, with p the momentum (6.16).

On $\partial\mathcal{K}_+$ the contact is C^1, so $\Upsilon' = 2\partial_\omega\mathcal{U} = 2\partial_\omega\mathcal{B} = \log\frac{6\mu^2}{\pi\omega}$ by (A.12). In (A.18) this gives $b^2 = (3\mu/\pi)^2$, hence the free-boundary condition

$$b = \frac{3\mu}{\pi}, \qquad q = \frac{\omega}{2\mu} = \frac{1}{2} + \frac{i\nu}{2\mu}; \qquad \text{in particular} \quad \operatorname{Im} b = 0, \quad \operatorname{Re} q = \tfrac{1}{2} \quad \text{on } \partial\mathcal{K}_+. \tag{R}$$

In the variables (b,q) the nonlinear condition $\nabla\mathcal{U}=\nabla\mathcal{B}$ has become linear; this is the reason for introducing them. The reflection $\omega\to-\omega$ acts as $(b,q)\to(iq,ib)$, because Υ' is odd, so that on $-\partial\mathcal{K}_+$ the conditions read $\operatorname{Re} q=0$ and $|\operatorname{Im} b|=\frac12$: there b is on an edge of the strip $\mathbb{S}$. The reflections in the lines $\operatorname{Re} q=0$ and $\operatorname{Re} q=\frac12$ compose to the translation $q\to q+1$, those in $\operatorname{Im} b=0$ and $\operatorname{Im} b=\frac12$ to $b\to b+i$, which suggests a solution that is periodic in both variables. Consider therefore the function $\cosh 2\pi b+\cos 2\pi q$ of ω. It is an entire function of (b^2,q^2), hence holomorphic in $\mathcal{N}$. It is even, because $\omega\to-\omega$ exchanges its two terms. It is real on $\partial\mathcal{K}_+$ by (R), since $\cos 2\pi(\frac12+is)=-\cosh 2\pi s$, and hence on all of $\partial\mathcal{N}$. So its imaginary part is harmonic in $\mathcal{N}$ and vanishes on $\partial\mathcal{N}$. Assume that it is bounded in $\mathcal{N}$. Then it is a real constant, by the Phragmén–Lindelöf principle, and the value at $\omega=0$, where $b=q=0$, is 2:

$$\begin{gathered}\cosh 2\pi b+\cos 2\pi q=2,\qquad\text{equivalently}\qquad \sin\pi q=\sinh\pi b,\\ \text{that is,}\qquad \sinh\pi b=i\sinh\pi p\quad\text{with } q=ip,\end{gathered}\tag{A.19}$$

since the first equation is $\sinh^2\pi b=\sin^2\pi q$ and the sign is fixed on $(0,\mu_*)$. This is the curve (1.4). (With $b=iX$ the first form is the energy surface $\cos 2\pi X+\cos 2\pi q=2$ of Harper's equation [83].) Together with $bq=3\omega/2\pi$ it determines b and q, hence Υ', as functions of ω:

$$\omega=\frac{2\pi}{3}\,b\,q,\qquad \sin\pi q=\sinh\pi b;\qquad \text{on } (0,\mu_*):\quad q=\frac{1}{\pi}\arcsin\sinh\pi b=i\,p(b).\tag{A.20}$$

The rescaled Mellin variable is the action, $\omega=\frac{2\pi i}{3}\,b\,p$, on the curve of section 4.

At the tip, where $\partial\mathcal{K}_+$ crosses the real axis, (R) gives $q=\frac12$ and $b=3\mu_*/\pi$, and (A.19) becomes $\sinh\pi b=1$:

$$b=x_1^*,\qquad \mu_*=\frac{\pi}{3}\,x_1^*=\tfrac13\operatorname{arcsinh}1=0.2937912,\qquad x_T=\frac{3}{\pi}\mu_*=x_1^*,\tag{A.21}$$

which is the threshold of Theorem 1. On the rest of $\partial\mathcal{K}_+$, (R) and $\sin(\frac{\pi}{2}+\frac{i\pi\nu}{2\mu})=\cosh\frac{\pi\nu}{2\mu}$ turn (A.19) into $\cosh\frac{\pi\nu}{2\mu}=\sinh 3\mu$:

$$\nu=\pm\nu_*(\mu),\qquad \nu_*(\mu):=\frac{2\mu}{\pi}\operatorname{arccosh}(\sinh 3\mu),\qquad \mu\ge\mu_*,\tag{A.22}$$

where $\sinh 3\mu\ge1$ precisely for $\mu\ge\mu_*$. Since $\nu_*(\mu)=\frac{6}{\pi}\mu^2-O(\mu e^{-6\mu})$, the non-contact set is a parabolic neighborhood of the ridge (figure 10(a)).

The solution. We now turn the outcome into definitions, which no longer depend on how they were found. Let

$$\begin{gathered}\mathcal{K}_+:=\{\mu+i\nu:\ \mu\ge\mu_*,\ |\nu|\le\nu_*(\mu)\},\qquad \mathcal{K}:=\mathcal{K}_+\cup(-\mathcal{K}_+),\qquad \mathcal{N}:=\mathbb{C}\setminus\mathcal{K},\\ \Upsilon'(\omega):=\log\frac{b}{q}\quad(\omega\in\mathcal{N}),\qquad \mathcal{U}(\omega):=\mathcal{B}(\mu_*)+\operatorname{Re}\int_{\mu_*}^{\omega}\Upsilon'(\omega')\,\mathrm{d}\omega'\quad(\omega\in\mathcal{N}),\qquad \mathcal{U}:=\mathcal{B}\ \text{ on }\mathcal{K},\end{gathered}\tag{A.23}$$

where b and q are the functions on $\mathcal{N}$ defined by (A.20) through part (i) below, the logarithm is the branch that vanishes at $\omega=0$, and the path runs in $\mathcal{N}\cup\{\mu_*\}$. Put $\mathcal{W}:=\mathcal{B}-\mathcal{U}$ and $\mathcal{N}^+:=\mathcal{N}\cap\{\nu>0\}$.

Result M3 (the solution of the obstacle problem)

(i) The relations (A.20) define q as a conformal map of $\mathcal{N}^+$ onto the half-strip $\{0<\operatorname{Re} q<\frac12,\ \operatorname{Im} q>0\}$. The side $\operatorname{Re} q=\frac12$ corresponds to the upper arc of $\partial\mathcal{K}_+$, the side $\operatorname{Im} q=0$ to the segment $(0,\mu_*)$, and the side $\operatorname{Re} q=0$ to $(-\mu_*,0]$ followed by the upper arc of $-\partial\mathcal{K}_+$. Hence Υ' is single-valued and holomorphic on $\mathcal{N}$.

(ii) $\mathcal{U}\in C^1(\mathbb{C})$; it is harmonic in $\mathcal{N}$, equal to $\mathcal{B}$ on $\mathcal{K}$, and even in μ and in ν.

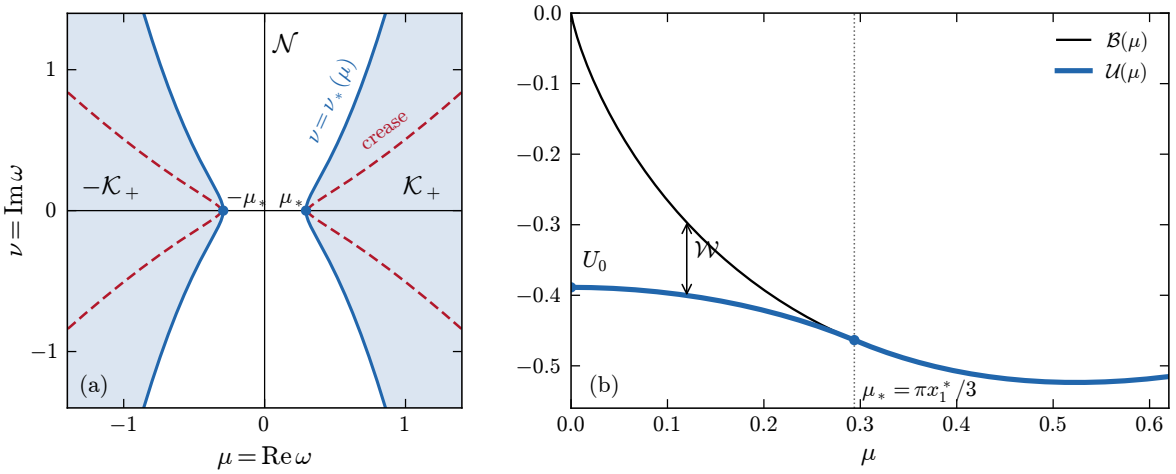


Figure 10: (a) The plane of $\omega = \mu + i\nu$, where $z = \frac{1}{2} + c'\omega$ is the Mellin variable. Shaded: the contact set $\mathcal{K} = \mathcal{K}_+ \cup (-\mathcal{K}_+)$. White: the non-contact set $\mathcal{N}$, which contains the ridge $\mu = 0$ of the obstacle. Solid: the free boundary $\nu = \pm\nu_*(|\mu|)$ of (A.22), whose four arcs meet at the tips $\omega = \pm\mu_*$. On the arcs b is real and $\geq x_1^*$, and $\nu_*(\frac{\pi}{3}x) = \frac{\pi}{2}x\,\rho_U(x)$: the width of the contact set is the zero law. Dashed: the four creases of appendix A.5, which leave the tips at 45° and carry the skeleton. (b) The obstacle $\mathcal{B}$ and the solution $\mathcal{U}$ on the positive real axis. They agree, with their first derivatives, for $\mu \geq \mu_*$; for $0 \leq \mu < \mu_*$ one has $\mathcal{W} = \mathcal{B} - \mathcal{U} > 0$, and $\mathcal{U}(0) = U_0$, the value of the extremal potential of section 6 at $b = 0$.

(iii) $\mathcal{W} > 0$ in $\mathcal{N}$, and $\mathcal{W}(\mu + i\nu) \leq \mathcal{W}(0) + \frac{\pi}{2}|\nu|$ on $\mathbb{C}$. In the quadrant $\mu, \nu > 0$ of $\mathcal{N}$, $\partial_\mu \mathcal{W} = 2\log\frac{3\mu}{\pi|b|} < 0$ and $\partial_\nu \mathcal{W} = 2\arg b > 0$.

(iv) ν_* is increasing on $[\mu_*, \infty)$ with $\nu_*(\mu_*) = 0$; hence $\{|\mu| \leq \mu_1\} \subset \mathcal{N}$ for every $\mu_1 < \mu_*$; and $\mu^2 \leq \frac{\pi}{3}(1 + |\nu|)$ on the closure of $\mathcal{N}$.

These properties are checked directly from the formulas, without the assumption made above. For (i) one uniformizes with $\sigma := \sinh^2 \pi b = \sin^2 \pi q$, so that $\omega = f(\sigma) := \frac{2}{3\pi}\,\mathrm{arcsinh}\,\sqrt{\sigma}\,\arcsin\sqrt{\sigma}$ on the plane cut along $(-\infty, -1]$ and $[1, \infty)$. For $\mathrm{Im}\,\sigma > 0$ one finds $0 < \arg b < \arg\sqrt{\sigma} < \arg q < \frac{\pi}{2}$, from $\tanh s < s < \tan s$, and then $\mathrm{Re}\,f' > 0$; since a half-plane is convex, f is one-to-one there, by the criterion of Noshiro and Warschawski [84, Thm. 2.16]. The upper and lower lips of the cut $[1, \infty)$ go to the two arcs of $\partial\mathcal{K}_+$, those of $(-\infty, -1]$ to the arcs of $-\partial\mathcal{K}_+$, and the branch points $\sigma = \pm 1$ to the tips. For (ii), on the upper arc $b = 3\mu/\pi$ is real and $q = 3\omega/(2\pi b)$, so that $\mathrm{Re}\,\Upsilon' = \log\frac{b}{|q|} = \log\frac{6\mu^2}{\pi|\omega|} = \partial_\mu\mathcal{B}$ and $-\mathrm{Im}\,\Upsilon' = \arg q = \arg\omega = \partial_\nu\mathcal{B}$, by (A.12); the values match as well, because the path in (A.23) may run along the arc, where $\mathrm{Re}(2\partial_\omega\mathcal{B}\,\mathrm{d}\omega) = \mathrm{d}\mathcal{B}$. For (iii), (A.12) and $|\omega| = \frac{2\pi}{3}|b||q|$ give the two components of $\nabla\mathcal{W}$; their signs follow from $3\mu = 2\pi\,\mathrm{Re}(bq) < \pi|b|$ and from the ordering of the arguments; and one integrates, along horizontal segments from the free boundary, where $\mathcal{W} = 0$, and up the imaginary axis from $\omega = 0$, where $\partial_\nu\mathcal{W} \leq \frac{\pi}{2}$. Part (iv) is elementary: $\frac{6}{\pi}\mu^2 - \frac{2\,\mathrm{arcsinh}\,1}{\pi}\mu \leq \nu_*(\mu) < \frac{6}{\pi}\mu^2$.

The value at the origin is that of the extremal potential of section 6. Indeed, by (iii) on the real segment, where $3\mu = 2\pi bq$, and by an integration by parts,

$$\mathcal{W}(0) = -\int_0^{x_1^*} 2\log(2q)\,\mathrm{d}\Big[\frac{2\pi}{3}\,b\,q\Big] = \frac{4\pi}{3}\int_0^{x_1^*} b\,\mathrm{d}q = \frac{2\pi}{3}\int_0^{x_1^*}(1-2q)\,\mathrm{d}b = -U_0 = 0.388748, \tag{A.24}$$

by (6.23) at $x = 0$, with $q = \frac{1}{\pi}\arcsin\sinh\pi b$; the boundary terms vanish because $2q = 1$ at the tip and $bq\log q \to 0$ at the origin. So $\mathcal{U}(0) = U_0 = U(0)$. The reason is that $m_g(0) = g(0)$: at exponential order $e^{c'U(0)}$ bounds $|g(0)|/M[g]$ by Proposition 6.4 at $b = 0$, and $e^{c'\mathcal{U}(0)}$ does so by (A.27) below at $\omega = -1/2c'$, the point $z = 0$; the two bounds are the same. Figure 10(b) shows $\mathcal{B}$ and $\mathcal{U}$ on the real axis.

A.4 Optimality at finite central charge

Result M1 is the argument of appendix A.2 carried out at finite c. Fix $x_T = x_1^* - \delta$ and $T = c' x_T^2/3$. For $g \in \bar{\mathcal{A}}$, $g \not\equiv 0$, let

$$p_g(\omega) := \log|m_g(\tfrac{1}{2} + c'\omega)| - \log(2\pi M[g]), \tag{A.25}$$

which is subharmonic on $\mathbb{C}$ and even in μ and in ν. There are four steps.

The obstacle inequality. For all $c \geq 25$ and $c'|\mu| \geq \frac{5}{2}$, $p_g(\omega) \leq c'\mathcal{B}(\omega) + k_a$ with $k_a = \frac{1}{2}\log(32\pi^2 a^5) + \frac{1}{10} < \frac{5}{2}\log c'$. What matters is that k_a depends neither on g nor on ω, because the inequality is used on all of $\partial\mathcal{N}$ and on entire vertical lines. It follows from (A.7) with $\theta_n \geq 1/2a^2$ uniformly in n; from Hölder's inequality between consecutive integer moments, where replacing a chord of the concave function $n \mapsto \log[(4\pi^2 a)^n/(n!)^2]$ by the function costs at most $\frac{1}{10}$; and from Stirling's formula with its exact remainder. Because $c' = 12a$ exactly, the main terms are exactly $c'\mathcal{B}(\omega)$. Had we scaled with c instead of c', the right side would contain the additional term $|\mu|\, c \log \frac{c}{c-1}$, which is unbounded on $\mathcal{N}$.

The comparison step. The obstacle inequality is sharp on $\partial\mathcal{N}$ and wasteful inside $\mathcal{N}$. Let Ω be an open set whose closure lies in a parabolic region $\{\mu^2 \leq A_0^2(1 + |\nu|)\}$ and whose boundary lies in $\{c'|\mu| \geq \frac{5}{2}\}$, and let u be continuous on the closure of Ω and harmonic in Ω, with $u \geq \mathcal{B}$ on $\partial\Omega$ and $\mathcal{B} - u$ bounded by a power of $1 + |\omega|$. Then

$$p_g \leq c'\, u + k_a \qquad \text{on the closure of } \Omega, \tag{A.26}$$

with the same k_a. Indeed $p_g - c'u - k_a$ is subharmonic in Ω and non-positive on $\partial\Omega$. In an unbounded domain one needs in addition that it does not grow too fast. This is the one delicate point, because the only bound available in the central strip is not uniform in g and c. No uniform bound is needed: the difference grows at most like a power of $|\nu|$, with a constant that depends on g and c, whereas a parabolic region is so thin that it carries positive harmonic functions that grow like $\exp(C\sqrt{|\nu|})$, for instance $\operatorname{Re}\cosh(\frac{\pi}{2A_0}\sqrt{1 - i\omega}) + \operatorname{Re}\cosh(\frac{\pi}{2A_0}\sqrt{1 + i\omega})$ plus a constant. Subtracting ε times such a function, applying the maximum principle on bounded pieces and letting $\varepsilon \to 0$ gives (A.26), and the constant has disappeared from the conclusion. The first application is $\Omega = \mathcal{N}$, $u = \mathcal{U}$, which is allowed by Result M3 (ii)–(iv), since $c'|\mu| \geq 24\mu_* > 7$ on $\partial\mathcal{N}$:

$$p_g(\omega) - c'\,\mathcal{B}(\omega) \;\leq\; -c'\,\mathcal{W}(\omega) + k_a \qquad (\omega \in \mathcal{N}). \tag{A.27}$$

The second application controls the tails of the inversion integral, where Result M3 gives no lower bound for $\mathcal{W}$: with Ω the strip $|\mu| < 1$ and u the harmonic function in it that equals $\mathcal{B}$ on its two sides, which is explicit by (A.9), one finds $p_g - c'\mathcal{B} \leq k_a + c'(0.68 - \eta_1 \log|\nu|)$ for $|\nu| \geq 1$ and $|\mu| \leq \frac{\pi}{3}x_T$, with $\eta_1 = (1 - \frac{\pi}{3}x_T)/\cosh 1$ and $c'\eta_1 > 7$: along a vertical line the integrand of (A.15) decays like a power $|\nu|^{-c'\eta_1}$, uniformly in g and c.

Mellin inversion at the saddle point. Put $z = \frac{1}{2} + c'(\xi + i\nu)$ in the inversion formula, multiply by $V(t) \leq e^{4\pi\sqrt{at}}$ and use Stirling's formula. The exponents that depend on t combine to a function of ξ that is non-positive and vanishes, to second order, only on the line (A.16), $\xi = \xi_t := \frac{\pi}{3}x$; on this line they cancel, and

$$V(t)\,|g(t)| \;\leq\; M[g]\; c'\, t^{-1/2}\, I_g(\xi_t), \qquad I_g(\xi) := \int_{\mathbb{R}} e^{(p_g - c'\mathcal{B})(\xi + i\nu)}\, \mathrm{d}\nu. \tag{A.28}$$

The times $0 < t \leq T$ correspond to $0 < \xi_t \leq \frac{\pi}{3}x_T$, and integrating $t^{-1/2}$ over this range gives $\int_0^T |g|\, V\, \mathrm{d}t \leq M[g]\, c'\, 2\sqrt{T}\, \sup_{0<\xi\leq\pi x_T/3} I_g(\xi)$.

Conclusion. By Result M3 (iv) the closed strip $|\mu| \leq \frac{\pi}{3}x_T$ lies in $\mathcal{N}$. This is the only place where $x_T < x_1^*$ is used, and it is essential: for $x_T = x_1^*$ the line $\operatorname{Re}\omega = \frac{\pi}{3}x_T$ touches the contact set at its tip, where $\mathcal{W} = 0$, and there is no exponential gain. Split I_g at $|\nu| = R_0 := e^{1.68/\eta_1}$. On the

inner part (A.27) gives an integrand at most $e^{k_a - c'\kappa}$, where κ is the minimum of $\mathcal{W}$ over the box $\{|\mu| \le \frac{\pi}{3}x_T,\ |\nu| \le R_0\}$; by the signs in Result M3 (iii) this minimum is attained on the real axis at $\mu = \frac{\pi}{3}x_T$, so that $\kappa = \kappa_M(\delta)$. The outer part is smaller than $e^{-c'}$. With $e^{k_a} < c'^{5/2}$ this is (A.1), with $C_\delta = 3R_0$. Finally, if g is weakly feasible at T, the half-mass condition and (A.1) give $0 < M[g] \le 2C_\delta\, c'^4 e^{-\kappa_M(\delta)c'} M[g]$, which is absurd for large c.

Comparison with Theorem 3. The inequality (A.1) is (6.1) with κ_M in place of the Cardy deficit κ. The two agree at the far end, $\kappa_M(x_1^*) = \mathcal{W}(0) = -U_0 = \kappa(x_1^*)$ by (A.24), and nowhere else: $\kappa_M(\delta) = 0.00037,\ 0.0090,\ 0.036,\ 0.16$ at $\delta = 0.01,\ 0.05,\ 0.1,\ 0.2$, against $\kappa(\delta) = 0.0026,\ 0.029,\ 0.083,\ 0.23$. Near the tip the contact of $\mathcal{U}$ with the obstacle is C^1, so that $\mathcal{W}$ vanishes to second order, $\mathcal{W}(\mu) = (\mu_* - \mu)^2/\mu_* + \dots$, and

$$\kappa_M(\delta) = \frac{\pi}{3x_1^*}\,\delta^2(1 + O(\delta)) = 3.73\,\delta^2(1 + O(\delta)), \qquad \text{whereas} \qquad \kappa(\delta) = 2.650\,\delta^{3/2}(1 + O(\delta)). \tag{A.29}$$

The reason is that (A.28) integrates along the line through the saddle point of the Cardy weight, and not through that of the functional. Used in this way the Mellin argument gives the first statement of Theorem 4, but in place of (6.3) only a correction of order $c'^{1/2}\log^{1/2} c'$. At exponential order nothing is lost on the other line: for $0 \le x \le x_1^*$,

$$U(x) = \mathcal{U}(\mu) + \mu \log \frac{3\mu}{2\pi e\, x^2} \qquad \text{at } \mu = \frac{2\pi}{3}\, x\, q(x), \quad \text{the point where } b(\mu) = x, \tag{A.30}$$

because the right side is stationary in μ there, both sides equal U_0 at $x = 0$, and both have the derivative $-\frac{4\pi}{3}q(x)$. The right side is the exponent that (A.15) produces for $|g(t)|/M[g]$ on the line through this point, where the integrand is largest at $\nu = 0$ because $\partial_\nu \mathcal{W} > 0$. So that line gives $|g|\,V \le M[g]\, e^{c'(U+L)+o(c')}$, that is, the Cardy deficit $\kappa(\delta)$ itself. We have not carried this out at finite c.

A.5 The skeleton of the contact set

A functional that attains the bound should have a symbol m_c with $\frac{1}{c'}\log|m_c(\frac{1}{2} + c'\omega)| \to \mathcal{U}(\omega)$ in $\mathcal{N}$. Its zeros then have the density c' times the Riesz measure of the limit. For the limit $\mathcal{U}$ itself this is the area measure $\mathrm{d}A/(\pi|\mu|)$ on $\mathcal{K}$, which gives no control of signs: for $t \ge T$ with $x_T > x_1^*$ the line (A.16) crosses $\mathcal{K}_+$, and the integrand of (A.15) has constant modulus along the whole segment $|\nu| \le \nu_*(\mu)$. But only the values of the limit in $\mathcal{N}$ enter the threshold. Inside $\mathcal{K}$ the measure may therefore be rearranged, as long as the potential stays below $\mathcal{B}$ and is unchanged in $\mathcal{N}$. Swept together as far as possible it becomes the potential-theoretic *skeleton* of $\mathcal{K}$ [85], a positive measure on four arcs, the *creases*, which issue from the tips (figure 10(a)). It is constructed by continuing $\mathcal{U}$ harmonically from $\mathcal{N}$ across the free boundary into $\mathcal{K}_+$, on a second sheet, until the continuation meets the elementary harmonic function $\operatorname{Re}\Upsilon_R$ of (A.13) along a curve.

The second sheet. By Result M3 (i), q is a conformal coordinate on $\mathcal{N}^+$ in which the upper arc of the free boundary is the line $\operatorname{Re} q = \frac{1}{2}$. We move the origin to the image of the tip and put

$$q = \frac{1}{2} + \frac{i\vartheta}{\pi}, \qquad \text{so that} \qquad \sinh \pi b = \cosh\vartheta, \qquad \omega(\vartheta) = \frac{1}{3}\,\pi b(\vartheta)\Big(1 + \frac{2i\vartheta}{\pi}\Big),$$
$$\pi b(\vartheta) = \vartheta + \log \frac{1 + e^{-2\vartheta} + \sqrt{1 + 6e^{-2\vartheta} + e^{-4\vartheta}}}{2}. \tag{A.31}$$

Then $\mathcal{N}^+$ is the half-strip $\{\operatorname{Re}\vartheta > 0,\ 0 < \operatorname{Im}\vartheta < \frac{\pi}{2}\}$, the upper arc of $\partial\mathcal{K}_+$ is the ray $\vartheta \ge 0$, the tip is $\vartheta = 0$, and the second sheet is reached through $\operatorname{Im}\vartheta < 0$. The map $\omega(\vartheta)$ is holomorphic in a full neighborhood of $\vartheta = 0$, which is the reason for using ϑ. On the negative imaginary axis

$q > \frac{1}{2}$ and $b = \frac{1}{\pi}\operatorname{arcsinh}\sin\pi q$ are real, and $\omega = \frac{2}{3}\,q\operatorname{arcsinh}(\sin\pi q)$ continues the segment $(0,\mu_*)$ beyond the tip into $\mathcal{K}$. It increases up to a maximum 0.34818 at $\vartheta = -i\vartheta_f$, $\vartheta_f = 0.520059$, and then decreases: the map folds the real axis back onto itself. We therefore work in the convex wedge

$$\{\vartheta = \vartheta_1 - i\vartheta_2 :\ \vartheta_1 > 0,\ 0 < \vartheta_2 < \vartheta_1 + \vartheta_f\}, \tag{A.32}$$

whose closure avoids the branch points of $b(\vartheta)$, because $\vartheta_f < \frac{\pi}{2} - \operatorname{arcsinh} 1 = 0.689$.

The step checked in interval arithmetic. Functions of ϑ on the second sheet are single-valued functions of ω in the upper half of $\mathcal{K}_+$ only if $\omega(\vartheta)$ covers it exactly once. It does: on the closed wedge, the corner $-i\vartheta_f$ excepted,

$$\operatorname{Re}(e^{-i\pi/8}\,\omega'(\vartheta)) > 0, \qquad \text{and} \qquad \operatorname{Im}\omega < 0 < \operatorname{Re}\omega \quad \text{on the slanted side } \vartheta_2 = \vartheta_1 + \vartheta_f. \tag{A.33}$$

The first statement gives injectivity, again by the criterion of Noshiro and Warschawski; the rotation is needed because $\arg\omega'$ fills the interval $(-\frac{\pi}{4}, \frac{\pi}{2})$ on the wedge. The second shows that the image contains the open upper half of $\mathcal{K}_+$. The corner, where ω' vanishes, and the far part $\vartheta_1 \ge 3$ of the wedge are treated by hand, with ω'' in a cone around $\omega''(-i\vartheta_f) = 0.491 > 0$ at the corner and with $\pi b(\vartheta) - \vartheta = O(e^{-2\vartheta_1})$ in the far part. What remains is compact, and it was checked in interval (ball) arithmetic with Arb [61], by bisection into boxes on each of which the enclosure of the function satisfies the inequality:

(I0) the location of the fold, $|\vartheta_f - 0.52005880928750816| \le 10^{-30}$;
(I1) $|\arg\omega''| < \frac{\pi}{8}$ on the square $\{0 \le \vartheta_1 \le \frac{1}{20},\ |\vartheta_2 - \vartheta_f| \le \frac{1}{20}\}$;
(I2) the first inequality of (A.33) on the part $\vartheta_1 \le 3$ of the closed wedge outside that square (2380 boxes; the smallest value is about 0.009, next to the corner);
(I3) the second inequality of (A.33) for $\frac{1}{20} \le \vartheta_1 \le 3$, and $\operatorname{Re}\omega \ge 0.287$ for $\vartheta_1 \le \frac{1}{20}$;
(I4) $|\lambda'(\zeta)| \le 2.18$ for $|\operatorname{Re}\zeta|, |\operatorname{Im}\zeta| \le e^{-6}$, where $\lambda(\zeta) = \log\frac{1}{2}[(1-\zeta) + \sqrt{1-6\zeta+\zeta^2}]$ is the logarithm in (A.31) at $\zeta = -e^{-2\vartheta}$; this bounds the far part.

This is the only place in this appendix where a computer is used. A consequence that is needed below is that $\arg b \in (-\pi, 0)$ and $\arg q \in (0, \frac{\pi}{2})$ on the wedge, with $\arg\omega = \arg b + \arg q$ for the principal values.

The continuation and the crease. On the first sheet $\Upsilon' = \log(b/q)$, and this expression is holomorphic in ϑ across the ray $\vartheta \ge 0$ and in the whole wedge. Hence

$$\begin{gathered} \Upsilon'_{II}(\omega) := \log\frac{b}{q}\Big|_{\vartheta(\omega)}, \qquad \Upsilon_{II}(\mu_*) := \mathcal{B}(\mu_*); \\ \mathcal{E} := \Upsilon_R - \Upsilon_{II}, \qquad \mathcal{E}' = 2\log(2q), \qquad \mathcal{E}(\omega) = \frac{(\omega-\mu_*)^2}{\mu_*} + O(|\omega-\mu_*|^3) \end{gathered} \tag{A.34}$$

defines the analytic continuation Υ_{II} of Υ across the upper arc, and through a full neighborhood of the tip, to the upper half of $\mathcal{K}_+$. We have used $\Upsilon'_R = \log\frac{6\omega}{\pi} = \log(2b) + \log(2q)$; the double zero of $\mathcal{E}$ at the tip is the C^1 contact of $\mathcal{U}$ with the obstacle. There are now two harmonic functions in the upper half of $\mathcal{K}_+$, and their order follows from the signs of the arguments. First, $\partial_\nu(\mathcal{B} - \operatorname{Re}\Upsilon_{II}) = 2\arg b < 0$, and $\operatorname{Re}\Upsilon_{II} = \mathcal{B}$ on the arc, so that $\operatorname{Re}\Upsilon_{II} < \mathcal{B}$ below it. Next, $\partial_\mu \operatorname{Re}\mathcal{E} = 2\log|2q| > 0$ and $\partial_\nu \operatorname{Re}\mathcal{E} = -2\arg q < 0$, while $\operatorname{Re}\mathcal{E} = -2\mathsf{D}_\mu(\nu_*(\mu)) < 0$ on the arc and $\operatorname{Re}\mathcal{E} = \mathcal{B} - \operatorname{Re}\Upsilon_{II} > 0$ on the real ray $\mu > \mu_*$. On each vertical segment $\operatorname{Re}\mathcal{E}$ therefore has exactly one zero, and

$$\mathcal{C} := \{\operatorname{Re}\mathcal{E} = 0\} = \{\nu = \nu_c(\mu),\ \mu > \mu_*\}, \qquad 0 < \nu_c < \nu_*, \qquad \nu_c'(\mu) = \frac{\log|2q|}{\arg q} > 0, \tag{A.35}$$

is a real-analytic curve, the *crease*, which leaves the tip at 45°. Heuristically it is an anti-Stokes line: a function that behaves like $e^{c'\Upsilon_R} + e^{c'\Upsilon_{II}}$ is dominated by one exponential on either side of it and has its zeros along it. We define

$$\mathcal{U}_{\mathrm{sk}} := \begin{cases} \mathcal{U} & \text{on the closure of } \mathcal{N}, \\ \max(\operatorname{Re}\Upsilon_R, \operatorname{Re}\Upsilon_{II}) & \text{on the upper half of } \mathcal{K}_+, \\ \mathcal{B} & \text{on the real rays } |\mu| \geq \mu_*, \end{cases} \tag{A.36}$$

continued by the symmetries under $\omega \to -\omega$ and $\omega \to \bar{\omega}$. Thus $\mathcal{U}_{\mathrm{sk}} = \operatorname{Re}\Upsilon_{II}$ between the free boundary and the crease, and $\mathcal{U}_{\mathrm{sk}} = \operatorname{Re}\Upsilon_R$ between the crease and the real axis. It is continuous, harmonic away from the four creases, subharmonic on $\mathbb{C}$, equal to $\mathcal{U}$ on $\mathcal{N}$, and

$$\mathcal{U}_{\mathrm{sk}} \leq \mathcal{B} \quad \text{on } \mathbb{C}, \qquad \text{with equality on the real rays } |\mu| \geq \mu_*. \tag{A.37}$$

The skeleton, parametrized by its mass. The Riesz measure $\mathfrak{n}_{\mathrm{sk}} := \frac{1}{2\pi}\nabla^2\mathcal{U}_{\mathrm{sk}}$ is carried by $\mathcal{C}$ and its three mirror images. Across $\mathcal{C}$ the gradient jumps by $|\mathcal{E}'|$, so that $\mathrm{d}\mathfrak{n}_{\mathrm{sk}} = \frac{1}{\pi}|\log 2q|\,\mathrm{d}s$ with respect to arc length, a positive real-analytic density that vanishes linearly at the tip. Along $\mathcal{C}$ the function $\mathcal{E}$ is purely imaginary, and the mass between the tip and a point of $\mathcal{C}$ is $\operatorname{Im}\mathcal{E}/2\pi$ there; it is unbounded. We parametrize the crease by its mass,

$$\mathcal{E}\big(\omega_*(\tau)\big) = 2\pi i\,\tau \quad (\tau \geq 0), \qquad \omega_*(\tau) = \mu_* + e^{i\pi/4}\sqrt{2\pi\mu_*\,\tau}\,\big(1 + O(\sqrt{\tau})\big) \quad (\tau \to 0), \tag{A.38}$$

so that $\mathfrak{n}_{\mathrm{sk}}$ is the sum of the images of $\mathrm{d}\tau$ under $\pm\omega_*$ and $\pm\bar{\omega}_*$. Jensen's formula and (A.37) give $\mathfrak{n}_{\mathrm{sk}}\{|\omega| \leq r\} \leq Cr\log(2+r)$, hence $\int_0^\infty |\omega_*|^{-2}\mathrm{d}\tau < \infty$, and then, as in the Hadamard factorization, $\mathcal{U}_{\mathrm{sk}}$ is the potential of its mass. With the normalization $\mathcal{U}_{\mathrm{sk}}(0) = \mathcal{U}(0) = U_0$,

$$\mathcal{U}_{\mathrm{sk}}(\omega) - U_0 = \int_0^\infty \log\Big|\Big(1 - \frac{\omega^2}{\omega_*(\tau)^2}\Big)\Big(1 - \frac{\omega^2}{\bar{\omega}_*(\tau)^2}\Big)\Big|\,\mathrm{d}\tau. \tag{A.39}$$

The error estimates of appendix A.7 need quantitative control of $\omega_*(\tau)$, which one obtains from $\omega_*' = i\pi/\log(2q)$ and from the explicit far field $\pi b \approx \vartheta$. The crease does not return to the real axis at any scale: $\operatorname{Im}\omega_* \geq a_0(\operatorname{Re}\omega_* - \mu_*)$ with a constant $a_0 \in (0,1]$, so that the creases stay out of the sector $\{\mu > \mu_*,\ |\nu| < a_0(\mu - \mu_*)\}$. Chord and arc are comparable, because $\arg\omega_*' \in (0, \frac{\pi}{2})$. Up to a constant factor the speed $|\omega_*'|$ decreases, but no faster than $\tau^{-1/2}$, which is its rate at the square-root tip; and $|\omega_*''| \leq C|\omega_*'|/\tau$. The delicate point is the far field, where the margin in the monotonicity of the speed is only logarithmic.

A.6 The functional

What is wanted, and what the skeleton provides. Suppose that a symbol has $|m_c(\frac{1}{2} + c'\omega)| = e^{c'\mathcal{H}(\omega)+o(c')}$. By Stirling's formula the modulus of the integrand $\Gamma(z)m_c(z)(2\pi t)^{-z}$ of the inversion integral at $z = \frac{1}{2} + c'(\mu + i\nu)$ is

$$\exp\big\{c'\big[\mathcal{B}(\mu) + \mathcal{H}(\mu) - \mu\log(4x^2)\big] + o(c')\big\} \times \exp\big\{c'\big[\mathcal{H}(\mu+i\nu) - \mathcal{H}(\mu) - \mathsf{D}_\mu(\nu)\big]\big\}, \qquad x = \sqrt{3t/c'}, \tag{A.40}$$

its value at the real point times its variation along the vertical line, and the weights of the vacuum series (A.5) are $e^{-c'\mathcal{B}(\mu)+o(c')}$ at $n = c'\mu$. Thus the saddle point lies where $(\mathcal{B}+\mathcal{H})'(\mu) = \log(4x^2)$; it dominates its line if $\mathcal{H}(\mu+i\nu) - \mathcal{H}(\mu) < \mathsf{D}_\mu(\nu)$ for $\nu \neq 0$; and the vacuum series is dominated by the terms near the maximum of $\mathcal{H} - \mathcal{B}$ on the positive axis.

The potential $\mathcal{H}_* := \mathcal{U}_{\mathrm{sk}} - U_0$ of the skeleton has all this, but only marginally. In the sector free of creases it is $\operatorname{Re}\Upsilon_R$ plus a constant, so that the saddle point for $x \geq x_1^*$ is on the real axis at $\mu = \frac{\pi}{3}x$. By (A.37), $\mathcal{H}_*(\mu+i\nu) - \mathcal{H}_*(\mu) \leq \mathcal{B}(\mu+i\nu) - \mathcal{B}(\mu) = \mathsf{D}_\mu(\nu)$ for $\mu \geq \mu_*$, but with equality on the free boundary: there $\operatorname{Re}\Upsilon_{II}$ contributes a conjugate pair of saddle points, which

by (R) lie on the same vertical line as the real one and have the same modulus, because $\mathcal{U}_{\rm sk} = \mathcal{B}$ at all three points. Hence $V\,g = r_1 + r_2\cos\Theta(t)$ with a real phase Θ and positive amplitudes r_1, r_2 of the same exponential order, whose ratio is not determined at this accuracy: the sign of g is marginal. Likewise $\mathcal{H}_* - \mathcal{B} = -U_0$ is constant on $[\mu_*, \infty)$, so that all the terms of the vacuum series beyond the tip, which have the wrong sign, are of the same exponential order as the largest one.

The design. A margin is created by thinning and dilating the skeleton. Let $\eta \in (0,1)$, $\eta_v > 0$ and $\iota > 0$ be three small parameters, and put

$$\begin{aligned} \mathcal{H}(\omega) &:= (1-\eta)\,\lambda\,\mathcal{H}_*(\omega/\lambda), \qquad \lambda := e^{\eta_v}\,(2x_1^*)^{-\eta}, \\ \mu_s := \lambda\,\mu_*, \qquad \mu_b &:= (1+\tfrac{\iota}{2})\,\mu_s, \qquad \mu_a := (1+\iota)\,\mu_s. \end{aligned} \tag{A.41}$$

The Riesz measure of $\mathcal{H}$ is the image of $\mathrm{d}\tau$ under the four arcs $\pm\omega_d$, $\pm\bar\omega_d$, where $\omega_d(\tau) := \lambda\,\omega_*(\tau/(1-\eta)\lambda)$, and the regularity properties of appendix A.5 hold for ω_d with the same constants, because they are invariant under dilations. Since $\lambda\mathcal{B}(\omega/\lambda) = \mathcal{B}(\omega) - |\mu|\log\lambda$ and $\lambda\mathsf{D}_{\mu/\lambda}(\nu/\lambda) = \mathsf{D}_\mu(\nu)$, the properties of $\mathcal{U}_{\rm sk}$ become the following.

(D1) $\mathcal{H}$ is subharmonic, finite and C^1 on the real axis, and even in μ and in ν; its Riesz measure is carried by four arcs that issue from the points $\pm\mu_s$, the *tips of the design*.

(D2) *Corridor.* In the sector $\{\mu > \mu_b,\ |\nu| < a_0(\mu - \mu_b)\}$, which is free of mass, $\mathcal{H} = (1-\eta)\,\mathrm{Re}\big[\omega\log\frac{6\omega}{\pi\lambda} - \omega\big] + \mathrm{const}$.

(D3) *Strict damping.* $\mathcal{H}(\mu + i\nu) - \mathcal{H}(\mu) \le (1-\eta)\,\mathsf{D}_\mu(\nu)$ for all $\mu \ge \mu_s$ and all real ν.

(D4) *Strict vacuum dominance.* $(\mathcal{H}-\mathcal{B})'(\mu) = -\eta\log\frac{\mu}{\mu_s} - \eta_v \le -\eta_v$ for $\mu \ge \mu_s$. Hence there are a point $\mu_v \in [\frac12\mu_s, \mu_s)$ and $\varepsilon_0 > 0$ with $(\mathcal{H}-\mathcal{B})(\mu) \le (\mathcal{H}-\mathcal{B})(\mu_v) - \varepsilon_0 - \eta_v(\mu - \mu_s)$ for all $\mu \ge \mu_s$.

The three parameters have three jobs. The reduction by $1-\eta$ makes the damping strict, but by itself it destroys (D4): for $\lambda = 1$ one finds $(\mathcal{H}-\mathcal{B})'(\mu) = -\eta\log\frac{6\mu}{\pi}$, which is positive just to the right of μ_* because $\frac{6}{\pi}\mu_* = 2x_1^* < 1$. The dilation restores (D4), with the margin $\eta_v = \log\lambda + \eta\log(2x_1^*)$; this requires $\lambda > (2x_1^*)^{-\eta} > 1$, so the tip moves outward, to $\lambda\mu_*$, as it must by Result M1. Finally ι keeps the saddle points that are used, $\mu \ge \mu_a$, away from the tip, where the zeros accumulate and no lower bound on the symbol is available. By (D2) the saddle points $\mu \ge \mu_a$ belong to $x \ge x_a$, where

$$\begin{aligned} 4x_a^2 &= \Big(\frac{6\mu_a}{\pi}\Big)^{2-\eta}\lambda^{-(1-\eta)}, \qquad \text{that is,} \\ x_a^2 = (x_1^*)^2\,e^{\eta_v}\,(2x_1^*)^{-2\eta}\,(1+\iota)^{2-\eta} &\ \longrightarrow\ (x_1^*)^2 \quad \text{as } (\eta,\eta_v,\iota)\to 0. \end{aligned} \tag{A.42}$$

The symbol. The Riesz measure of $c'\mathcal{H}$ is $c'\mathrm{d}\tau$ along each arc. We cut every arc into cells of unit mass, replace the mass of each cell by a unit point mass at its midpoint in mass, and let these points be the zeros:

$$\begin{gathered} \omega_j := \omega_d\Big(\frac{j-\frac12}{c'}\Big) \quad (j = 1,2,\dots), \qquad P_c(\omega) := \prod_{j\ge1}\Big(1-\frac{\omega^2}{\omega_j^2}\Big)\Big(1-\frac{\omega^2}{\bar\omega_j^2}\Big), \\ m_c(\tfrac12 + c'\omega) := \omega\,(\omega^2 - \mu_s^2)\,P_c(\omega). \end{gathered} \tag{A.43}$$

There is no integrality condition, so c is an arbitrary real number. By (A.39), $\log|P_c|$ is the midpoint rule, with step $1/c'$, for the integral $c'\mathcal{H}$. The set of zeros is invariant under $\omega \to -\omega$ and $\omega \to \bar\omega$, so P_c is even, real on the real axis and positive there. The zero at $\omega = 0$ makes the symbol odd, and the pair $\pm\mu_s$ puts its only sign change on the positive axis at the tip of the design. What the rest of the argument uses is the following list, in which $\delta_c = C/c'$.

(P1) m_c is entire, real on $\mathbb{R}$, and $m_c(1-z) = -m_c(z)$.

(P2) $\log|m_c(\frac12+c'\omega)| \le c'[\mathcal{H}(\omega)+\delta_c(1+|\omega|)]$ for all ω with $\mu \ge \mu_s$, and $\ge c'[\mathcal{H}(\omega)-\delta_c(1+|\omega|)]$ in the corridor of (D2) and on a real interval around μ_v.
(P3) $m_c(\frac12+c'\mu) > 0$ for real $\mu > \mu_s$, and $m_c(n+1) \le 0$ for the integers $n \ge 1$ with $n+\frac12 < c'\mu_s$.
(P4) $|\Gamma(z)m_c(z)| \le C_c\, e^{-a_c|\operatorname{Im} z|}$ for $-\frac12 \le \operatorname{Re} z \le \frac12 + c'\mu_a$ and $|\operatorname{Im} z| \ge 1$, with $a_c > 0$.

The upper bound in (P2) is needed in the whole half-plane to the right of the tip, the arcs included, on which the zeros lie; the lower bound only away from the zeros. (P1) and (P3) are read off from the product. (P2) and (P4) are the subject of appendix A.7; the content is that the error of the midpoint rule is $O(1+|\omega|)$, with no factor c'.

From the symbol to the functional. For $t > 0$ let

$$g_c(t) := \frac{1}{2\pi i} \int_{\operatorname{Re} z = s_0} (2\pi t)^{-z}\, \Gamma(z)\, m_c(z)\, \mathrm{d}z, \tag{A.44}$$

which by (P4) does not depend on $s_0 > 0$, and is real by (P1). Moving the line to $\operatorname{Re} z = -\frac12$ one crosses the pole of Γ at $z = 0$ and finds $g_c(t) = m_c(0) + O(t^{1/2})$, so g_c is continuous on $[0,\infty)$. Next, $\hat g_c = -g_c$: the Laplace transform of g_c is $F(\beta) = \frac{1}{2\pi i}\int_{\operatorname{Re} z=1/2} \frac{\pi}{\sin \pi z}\, m_c(z)\, \frac{\beta^{z-1}}{2\pi}\, \mathrm{d}z$, the substitution $z \to 1-z$ preserves the line and $\sin \pi z$ and changes the sign of m_c, hence $F(1/\beta) = -\beta F(\beta)$, which is $\hat g_c = -g_c$ by (2.8). *In Mellin space the Fourier constraint costs nothing: every odd symbol with enough decay gives a functional, and all the work is in the signs.* Finally the decay. For every $s_0 > 0$, $|g_c(t)| \le (2\pi t)^{-s_0} J(s_0)$ with $J(s_0) := \frac{1}{2\pi}\int |\Gamma m_c|(s_0+iy)\, \mathrm{d}y$. By (P2) and (D3), $|\Gamma m_c|$ decays exponentially along the lines to the right of the tip as soon as $\delta_c \le \eta/8$, and since $\mathcal{H}(\mu) = (1-\eta)\mu\log\mu + O(\mu)$ one finds $\log J(\frac12 + c'\mu) \le c'[(2-\eta)\mu\log\mu + C\mu]$. This is smaller than $\log[\Gamma(2s_0)(8\pi\alpha)^{-s_0}]$ at $s_0 = \frac12 + c'\mu$ for every $\alpha > 0$, up to a constant that depends on α and c, and the choice $2s_0 = 4\pi\sqrt{\alpha t}$ then gives

$$|g_c(t)| \le C_{\alpha,c}\, e^{-4\pi\sqrt{\alpha t}} \qquad \text{for every } \alpha > 0. \tag{A.45}$$

In particular $\int_0^\infty |g_c|\, \mathrm{d}t < \infty$ and $M[g_c] < \infty$, because $V \le e^{4\pi\sqrt{at}}$: $g_c \in \bar{\mathcal{A}}$. Here $\eta > 0$ is essential twice. Without the margin $\eta \mathsf{D}_\mu(\nu)$ the error $c'\delta_c|\nu|$ that (P2) allows would make the bound non-integrable along the line; and for $\eta = 0$ the symbol would grow at the critical rate $\mu\log\mu$, for which one obtains (A.45) only up to some finite α.

The sign of g_c. Fix c and t, and let $I(\omega) := \Gamma(z)m_c(z)(2\pi t)^{-z}$, so that $g_c(t) = \frac{c'}{2\pi}\int_{\mathbb{R}} I(\mu+i\nu)\, \mathrm{d}\nu$ for every $\mu > 0$; by (P3), $I > 0$ on the real axis for $\mu > \mu_s$. If x is confined to a compact set this is a standard problem with the large parameter c'. What is delicate is that positivity is required for all $t \ge T$ at fixed c: as $t \to \infty$ the saddle point μ_t moves off to infinity, the only large parameter is $c'\mu_t$, and the errors $c'\delta_c(1+|\omega|)$ that (P2) allows are not small. The resolution is that everything is invariant under dilations of ω: the corridor is a sector, the error is relative, and the profile in (D2), like Stirling's exponent, is homogeneous of degree one up to terms linear in ω. The saddle-point expansion at μ then has $1/\sqrt{c'\mu}$ as its only parameter, uniformly for $\mu \ge \mu_a$. In the corridor $\log m_c$ is holomorphic and real on the axis, and the difference Q_c between $\frac{1}{c'}\log m_c$ and the holomorphic profile of (D2) has $|\operatorname{Re} Q_c| \le \delta_c(1+|\omega|)$. A disc of radius proportional to μ around $\mu \ge \mu_a$ lies in the corridor, and the gradient estimate for harmonic functions and Cauchy's estimates give $|Q_c'| \le C\delta_c$, $|Q_c''| \le C\delta_c/\mu$ and $|Q_c'''| \le C\delta_c/\mu^2$ there. It follows that the equation $\partial_\mu \log I = 0$ has exactly one solution $\mu_t \ge \mu_a$ for every $t \ge T_{\mathcal{H}}(c) := \frac13 c' x_a^2 \exp[C(\delta_c + c'^{-2})]$, that $-\partial_\mu^2 \log I$ lies between $c'/2\mu_t$ and $3c'/\mu_t$ there, and that the third derivative is at most Cc'/μ^2 on the disc. It is essential to expand at this exact saddle point: the saddle point of the limit profile differs from it by $O(\delta_c\mu)$, which exceeds the width $\sqrt{\mu/c'}$ of the Gaussian as $\mu \to \infty$. On the window $|\nu| \le r\mu_t$, with a small constant r, the integrand is a Gaussian up to a relative error $O((c'\mu_t)^{-1/2})$. On the tails $|\nu| \ge r\mu_t$ one

leaves the corridor and has only upper bounds; (D3), (P2) and $\mathsf{D}_\mu(\nu) \geq \nu^2/2(\mu + |\nu|)$ give $|I(\mu_t + i\nu)|/I(\mu_t) \leq \sqrt{2}\exp(-c'\gamma|\nu|)$ with $\gamma > 0$. Altogether

$$g_c(t) = \frac{c'}{2\pi}\, I(\mu_t)\, \Big(\frac{2\pi}{-\partial_\mu^2 \log I(\mu_t)}\Big)^{1/2} [1 + \epsilon_c(t)], \qquad |\epsilon_c(t)| \leq \frac{C}{\sqrt{c'\mu_a}} \leq \frac{1}{2} \qquad \text{for all } t \geq T_{\mathcal{H}}(c), \tag{A.46}$$

and $g_c(t) > 0$ because $I(\mu_t) > 0$.

The sign of the vacuum value. By (A.5) and Stirling's formula,

$$(g_c)_{\text{vac}} = \frac{1}{\sqrt{\pi^2 c'/3}} \sum_{n \geq 2} \theta_n\, e^{\epsilon_n}\, e^{-c'\mathcal{B}(\mu_n)}\, [-m_c(\tfrac{1}{2} + c'\mu_n)], \qquad \mu_n := \frac{n + \frac{1}{2}}{c'}, \quad 0 \leq \epsilon_n \leq \tfrac{1}{2}\log 2. \tag{A.47}$$

All the terms with $\mu_n < \mu_s$ are non-negative by (P3). We keep the one nearest to μ_v; by the lower bound in (P2) it is at least $\exp\{c'[(\mathcal{H} - \mathcal{B})(\mu_v) - \delta_c(1 + \mu_v)] - C\}$. The terms with $\mu_n \geq \mu_s$ have the wrong sign. By (P2) and (D4) the modulus of such a term is at most $\exp c'[(\mathcal{H} - \mathcal{B})(\mu_v) - \varepsilon_0 + \delta_c(1 + \mu_s) - (\eta_v - \delta_c)(\mu_n - \mu_s)]$; the points μ_n have spacing $1/c'$, so this is a geometric series, and its sum is at most $1 + 2/\eta_v$ times its first term. Hence $(g_c)_{\text{vac}} > 0$ as soon as $\delta_c(2 + \mu_v + \mu_s) \leq \frac{1}{2}\varepsilon_0$: the wrong-sign terms are smaller by the factor $e^{-c'\varepsilon_0/2}$.

Conclusion. Let $x_g > x_1^*$. By (A.42) we choose η, η_v and ι, depending only on x_g, such that $x_a < \frac{1}{2}(x_1^* + x_g)$. This fixes the design, its μ_v and ε_0, and then all the constants above. Since $\delta_c \to 0$, there is $c_0(x_g)$ such that for $c \geq c_0(x_g)$ the smallness conditions on δ_c hold and $T_{\mathcal{H}}(c) \leq c' x_g^2/3$. For every such real c the function g_c of (A.44) lies in $\bar{\mathcal{A}}$, is positive on $[c'x_g^2/3, \infty)$ and has $(g_c)_{\text{vac}} > 0$. This is Result M2.

A.7 Discretization of the skeleton

It remains to justify (P2) and (P4). In electrostatic language, $c'\mathcal{H}$ is the potential of a line charge of density $c'\mathrm{d}\tau$ in the mass parameter of the arcs, and $\log|P_c|$ is that of unit point charges at the mass midpoints of the cells. The claim is that the difference is $O(1)$, uniformly in c and in the point of observation:

$$\log|P_c(\omega)| \leq c'\mathcal{H}(\omega) + C \quad \text{for all } \omega \in \mathbb{C}, \qquad \log|P_c(\omega)| \geq c'\mathcal{H}(\omega) - C \quad \text{if } \operatorname{dist}(\omega, \text{arcs}) \geq C\,\ell_1, \tag{A.48}$$

where ℓ_j is the length of the j-th cell, and $\ell_1 \leq Cc'^{-1/2} \to 0$. The upper bound holds everywhere, also on the arcs, where the zeros lie; the lower bound cannot, since P_c vanishes there. For one arc and a point w let

$$e_j(w) := c' \int_{I_j} \log\Big|\frac{\omega_j - w}{\omega_d(\tau) - w}\Big|\, \mathrm{d}\tau, \qquad I_j = \Big[\frac{j-1}{c'}, \frac{j}{c'}\Big], \tag{A.49}$$

be the error made when the mass of the j-th cell is concentrated at its midpoint in mass. There are three regimes. *Near cells*, the cell nearest to w and its two neighbors: no cancellation is needed, because a logarithmic singularity is integrable against a mass that is spread evenly; chord and arc being comparable and the mass per unit length being at most C/ℓ_j, one finds $-\log(1 + \ell_j/|\omega_j - w|) \leq e_j(w) \leq C$ for every cell and every w. *Far cells*: $e_j(w)$ is the error of the midpoint rule for $\tau \mapsto \log(\omega_d(\tau) - w)$; the linear term of the Taylor expansion about the midpoint integrates to zero, and the second derivative, with $|\omega_d''| \leq C|\omega_d'|/\tau$, gives

$$|e_j(w)| \leq C\Big[\frac{1}{j-1}\,\frac{\ell_j}{d_j} + \frac{\ell_j^2}{d_j^2}\Big] \qquad (j \geq 2), \qquad d_j := \operatorname{dist}(w, \text{cell } j). \tag{A.50}$$

The second term is the quadrupole field of the cell. The first is a residual dipole, present because the mass midpoint of a cell is its center of mass only if the speed is constant along it. Since the speed decreases no faster than $\tau^{-1/2}$, the lengths of the cells between the j-th and the one nearest to w are comparable with ℓ_j in the sense that $\ell_j/d_j \le C[\frac{1}{j-1} + \frac{1}{k}]$, where k is the number of cells in between, and this is square-summable, uniformly in w and c. *The tip*: there $\omega_d - \mu_s \propto \sqrt{\tau}$, and $|\omega_d''| \propto \tau^{-3/2}$ is not integrable, so (A.50) has no analogue for the first cell, however far w is from it. This is harmless, because the bound for near cells holds for every cell and uses no second derivative; the first cell is always counted among the near ones. Summing over the cells and over the four arcs gives (A.48).

With the prefactor $\omega(\omega^2 - \mu_s^2)$, which is at most $(\mu_s + |\omega|)^3$ and is bounded below in the corridor and near μ_v, (A.48) is (P2) with $\delta_c = C/c'$, for all c so large that $C\ell_1$ is smaller than the distance from the arcs to the corridor and to the interval around μ_v. For (P4), the dilated form of (A.37) and $\mathsf{D}_\mu(\nu) \le \frac{\pi}{2}|\nu|$ give $\mathcal{H}(\omega) \le (1-\eta)\frac{\pi}{2}|\nu| + C$ for $|\mu| \le \mu_a$, and $|\Gamma(z)| \le C(1+|\operatorname{Im} z|)^{\operatorname{Re} z - 1/2} e^{-\pi|\operatorname{Im} z|/2}$; so $\Gamma(z) m_c(z)$ decays like $e^{-\eta\pi|\operatorname{Im} z|/2}$ up to a power. Here again $\eta > 0$ is indispensable: it is the only margin against the decay of the Gamma function.

A.8 A dictionary, and remarks

The strip and the Mellin plane. The arguments of section 6 and of appendix A.4 have the same skeleton: a holomorphic function attached to g, a bound on part of a boundary that comes from the vacuum, the maximum principle for the logarithm of the modulus, and the half-mass condition. They are carried out in conjugate variables. In section 6 the function is $G(b)$ on the strip $\mathbb{S}$, and the variable is b. Here it is m_g on the plane, and the variable is the action $\omega = \frac{2\pi i}{3} bp$ (A.20), as one expects of a Mellin transform, which diagonalizes dilations. The two profiles, $u_g(b)$ of (6.13) and the left side of (A.11), are related at exponential order by the saddle point of the Mellin transform, that is, by a Legendre transformation in $\log t$. The correspondence is as follows.

- The Fourier transform is the quarter-turn $(p, b) \mapsto (b, -p)$ of section 4 on the strip, and the reflection $\omega \to -\omega$, which acts as $(b, q) \to (iq, ib)$, in the plane.
- The vacuum is the point $b = \frac{i}{2}$ on an edge of the strip, and gives the boundary value 0 on the edges (Lemma 6.1). In the plane every Taylor coefficient of the Cardy weight gives a bound on a vertical line; together they are the obstacle $\mathcal{B}$.
- The Cardy line $-L$ on the slits $|x| \ge x_1^*$ corresponds to the obstacle on the contact set. The tips $b = \pm x_1^*$ of the slits are the tips $\omega = \pm\frac{\pi}{3} x_1^*$ of $\mathcal{K}$; on the free boundary b is real and runs over the band $x \ge x_1^*$, and $q = ip(x + i0)$ there. The edges $|\operatorname{Im} b| = \frac{1}{2}$ of the strip appear as the free boundary of $-\mathcal{K}_+$.
- The extremal potential U corresponds to $\mathcal{U}$, and $U(0) = \mathcal{U}(0) = U_0$ (A.24). The exponents differ away from that point, (A.29): at the tips $U + L$ vanishes to order $\frac{3}{2}$, and $\mathcal{W}$ to order 2.
- The charge of U sits on the slits, with the density ρ_U of (6.21). The charge of $\mathcal{U}$ is the area measure $\mathrm{d}A/\pi|\mu|$ on $\mathcal{K}$, and the two have the same projection: by (A.22),

$$\int_{-\nu_*(\mu)}^{\nu_*(\mu)} \frac{\mathrm{d}\nu}{\pi\mu}\,\mathrm{d}\mu = \frac{4}{\pi^2}\operatorname{arccosh}(\sinh 3\mu)\,\mathrm{d}\mu = \rho_U(x)\,\mathrm{d}x \qquad \text{at } \mu = \frac{\pi}{3}\,x. \tag{A.51}$$

Zeros. By Theorem 7 the zeros of G in the strip, for any sequence that attains Λ_V, follow the one law ρ_U. The zeros of the symbol are not rigid in this sense: the argument of appendix A.2 fixes their limiting distribution only up to rearrangements inside $\mathcal{K}$ that leave the potential in $\mathcal{N}$ unchanged, and appendix A.5 uses this freedom. The two statements concern the zeros of different functions.

Three functionals. The functional of Theorem 5 places the zeros of G on the band, along the Cardy line, where positivity is an inequality between two numbers that a computer certifies; it is

sharp to order $c^{1/3}$. The functional of section 9 places no zeros at all; it is one transform of one real seed, and it stays below the Cardy line by a fixed margin. The functional of this appendix places the zeros of the Mellin symbol on the creases; the constraint $\hat{g} = -g$ is automatic, and positivity comes from one real saddle point that dominates a conjugate pair by the margin η. In the last two constructions the margin is bought in the same way, by moving the tip outward: the deformation $\gamma < \pi$ of section 9 borrows the extremal profile of a heavier theory, with c' replaced by $(\pi/\gamma)^2 c'$ (9.13), and so does the dilation of (A.41), since $c'\lambda\,\mathcal{H}_*(\omega/\lambda)$ is the potential of the skeleton with c' replaced by $\lambda c'$, at the same z. Neither gives a rate.

The problem on a strip. In the $U(1)^c$ problem the vacuum sits at the origin, on the boundary of the half line of the Mellin transform, and the proof of [13, Ch. 1] works on a strip in the Mellin variable, whose width is the dimension. Here the vacuum sits at $t = -a$, off the half line. It cannot be reached by the transform, and enters only through the expansion (A.4) of its S-image; the strip is replaced by the unknown set $\mathcal{N}$, and the value of the slope is fixed by a free-boundary condition. In the variable b the same vacuum is a boundary point of a fixed strip (section 6.3), and no free boundary has to be found, although the largest useful slit is again characterized by tangency (section 6.6).

B Bessel functions and the Cardy weight

This appendix collects the properties of the Cardy kernel $K_\alpha(t) = I_0(4\pi\sqrt{\alpha t})$ and of the weight $V = K_a - 2K_{a-1} + K_{a-2}$, $\rho_C = 2\pi V$, that the proofs of Parts III and IV use: the continuation of the eigen-identity below the BTZ threshold (Lemma B.1), the comparison of V with K_a and with $e^{c'L}$ (Lemma B.2), the window at the threshold where V degenerates (Lemma B.3), and two-sided asymptotes of I_0 and V with explicit remainders (Lemma B.4). The first three are used from section 6.3 on; the fourth is needed in section 7.9, appendix G and section 8.2. Everything is proved by hand from the integral representation, the power series and the recurrences of I_ν [67, §§10.25, 10.29, 10.32]. Throughout, $c \geq 40$, that is $c' \geq 39$ and $a = c'/12 \geq 3.25$, which enters only through the numerical values in the proofs. We write $w_\alpha = 4\pi\sqrt{\alpha t}$ and $t = c'x^2/3$ with $x \geq 0$, so that $w_a = c'L(x)$, $L(x) = \frac{2\pi}{3}|x|$.

B.1 Continuation of the eigen-identity

Since $K_\alpha(t) = \sum_{k\geq 0}(4\pi^2\alpha t)^k/(k!)^2$ is entire in α, the eigen-identity of section 2.4 makes sense for complex α. We show that it converges on a parabolic region, with vertex at the vacuum $-\alpha = -a$ and focus at the threshold, on which K_a dominates the kernel; in the variable b of section 2.5, $\alpha = -c'b^2/3$, this region is the closed strip $|\operatorname{Im} b| \leq \frac{1}{2}$.

Lemma B.1 (proved). *Let $\mathcal{D}_a = \{\alpha \in \mathbb{C} : |\operatorname{Re}\sqrt{\alpha}| \leq \sqrt{a}\}$, the closed region $\operatorname{Re}\alpha \leq a - (\operatorname{Im}\alpha)^2/4a$ bounded by a parabola; it contains $(-\infty, a]$. For $\alpha \in \mathcal{D}_a$ and $t \geq 0$,*

$$|K_\alpha(t)| \leq K_{(\operatorname{Re}\sqrt{\alpha})^2}(t) \leq K_a(t). \tag{B.1}$$

For $g \in \bar{\mathcal{A}}$ the integral in

$$g(-\alpha) = -2\pi \int_0^\infty g\,K_\alpha\,\mathrm{d}t, \qquad |g(-\alpha)| \leq 2\pi \int_0^\infty |g|\,K_a\,\mathrm{d}t \leq 2\pi(87 + 78\,a\,c')M[g], \tag{B.2}$$

converges absolutely, uniformly in $\alpha \in \mathcal{D}_a$. It defines a function that is continuous on $\mathcal{D}_a$, holomorphic in the interior, and equal to the given $g(s)$ at $\alpha = -s \leq 0$. In particular $g_{\mathrm{vac}} = g(-a) - 2g(-a+1) + g(-a+2) = -\int_0^\infty g\,\rho_C\,\mathrm{d}t$, with an absolutely convergent integral.

Proof. The representation $I_0(z) = \frac{1}{\pi}\int_0^\pi e^{z\cos\theta}\,\mathrm{d}\theta$ [67, §10.32] gives $|I_0(z)| \le I_0(|\mathrm{Re}\,z|)$; since $\mathrm{Re}(4\pi\sqrt{\alpha t}) = 4\pi\sqrt{t}\,\mathrm{Re}\,\sqrt{\alpha}$ and I_0 increases on $[0,\infty)$, this is (B.1). For the rest we use Lemmas B.2 and B.3 below, whose proofs do not use the present lemma. By Lemma B.2(b), $K_a < 214$ on $[0, 4/c']$ and $K_a \le 310\,a\max(1,t^{-1})V \le 78\,a\,c'V$ on $[4/c',\infty)$, so that $\int_0^\infty |g|K_a\,\mathrm{d}t \le 214\int_0^{4/c'}|g|\,\mathrm{d}t + 78\,a\,c'M[g]$. This is finite, because $M[g] < \infty$ and $\int_0^\infty |g|\,\mathrm{d}t = \frac{1}{2\pi}\|g(|\mathbf{r}|^2/2)\|_{L^1(\mathbb{R}^2)} < \infty$ by the definition of $\bar{\mathcal{A}}$ (section 2.6), and Lemma B.3 bounds the first term by $87M[g]$. By (B.1) the integrand in (B.2), which is entire in α, is dominated by $|g|K_a$ for all $\alpha \in \mathcal{D}_a$ at once; dominated convergence gives the uniform absolute convergence, the continuity and the holomorphy in the interior. Finally, $K_{-s}(t) = J_0(4\pi\sqrt{st})$ for $s \ge 0$, and (B.2) at $\alpha = -s$ is the relation $\hat{g} = -g$ written as a Hankel transform of order zero (section 2.3). □

B.2 The weight

The weight V is a second difference of $\alpha \mapsto K_\alpha(t)$ with unit step, yet it is comparable to the single kernel K_a: up to a polynomial factor as soon as $t \ge 4/c'$, and up to the factor 0.9 beyond $t = \xi_1^* c'$, where K_{a-1} and K_{a-2} are exponentially smaller than K_a. The proof writes V as an average of $\partial_\alpha^2 K_\alpha$, a multiple of I_2, and compares Bessel functions at the nearby arguments w_a, w_{a-1}, w_{a-2} through the logarithmic derivative I_1/I_0.

Lemma B.2 (proved)**.** *Let $c \ge 40$, $t > 0$ and $x = \sqrt{3t/c'}$.*

(a) *The weight obeys*

$$\frac{4\pi^2 t}{a-2}\,I_2(w_{a-2}) \le V(t) \le \frac{4\pi^2 t}{a}\,I_2(w_a), \tag{B.3}$$

and $V(t) = \sum_{k\ge 2} v_k t^k$ with $v_k \ge 0$, $v_2 = 8\pi^4$; hence V is positive and increasing on $(0,\infty)$, and $V(t) \ge 8\pi^4 t^2$.

(b) $K_a(t) \le I_0(4\pi/\sqrt{3}) < 214$ *for* $t \le 4/c'$, *and* $K_a(t) \le 310\,a\max(1,t^{-1})\,V(t)$ *for* $t \ge 4/c'$.

(c) $V(t) \ge 0.9\,K_a(t)$ *for* $t \ge \xi_1^* c'$.

(d) $V(t) \le \frac{4\pi^2 t}{a}\,K_a(t) \le \frac{4\pi^2 t}{a}\,e^{c'L(x)}$.

(e) $\log K_a(t) \le c'L(x)$ *for all* x, *and* $\log K_a(t) \ge c'L(x) - \frac{1}{2}\log(c'L(x)) - 2$ *for* $x \ge x_1^*$.

Proof. We use four facts about $I_n(w)$, $w > 0$, which follow from $I_n(w) = \frac{1}{\pi}\int_0^\pi e^{w\cos\theta}\cos n\theta\,\mathrm{d}\theta$ and from the recurrences $I_0' = I_1$, $I_1' = I_2 + I_1/w$, $I_0 - I_2 = (2/w)I_1$ [67, §§10.29, 10.32]. (i) $0 \le I_1 \le I_0 \le e^w$; hence $(1-2/w)I_0 \le I_2 \le I_0$, and $I_0 \le 2I_2$ for $w \ge 4$. (ii) $\log I_0$ is convex, I_0 being the Laplace transform of a positive measure on $[-1,1]$, and its derivative I_1/I_0 lies in $[0,1)$; hence $e^{-(w-w')}I_0(w) \le I_0(w') \le e^{-(w-w')\,(I_1/I_0)(w')}\,I_0(w)$ for $0 < w' \le w$. (iii) $I_1(w)/I_0(w) \ge 1 - 1/w$ for $w \ge 10$. (iv) $I_0(w) \ge e^{w-1/2}/(\pi\sqrt{w})$ for $w \ge 1$, as one sees by restricting the integral to $0 \le \theta \le w^{-1/2}$, where $\cos\theta \ge 1 - 1/2w$. To prove (iii) we substitute $u = 1 - \cos\theta$ in the integrals for $I_0 - I_1$ and I_0:

$$1 - \frac{I_1(w)}{I_0(w)} = \frac{\int_0^2 u\,e^{-wu}\,(u(2-u))^{-1/2}\,\mathrm{d}u}{\int_0^2 e^{-wu}\,(u(2-u))^{-1/2}\,\mathrm{d}u} \le \frac{\frac{\sqrt{\pi}}{2}\,w^{-3/2} + 3e^{-w}}{\frac{1}{\sqrt{2}}\bigl(\sqrt{\pi/w} - e^{-w}/w\bigr)}.$$

In the numerator we use $(2-u)^{-1/2} \le 1$ on $[0,1]$, and $e^{-wu} \le e^{-w}$, $\int_1^2 \sqrt{u/(2-u)}\,\mathrm{d}u \le 3$ on $[1,2]$; in the denominator, $(2-u)^{-1/2} \ge 2^{-1/2}$ on $[0,1]$ and $\int_1^\infty e^{-wu}u^{-1/2}\,\mathrm{d}u \le e^{-w}/w$. The right-hand side is 0.071 at $w = 10$, and w times it decreases for $w \ge 10$.

(a) Fix t and let $f(\alpha) = K_\alpha(t) = I_0(w_\alpha)$. Since $\partial_\alpha w_\alpha = w_\alpha/2\alpha$, the recurrences give

$$f''(\alpha) = \frac{w_\alpha^2}{4\alpha^2}\Bigl(I_1'(w_\alpha) - \frac{I_1(w_\alpha)}{w_\alpha}\Bigr) = \frac{4\pi^2 t}{\alpha}\,I_2(w_\alpha) = 64\pi^4 t^2\,\frac{I_2(w_\alpha)}{w_\alpha^2} \ge 0,$$

which is non-decreasing in α because $I_2(s)/s^2 = \sum_{k\ge 0}(s/2)^{2k}/(4\,k!\,(k+2)!)$ is non-decreasing in s. Since $V(t) = \int_{-1}^1 (1-|u|)\,f''(a-1+u)\,\mathrm{d}u$ is a weighted mean of f'' over $[a-2,a]$, (B.3)

follows. The power series of K_α gives $v_k = (4\pi^2)^k (k!)^{-2}\,[a^k - 2(a-1)^k + (a-2)^k]$, which vanishes for $k = 0, 1$, equals $8\pi^4$ for $k = 2$, and is non-negative because $\alpha \mapsto \alpha^k$ is convex on $[a-2, a] \subset [0, \infty)$.

(b) K_a increases with t, and $w_a = 4\pi/\sqrt{3}$ at $t = 4/c' = 1/3a$, where $I_0(4\pi/\sqrt{3}) = 213.6$. For $t \ge 4/c'$ we have $w_{a-2} \ge 4\pi\sqrt{(1-2/a)/3} \ge 4.49$ because $a \ge 3.25$, so (B.3) and (i) give $V \ge \frac{4\pi^2 t}{a-2} \cdot \frac{1}{2} I_0(w_{a-2}) \ge \frac{2\pi^2 t}{a} K_{a-2}$. By (ii), $K_a \le e^{w_a - w_{a-2}} K_{a-2}$ with $w_a - w_{a-2} = 8\pi\sqrt{t/a}\,/(1 + \sqrt{1-2/a})$. For $4/c' \le t \le \xi_1^* c' = 12\,\xi_1^* a$ this difference is at most $8\pi\sqrt{12\,\xi_1^*}/(1 + \sqrt{1-2/3.25}) \le 8\pi \cdot 0.5611/1.62 \le 8.71$, and $e^{8.71}/2\pi^2 \le 308$, so $K_a \le 308\,(a/t)\,V$. For $t \ge \xi_1^* c'$, (c) gives $K_a \le V/0.9$. In both ranges this is at most $310\,a \max(1, t^{-1}) V$.

(c) Since $K_{a-2} \ge 0$, we have $V \ge K_a - 2K_{a-1} = K_a(1 - 2\vartheta)$ with $\vartheta = I_0(w_{a-1})/I_0(w_a) \le \exp(-(w_a - w_{a-1})\,(I_1/I_0)(w_{a-1}))$ by (ii). For $t \ge \xi_1^* c' = 12\,\xi_1^* a$ we have $w_a - w_{a-1} = 4\pi\sqrt{t}/(\sqrt{a} + \sqrt{a-1}) \ge 2\pi\sqrt{t/a} \ge 2\pi\sqrt{12\,\xi_1^*} \ge 3.525$ and $w_{a-1} \ge 4\pi\sqrt{12\,\xi_1^*\,a(a-1)} \ge 19$, so that $(I_1/I_0)(w_{a-1}) \ge 0.947$ by (iii). Hence $\vartheta \le e^{-3.33} \le 0.036$ and $1 - 2\vartheta \ge 0.9$.

(d) This is the upper bound in (B.3) with $I_2 \le I_0 \le e^w$ from (i) and $w_a = c' L(x)$.

(e) $K_a(t) = I_0(w)$ with $w = c' L(x)$, and $I_0(w) \le e^w$. For $x \ge x_1^*$ we have $w \ge c' L(x_1^*) \ge 22$, and (iv) gives $\log I_0(w) \ge w - \frac{1}{2}\log w - \frac{1}{2} - \log\pi \ge w - \frac{1}{2}\log w - 2$. □

B.3 The window at the BTZ threshold

Near the threshold the weight degenerates, $V(t) \simeq 8\pi^4 t^2$, while K_a stays of order one, so $M[g]$ does not control $\int |g| K_a\,\mathrm{d}t$ there through V. The control comes from the eigen-identity itself: g is minus its own Hankel transform, so $\sup|g|$ is bounded by the L^1 norm of g, and the part of that norm which comes from a fixed neighborhood of $t = 0$ can be absorbed.

Lemma B.3 (proved)**.** *For every $g \in \bar{\mathcal{A}}$,*

$$\int_0^\infty |g|\,\mathrm{d}t \le \frac{4}{\pi^2}\,M[g], \qquad \sup_{t \ge 0}|g(t)| \le \frac{8}{\pi}\,M[g], \tag{B.4}$$

and consequently $\int_0^{4/c'} |g|\,K_a\,\mathrm{d}t \le 214 \cdot \frac{4}{\pi^2}\,M[g] \le 87\,M[g]$ for $c \ge 40$.

Proof. Write $\|g\|_1 = \int_0^\infty |g|\,\mathrm{d}t$, which is finite by the definition of $\bar{\mathcal{A}}$. The relation $\hat{g} = -g$ of Definition 2.5, in the form (2.9), gives $\sup|g| \le 2\pi\|g\|_1$ because $|J_0| \le 1$. We split $\|g\|_1$ at $t_* = 1/4\pi$. Below, $\int_0^{t_*} |g|\,\mathrm{d}t \le t_* \sup|g| \le \frac{1}{2}\|g\|_1$. Above, $V(t) \ge V(t_*) \ge 8\pi^4 t_*^2 = \pi^2/2$ by Lemma B.2(a), so $\int_{t_*}^\infty |g|\,\mathrm{d}t \le \frac{2}{\pi^2} M[g]$. Adding the two and rearranging gives the first bound of (B.4), the second follows from $\sup|g| \le 2\pi\|g\|_1$, and the last statement from Lemma B.2(b). □

B.4 The two-sided Bessel asymptote

The vacuum inequality of section 7.9 needs V to relative accuracy $O(1/c')$ on both sides of the tip, from below on the lobe and from above on the band, and section 8.2 needs an upper bound on I_0 valid for all arguments. We write $\mathrm{as}(z) = e^z/\sqrt{2\pi z}$. The two-sided bound on I_0 comes from the integral representation with $u = 1 - \cos\theta$,

$$I_0(z) = \frac{e^z}{\pi} \int_0^2 \frac{e^{-zu}}{\sqrt{u(2-u)}}\,\mathrm{d}u, \tag{B.5}$$

by bounding $(2-u)^{-1/2}$ below by its value at $u = 0$ and above by a chord; the asymptote of V follows by expanding w_{a-1} and w_{a-2} around w_a.

Lemma B.4 (proved)**.** (a) *For $z \ge 2$,*

$$(1 - e^{-2z})\,\mathrm{as}(z) \le I_0(z) \le \Big(1 + \frac{0.36}{z}\Big)\mathrm{as}(z) + \frac{2}{\pi}. \tag{B.6}$$

(b) *Let $c \ge 40$ and $t = c'x^2/3$ with $x \ge x_1^*/2$, in particular with x in the window $|x - x_1^*| \le 0.1$. Then, with an absolute constant C_V,*

$$V(t) = \mathrm{as}(c'L(x))\Big[\big(1 - e^{-4\pi x}\big)^2 + \varepsilon_V(x)\Big], \qquad |\varepsilon_V(x)| \le \frac{C_V}{c'}. \tag{B.7}$$

(c) *For all $z \ge 0$, $I_0(z) \le 1.18\, e^z/\sqrt{1+z}$.*

Proof. (a) Lower bound: $(2-u)^{-1/2} \ge 2^{-1/2}$ in (B.5) gives $I_0(z) \ge \frac{e^z}{\pi\sqrt{2}}\big[\sqrt{\pi/z} - \int_2^\infty e^{-zu}u^{-1/2}\,\mathrm{d}u\big]$, and $\int_2^\infty e^{-zu}u^{-1/2}\,\mathrm{d}u \le e^{-2z}/(z\sqrt{2}) \le \sqrt{\pi/z}\,e^{-2z}$ for $z \ge 1/2\pi$. Upper bound: on $0 \le u \le 1$ the convex function $(1-u/2)^{-1/2} = \sqrt{2}\,(2-u)^{-1/2}$ lies below its chord $1+(\sqrt{2}-1)u$, so this part of (B.5) is at most $\frac{e^z}{\pi\sqrt{2}}\big[\Gamma(\tfrac12)z^{-1/2} + (\sqrt{2}-1)\Gamma(\tfrac32)z^{-3/2}\big] = \mathrm{as}(z)(1 + \frac{\sqrt{2}-1}{2z}) \le \mathrm{as}(z)(1+\frac{0.36}{z})$; on $1 \le u \le 2$ we use $e^{-zu} \le e^{-z}$ and $\int_1^2 (u(2-u))^{-1/2}\,\mathrm{d}u \le \int_1^2 (2-u)^{-1/2}\,\mathrm{d}u = 2$, which contributes at most $2/\pi$.

(b) Let $z_0 = c'L(x)$, $q_j = 12j/c' \le 24/39$ and $z_j = w_{a-j} = z_0\sqrt{1-q_j}$ for $j = 0,1,2$, so that $V = I_0(z_0) - 2I_0(z_1) + I_0(z_2)$. Since $z_0 q_j/2 = 4\pi j x$,

$$z_j = z_0 - 4\pi j x - \delta_j, \qquad 0 \le \delta_j = z_0\big[1 - \tfrac{q_j}{2} - \sqrt{1-q_j}\big] \le \frac{z_0\, q_j^2}{8(1-q_j)} = \frac{12\pi x\, j^2}{c' - 12j},$$

and $z_j \ge z_2 \ge 0.62\, z_0 \ge 1.29\, c'x \ge 0.18\, c' \ge 7$. Thus (a) applies to each z_j: $I_0(z_j) = \mathrm{as}(z_j)(1+\lambda_j) + r_j$ with $-e^{-2z_j} \le \lambda_j \le 0.36/z_j$ and $0 \le r_j \le 2/\pi$. Moreover $\mathrm{as}(z_j) = \mathrm{as}(z_0)\, e^{-4\pi jx}\, e^{-\delta_j}(1-q_j)^{-1/4}$, and $1 \le (1-q_j)^{-1/4} \le 1 + 11/c'$ for $c' \ge 39$. Therefore

$$\frac{V}{\mathrm{as}(z_0)} = \sum_{j=0}^{2} (-1)^j \tbinom{2}{j}\, e^{-4\pi jx}\,(1+\zeta_j) + R, \qquad 1+\zeta_j = e^{-\delta_j}(1-q_j)^{-1/4}(1+\lambda_j), \qquad |R| \le \frac{4/\pi}{\mathrm{as}(z_0)}.$$

The sum without the ζ_j is $(1-e^{-4\pi x})^2$, so $|\varepsilon_V| \le \sum_j \binom{2}{j} e^{-4\pi jx}|\zeta_j| + |R|$. The three factors of $1+\zeta_j$ lie in $[1-\delta_j, 1]$, $[1, 1+11/c']$ and $[1-e^{-2z_2}, 1+0.36/z_2]$, whence $|\zeta_j| \le \delta_j + 11/c' + 1/z_2$. Each contribution is at most an absolute constant times $1/c'$, uniformly in $x \ge x_1^*/2$: $1/z_2 \le 1/(0.18\, c')$; $e^{-4\pi jx}\delta_j \le 12\pi j^2\, x\, e^{-4\pi jx}/(0.38\, c')$ with $x\, e^{-4\pi jx} \le 1/(4\pi e j)$ for $j = 1,2$, while $\delta_0 = 0$; and $\mathrm{as}(z_0) \ge z_0 \ge 0.18\, c'$, because $e^z \ge \sqrt{2\pi}\, z^{3/2}$ for $z \ge 2$.

(c) For $0 \le z \le 2$, the series $I_0(z) = \sum_{k\ge0}(z^2/4)^k/(k!)^2 \le e^{z^2/4}$ and $\sqrt{1+z} \le e^{z/2}$ give $e^{-z}I_0(z)\sqrt{1+z} \le e^{-z(2-z)/4} \le 1$. For $z \ge 2$, $I_0(z) = \frac{1}{\pi}\int_0^\pi e^{z\cos\theta}\,\mathrm{d}\theta$ and $1 - \cos\theta \ge 2\theta^2/\pi^2$ on $[0,\pi]$ give $I_0(z) \le \frac{e^z}{\pi}\int_0^\infty e^{-2z\theta^2/\pi^2}\,\mathrm{d}\theta = e^z\sqrt{\pi/8z}$, so that $e^{-z}I_0(z)\sqrt{1+z} \le \sqrt{\pi(1+z)/8z} \le \sqrt{3\pi/16} < 1$. Thus $e^{-z}I_0(z)\sqrt{1+z} \le 1$ for all $z \ge 0$, which is more than (c) asserts. □

C Potential theory on the slit strip

This appendix proves the lemmas of potential theory behind sections 6.5 to 6.8: the conformal map and the harmonic measure of D, the entropy of that measure, the Poisson–Jensen and Jensen inequalities on D, the edge bound, Proposition 6.4, and the last inequality of Lemma 6.7. Appendix I uses Lemma C.4 and (C.15) again. From appendix B we take Lemmas B.1 to B.3. Throughout, $c \ge 40$, $D = D_{x_1^*}$, $G(b) = g(c'b^2/3)$ with $g \in \bar{\mathcal{A}}$, and C is an absolute constant whose value may change from line to line.

C.1 The map and harmonic measure

For $z \in \mathbb{H}$ let $b(z) = \frac{1}{2\pi}\big[\log(z-1) - \log z - \log(z+1)\big]$, with all three arguments in $(0,\pi)$, be the map of Lemma 6.3. We write σ for a point of the real axis bounding $\mathbb{H}$, and $\sigma_* := 1 - \sqrt{2}$, $\sigma^* := 1 + \sqrt{2}$, so that

$$b'(z) = \frac{1}{2\pi}\Big[\frac{1}{z-1} - \frac{1}{z} - \frac{1}{z+1}\Big] = -\frac{(z-\sigma_*)(z-\sigma^*)}{2\pi\, z\,(z^2-1)}. \tag{C.1}$$

Lemma C.1 (proved)**.** (a) *The map b is a conformal bijection of $\mathbb{H}$ onto D. The preimage z_w of $w \in D$ is the unique root in $\mathbb{H}$ of*

$$e^{2\pi w} z^2 + (e^{2\pi w} - 1)z + 1 = 0. \tag{C.2}$$

(b) *b extends continuously to $\mathbb{R} \setminus \{-1, 0, 1\}$ and realizes the boundary correspondence stated in Lemma 6.3. It is monotonic on $(0, 1)$ and on $(-\infty, -1)$, and it maps each of $(-1, \sigma_*]$ and $[\sigma_*, 0)$ monotonically onto $[x_1^*, \infty)$, the two intervals giving the two lips of the right slit; likewise $(1, \sigma^*]$, $[\sigma^*, \infty)$ and the left slit.*

(c) *For $b \in D$ let ω_b be the image under this map of the Poisson measure $\frac{\operatorname{Im} z_b}{\pi|\sigma - z_b|^2}\,\mathrm{d}\sigma$ of $\mathbb{H}$ seen from z_b. It is the harmonic measure of D seen from b, a probability measure on ∂D in which the two lips of a slit count separately. On the slits it has the positive density (the two lips added)*

$$\omega_b'(x) := \frac{\mathrm{d}\omega_b}{\mathrm{d}x}(x) = \sum_{\sigma \in \mathbb{R}:\ b(\sigma) = x} \frac{\operatorname{Im} z_b}{\pi|\sigma - z_b|^2} \frac{1}{|b'(\sigma)|}, \qquad \frac{1}{|b'(\sigma)|} = \frac{2\pi|\sigma|\,|\sigma^2 - 1|}{|\sigma - \sigma_*|\,|\sigma - \sigma^*|}, \tag{C.3}$$

and on an edge the same with the single preimage. For every $X > |\operatorname{Re} b|$, and with an absolute constant C_M,

$$\omega_b(\{\tilde{b} \in \partial D :\ |\operatorname{Re} \tilde{b}| \geq X\}) \leq 2\sqrt{2}\, e^{-\frac{\pi}{2}(X - |\operatorname{Re} b|)}, \qquad \int_{\partial D} (1 + |\operatorname{Re} \tilde{b}|)\, \mathrm{d}\omega_b(\tilde{b}) \leq C_M (1 + |\operatorname{Re} b|). \tag{C.4}$$

Proof. For (a) we turn $b(z) = w$ into the quadratic (C.2) and count its roots in $\mathbb{H}$ by continuity in w: a root can leave $\mathbb{H}$ only through the real axis, which happens exactly when w is on a slit.

(a) For fixed $z \in \mathbb{H}$ the angle $\arg(z - \sigma) \in (0, \pi)$ increases with $\sigma \in \mathbb{R}$, so $\pi > \arg(z-1) > \arg z > \arg(z+1) > 0$ and $2\pi \operatorname{Im} b(z) = \arg(z-1) - \arg z - \arg(z+1) \in (-\pi, \pi)$: b maps $\mathbb{H}$ into $\mathbb{S}$. For $w \in \mathbb{S}$, $b(z) = w$ is equivalent to $\frac{z-1}{z(z+1)} = e^{2\pi w}$, which is (C.2) (the imaginary parts then agree, $2\pi \operatorname{Im} b(z)$ and $2\pi \operatorname{Im} w$ being congruent modulo 2π and both in $(-\pi, \pi)$). The two roots depend continuously on w and stay finite. A real root σ (necessarily $\sigma \neq 0, \pm 1$) forces $e^{2\pi w} = \frac{\sigma - 1}{\sigma(\sigma+1)}$ to be real, hence positive because $|\operatorname{Im} w| < \frac{1}{2}$, and the discriminant $(e^{2\pi w} - 1)^2 - 4e^{2\pi w}$ to be non-negative, that is $e^{2\pi w} \notin ((\sqrt{2} - 1)^2, (\sqrt{2} + 1)^2)$; since $e^{2\pi x_1^*} = (\sqrt{2} + 1)^2$, this says that w is real with $|w| \geq x_1^*$, and then both roots are real. Hence the number of roots in $\mathbb{H}$ is constant on the connected set D, where it equals its value 1 at $w = 0$ ($z^2 + 1 = 0$), and it is 0 on the slits: b is a bijection of $\mathbb{H}$ onto D.

(b) On $(0, 1)$, $(-1, 0)$, $(1, \infty)$, $(-\infty, -1)$ the angles $(\arg(\sigma - 1), \arg \sigma, \arg(\sigma + 1))$ are $(\pi, 0, 0)$, $(\pi, \pi, 0)$, $(0, 0, 0)$, (π, π, π), so $\operatorname{Im} b = \frac{1}{2}, 0, 0, -\frac{1}{2}$. On $(-1, 0)$ the modulus $\left|\frac{\sigma - 1}{\sigma(\sigma+1)}\right|$ decreases from $+\infty$ to its minimum $(1 + \sqrt{2})^2$ at σ_* and increases back, so $\operatorname{Re} b$ sweeps $[x_1^*, \infty)$ twice; by (C.1) b' has opposite signs on the two halves, and since b preserves orientation, points of $\mathbb{H}$ near the two halves go to opposite sides of the slit. The interval $(1, \infty)$ is treated in the same way, with the maximum $(\sqrt{2} - 1)^2$ of the modulus at σ^*. On $(0, 1)$ and $(-\infty, -1)$, $b' \neq 0$ and $\operatorname{Re} b$ runs monotonically over $\mathbb{R}$. Finally $i(i + 1) = i - 1$ gives $b(i) = 0$, and at $\sigma = \sqrt{2} - 1$ one has $|\sigma - 1| = 2 - \sqrt{2} = \sigma(\sigma + 1)$, so $b = \frac{i}{2}$.

(c) Composition with the map takes harmonic functions on D to harmonic functions on $\mathbb{H}$ (equivalently, Brownian paths to Brownian paths), so by Poisson's formula on $\mathbb{H}$, $\int \varphi\, \mathrm{d}\omega_b$ solves the Dirichlet problem on D with boundary values φ; this is the definition of harmonic measure [63, §4.3]. The density (C.3) is the change of variables $x = b(\sigma)$ on each of the two intervals that cover a slit. For the tails we compare with an explicit harmonic function (a barrier): $\psi_X(w) := \cosh(\frac{\pi}{2} \operatorname{Re} w) \cos(\frac{\pi}{2} \operatorname{Im} w) / (\cos \frac{\pi}{4} \cosh \frac{\pi}{2} X)$ is harmonic and non-negative on $\bar{\mathbb{S}}$, and is ≥ 1 where $|\operatorname{Re} w| = X$. The exit probability $w \mapsto \omega_w(\{|\operatorname{Re} \tilde{b}| \geq X\})$ is harmonic on D, lies in $[0, 1]$, and vanishes on the part of ∂D where $|\operatorname{Re} \tilde{b}| < X$; by the maximum

principle on the bounded domain $D \cap \{|\operatorname{Re} w| < X\}$ it is at most ψ_X there, and $\psi_X(b) \le \sqrt{2}\cosh(\frac{\pi}{2}\operatorname{Re} b)/\cosh(\frac{\pi}{2}X) \le 2\sqrt{2}\,e^{-\frac{\pi}{2}(X-|\operatorname{Re} b|)}$. Using this for $X = |\operatorname{Re} b| + n$, $n \ge 1$, we get $\int(1+|\operatorname{Re}\tilde{b}|)\,\mathrm{d}\omega_b \le (2+|\operatorname{Re} b|) + \sum_{n\ge1}(2+|\operatorname{Re} b|+n)\,2\sqrt{2}\,e^{-\pi n/2}$, which is the second bound. □

C.2 Entropy

Jensen's inequality in appendix C.3 costs the entropy of harmonic measure on the slits, which we bound here. We write $\log^+ t := \max(\log t, 0)$.

Lemma C.2 (proved)**.** (i) *For every compact $Q \subset D$ there is a constant $C'_Q < \infty$ such that for all $b \in Q$*

$$\int_{|x|\ge x_1^*} \frac{\mathrm{d}\omega_b}{\mathrm{d}x}\left|\log\frac{\mathrm{d}\omega_b}{\mathrm{d}x}\right|\mathrm{d}x \le C'_Q. \tag{C.5}$$

(ii) *There is an absolute constant C_H such that for every real $b \in (-x_1^*, x_1^*)$, at distance $\delta := x_1^* - |b|$ from the nearer tip,*

$$\int_{|x|\ge x_1^*} \frac{\mathrm{d}\omega_b}{\mathrm{d}x}\,\log^+\frac{\mathrm{d}\omega_b}{\mathrm{d}x}\,\mathrm{d}x \le C_H + 5\log\frac{1}{\delta}. \tag{C.6}$$

Proof. By (C.3), ω'_b is the Poisson kernel times the Jacobian $1/|b'|$. The Jacobian has an inverse square-root singularity at each tip: the map folds the real axis there, so $r := x - x_1^*$ is quadratic in $\sigma - \sigma_*$. At the ends it decays like $e^{-2\pi x}$. Since $r^{-1/2}\log r$ is integrable, (i) follows as long as the Poisson kernel is bounded. In (ii) it is not, because z_b approaches the real axis when b approaches a tip, and we keep track of $\operatorname{Im} z_b$.

The Jacobian on the right slit. For $\sigma \in (-1, 0)$ we have $|\sigma|\,|\sigma^2 - 1| \le 1$ and $|\sigma - \sigma^*| \ge 1 + \sqrt{2}$, so $1/|b'(\sigma)| \le 2.61/|\sigma - \sigma_*|$. If $|\sigma - \sigma_*| \le 0.3$, every u between σ_* and σ has $|u| \ge 0.114$, $|u^2 - 1| \ge 0.48$ and $|u - \sigma^*| \le 3.14$, so $|b'(u)| \le 9.5|u - \sigma_*|$ by (C.1) and, integrating, $r = b(\sigma) - b(\sigma_*) \le 4.75\,(\sigma - \sigma_*)^2$. Therefore $1/|b'(\sigma)| \le 5.7\,r^{-1/2}$ if $|\sigma - \sigma_*| \le 0.3$, and $1/|b'(\sigma)| \le 8.7$ otherwise. At the ends $\sigma \to 0^-$ and $\sigma \to -1^+$ one reads off $x = \frac{1}{2\pi}\log\frac{1}{|\sigma|} + O(1)$, resp. $x = \frac{1}{2\pi}\log\frac{2}{|\sigma+1|} + O(|\sigma+1|)$, and $1/|b'| \le C|\sigma|$, resp. $C|\sigma+1|$; in both cases $1/|b'(\sigma)| \le Ce^{-2\pi x}$.

(i) For $b \in Q$ the preimage z_b stays in a compact subset of $\mathbb{H}$, so the Poisson kernel is at most $C''_Q(1+\sigma^2)^{-1}$, and the Jacobian bounds give $0 < \omega'_b(x) \le C''_Q(r^{-1/2}1_{r\le1} + e^{-2\pi x})$ on the right slit. Where $\omega'_b \le 1$ we use $\omega'_b|\log\omega'_b| \le \sqrt{\omega'_b} \le C''_Q(r^{-1/4} + e^{-\pi x})$, which is integrable; the set where $\omega'_b \ge 1$ lies in a bounded neighborhood of the tip, where $\omega'_b\log\omega'_b \le C''_Q r^{-1/2}\log(C''_Q/r)$ is integrable. The left slit is the mirror image, because $b(-1/z) = -b(z)$.

(ii) By the same symmetry we may take $0 \le b < x_1^*$. Put $\lambda := e^{2\pi b} \in [1, \lambda_+)$ and $\lambda_\pm := (\sqrt{2} \pm 1)^2$. The discriminant of (C.2) is $(\lambda - \lambda_+)(\lambda - \lambda_-) < 0$, the two roots are complex conjugate with product $1/\lambda \le 1$, and

$$\operatorname{Im} z_b = \frac{\sqrt{(\lambda_+ - \lambda)(\lambda - \lambda_-)}}{2\lambda}, \qquad \operatorname{Re} z_b = \frac{1-\lambda}{2\lambda} \le 0, \qquad 0.3\sqrt{\delta} \le \operatorname{Im} z_b \le 1. \tag{C.7}$$

The lower bound holds because $\lambda_+ - \lambda = \lambda_+(1 - e^{-2\pi\delta}) \ge \lambda_+ \cdot 0.46 \cdot 2\pi\delta \ge 16.8\,\delta$ (the chord of the concave function $1 - e^{-u}$ over $[0, 2\pi x_1^*]$), $\lambda - \lambda_- \ge 1 - \lambda_- \ge 0.82$ and $2\lambda \le 2\lambda_+ \le 11.7$. The Poisson kernel is at most $1/(\pi \operatorname{Im} z_b)$, so adding the two preimages of $x = x_1^* + r$ and using the Jacobian bounds,

$$\omega'_b(x) \le W(r) := \frac{1}{\pi\,\operatorname{Im} z_b}(11.4\,r^{-1/2} + 17.4), \qquad \log^+ W(r) \le \log\frac{1}{\operatorname{Im} z_b} + \tfrac{1}{2}\log^+\frac{1}{r} + 3. \tag{C.8}$$

Since $\log^+$ is non-decreasing and $\omega'_b \le W$, $\omega'_b\log^+\omega'_b \le \omega'_b\log^+ W$; and since ω_b has total mass 1,

$$\int_{x\ge x_1^*} \omega'_b\log^+\omega'_b\,\mathrm{d}x \le \log\frac{1}{\operatorname{Im} z_b} + 3 + \tfrac{1}{2}\int_{x\ge x_1^*}\omega'_b(x)\,\log^+\frac{1}{r}\,\mathrm{d}x. \tag{C.9}$$

We split the last integral at $r = (\operatorname{Im} z_b)^2 \le 1$. Below it we use $\omega_b' \le W$ and compute, with $y := \operatorname{Im} z_b \le 1$, $\int_0^{y^2} W \log\frac{1}{r}\,\mathrm{d}r = \frac{1}{\pi y}\big[22.8\,y(2\log\frac{1}{y}+2) + 17.4\,y^2(2\log\frac{1}{y}+1)\big] \le 15\log\frac{1}{y} + 25$ (using $y\log\frac{1}{y} \le e^{-1}$). Above it, $\log^+\frac{1}{r} \le 2\log\frac{1}{\operatorname{Im} z_b}$. Altogether the left side of (C.9) is at most $10\log\frac{1}{\operatorname{Im} z_b} + 16 \le 5\log\frac{1}{\delta} + 29$ by (C.7). On the left slit, where $\sigma \ge 1$, we have $|\sigma - z_b| \ge \sigma$ because $\operatorname{Re} z_b \le 0$, so the Poisson kernel is at most $1/(\pi\sigma^2)$ whatever δ is; the Jacobian on $(1,\infty)$ has the same structure as on $(-1,0)$ (the tip at σ^*, the ends at 1 and ∞). Hence $\omega_b'(x) \le C\big(|x+x_1^*|^{-1/2}1_{|x+x_1^*|\le 1} + e^{-2\pi|x|}\big)$ there, with an absolute C, and as in (i) the left slit contributes an absolute constant. □

C.3 Poisson–Jensen and Jensen on the slits

Lemma C.3 (proved)**.** *Let $g \in \bar{\mathcal{A}} \setminus \{0\}$, $b \in D$, and $\omega_b' = \mathrm{d}\omega_b/\mathrm{d}x$ as in (C.3).*

(a) (Poisson–Jensen.) *The potential at b is at most the mean of its boundary values over harmonic measure,*

$$\log|G(b)| \le \int_{\partial D} \log|G|\,\mathrm{d}\omega_b = \int_{|x|\ge x_1^*} \log|G(x)|\,\omega_b'(x)\,\mathrm{d}x + \int_{E_+\cup E_-} \log|G|\,\mathrm{d}\omega_b, \tag{C.10}$$

whether or not G has zeros in D or on ∂D.

(b) (Jensen on the slits.) *Let $m_b := \omega_b(\{|x| \ge x_1^*\}) \in (0,1)$ be the probability of exit through a slit. Then, with an absolute constant C,*

$$\begin{aligned}\int_{|x|\ge x_1^*} \log|G|\,\omega_b'\,\mathrm{d}x \le\ & -c'\int_{|x|\ge x_1^*} L\,\omega_b'\,\mathrm{d}x + m_b\log M[g] + \int_{|x|\ge x_1^*} \omega_b'\log\omega_b'\,\mathrm{d}x \\ & + \frac{m_b}{2}\log c' + C(1+|\operatorname{Re} b|).\end{aligned} \tag{C.11}$$

Proof. (a) We move the problem to the unit disk, where G becomes a bounded holomorphic function, to which the classical fact quoted after (6.8) applies. Let $F(w) := G(b(i\frac{1+w}{1-w}))$ for $|w| < 1$, the inner map being the Möbius map of the disk onto $\mathbb{H}$. By section 6.3, G is bounded and continuous on $\bar{\mathbb{S}}$, so F is bounded and holomorphic; and $F \not\equiv 0$, because G is holomorphic on the connected set $\mathbb{S}$ and $G(x) = g(c'x^2/3)$ does not vanish identically on the real axis. For such F the radial limits F^* exist almost everywhere on the unit circle, $\log|F^*|$ is integrable, and $F = F_{\mathrm{in}}F_{\mathrm{out}}$, where $|F_{\mathrm{in}}| \le 1$ (this factor carries the zeros) and $\log|F_{\mathrm{out}}|$ is the Poisson integral of $\log|F^*|$ [64, Ch. II, Thm. 4.1 and Cor. 4.2], [65, Thms. 17.16–17.17]. Hence $\log|F(w)|$ is at most that Poisson integral. By Lemma C.1(b) the composite map extends continuously to the circle minus four points, so F^* is the composition of G with it almost everywhere, and carrying the Poisson measure of the disk to ∂D gives ω_b by Lemma C.1(c).

(b) This is Jensen's inequality (6.9) with $w = \omega_b'/m_b$ and $K = K_a$, with the constants tracked. On the slits put $\ell(x) := \log K_a(c'x^2/3)$ and write $\log|G| = \log(|G|e^{\ell}/\omega_b') - \ell + \log\omega_b'$. Jensen's inequality for the probability measure $\omega_b'\mathrm{d}x/m_b$, followed by Lemma 6.2, gives

$$\begin{aligned}\int_{|x|\ge x_1^*} \log\frac{|G|e^{\ell}}{\omega_b'}\,\omega_b'\,\mathrm{d}x &\le m_b\log\Big(\frac{1}{m_b}\int_{|x|\ge x_1^*}|G|K_a\,\mathrm{d}x\Big) \\ &\le m_b\log M[g] + m_b\log\frac{12}{c'm_b} \le m_b\log M[g] + \frac{1}{e},\end{aligned} \tag{C.12}$$

since $12/c' < 1$ and $m\log\frac{1}{m} \le e^{-1}$. By Lemma B.2(e), $-\ell(x) \le -c'L(x) + \frac{1}{2}\log(c'L(x)) + 2$ for $|x| \ge x_1^*$, and, since $\log L \le L = \frac{2\pi}{3}|x|$, $\int_{|x|\ge x_1^*}(\frac{1}{2}\log(c'L)+2)\omega_b'\,\mathrm{d}x \le \frac{m_b}{2}\log c' + \int_{\partial D}(2+\frac{1}{2}L)\mathrm{d}\omega_b \le \frac{m_b}{2}\log c' + C(1+|\operatorname{Re} b|)$ by (C.4). The term $\log\omega_b'$ gives the entropy, which converges absolutely by Lemma C.2(i). Adding the three contributions gives (C.11). □

C.4 The edge bound and the proof of the majorant proposition

Lemma C.4 (proved)**.** *This is Lemma 6.1, with the supremum taken over the closed strip. There is an absolute constant C such that for all $c \geq 40$, all $g \in \bar{\mathcal{A}}$ and all real x,*

$$|G(x \pm \tfrac{i}{2})| \leq 2\pi \int_0^\infty |g|\, K_a \,\mathrm{d}t \leq C\, a\, c'\, M[g], \quad \textit{hence} \quad \log|G(x \pm \tfrac{i}{2})| \leq \log M[g] + 2\log c' + C, \tag{C.13}$$

uniformly in x and in g (in particular in the order P). The same bound holds for $\sup_{\bar{\mathbb{S}}}|G|$.

Proof. Let $b \in \bar{\mathbb{S}}$ and $\alpha := -c'b^2/3$, so that $G(b) = g(-\alpha)$. Then $\sqrt{\alpha} = \pm i\sqrt{c'/3}\, b$ and $(\operatorname{Re}\sqrt{\alpha})^2 = \frac{c'}{3}(\operatorname{Im} b)^2 \leq \frac{c'}{12} = a$, with equality on the edges $b = x \pm \frac{i}{2}$, for every real x. So α lies in the region $\mathcal{D}_a$ of Lemma B.1, where $|K_\alpha| \leq K_a$ by (B.1), and (B.2) gives $|G(b)| \leq 2\pi \int_0^\infty |g| K_a \,\mathrm{d}t \leq 2\pi(87 + 78\, a\, c')M[g] \leq C\, a\, c'\, M[g]$. The polynomial factor comes from $K_a \leq 78\, a\, c'\, V$ for $t \geq 4/c'$ (Lemma B.2(b)) and from $\int_0^{4/c'} |g|\, K_a \,\mathrm{d}t \leq 87 M[g]$ on the window at the BTZ threshold (Lemma B.3). Finally $\log(C\, a\, c') = 2\log c' + \log \frac{C}{12}$. □

Proof of Proposition 6.4. The idea is described in section 6.5. Let $h(b) := -\int_{|x| \geq x_1^*} L \,\mathrm{d}\omega_b$. Inserting (C.11) and (C.13) (with $\omega_b(E_+ \cup E_-) = 1 - m_b$) into (C.10), and using $\frac{1}{2}m_b + 2(1 - m_b) \leq 2$ for the coefficient of $\log c'$, we get for every $b \in D$, every $g \in \bar{\mathcal{A}} \setminus \{0\}$ and every $c \geq 40$

$$\log|G(b)| \leq c'\, h(b) + \log M[g] + \int_{|x| \geq x_1^*} \omega_b' \log \omega_b' \,\mathrm{d}x + 2\log c' + C(1 + |\operatorname{Re} b|). \tag{C.14}$$

It remains to recognize h. By Lemma C.1(c), $h \circ b$ is the Poisson integral on $\mathbb{H}$ of the function equal to $-L(\operatorname{Re} b(\sigma))$ on $(-1, 0) \cup (1, \infty)$ and to 0 on $(0, 1) \cup (-\infty, -1)$. This function is continuous on $\mathbb{R} \setminus \{-1, 0, 1\}$, in particular at σ_* and σ^*, and, by (C.4), integrable against the Poisson measure. Hence h is harmonic on D, takes the boundary values $-L$ on both lips of the slits and at the two tips and 0 on the edges, continuously, and grows at most linearly, $|h(b)| \leq \frac{2\pi}{3} C_M (1 + |\operatorname{Re} b|)$. It is therefore the function $U_{x_1^*}$ of Proposition 6.4, which these properties determine uniquely (part (d) of the proof of Lemma 6.5, where it is also shown that $U_{x_1^*} = U$):

$$U_{x_1^*}(b) = -\int_{|x| \geq x_1^*} L(x) \,\mathrm{d}\omega_b(x) \leq 0 \qquad (b \in D). \tag{C.15}$$

For b in a compact set $Q \subset D$ the entropy in (C.14) is at most C_Q' by Lemma C.2(i) and $|\operatorname{Re} b|$ is bounded; dividing by c' gives $u_g(b) \leq U_{x_1^*}(b) + C_Q(1 + \log c')/c'$ with $C_Q := \max(2,\, C_Q' + C \sup_Q(1 + |\operatorname{Re} b|))$, which depends on Q only. □

Dependence on the distance to the tip. For real $b = x \in (-x_1^*, x_1^*)$ we use Lemma C.2(ii) in (C.14) instead, the entropy being at most $\int \omega_b' \log^+ \omega_b' \,\mathrm{d}x$. With $U_{x_1^*} = U$ this gives, with an absolute constant C and for all $c \geq 40$ and $g \in \bar{\mathcal{A}} \setminus \{0\}$,

$$\log|G(x)| \leq c'\, U(x) + \log M[g] + 5\log \frac{1}{x_1^* - |x|} + 3\log c' + C \qquad (|x| < x_1^*). \tag{C.16}$$

The argument gives $2\log c'$; we state $3\log c'$, as in the count of powers of c' in section 6.7.

C.5 Strict deficit

We prove the last inequality of Lemma 6.7. By that lemma, $\kappa(\delta) = \frac{4}{3}\int_0^\delta \big[\frac{\pi}{2} - \arcsin(\sinh \pi(x_1^* - u))\big] \mathrm{d}u$ for $0 < \delta \leq x_1^*$, and we bound the integrand from below by its square-root behavior at the tip. First, $\frac{\pi}{2} - \arcsin y = \arccos y \geq \sqrt{2(1 - y)}$ for $0 \leq y \leq 1$: both sides vanish at $y = 1$, and $\frac{\mathrm{d}}{\mathrm{d}y} \arccos y = -(1 - y)^{-1/2}(1 + y)^{-1/2} \leq -(2(1 - y))^{-1/2} = \frac{\mathrm{d}}{\mathrm{d}y}\sqrt{2(1 - y)}$. Second, since

$\sinh \pi x_1^* = 1$, we have $1 - \sinh \pi(x_1^* - u) = \int_{x_1^*-u}^{x_1^*} \pi \cosh(\pi v)\, \mathrm{d}v \geq \pi u$ for $0 \leq u \leq x_1^*$. Hence the integrand is at least $\sqrt{2\pi u}$, and

$$\kappa(\delta) \geq \frac{4}{3}\sqrt{2\pi} \int_0^\delta \sqrt{u}\, \mathrm{d}u = \frac{8\sqrt{2\pi}}{9}\, \delta^{3/2} = 2.228\ldots\, \delta^{3/2} \qquad (0 < \delta \leq x_1^*). \tag{C.17}$$

D The zero law on the strip

This appendix proves the two statements of section 7 that tie the comb B to the extremal potential U: the Riesz representation (Lemma 7.1; on the real axis it is the continuum limit of the sums of appendix F) and the edge-phase lemma (Lemma 7.6; its sharper form Lemma D.2 is what verifies (SD2) in appendix E.4). A Poisson identity (Lemma D.1) links the two, and appendix D.4 derives the eikonal identity of section 7.6.

Throughout, $b = x + iy$, and $b = v + \frac{i}{2}$ on E_+; $A \lesssim B$ means $A \leq CB$ with C depending at most on the width δ_1 of appendix D.3. Besides U we use the complex potential of Lemma 6.5,

$$\mathcal{U}(b) := U_0 - \frac{4\pi i}{3} \int_0^b p(b')\, \mathrm{d}b', \qquad \operatorname{Re} \mathcal{U} = U, \qquad \mathrm{d}U = \tfrac{4\pi}{3}(\operatorname{Im} p\, \mathrm{d}x + \operatorname{Re} p\, \mathrm{d}y), \tag{D.1}$$

analytic on D, with p continuous up to E_+ and $p(v + \frac{i}{2}) = F(v)$. We recall from Lemma 6.5 and Definition 6.6 that U is harmonic on D, continuous on $\bar{\mathbb{S}}$, zero on $E_\pm$, equal to $-L$ on both lips of the slits, and $|U(b)| \leq L(|x|) + C$; and that U is subharmonic on $\mathbb{S}$ with charge $\frac{1}{2\pi}\Delta U = \rho_U(|x|)\, \mathrm{d}x \otimes \delta_0(\mathrm{d}y)$ in the sense of distributions (across the slits U is continuous, ∇U is locally bounded, and $\partial_y U$ jumps by $2\pi\rho_U(|x|)$). We also use $\partial_w \log\tanh \frac{\pi w}{2} = \pi/\sinh \pi w$ and, for real u, θ, $|\sinh \pi(u + i\theta)|^2 = \sinh^2 \pi u + \sin^2 \pi\theta$.

D.1 Riesz representation of U

Proof of Lemma 7.1. Plan. The superposition u of the kernels $\log|T_{x'}|$ at density ρ_U has the charge, the edge values and the growth of U; so $U - u$ is harmonic, and vanishes by Phragmén–Lindelöf.

The kernel. By (T1) and (T4), $b \mapsto \log|T_{x'}(b)| = \log\left|\tanh \frac{\pi(b-x')}{2}\right| + \log\left|\tanh \frac{\pi(b+x')}{2}\right|$ is harmonic on $\mathbb{S} \setminus \{\pm x'\}$, vanishes on $E_\pm$, and has unit logarithmic poles at $\pm x'$: it is minus the Green's function of $\mathbb{S}$ with poles at $\pm x'$ ($b \mapsto \tanh \frac{\pi b}{2}$ maps $\mathbb{S}$ conformally onto the unit disk). From $T_{x'} = (\cosh \pi b - \cosh \pi x')/(\cosh \pi b + \cosh \pi x')$,

$$\big|\log|T_{x'}(b)|\big| \lesssim e^{-\pi|x'-|x||} \qquad (b \in \bar{\mathbb{S}},\ |x' - |x|| \geq 1). \tag{D.2}$$

The superposition. Since $\rho_U(x') \lesssim 1 + x'$, the integral $u(b) := \int_{x_1^*}^\infty \rho_U(x') \log|T_{x'}(b)|\, \mathrm{d}x'$ converges absolutely and locally uniformly on $\bar{\mathbb{S}}$ (the logarithmic singularity at $x' = |x|$, $y = 0$ is integrable). Hence u is subharmonic on $\mathbb{S}$ with the same charge as U, continuous on $\bar{\mathbb{S}}$ with $u = 0$ on $E_\pm$ (dominated convergence), and $|u(b)| \leq C(1 + |x|)$ by (D.2).

Uniqueness. The difference $d := U - u$ satisfies $\Delta d = 0$ in the sense of distributions, so it is harmonic on $\mathbb{S}$ (Weyl's lemma [63, §3.7]); it is continuous on $\bar{\mathbb{S}}$, vanishes on $E_\pm$, and $|d(b)| \leq C'(1 + |x|)$. For $\epsilon > 0$ the function $d - \epsilon \cosh 2x \cos 2y$ is harmonic on $\mathbb{S}$, is ≤ 0 on $E_\pm$ because $\cos 1 > 0$, and is negative on the cross-cuts $|x| = X$ once X is large; by the maximum principle it is ≤ 0 on $\mathbb{S}$. Letting $\epsilon \to 0$, and repeating the argument with $-d$, we get $d \equiv 0$. □

D.2 The Poisson identity

Lemma D.1 (Poisson identity; proved)**.** *For every real v,*

$$2\pi \int_{x_1^*}^\infty N'(x')\,[\operatorname{sech} \pi(v - x') + \operatorname{sech} \pi(v + x')]\, \mathrm{d}x' = \frac{4\pi}{3}\, F(v). \tag{D.3}$$

Proof. Plan. Both sides are the normal derivative $\partial_y U$ at the point $v+\frac{i}{2}$ of E_+, taken from inside the strip: the right side from the closed form (D.1), the left side from the Riesz representation.

By (D.1), $\partial_y U = \frac{4\pi}{3}\operatorname{Re} p$ on D and p is continuous up to E_+, so $\lim_{y\uparrow 1/2}\partial_y U(v+iy) = \frac{4\pi}{3}F(v)$. By (T4) each kernel $\log|T_{x'}|$ is harmonic on $0<y<1$, with $\partial_y \log|T_{x'}| = \operatorname{Re}[i\,\partial_b \log T_{x'}]$ and $\partial_b \log T_{x'}(b) = \pi/\sinh\pi(b-x') + \pi/\sinh\pi(b+x')$. On $\frac14 \le y \le \frac34$ the latter is at most $2\sqrt{2}\,\pi$ in modulus and is $\lesssim e^{-\pi|x'-|x||}$ for $|x'-|x|| \ge 1$; as $N'(x') \lesssim 1+x'$, the integral u of appendix D.1 and its first derivatives converge there locally uniformly. So u extends harmonically across E_+ and may be differentiated under the integral sign: at $b = v+\frac{i}{2}$, $\sinh\pi(v\mp x'+\frac{i}{2}) = i\cosh\pi(v\mp x')$ gives $\partial_y \log|T_{x'}| = \pi[\operatorname{sech}\pi(v-x') + \operatorname{sech}\pi(v+x')]$, the inward normal derivative of the Green's function at the edge, and with $\rho_U = 2N'$ (Definition 6.6) the value $\partial_y u(v+\frac{i}{2})$ is the left side of (D.3). As $U = u$ on $\mathbb{S}$ by Lemma 7.1 and u is C^1 across E_+, the two values agree. □

D.3 The edge phase

Fix $\delta_1 \in (0, \frac14]$ and let $\mathcal{N}_{\delta_1} := \{b : |y-\frac12| \le \delta_1\}$ be the thin two-sided strip about E_+, as in (E.2). For $\operatorname{Re}\zeta \ge x_1^*$ and $|\operatorname{Im}\zeta| \le \frac18$ the factor T_ζ has neither zeros nor poles at distance less than $\frac18$ from $\mathcal{N}_{\delta_1}$, by (T4), and $T_\zeta \to -1$ as $\operatorname{Re}\zeta \to \infty$. We write

$$\varphi_\zeta(b) := \log(-T_\zeta(b)), \qquad \partial_b\varphi_\zeta(b) = \frac{\pi}{\sinh\pi(b-\zeta)} + \frac{\pi}{\sinh\pi(b+\zeta)}, \tag{D.4}$$

for the branch on $\mathcal{N}_{\delta_1}$ that is continuous in (b,ζ) and tends to 0 as $\operatorname{Re}\zeta\to\infty$. It is analytic in b and in ζ, $\operatorname{Re}\varphi_\zeta = \log|T_\zeta|$, and $\varphi_\zeta(\frac{i}{2}) = 0$ by (T3). Since $|\sinh\pi(u+i\theta)| \ge |\sin\pi\theta|$, on $\mathcal{N}_{\delta_1}$ both $|\partial_b\varphi_\zeta|$ and $|\partial_\zeta\varphi_\zeta|$ are at most $2\pi/\cos\pi(\delta_1+|\operatorname{Im}\zeta|)$, and

$$|\varphi_\zeta(b)| \lesssim \min(1, e^{-\pi(\operatorname{Re}\zeta-|x|)}), \qquad |\partial_b^i\partial_\zeta^j\varphi_\zeta(b)| \lesssim e^{-\pi|\operatorname{Re}\zeta-|x||} \quad (1 \le i+j \le 4). \tag{D.5}$$

As $x \to \pm\infty$ at fixed ζ, $T_\zeta \to +1$ and $\varphi_\zeta \to \mp i\pi$, so only the derivatives decay on both sides. In the comb, $\varepsilon_n \le \eta_0(\chi_3-\chi_2) \lesssim c'^{-2/3}$ (the spacings decrease along the band because N' increases), and we take c large enough that $\max_n \varepsilon_n \le \frac18$. On $\mathcal{N}_{\delta_1}$ we fix the branch

$$\log B := \log T_{\chi_2} + \sum_{n\ge3}\big[\varphi_{\chi_n+i\varepsilon_n} + \varphi_{\chi_n-i\varepsilon_n}\big], \qquad \log T_{\chi_2} := i\pi + \varphi_{\chi_2}, \tag{D.6}$$

that is, $\log T_{\chi_2}(\frac{i}{2}) = i\pi$ (T3); the sum converges absolutely and locally uniformly by (D.5). Lemma 7.6 is the restriction to E_+ of the following statement.

Lemma D.2 (Edge phase; proved)**.** *On $\mathcal{N}_{\delta_1}$ let*

$$\Phi_0(b) := \int_{x_1^*}^{\infty} \rho_U(x')\,\varphi_{x'}(b)\,\mathrm{d}x'. \tag{D.7}$$

(a) *Φ_0 is analytic on $\mathcal{N}_{\delta_1}$, $\operatorname{Re}\Phi_0 = 0$ on E_+, $\Phi_0(\frac{i}{2}) = 0$, and*

$$\Phi_0^{(j+1)}(v+\tfrac{i}{2}+iy') = -\frac{4\pi i}{3}F^{(j)}(v+iy') \qquad (v\in\mathbb{R},\ |y'|\le\delta_1,\ j=0,\dots,3); \tag{D.8}$$

in particular $\partial_v \operatorname{Im}\Phi_0(v+\frac{i}{2}) = -\frac{4\pi}{3}F(v)$. Here $F(w) = \frac{1}{\pi}\operatorname{arcsinh}(\cosh\pi w)$ is analytic in $|\operatorname{Im} w| < \frac12$; it is even, $F(0) = x_1^*$, $F'' > 0$ on $\mathbb{R}$ and $0 < F' < 1$ on $(0,\infty)$. The constants $C_2 := \sup_{\mathcal{N}_{\delta_1}}|\Phi_0'''|$ and $C_3 := \sup_{\mathcal{N}_{\delta_1}}|\Phi_0''''|$ are finite and depend on δ_1 only.

(b) *On $\mathcal{N}_{\delta_1}$, $\log B = c'\Phi_0 + \Phi_1$ with*

$$\Phi_1 = i\pi - 2n_1\bar\varphi + \Delta_{\mathrm{det}} + R_{\mathrm{EM}}, \qquad \Delta_{\mathrm{det}} := \sum_{n\ge3}\big[\varphi_{\chi_n+i\varepsilon_n} + \varphi_{\chi_n-i\varepsilon_n} - 2\varphi_{\chi_n}\big], \tag{D.9}$$

in this order the sign of the simple zero ($B(\frac{i}{2}) = -1$), the charge of the law that is absent from the comb (n_1 sites spread over $[x_1^*,\chi_2]$), the detuning, and the discreteness of the sites; $\bar\varphi := N(\chi_2)^{-1}\int_{x_1^*}^{\chi_2} N'(x')\,\varphi_{x'}\,\mathrm{d}x' = \varphi_{x_1^*} + O((n_1/c')^{2/3})$, and R_{EM} is defined in (D.11).

(c) $\operatorname{Re}\Phi_1 = 0$ *on* E_+, *and* $\sup_{\mathcal{N}_{\delta_1}}|\operatorname{Re}\Phi_1| \le M_0$, $\sup_{\mathcal{N}_{\delta_1}}|\Phi_1'| \le M_1$, $\sup_{\mathcal{N}_{\delta_1}}|\Phi_1''| \le M_1'$ *with constants depending on* (n_1, η_0, δ_1) *only, given in* (D.12). *Moreover, with* C *and* C_{EM} *depending on* δ_1 *only, uniformly in* $x = \operatorname{Re} b$,

$$|\Delta_{\det}^{(i)}| \le C\eta_0^2\, c'^{-2/3}, \qquad |R_{\mathrm{EM}}^{(i)}| \le C_{\mathrm{EM}}\, c'^{-2/3} \qquad (i = 0, 1, 2;\ b \in \mathcal{N}_{\delta_1}). \tag{D.10}$$

In particular Φ_1, Φ_1' *and* Φ_1'' *are bounded on* $\mathcal{N}_{\delta_1}$ *uniformly in* c'.

Proof. Plan. Part (a) is the Poisson identity read along the edge, together with the Riesz representation, which identifies Φ_0 with $\mathcal{U}$ continued across E_+. Part (b) is Euler–Maclaurin summation in the continuous site index. Part (c) bounds the terms of Φ_1 one by one from the decay (D.5) of the kernel and the behavior of N at the tip.

(a). By (D.5) and $\rho_U(x') \lesssim 1 + x'$, the integral (D.7) and its b-derivatives converge absolutely and locally uniformly on $\mathcal{N}_{\delta_1}$, so Φ_0 is analytic there. On E_+, $\operatorname{Re}\varphi_{x'} = \log|T_{x'}| = 0$ by (T1), so $\operatorname{Re}\Phi_0 = 0$; and $\varphi_{x'}(\frac{i}{2}) = 0$ gives $\Phi_0(\frac{i}{2}) = 0$. By (D.4), $\partial_b\varphi_{x'}(v + \frac{i}{2}) = -i\pi[\operatorname{sech}\pi(v - x') + \operatorname{sech}\pi(v + x')]$, whence $\Phi_0'(v + \frac{i}{2}) = -\frac{4\pi i}{3}F(v)$ by Lemma D.1. Next, $\operatorname{Re}\Phi_0 = U = \operatorname{Re}\mathcal{U}$ on $\mathcal{N}_{\delta_1} \cap \mathbb{S}$ by Lemma 7.1; this set does not meet the slits, as $\delta_1 \le \frac{1}{4}$, and two analytic functions with equal real parts differ by an imaginary constant, so $\Phi_0 = \mathcal{U} + i\gamma_0$ and $\Phi_0' = -\frac{4\pi i}{3}p$ there: Φ_0 is the complex potential continued across E_+. This continues p analytically to $\mathcal{N}_{\delta_1}$, with $p(w + \frac{i}{2}) = F(w)$ for $|\operatorname{Im} w| \le \delta_1$, which is (D.8). Differentiating, $F'(w) = \sinh\pi w\,(1 + \cosh^2\pi w)^{-1/2}$ and $F''(w) = 2\pi\cosh\pi w\,(1 + \cosh^2\pi w)^{-3/2}$, as in (E.30), which for real w gives the sign statements. In $|\operatorname{Im} w| \le \frac{1}{2}$ the only singularities of F are where $\cosh\pi w = \pm i$, on $|\operatorname{Im} w| = \frac{1}{2}$; so F'' and F''' are continuous on $|\operatorname{Im} w| \le \delta_1$, they tend to 0 as $|\operatorname{Re} w| \to \infty$, and $C_2 = \frac{4\pi}{3}\sup_{|\operatorname{Im} w|\le\delta_1}|F''|$, $C_3 = \frac{4\pi}{3}\sup_{|\operatorname{Im} w|\le\delta_1}|F'''|$ are finite.

(b). Let $\chi(n) := N^{-1}((n - \frac{1}{4})/c')$ for real $n \ge 2$, so that $\chi(n) = \chi_n$ at integers and $\chi'(n) = 1/(c'N'(\chi(n)))$; as $(n - \frac{1}{4})/c' \ge n_1/c' > 0$ the tip is avoided, and $f(n) := 2\varphi_{\chi(n)}(b)$ is smooth and decays with its derivatives like $e^{-\pi(\chi(n) - |x|)}$. By (D.6) and the definition of $\Delta_{\det}$, $\log B = i\pi - \varphi_{\chi_2} + \sum_{n\ge2} f(n) + \Delta_{\det}$. The second-order Euler–Maclaurin formula gives

$$\sum_{n\ge2} f(n) = \int_2^\infty f\,\mathrm{d}n + \frac{1}{2}f(2) + R_{\mathrm{EM}}, \qquad R_{\mathrm{EM}} := -\frac{1}{12}f'(2) + R_2, \tag{D.11}$$

with $|R_2| \le \frac{1}{12}\int_2^\infty|f''|\,\mathrm{d}n$, and the substitution $x' = \chi(n)$, $\mathrm{d}n = c'N'(x')\,\mathrm{d}x'$ turns the integral into $c'\int_{\chi_2}^\infty 2N'\varphi_{x'}\,\mathrm{d}x' = c'\Phi_0 - 2c'N(\chi_2)\,\bar\varphi = c'\Phi_0 - 2n_1\bar\varphi$. With $\frac{1}{2}f(2) = \varphi_{\chi_2}$ this is (D.9). The estimate for $\bar\varphi$ follows from $|\partial_{x'}\varphi_{x'}| \le 2\pi/\cos\pi\delta_1$ and $\chi_2 - x_1^* \asymp (n_1/c')^{2/3}$. For the latter we use no certified constant. Part (d) of the proof of Lemma F.2 shows that $\Phi := \rho_U^2$ has $\Phi(x_1^*) = 0$, $\Phi'(x_1^*) = 9\kappa_{\mathrm{tip}}^2$ and $0 \le \Phi'' \le \frac{32}{9}$ on $[x_1^*, \infty)$. Hence

$$9\kappa_{\mathrm{tip}}^2\, r \ \le\ \rho_U(x_1^* + r)^2 \ \le\ 9\kappa_{\mathrm{tip}}^2\, r + \tfrac{16}{9}r^2 \qquad (r > 0),$$

and $\frac{16}{9}r^2 \le \frac{5}{4}\cdot 9\kappa_{\mathrm{tip}}^2 r$ for $r \le 1$, because $16/(81\kappa_{\mathrm{tip}}^2) = \pi/(2\sqrt{2}) \le \frac{5}{4}$. Integrating $N' = \frac{1}{2}\rho_U$, we get $\kappa_{\mathrm{tip}}r^{3/2} \le N(x_1^* + r)$ for every $r > 0$, and $N(x_1^* + r) \le \frac{3}{2}\kappa_{\mathrm{tip}}r^{3/2}$ for $r \le 1$. We use this at $r = \chi_2 - x_1^*$, where $c'N(\chi_2) = n_1$; the first bound gives $r \le n_1^{2/3}\ell_c$, which is at most 1 for $c' \ge 5$.

(c). Each term of (D.9) is analytic on $\mathcal{N}_{\delta_1}$. First, $\bar\varphi$ is an average of $\varphi_{x'}$ over x', so $|\partial_b(2n_1\bar\varphi)| \le n_1\cdot 4\pi/\cos\pi\delta_1$ and $|\partial_b^2(2n_1\bar\varphi)| \le n_1\sup_{x'}\sup_{\mathcal{N}_{\delta_1}}|2\partial_b^2\varphi_{x'}|$. Second, each summand of $\Delta_{\det}$ is a second difference in ζ of the analytic function $\zeta \mapsto \varphi_\zeta(b)$: $\varphi_{\chi+i\varepsilon} + \varphi_{\chi-i\varepsilon} - 2\varphi_\chi = -\int_0^\varepsilon(\varepsilon - s)[\partial_\zeta^2\varphi_{\chi+is} + \partial_\zeta^2\varphi_{\chi-is}]\,\mathrm{d}s$, which with up to two b-derivatives is $\lesssim \varepsilon^2 e^{-\pi|\chi - |x||}$ by (D.5). With $\varepsilon_n = \eta_0(\chi_{n+1} - \chi_n)$ and $\chi_{n+1} - \chi_n \le \chi_3 - \chi_2 \asymp c'^{-2/3}$,

$$|\Delta_{\det}^{(i)}(b)| \lesssim \sum_{n\ge3}\varepsilon_n^2 e^{-\pi|\chi_n - |x||} \le \eta_0^2\,(\chi_3 - \chi_2)\sum_{n\ge3}(\chi_{n+1} - \chi_n)\,e^{-\pi|\chi_n - |x||} \lesssim \eta_0^2\, c'^{-2/3},$$

the last sum being, up to the factor $e^{\pi s} \le e^{\pi}$ with $s = \chi_3 - \chi_2$ the largest spacing, a Riemann sum for $\int e^{-\pi|x'-|x||}\mathrm{d}x' \le 2/\pi$. Third, the remainder: at $x' = \chi(n)$, $f'(n) = 2\partial_{x'}\varphi_{x'}/(c'N')$ and $f''(n) = 2\partial^2_{x'}\varphi_{x'}/(c'N')^2 - 2\partial_{x'}\varphi_{x'}\,N''/(c'^2N'^3)$. Near the tip $N'(x') \asymp (x'-x_1^*)^{1/2}$ and $|N''(x')| \asymp (x'-x_1^*)^{-1/2}$, deep in the band $N'(x') \asymp x'$ (for $0 < x' - x_1^* \le 1$ by the bounds for ρ_U^2 in part (b) of this proof and by (F.13), since $N' = \frac{1}{2}\rho_U$ and $N'' = \frac{1}{2}\rho_U\,(\log\rho_U)'$; beyond, by (6.21)), and $\chi_2 - x_1^* \asymp \ell_c$, so $c'N'(\chi_2) \asymp c'\ell_c^{1/2} \asymp c'^{2/3}$ and $|f'(2)| \lesssim c'^{-2/3}$. Likewise, by (D.5),

$$\int_2^\infty |f''|\,\mathrm{d}n = \int_{\chi_2}^\infty |f''|\,c'N'\,\mathrm{d}x' \lesssim \frac{1}{c'}\int_{\chi_2}^\infty \Big[\frac{|\partial^2_{x'}\varphi_{x'}|}{N'} + \frac{|\partial_{x'}\varphi_{x'}||N''|}{N'^2}\Big]\mathrm{d}x' \lesssim \frac{1+\ell_c^{-1/2}}{c'} \lesssim c'^{-2/3}$$

uniformly in x, the integrand being $\lesssim (x'-x_1^*)^{-1/2} + (x'-x_1^*)^{-3/2}$ for $x' \le x_1^* + 1$ and $\lesssim e^{-\pi|x'-|x||}/x'$ beyond. The same computation with ∂_b, ∂_b^2 applied under the sums and integrals bounds R'_{EM} and R''_{EM}; this is (D.10), with C_{EM} the resulting constant. Adding the contributions and using $c'^{-2/3} \le 1$, the bounds of the statement hold with

$$M_1 := (n_1+1)\frac{4\pi}{\cos\pi\delta_1} + C\eta_0^2 + C_{\mathrm{EM}}, \qquad M_0 := M_1\delta_1, \tag{D.12}$$

and likewise for M_1' with $\sup|2\partial_b^2\varphi_{x'}|$ in place of $4\pi/\cos\pi\delta_1$ (the $+1$ is a crude allowance for the simple zero, which contributes only the constant $i\pi$); Φ_1 itself is bounded by (D.9), $|\varphi_{x'}| \lesssim 1$ and (D.10). Finally $\mathrm{Re}\,\Phi_1 = 0$ on E_+, because $\mathrm{Re}\log B = \log|B| = 0$ there (Proposition 7.2) and $\mathrm{Re}\,\Phi_0 = 0$ by (a); integrating Φ_1' vertically from the edge, $|\mathrm{Re}\,\Phi_1(v+\frac{i}{2}+iy')| \le M_1|y'| \le M_0$. □

D.4 The eikonal identity

[ORIENTATION] At order c' the phase of the integrand of the edge representation (Lemma 7.3(c)) is $c'[\mathrm{Im}\,\Phi_0(v+\frac{i}{2}) + \frac{4\pi}{3}xv]$; by (D.8) it is stationary where $F(v) = x$, that is at $v = \pm v_0(x)$. Along the saddle $b_0(x) = v_0(x) + \frac{i}{2}$, with $k_x = \frac{4\pi}{3}c'x$,

$$\frac{\mathrm{d}}{\mathrm{d}x}\Big[c'\,\mathrm{Im}\,\Phi_0(b_0) + k_x v_0\Big] = \Big(c'\partial_v\,\mathrm{Im}\,\Phi_0(v_0+\tfrac{i}{2}) + k_x\Big)v_0' + \frac{4\pi}{3}c'v_0 = \pi c'\rho_U(x) = \Psi'(x), \tag{D.13}$$

the bracket vanishing by stationarity, and the last two steps being $v_0 = \frac{3}{4}\rho_U$ and $\Psi = 2\pi\nu - \pi$ with $\nu' = c'N' = \frac{1}{2}c'\rho_U$. Since $v_0(x_1^*) = 0$, $\Phi_0(\frac{i}{2}) = 0$ and $N(x_1^*) = 0$, the integrated form is $c'\,\mathrm{Im}\,\Phi_0(b_0(x)) + k_x v_0(x) = 2\pi c'N(x)$ for $x \ge x_1^*$. The omitted sites and the node phase live in Φ_1 and do not enter.

E Two-saddle steepest descent with a uniform remainder

This appendix proves Lemma 7.7: for band points $x \ge x_I$, $\hat{h}_0(c'x^2/3)$ is the sum $\mathrm{Amp}\cos\hat{\Psi}$ of two saddle-point contributions, up to a relative remainder $\varepsilon_{\mathrm{sd}}$ that is bounded explicitly and tends to zero uniformly in x (Lemma E.1, Corollary E.2), and obeys a global bound that decays in x (Corollary E.3). The comb enters only through the edge representation of Lemma 7.3(c) and the edge phases Φ_0, Φ_1 of Lemma 7.6, which we abstract into hypotheses (SD1)–(SD4) and verify in appendix E.4.

The idea. On E_+ the integrand of the edge representation is $e^{-c'L(x)}$ times an integrable profile times a pure phase $e^{i[\Theta_0(v)+k_x v]}$, where $\Theta_0(v) := c'\,\mathrm{Im}\,\Phi_0(v+\frac{i}{2})$ has $\Theta_0' = -\frac{4\pi}{3}c'F$ and $k_x = \frac{4\pi}{3}c'x$. The phase is stationary at $v = \pm v_0(x)$, where $F(v_0) = x$, with second derivative $\mp c'\alpha_x$, $\alpha_x = \frac{4\pi}{3}F'(v_0)$. The two contributions are complex conjugates, and ordinary stationary phase gives their sum as $\mathrm{Amp}\cos\hat{\Psi}$ with

$$\tfrac{1}{2}\,\mathrm{Amp}(x)\,e^{i\hat{\Psi}(x)} = \frac{2\pi c'}{3}\,h_0(b_0)\,H_0^{(1)}(k_x b_0)\,b_0\,e^{-i\pi/4}\sqrt{\frac{2\pi}{c'\alpha_x}}, \qquad b_0 = v_0 + \tfrac{i}{2}, \tag{E.1}$$

up to relative corrections that are $O(1/c')$ *at fixed* x. Toward the tip, however, the two points coalesce at $v = 0$ and $\alpha_x \to 0$, whereas section 7.7 needs the corrections small on all of $[x_I, \infty)$, with $x_I \to x_1^*$ as $c \to \infty$. The proof therefore uses an explicit contour: at height u above the edge the oscillating factor has modulus $\exp(\frac{4\pi}{3}c'u[F(v) - x])$ up to a cubic error, so running above the edge between the saddles and below it outside them gains a factor exponentially small in c', at rates given by the chord slope s_{ch} and the curvature α_x. At the saddle the first-order terms are odd and cancel, leaving terms of order $1/(c'\alpha_x^k)$, $k = 1, 2, 3$, with explicit constants. Near the tip v_0, α_x and s_{ch} vanish like $(x - x_1^*)^{1/2}$, and the remainder is governed by $c' \min\{1, v_0\}^3 \asymp c'(x - x_1^*)^{3/2}$.

E.1 Setting and hypotheses

Throughout, $c' \geq 39$, $\delta_1 \in (0, \frac{1}{4}]$ is fixed, and $k_x = \frac{4\pi}{3}c'x$, so that $k_x/2 = c'L(x)$; a *band point* is an $x > F(0)$, with F as in (SD2) below. Near the upper edge we write

$$b = v + i(\tfrac{1}{2} + u), \qquad v = \operatorname{Re} b, \quad u = \operatorname{Im} b - \tfrac{1}{2}, \qquad \mathcal{N}_\delta := \{b : \ |u| \leq \delta\}, \tag{E.2}$$

so that u is the height above E_+ and $\mathcal{N}_\delta$ is a thin two-sided strip around it (the letters u, r, ℓ, q have this meaning in this appendix only). For $\operatorname{Im} z \geq 0$ and on principal branches,

$$H_0^{(1)}(z) = \sqrt{\frac{2}{\pi z}}\, e^{i(z-\pi/4)}(1 + \varepsilon_H(z)), \qquad |\varepsilon_H(z)| \leq \frac{1}{4|z|}\, e^{1/(4|z|)} \leq \frac{0.33}{|z|} \quad (|z| \geq 1), \tag{E.3}$$

by [67, (10.17.13)–(10.17.15)] with $\nu = 0$ and one term. Let h_0 have the following properties.

(SD1) *Edge representation and symmetry.* The function h_0 is even, real on $\mathbb{R} \cup i\mathbb{R}$ and analytic on a neighborhood of $\bar{\mathbb{S}} \cup \mathcal{N}_{\delta_1}$, and $|h_0(b)| \leq Ce^{-\mu|\operatorname{Re} b|}$ for some $\mu > 0$ on $\mathcal{N}_{\delta_1} \cap \bar{\mathbb{S}} = \{\frac{1}{2} - \delta_1 \leq \operatorname{Im} b \leq \frac{1}{2}\}$. (Nothing is assumed as $|\operatorname{Re} b| \to \infty$ above E_+, where for the comb $|h_0|$ grows like $e^{\frac{4\pi}{3}c'F(v)u}$.) With $\mathcal{I}(b) := h_0(b)\, H_0^{(1)}(k_x b)\, b$,

$$\hat{h}_0(c'x^2/3) = \frac{2\pi c'}{3} \int_{E_+} \mathcal{I}(b)\, \mathrm{d}b, \qquad \mathcal{I}(-\bar{b}) = \overline{\mathcal{I}(b)} \quad (b \in E_+). \tag{E.4}$$

(SD2) *Phase–amplitude split.* On $\mathcal{N}_{\delta_1}$, $h_0 = \pm\, e^{c'\Phi_0} e^{\Phi_1}\, \mathcal{E}$ with a fixed sign, where Φ_0, Φ_1 and the outer factor $\mathcal{E}$ are analytic, $\mathcal{E}$ has no zeros, and: (a) $\operatorname{Re}\Phi_0 = 0$ on E_+; (b) the function $F(v) := \frac{3i}{4\pi}\Phi_0'(v + \frac{i}{2})$, which is real for real v by (a), is even, strictly increasing and convex on $[0, \infty)$, tends to infinity, satisfies $\frac{\pi}{3}c'F(0) \geq 11$, and extends analytically to $|\operatorname{Im} v| \leq \delta_1$; (c) $C_2 := \sup_{\mathcal{N}_{\delta_1}} |\Phi_0'''| = \frac{4\pi}{3} \sup_{|\operatorname{Im} v| \leq \delta_1} |F''|$ and $C_3 := \sup_{\mathcal{N}_{\delta_1}} |\Phi_0''''|$ are finite; (d) $M_1 := \sup_{\mathcal{N}_{\delta_1}} |\Phi_1'|$ and $M_1' := \sup_{\mathcal{N}_{\delta_1}} |\Phi_1''|$ are finite and independent of c; (e) $\operatorname{Re}\Phi_1 = 0$ on E_+ (used only to drop the factor $e^{\operatorname{Re}\Phi_1(b_0)} = 1$ from the amplitude).

(SD3) *Outer factor.* $M_{\mathcal{E}} := \sup_{\mathcal{N}_{\delta_1}} |\mathcal{E}'/\mathcal{E}|$ and $M_{\mathcal{E}}' := \sup_{\mathcal{N}_{\delta_1}} |(\mathcal{E}'/\mathcal{E})'|$ are finite.

(SD4) *Saddle, curvature and chord slope.* With $v_0 = v_0(x) > 0$ the unique solution of $F(v_0) = x$,

$$b_0 := v_0 + \tfrac{i}{2}, \qquad \alpha_x := \frac{4\pi}{3} F'(v_0) > 0, \qquad s_{\mathrm{ch}} := \frac{x - F(0)}{v_0} > 0. \tag{E.5}$$

In appendices E.1 to E.3 the letters F and v_0 refer to (SD2) and (SD4); for the comb they are the edge function and the map of section 7.1, and $F(0) = x_1^*$. The dependence on c' that is not in $e^{c'\Phi_0}$ or in the exponential of the Hankel function is collected in the amplitude, defined on $\mathcal{N}_{\delta_1}$ (where $\operatorname{Im} b \geq \frac{1}{4}$) with the principal square root by

$$A(b) := \pm\, \mathcal{E}(b)\, e^{\Phi_1(b)}\, b^{1/2}(1 + \varepsilon_H(k_x b)), \qquad M \geq \sup_{\mathcal{N}_{\delta_1}} |A'/A|, \qquad M' \geq \sup_{\mathcal{N}_{\delta_1}} |(A'/A)'|. \tag{E.6}$$

One may take $M = M_{\mathcal{E}} + M_1 + 2 + C$ and $M' = M'_{\mathcal{E}} + M'_1 + 8 + C$ with an absolute constant C, so that M and M' do not depend on x or on c: the square root contributes $1/(2|b|) \le 2$ and $1/(2|b|^2) \le 8$, and the Hankel factor at most C/k_x to each. Indeed the reference for (E.3) bounds ε_H, continued analytically, by $C/|z|$ in the larger sector $-\frac{\pi}{2} \le \operatorname{ph} z \le \frac{3\pi}{2}$, which contains the disk of radius $|z|/2$ about every z with $\operatorname{Im} z \ge 0$; Cauchy's estimate then bounds $|z^2\varepsilon'_H(z)|$ and $|z^3\varepsilon''_H(z)|$ by an absolute constant, and $|k_x b| \ge k_x/4 = \frac{\pi}{3}c'x \ge \frac{\pi}{3}c'F(0) \ge 11$ on $\mathcal{N}_{\delta_1}$ at every band point, by (SD2)(b).

E.2 Statements

Lemma E.1 (Two-saddle steepest descent; proved)**.** *Assume (SD1)–(SD4). Put*

$$\ell := \min\{1,\ \sqrt{2}\,\delta_1,\ v_0,\ \alpha_x/C_2,\ 2\sqrt{2}\,\pi s_{\mathrm{ch}}/C_2,\ 1/M,\ 1/\sqrt{M'}\}, \qquad u_0 := \ell/\sqrt{2}, \tag{E.7}$$

and $r_1 := \min\{\ell,\ (6/(c'C_2))^{1/3}\}$*, and suppose that* c' *is so large that*

$$\text{(i)}\ \ \tfrac{2\pi}{3}\,c'u_0 s_{\mathrm{ch}} \ge M, \qquad \text{(ii)}\ \ c'\alpha_x u_0 \ge 2M, \qquad \text{(iii)}\ \ c'\alpha_x \ge 8. \tag{E.8}$$

Then

$$\hat{h}_0(c'x^2/3) = \mathrm{Amp}(x)\big[\cos\hat{\Psi}(x) + \varepsilon_{\mathrm{sd}}(x)\big], \qquad |\varepsilon_{\mathrm{sd}}(x)| \le \bar{\varepsilon}_{\mathrm{sd}}(x) := \varepsilon_{\mathrm{core}} + 2\varepsilon_{\mathrm{tr}} + \varepsilon_{\mathrm{mid}} + \varepsilon_{\mathrm{far}}, \tag{E.9}$$

where $\varepsilon_{\mathrm{sd}}$ *is real and, with* $\Theta_0(v) = c'\operatorname{Im}\Phi_0(v + \frac{i}{2})$*,*

$$\mathrm{Amp}(x) = 2\,e^{-c'L(x)}\,|\mathcal{E}(b_0)|\,e^{\operatorname{Re}\Phi_1(b_0)}\,|1 + \varepsilon_H(k_x b_0)|\,\Big(\frac{|b_0|}{xF'(v_0)}\Big)^{1/2}, \tag{E.10}$$

$$\hat{\Psi}(x) = \Theta_0(v_0) + k_x v_0 - \tfrac{\pi}{2} + \arg A(b_0), \tag{E.11}$$

$$\arg A(b_0) = \arg(\pm 1) + \operatorname{Im}\Phi_1(b_0) + \arg\mathcal{E}(b_0) + \tfrac{1}{2}\arctan\tfrac{1}{2v_0} + \arg\big(1 + \varepsilon_H(k_x b_0)\big),$$

and the four parts of the remainder, from the core of the saddle, the transition to the valleys, the middle piece and the far pieces of the contour, are, with $K_A := 4.5M^2 + 1.625M'$*,*

$$\varepsilon_{\mathrm{core}} = \frac{K_A}{c'\alpha_x} + \frac{\frac{1}{8}C_3 + \frac{1}{2}MC_2 + K_A C_2}{c'\alpha_x^2} + \frac{(0.57 + 0.52M)\,C_2^2}{c'\alpha_x^3}, \tag{E.12}$$

$$\varepsilon_{\mathrm{tr}} = \frac{3e^{M\ell}}{\sqrt{2\pi}}\,\frac{e^{-c'\alpha_x r_1^2/3}}{r_1\sqrt{c'\alpha_x}}, \quad \varepsilon_{\mathrm{mid}} = \frac{3e^{Mu_0}}{2\pi}\sqrt{\frac{\alpha_x}{2\pi c'}}\,\frac{e^{-\frac{\pi}{3}c's_{\mathrm{ch}}u_0^2}}{s_{\mathrm{ch}}u_0}, \quad \varepsilon_{\mathrm{far}} = \sqrt{\frac{2}{\pi}}\,e^{Mu_0}\,\frac{e^{-c'\alpha_x u_0^2/4}}{u_0\sqrt{c'\alpha_x}}. \tag{E.13}$$

Here Amp *and* $\hat{\Psi}$ *contain the exact* $\varepsilon_H(k_x b_0)$ *and obey (E.1) identically; by (SD2)(e), (E.3),*

$$\mathrm{Amp}(x)\,e^{c'L(x)} = 2\,|\mathcal{E}(b_0)|\Big(\frac{|b_0|}{xF'(v_0)}\Big)^{1/2}(1 + O(1/c')), \qquad |O(1/c')| \le \frac{0.33}{|k_x b_0|}. \tag{E.14}$$

Corollary E.2 (Uniformity; proved)**.** *Assume in addition that* $\sup_{[0,\infty)} F' < \infty$*, and let* $\delta_1, C_2, C_3, M, M'$ *be fixed. Suppose that along a family of band points* $x \ge x_I(c)$ *one has* $c'\min\{\alpha_x, s_{\mathrm{ch}}, v_0\}^3 \ge c'^{\gamma}$ *for some* $\gamma > 0$*. Then for* c *large the conditions (E.8) hold on* $[x_I(c), \infty)$*, and* $\bar{\varepsilon}_{\mathrm{sd}} \to 0$ *uniformly there as* $c \to \infty$*, at the rate*

$$\bar{\varepsilon}_{\mathrm{sd}} \le K\,(1 + M^2 + M')\Big[\frac{1}{c'\alpha_x} + \frac{C_3}{c'\alpha_x^2} + \frac{C_2^2}{c'\alpha_x^3}\Big] + C\,e^{-c_* c'^{\gamma/3}}, \tag{E.15}$$

with K *absolute and* $C, c_* > 0$ *depending only on* γ*,* $\sup F'$ *and the fixed constants.*

Corollary E.3 (Global band bound; proved)**.** *Under the hypotheses of Corollary E.2, for* c *large and every* $x \ge x_I(c)$*,*

$$|\hat{h}_0(c'x^2/3)| \le \mathrm{Amp}(x)(1 + \bar{\varepsilon}_{\mathrm{sd}}) \le 2(1 + \bar{\varepsilon}_{\mathrm{sd}})|\mathcal{E}(b_0)|\Big(\frac{|b_0|}{xF'(v_0)}\Big)^{1/2}(1 + O(1/c'))\,e^{-c'L(x)}. \tag{E.16}$$

For the comb, where $\mathcal{E} = \operatorname{sech}^2\frac{\pi b}{2}$ *and* F *is the edge function of section 7.1, the right-hand side is at most* $C_{\mathrm{glob}}\,F'(v_0)^{-1/2}\,e^{-\pi v_0}\,e^{-c'L(x)}$ *with* C_{glob} *absolute;* $C_{\mathrm{glob}} = 2^5$ *will do once* $\bar{\varepsilon}_{\mathrm{sd}} \le 1$*.*

E.3 Proofs

Proof of Lemma E.1. Plan. On $\mathcal{N}_{\delta_1}$ we factor the integrand into $e^{c'\varphi}$, which carries the dependence on c', and an amplitude A, and keep $\operatorname{Re} b > 0$ by symmetry (Step 1); read off from (SD2) how $|e^{c'\varphi}|$ behaves off the edge (Step 2); choose the contour and justify the deformation (Step 3); bound the pieces away from the saddles (Step 4); expand at a saddle (Step 5); assemble (Step 6).

Step 1: factorization and symmetry. By (SD2), (E.3) and (E.6), for $b \in \mathcal{N}_{\delta_1}$,

$$\mathcal{I}(b) = \sqrt{\frac{2}{\pi k_x}}\, e^{-i\pi/4}\, e^{-k_x/2}\, e^{c'\varphi(b)} A(b), \qquad \varphi(b) := \Phi_0(b) + \frac{4\pi i}{3}\, x\,(b - \tfrac{i}{2}), \tag{E.17}$$

since $c'\varphi = c'\Phi_0 + ik_x(b - \frac{i}{2})$. The symmetry in (E.4) extends from E_+ to $\mathcal{N}_{\delta_1}$ by the identity theorem, and on a contour $b(v)$ whose height $u(v)$ is even in v one has $b'(-v) = \overline{b'(v)}$, so that the part with $v < 0$ contributes the complex conjugate of the part with $v > 0$. Hence, for every such contour $\Gamma \subset \mathcal{N}_{\delta_1}$ to which E_+ can be deformed,

$$\hat{h}_0(c'x^2/3) = \frac{2\pi c'}{3}\sqrt{\frac{2}{\pi k_x}}\, e^{-k_x/2} \cdot 2\operatorname{Re}\big[e^{-i\pi/4} J_+\big], \qquad J_+ := \int_{\Gamma \cap \{\operatorname{Re} b > 0\}} e^{c'\varphi} A \,\mathrm{d}b. \tag{E.18}$$

Step 2: the phase near the edge. By (SD2)(a),(b), on E_+ one has $\operatorname{Re}\varphi = 0$ and $\varphi'(v + \frac{i}{2}) = \frac{4\pi i}{3}\,(x - F(v))$. Thus $|e^{c'\varphi}| = 1$ on E_+, the critical points of φ there are b_0 and its mirror image $-\bar{b}_0$, and $\varphi''(b_0) = -i\alpha_x$. For real v the k-th derivative of $u \mapsto \operatorname{Re}\varphi(v + i(\frac{1}{2} + u))$ is $\operatorname{Re}[i^k \varphi^{(k)}]$. At $u = 0$ the function vanishes, its first derivative is $\frac{4\pi}{3}(F(v) - x)$, and its second derivative is zero because $\varphi''(v + \frac{i}{2}) = -\frac{4\pi i}{3} F'(v)$ is imaginary; its third derivative is bounded by $|\Phi_0'''| \le C_2$. By Taylor's theorem, for $|u| \le \delta_1$,

$$\operatorname{Re}\varphi(v + i(\tfrac{1}{2} + u)) = \frac{4\pi}{3}\, u\,[F(v) - x] + R_3, \qquad |R_3| \le \tfrac{1}{6}\, C_2 |u|^3. \tag{E.19}$$

So $|e^{c'\varphi}|$ decreases above the edge where $|v| < v_0$ and below it where $|v| > v_0$: two valleys, which meet at the saddles. By convexity the chord slope $(F(v_0) - F(v))/(v_0 - v)$ increases with v, so its infimum over $[0, v_0)$ is s_{ch}, and the graph of F lies above its tangent at v_0:

$$x - F(v) \ge s_{\mathrm{ch}}\,(v_0 - v) \;\; (0 \le v \le v_0), \quad F(v) - x \ge F'(v_0)(v - v_0) = \tfrac{3\alpha_x}{4\pi}(v - v_0) \;\; (v \ge v_0). \tag{E.20}$$

Finally, by Taylor's theorem at b_0, for $b_0 + w \in \mathcal{N}_{\delta_1}$ and $\varphi_{\ge 3}(w) := \varphi(b_0 + w) - \varphi(b_0) + \frac{i\alpha_x}{2} w^2$,

$$|\varphi_{\ge 3}(w)| \le \tfrac{1}{6} C_2 |w|^3, \qquad |\varphi_{\ge 3}(w) - \tfrac{1}{6}\varphi'''(b_0) w^3| \le \tfrac{1}{24} C_3 |w|^4. \tag{E.21}$$

Step 3: the contour. Let Γ run from left to right through $\Gamma^-_{\mathrm{far}}, \Gamma^-_{\mathrm{loc}}, \Gamma_{\mathrm{mid}}, \Gamma^+_{\mathrm{loc}}, \Gamma^+_{\mathrm{far}}$, where

$$\begin{aligned} &\Gamma^{\mp}_{\mathrm{far}}: \; b = v + i(\tfrac{1}{2} - u_0), \quad \mp v \ge v_0 + u_0; && \Gamma^-_{\mathrm{loc}}: \; b = -\bar{b}_0 + r\, e^{i\pi/4}, \quad r \in [-\ell, \ell]; \\ &\Gamma_{\mathrm{mid}}: \; b = v + i(\tfrac{1}{2} + u_0), \quad |v| \le v_0 - u_0; && \Gamma^+_{\mathrm{loc}}: \; b = b_0 + r\, e^{-i\pi/4}, \quad r \in [-\ell, \ell]. \end{aligned} \tag{E.22}$$

It follows the valleys at distance u_0 from the edge, crosses the two saddles along their directions of steepest descent, and lies above E_+ only on the bounded piece Γ_{mid} and the adjacent halves of $\Gamma^{\pm}_{\mathrm{loc}}$. The pieces join, since $b_0 \mp \ell e^{-i\pi/4} = (v_0 \mp u_0) + i(\frac{1}{2} \pm u_0)$; the local pieces do not overlap, since $\ell \le v_0$; the height is even in v; and $\Gamma \subset \mathcal{N}_{u_0} \subset \mathcal{N}_{\delta_1}$, where $\mathcal{I}$ is analytic by (SD1) (the Hankel function and $b^{1/2}$ are analytic in $\operatorname{Im} b > 0$). The region between E_+ and Γ is bounded apart from two half-strips in $\{-u_0 \le u \le 0\} \subset \bar{\mathbb{S}}$. On their closing segments $\operatorname{Re} b = \pm X$ one has $|H_0^{(1)}(k_x b)\, b| \le C|b|^{1/2}$ by (E.3), so these contribute at most $Cu_0 X^{1/2} \sup_{-u_0 \le u \le 0} |h_0(\pm X + i(\frac{1}{2} + u))| \to 0$ as $X \to \infty$, by the decay in (SD1). By Cauchy's theorem $\int_{E_+} \mathcal{I}\,\mathrm{d}b = \int_\Gamma \mathcal{I}\,\mathrm{d}b$, and (E.18) holds for Γ.

Step 4: the middle and far pieces. Put $\mathcal{G} := |A(b_0)|\sqrt{2\pi/(c'\alpha_x)}$. On $\Gamma_{\rm mid}$ with $0 \le v \le v_0 - u_0$ let $s := v_0 - v$. Then (E.19) and (E.20) give $c'\,\mathrm{Re}\,\varphi \le -\frac{4\pi}{3}c'u_0 s_{\rm ch}\,s + \frac{1}{6}c'C_2u_0^3$, and integrating A'/A from b_0 along a path of length $s+u_0$ gives $|A(b)| \le |A(b_0)|\,e^{Ms+Mu_0}$. Condition (i) absorbs e^{Ms} into half of the linear decay, and $u_0 \le 2\pi s_{\rm ch}/C_2$ gives $\frac{1}{6}c'C_2u_0^3 \le \frac{\pi}{3}c's_{\rm ch}u_0^2$, so that

$$\begin{aligned}\Big|\int_{\Gamma_{\rm mid},\,v\ge 0} e^{c'\varphi}A\,\mathrm{d}b\Big| &\le |A(b_0)|\,e^{Mu_0+\frac{\pi}{3}c's_{\rm ch}u_0^2}\int_{u_0}^{\infty} e^{-\frac{2\pi}{3}c'u_0 s_{\rm ch}\,s}\,\mathrm{d}s\\ &= |A(b_0)|\,\frac{3\,e^{Mu_0-\frac{\pi}{3}c's_{\rm ch}u_0^2}}{2\pi c's_{\rm ch}u_0} = \mathcal{G}\,\varepsilon_{\rm mid}.\end{aligned} \tag{E.23}$$

On $\Gamma^+_{\rm far}$ let $s := v - v_0 \ge u_0$. The second bound of (E.20) gives $c'\,\mathrm{Re}\,\varphi \le -c'\alpha_x u_0\,s + \frac{1}{6}c'C_2u_0^3$, and $|A(b)| \le |A(b_0)|\,e^{Ms+Mu_0}$. By condition (ii) and $\frac{1}{6}C_2u_0^3 \le \frac{1}{4}\alpha_x u_0^2$ (from $u_0 \le \ell \le \alpha_x/C_2$),

$$\Big|\int_{\Gamma^+_{\rm far}} e^{c'\varphi}A\,\mathrm{d}b\Big| \le |A(b_0)|e^{Mu_0+\frac{1}{4}c'\alpha_x u_0^2}\int_{u_0}^{\infty} e^{-\frac{1}{2}c'\alpha_x u_0 s}\mathrm{d}s = |A(b_0)|\frac{2e^{Mu_0-\frac{1}{4}c'\alpha_x u_0^2}}{c'\alpha_x u_0} = \mathcal{G}\varepsilon_{\rm far}. \tag{E.24}$$

Step 5: the saddle. On $\Gamma^+_{\rm loc}$ we have $b = b_0 + w$ with $w = re^{-i\pi/4}$, and $-\frac{i\alpha_x}{2}w^2 = -\frac{1}{2}\alpha_x r^2$ is real. By (E.21) and $\ell \le \alpha_x/C_2$, with $q(r) := c'\varphi_{\ge 3}(re^{-i\pi/4})$,

$$c'\big[\varphi(b) - \varphi(b_0)\big] = -\tfrac{1}{2}c'\alpha_x r^2 + q(r), \qquad |q(r)| \le \tfrac{1}{6}c'C_2|r|^3 \le \tfrac{1}{6}c'\alpha_x r^2, \tag{E.25}$$

so that $\mathrm{Re}\,c'[\varphi - \varphi(b_0)] \le -\frac{1}{3}c'\alpha_x r^2$ on the whole segment. We split it into the core $|r| \le r_1$, where $|q| \le \frac{1}{6}c'C_2r_1^3 \le 1$, and the transition part $r_1 < |r| \le \ell$. On the latter $|A| \le |A(b_0)|e^{M\ell}$, so

$$\Big|\int_{r_1<|r|\le\ell} e^{c'[\varphi-\varphi(b_0)]}A\,\mathrm{d}r\Big| \le 2|A(b_0)|e^{M\ell}\int_{r_1}^{\infty} e^{-c'\alpha_x r^2/3}\mathrm{d}r \le |A(b_0)|e^{M\ell}\frac{3e^{-c'\alpha_x r_1^2/3}}{c'\alpha_x r_1} = \mathcal{G}\varepsilon_{\rm tr}. \tag{E.26}$$

On the core, integrating A'/A twice along the segment gives $A(b_0+w) = A(b_0)\exp(\mathsf{a}_1 w + \mathsf{r}_2)$ with $\mathsf{a}_1 := A'(b_0)/A(b_0)$, $|\mathsf{a}_1| \le M$ and $|\mathsf{r}_2| \le \frac{1}{2}M'r^2$. As $|r| \le \ell \le \min\{1/M, 1/\sqrt{M'}\}$, the exponent z has $|z| \le \frac{3}{2}$ and $|z|^2 \le (2M^2 + \frac{1}{2}M')r^2$, and $|e^z - 1 - z| \le \frac{1}{2}|z|^2e^{|z|} \le 2.25|z|^2$ gives $A/A(b_0) = 1 + \mathsf{a}_1 w + \mathsf{a}_2$ with $|\mathsf{a}_2| \le [\frac{1}{2}M' + 2.25(2M^2 + \frac{1}{2}M')]r^2 = K_A r^2$. Likewise $e^q = 1 + q + q_2$ with $|q_2| \le \frac{e}{2}|q|^2$, and $q = \frac{1}{6}c'\varphi'''(b_0)w^3 + q_4$ with $|q_4| \le \frac{1}{24}c'C_3r^4$ by (E.21). So

$$e^{c'[\varphi(b)-\varphi(b_0)]}\,\frac{A(b)}{A(b_0)} = e^{-c'\alpha_x r^2/2}\Big\{1 + \big[\mathsf{a}_1 w + \tfrac{1}{6}c'\varphi'''(b_0)w^3\big] + \mathrm{Rest}(r)\Big\}, \tag{E.27}$$

where the bracket is odd in r and integrates to zero over $[-r_1, r_1]$, and where

$$|\mathrm{Rest}| \le K_A r^2 + \frac{c'C_3r^4}{24} + \frac{Mc'C_2r^4}{6} + \frac{e\,(c'C_2)^2r^6}{72} + \Big(1+\frac{e}{2}\Big)\frac{K_Ac'C_2|r|^5}{6} + \frac{e\,M(c'C_2)^2|r|^7}{72}; \tag{E.28}$$

the terms are, in order, a_2; q_4; $\mathsf{a}_1 w\,q$; q_2; $\mathsf{a}_2(q+q_2)$, with $|q+q_2| \le (1+\frac{e}{2})|q|$ for $|q| \le 1$; and $\mathsf{a}_1 w\,q_2$. We integrate against $e^{-c'\alpha_x r^2/2}$ over $\mathbb{R}$, using $\int_{\mathbb{R}} r^{2n}e^{-sr^2/2}\mathrm{d}r = \sqrt{2\pi/s}\,(2n-1)!!\,s^{-n}$ and $\int_{\mathbb{R}}|r|^{2n+1}e^{-sr^2/2}\mathrm{d}r = n!\,(2/s)^{n+1}$ with $s = c'\alpha_x$. Relative to $\sqrt{2\pi/(c'\alpha_x)}$, the four even terms give $K_A/(c'\alpha_x)$, $\frac{1}{8}C_3/(c'\alpha_x^2)$, $\frac{1}{2}MC_2/(c'\alpha_x^2)$ and $\frac{15e}{72}C_2^2/(c'\alpha_x^3)$, and the two odd terms give $2.51\,(c'\alpha_x)^{-1/2}K_AC_2/(c'\alpha_x^2)$ and $1.45\,(c'\alpha_x)^{-1/2}MC_2^2/(c'\alpha_x^3)$, which condition (iii) bounds by $K_AC_2/(c'\alpha_x^2)$ and $0.52\,MC_2^2/(c'\alpha_x^3)$; the sum is $\varepsilon_{\rm core}$. Completing the Gaussian costs $\int_{|r|>r_1} e^{-c'\alpha_x r^2/2}\mathrm{d}r \le 2e^{-c'\alpha_x r_1^2/2}/(c'\alpha_x r_1) \le \sqrt{2\pi/(c'\alpha_x)}\,\varepsilon_{\rm tr}$. Altogether, with $\mathrm{d}b = e^{-i\pi/4}\mathrm{d}r$,

$$\int_{\Gamma^+_{\rm loc}} e^{c'\varphi}A\,\mathrm{d}b = e^{c'\varphi(b_0)}A(b_0)\,e^{-i\pi/4}\sqrt{\frac{2\pi}{c'\alpha_x}}\,(1+\varepsilon_{\rm loc}), \qquad |\varepsilon_{\rm loc}| \le \varepsilon_{\rm core} + 2\varepsilon_{\rm tr}. \tag{E.29}$$

Step 6: assembly. Let $\mathcal{Z} := e^{-i\pi/2}e^{c'\varphi(b_0)}A(b_0)\sqrt{2\pi/(c'\alpha_x)}$, so that $|\mathcal{Z}| = \mathcal{G}$, as $|e^{c'\varphi(b_0)}| = 1$. By (E.23), (E.24) and (E.29), $e^{-i\pi/4}J_+ = \mathcal{Z}(1+\varepsilon_{\rm loc}) + \mathcal{R}$ with $|\mathcal{R}| \le \mathcal{G}(\varepsilon_{\rm mid} + \varepsilon_{\rm far})$, hence

$2\,\mathrm{Re}[e^{-i\pi/4}J_+] = 2\mathcal{G}[\cos\arg\mathcal{Z} + \varepsilon_{\mathrm{sd}}]$ with $\varepsilon_{\mathrm{sd}}$ real and $|\varepsilon_{\mathrm{sd}}| \le \bar\varepsilon_{\mathrm{sd}}$. Then (E.18) gives (E.9) with $\mathrm{Amp} = \frac{2\pi c'}{3}\sqrt{2/(\pi k_x)}\,e^{-k_x/2}\cdot 2\mathcal{G}$ and $\hat\Psi = \arg\mathcal{Z} = c'\,\mathrm{Im}\,\varphi(b_0) - \frac{\pi}{2} + \arg A(b_0)$, which is (E.11) because $c'\varphi(b_0) = c'\Phi_0(b_0) + ik_xv_0$. With $k_x = \frac{4\pi}{3}c'x$ and $\alpha_x = \frac{4\pi}{3}F'(v_0)$ this is $\mathrm{Amp} = 2e^{-c'L}|A(b_0)|/\sqrt{xF'(v_0)}$, and (E.10) and the expression for $\arg A(b_0)$ follow from (E.6) with $\arg b_0^{1/2} = \frac12\arctan\frac{1}{2v_0}$. Finally $\frac12\mathrm{Amp}\,e^{i\hat\Psi}$ is $\frac{2\pi c'}{3}$ times the prefactor of (E.17) times $e^{i\pi/4}\mathcal{Z}$, which is (E.1). □

Proof of Corollaries E.2 and E.3. Plan. We bound the window ℓ from below by the controlling quantity and inspect (E.12)–(E.13). Let $m := \min\{\alpha_x, s_{\mathrm{ch}}, v_0\}$ and $\bar m := \min\{1, m\}$. By (E.7), $\ell \ge c_\ell\bar m$ with $c_\ell := \min\{1, \sqrt2\delta_1, 1/C_2, 1/M, 1/\sqrt{M'}\}$, and the hypothesis gives $c'\bar m^3 \ge c'^\gamma$ (we may take $\gamma \le 1$), so that $c'\bar m^2$ and $c'\bar m$ tend to infinity and (E.8) holds. In (E.12) we use $C_2/\alpha_x^2 \le \frac12(1/\alpha_x + C_2^2/\alpha_x^3)$ and $M \le \frac12(1+M^2)$; this gives the bracket of (E.15). The exponents in (E.13) are $\frac13 c'\alpha_x r_1^2$, $\frac{\pi}{6}c's_{\mathrm{ch}}\ell^2$ and $\frac18 c'\alpha_x\ell^2$. Those with ℓ are at least $\frac18 c_\ell^2\,c'\bar m^3$, and when $r_1 < \ell$ the first equals $\frac13\cdot 6^{2/3}(c'\alpha_x^3/C_2^2)^{1/3} \ge C_2^{-2/3}(c'\bar m^3)^{1/3}$; so all three are at least $2c_*c'^{\gamma/3}$ for a suitable $c_* > 0$. The prefactors of $\varepsilon_{\mathrm{tr}}$ and $\varepsilon_{\mathrm{far}}$ are bounded, because $e^{M\ell} \le e$ and $r_1\sqrt{c'\alpha_x}$, $u_0\sqrt{c'\alpha_x}$ are the square roots of multiples of the exponents; that of $\varepsilon_{\mathrm{mid}}$ is at most a power of c', because $\alpha_x \le \frac{4\pi}{3}\sup F'$ and $s_{\mathrm{ch}}u_0 \ge c_\ell\bar m^2/\sqrt2$ with $\bar m \ge c'^{-(1-\gamma)/3}$, and a power of c' times $e^{-2c_*c'^{\gamma/3}}$ is at most $Ce^{-c_*c'^{\gamma/3}}$. This proves Corollary E.2. The first inequality of (E.16) follows from (E.9) and $|\cos\hat\Psi + \varepsilon_{\mathrm{sd}}| \le 1 + \bar\varepsilon_{\mathrm{sd}}$, the second from (E.14). For the comb, $|\mathrm{sech}^2\frac{\pi b_0}{2}| = 2/\cosh\pi v_0 \le 4e^{-\pi v_0}$ (Proposition 7.2); $F(v) \ge v$ gives $v_0 \le x$, so that $|b_0|/x \le (1 + 1/(4(x_1^*)^2))^{1/2} \le 2.05$; and $1 + \bar\varepsilon_{\mathrm{sd}} \le 2$ once $\bar\varepsilon_{\mathrm{sd}} \le 1$. Hence $2\cdot 2\cdot 4\cdot\sqrt{2.05}\,(1 + O(1/c')) \le 2^5$. □

E.4 Verification for the comb

We verify the hypotheses for the function $h_0 = \mathrm{sech}^2\frac{\pi b}{2}\,B$ of section 7.2, with $\delta_1 = \frac14$, $\mathcal{E} = \mathrm{sech}^2\frac{\pi b}{2}$ and the phases Φ_0, Φ_1 of Lemma 7.6.

(SD1). Each factor T_ζ is even, and the zeros are real or form conjugate pairs, so h_0 is even and real on $\mathbb{R}\cup i\mathbb{R}$. By (T4) the poles of B lie at $|\mathrm{Im}\,b| \ge 1 - \max_n\varepsilon_n > \frac34$ for c large, since $\varepsilon_n \lesssim c'^{-2/3}$ (appendix D.3); those of $\mathcal{E}$ lie on $|\mathrm{Im}\,b| = 1$. The edge representation is Lemma 7.3(c), and the symmetry follows from $h_0(-\bar b) = \overline{h_0(b)}$ and $H_0^{(1)}(-\bar z) = -\overline{H_0^{(1)}(z)}$. For the decay, $|\cosh\frac{\pi}{2}(v+iy)|^2 = \frac12(\cosh\pi v + \cos\pi y) \ge \frac12\cosh\pi v$ for $\frac14 \le y \le \frac12$ and $|B| \le 1$ on $\bar{\mathbb{S}}$ (Proposition 7.2) give $|h_0| \le 2/\cosh\pi v \le 4e^{-\pi|v|}$ on $\mathcal{N}_{1/4}\cap\bar{\mathbb{S}}$, so $\mu = \pi$.

(SD2), with the sign +. We use Lemma 7.6 in the form of Lemma D.2, which holds on the two-sided strip $\mathcal{N}_{1/4}$ and not only on E_+. By its part (a), Φ_0 is analytic on $\mathcal{N}_{1/4}$, with $\mathrm{Re}\,\Phi_0 = 0$ and $\Phi_0' = -\frac{4\pi i}{3}F(v)$ on E_+, where $F(v) = \frac1\pi\,\mathrm{arcsinh}(\cosh\pi v)$ is analytic in $|\mathrm{Im}\,v| < \frac12$, and C_2, C_3 are finite. This F is even, $F(0) = x_1^*$ with $\frac{\pi}{3}c'x_1^* \ge 13\pi x_1^* > 11$, and

$$F'(v) = \frac{\sinh\pi v}{\sqrt{1+\cosh^2\pi v}} \in (0,1) \quad (v>0), \qquad F''(v) = \frac{2\pi\cosh\pi v}{(1+\cosh^2\pi v)^{3/2}} > 0, \tag{E.30}$$

so F is strictly increasing and convex, with $F(v) \ge v$ and $\sup F' = 1$. By (T4) the zeros of B lie at heights 0 and $\pm\varepsilon_n$ modulo 2, none of them in $\mathcal{N}_{1/4}$, so that $\Phi_1 = \log B - c'\Phi_0$ is analytic there; the sign of the simple zero, $B(\frac{i}{2}) = -1$, is the constant $i\pi$ in Φ_1, which is why the sign in (SD2) is +. Part (c) bounds Φ_1' and Φ_1'' on $\mathcal{N}_{1/4}$ uniformly in c' and $\mathrm{Re}\,b$, so that M_1 and M_1' depend on (n_1,η_0) only. Finally $\mathrm{Re}\,\Phi_1 = 0$ on E_+ because $|B| = 1$ and $\mathrm{Re}\,\Phi_0 = 0$ there.

(SD3). The factor $\mathcal{E}$ is analytic and zero-free in $|\mathrm{Im}\,b| < 1$, with $\mathcal{E}'/\mathcal{E} = -\pi\tanh\frac{\pi b}{2}$. As $|\tanh\frac{\pi}{2}(v+iy)|^2 = (\cosh\pi v - \cos\pi y)/(\cosh\pi v + \cos\pi y)$, $M_{\mathcal{E}} = \pi\tan\frac{3\pi}{8}$ and $M_{\mathcal{E}}' = \frac{\pi^2}{2}\sec^2\frac{3\pi}{8}$.

(SD4) *and the hand-off.* Here v_0 is given by $\cosh\pi v_0 = \sinh\pi x$. Since $F'(0) = 0$, $F''(0) = \pi/\sqrt2 > 0$ and F' is positive and increasing, the ratios $F'(v)/v$ and $\frac{1}{v^2}\int_0^v F'$ are bounded below on $(0,1]$, and $F'(v)$ and $\frac1v\int_0^v F'$ are increasing for $v \ge 1$; hence $\min\{\alpha_x, s_{\mathrm{ch}}, v_0\} \ge c_F\min\{1, v_0\}$

with an absolute $c_F > 0$. Near the tip $v_0 \simeq (2(x-x_1^*)/F''(0))^{1/2}$, so that $c' \min\{1, v_0\}^3$ is at least a positive multiple of $c'^{\,1-3\theta_{\rm on}/2}$ on $[x_I, \infty)$, and Corollary E.2 applies with any $\gamma < 1 - \frac{3}{2}\theta_{\rm on}$, provided $\theta_{\rm on} < \frac{2}{3}$. With $\sigma := c' \min\{1, v_0\}^3$, every term of $\bar\varepsilon_{\rm sd}$ is then at most a multiple of $1/\sigma$: for $\varepsilon_{\rm core}$ this is (E.15), and in (E.13), where $\alpha_x \asymp s_{\rm ch} \asymp u_0 \asymp \min\{1, v_0\}$, the exponents are bounded below by multiples of $\sigma^{1/3}$, σ, σ, the prefactors are bounded for $\sigma \ge 1$, and $\sigma e^{-c_* \sigma^{1/3}}$ is bounded. Thus, with C depending on (n_1, η_0) only and for $c \ge c(n_1, \eta_0, \theta_{\rm on})$,

$$|\varepsilon_{\rm sd}(x)| \le \bar\varepsilon_{\rm sd}(x) \le \frac{C}{c' \min\{1, v_0(x)\}^3} \qquad (x \ge x_I), \tag{E.31}$$

which is $O(1/c')$ deep in the band and $O((c'(x - x_1^*)^{3/2})^{-1})$ toward the onset, at most $Cc'^{-(1-3\theta_{\rm on}/2)}$ at x_I. With (E.9), (E.14) and Corollary E.3 this is Lemma 7.7. At x_I the term $\varepsilon_{\rm tr}$ decays only like $\exp(-\text{const} \cdot c'^{(1-3\theta_{\rm on}/2)/3})$, which is why $\theta_{\rm on}$ is taken well below $\frac{2}{3}$.

F The comb on the real axis

This appendix proves the statements of section 7.5 about the comb on the real axis, namely Proposition 7.4 and Lemma 7.5(a)–(c), (d1), (e), (f), and from them the floor of Lemma 7.9, the overshoot bound of Lemma 7.11 and the first-cell bounds of Lemma 7.12; appendix G takes appendices F.1 to F.4 and Lemmas F.8 to F.10 as input. Each statement carries its own tag, and a statement that contains or uses a certified constant names the row of table 4 on which it rests.

As in section 7.5, the logarithm of the comb is a sum over the sites of the site weight f_x of (F.1), a Riemann sum of unit step in the site index for the potential $U = -L$ (Lemma 7.1). On either side of x, apart from the sites far to the left of x, the summand is concave along the sites, so the trapezoid and midpoint rules bound the sum by the integral with no remainder. What is left over is explicit: the potential $c'\mathcal{P}$ of the charge $2n_1$ below the first kept site, the half cell $\mathcal{J}_{\rm end}$ there, and the few sites nearest to x. Appendices F.1 to F.3 provide the tools, appendix F.5 the two-sided bounds, and appendices F.4, F.6 and F.7 the consequences. The constants that appendix G needs are explicit: $C_J \le 0.65$ (Lemma F.8), $C_{\rm det} \le 16.6$ (Lemma F.7), and the coefficient 94 of $\frac{1}{n}$ in (F.46).

Notation. Throughout, $(m, k_\infty, n_1, \eta_0) = (1, \frac{1}{4}, \frac{7}{4}, \frac{1}{4})$, the outer factor is $\operatorname{sech}^2(\pi x/2)$, and $c \ge c_0^{\rm att}$. The letter C denotes an absolute constant, which may change from line to line; a subscript records a dependence. We recall the zero law $\rho_U(y) = \frac{4}{3\pi} \operatorname{arccosh}(\sinh \pi y)$ on $y \ge x_1^*$ and its counting function $N(y) = \frac{1}{2}\int_{x_1^*}^{y} \rho_U$. For $x \ge 0$ the *site weight* is

$$f_x(y) := \log|T_y(x)| = \log\Big|\tanh\frac{\pi(x-y)}{2}\Big| + \log\tanh\frac{\pi(x+y)}{2} \;\le 0, \qquad y > 0. \tag{F.1}$$

The *site map* $a \mapsto \chi_a$, $a \ge \frac{1}{4}$, is defined by $c'N(\chi_a) = a - \frac{1}{4}$. It interpolates the sites, starts at $\chi_{1/4} = x_1^*$, and satisfies

$$\mathrm{d}a = \tfrac{c'}{2}\rho_U(\chi_a)\,\mathrm{d}\chi_a, \qquad \chi_a' = \frac{2}{c'\rho_U(\chi_a)}, \qquad \chi_a'' = -(\chi_a')^2\,(\log\rho_U)'(\chi_a), \tag{F.2}$$

where a prime on χ_a is a derivative in a. We write $\varphi(a) := f_x(\chi_a)$ when x is fixed, $\ell_k := \chi_{k+1} - \chi_k$ for the spacing, and $\varepsilon_k = \eta_0\ell_k$ for the heights of the detuned zeros. A point x of cell n, $\chi_n < x < \chi_{n+1}$, has the position $u := (x - \chi_n)/\ell_n \in (0,1)$ in its cell. The index k always labels a site, j is the number of pairs kept exactly on each side of x, and a, a' are real site indices (in this appendix a never denotes $c'/12$). The product formula reads

$$\log|B^0(x)| = f_x(\chi_2) + 2\sum_{k\ge3} f_x(\chi_k), \qquad \log|B(x)| = f_x(\chi_2) + \sum_{k\ge3}\log q_k(x), \tag{F.3}$$

where, with $\gamma_k := \cos \pi\varepsilon_k$,

$$q_k(x) := |T_{\chi_k+i\varepsilon_k}(x)\, T_{\chi_k-i\varepsilon_k}(x)| = \prod_{\pm} \frac{\cosh \pi(\chi_k \mp x) - \gamma_k}{\cosh \pi(\chi_k \mp x) + \gamma_k} \tag{F.4}$$

is the modulus of a detuned pair; for $\varepsilon_k = 0$ it is $T_{\chi_k}(x)^2$. Since $\cosh 2z - \cos 2v = 2(\sinh^2 z + \sin^2 v)$ and $\cosh 2z + \cos 2v = 2(\cosh^2 z - \sin^2 v)$, each of the two factors of q_k equals $(\sinh^2 z + \sin^2 v)/(\cosh^2 z - \sin^2 v)$ with $z = \frac{\pi}{2}(\chi_k \mp x)$ and $v = \frac{\pi}{2}\varepsilon_k$. Both sums converge, because $|f_x(y)| \le Ce^{-\pi(y-x)}$ for $y \ge x+1$. On the real axis $h_0 = \operatorname{sech}^2(\pi x/2)\, B(x)$ with $t = c'x^2/3$, and $B < 0$ on $[0, \chi_2)$, $B \ge 0$ beyond. The continuum counterparts of the sums are

$$I_x(a) := \int_a^\infty f_x(\chi_{a'})\, \mathrm{d}a' = \frac{c'}{2} \int_{\chi_a}^\infty \rho_U f_x \, \mathrm{d}y, \qquad \mathcal{P}_Y(x) := -\int_{x_1^*}^Y \rho_U(y) f_x(y)\, \mathrm{d}y \ \ge 0, \tag{F.5}$$

so that $\mathcal{P} = \mathcal{P}_{\chi_2}$ and $c' \int_{x_1^*}^{\chi_a} \rho_U \, \mathrm{d}y = 2(a - \frac{1}{4})$, which is $2n_1$ for $a = 2$. Since $U(x) = \int \rho_U(y) \log|T_y(x)|\, \mathrm{d}y$ is the potential of the law, Lemma 7.1 gives

$$2I_x(a) = c'U(x) + c'\mathcal{P}_{\chi_a}(x), \qquad U(x) = -L(x) \ \text{ for } x \ge x_1^*. \tag{F.6}$$

Finally, in this notation the end correction, the level and the normalized comb of section 7.5 are

$$\begin{gathered} \mathcal{J}_{\mathrm{end}}(x) = f_x(\chi_2) - 2\int_2^{5/2} \varphi(a)\, \mathrm{d}a, \qquad \mathrm{Lev} = 4 \operatorname{sech}^2 \tfrac{\pi x}{2}\, e^{-c'L + c'\mathcal{P} + \mathcal{J}_{\mathrm{end}}}, \\ \frac{h_0}{\mathrm{Lev}} = \tfrac{1}{4}|B|\, e^{c'L - c'\mathcal{P} - \mathcal{J}_{\mathrm{end}}} \qquad (x > \chi_2). \end{gathered} \tag{F.7}$$

The conditions on the size of c are conditions on the Airy length ℓ_c (notation of Lemma F.2). We take c_0^{att} so large that three of them hold for $c \ge c_0^{\mathrm{att}}$. Statements in the Airy window are made under the hypothesis $\ell_c \varsigma_{\max} \le 0.3$ and are applied in this appendix with $\varsigma_{\max} \le \hat{\varsigma}_{10} \le 4.57$, so that we require $\ell_c \hat{\varsigma}_{10} \le 0.3$; this implies $\chi_6 - \chi_2 \ge \ell_c$, which is used for (F.36). The far-left loss requires $\ell_c \hat{\varsigma}_{602} \le 0.24$, where $\hat{\varsigma}_{602} \le 71.3$, and $C\ell_c \le 0.004$ with an absolute constant C which we do not evaluate (Lemma F.6(d)). The remaining conditions depend on a parameter. A statement on a far band $x \ge x_1^* + r$ with $r > 0$ fixed is made for c so large, depending on r, that $\chi_6 \le x_1^* + r/2$; the band then lies in the cells $n \ge 6$. The bracket for $j = 4$ in Proposition 7.4 holds on the cells $n \ge \epsilon c'$ for c large depending on ϵ.

F.1 The law near the tip

We prove that the site weight is monotone and concave along the sites (Lemma F.1), expand the law at the tip (Lemma F.2), and deduce the form of the comb in the Airy window, which gives Lemma 7.5(b) and (d1). Near the tip the law is the square-root density of a soft edge: the sites sit at $\varsigma_k \approx (k - \frac{1}{4})^{2/3}$, and the logarithm of each Blaschke factor is that of a scaled distance plus $\log \ell_c$ plus a constant. Rows 9 and 10 of table 4 are used.

Lemma F.1 (Monotone and concave summands; proved, computer-assisted)**.** *Let $x \ge 0$.*

(a) *For $y > 0$, $y \ne x$,*

$$\partial_y f_x(y) = \sum_{\pm} \frac{\pi}{\sinh \pi(y \pm x)}, \qquad \partial_y^2 f_x(y) = -\pi^2 \sum_{\pm} \frac{\cosh \pi(y \pm x)}{\sinh^2 \pi(y \pm x)} < 0. \tag{F.8}$$

Thus f_x is increasing and concave on (x, ∞), and decreasing and concave on $(0, x)$. For $0 < y < x$, $|\partial_y f_x| \le 1/(x-y)$ and $|\partial_y^2 f_x|/|\partial_y f_x| \ge \pi \coth \pi(x-y) \ge \max\{\pi, 1/(x-y)\}$.

(b) *ρ_U is positive, increasing and concave on (x_1^*,∞), and ρ_U^2/N is non-increasing there. Hence $a\mapsto\chi_a$ is increasing and concave, the spacings ℓ_k decrease, $\ell_k\le\chi_k'$ and $\ell_k\ge\chi_{k+1}'$, the mean spacing $(\chi_a-x_1^*)/(a-\frac14)$ decreases in a, and*

$$1\le\frac{\chi_a'}{\chi_{a'}'}=\frac{\rho_U(\chi_{a'})}{\rho_U(\chi_a)}\le\Big(\frac{a'-\frac14}{a-\frac14}\Big)^{1/2}\qquad(\tfrac14<a\le a').\tag{F.9}$$

(c) *φ is increasing and concave on $\{a:\chi_a>x\}$ and decreasing on $\{a:\chi_a<x\}$. It is concave on $\{a:y_{\rm thr}(x)\le\chi_a<x\}$, where*

$$y_{\rm thr}(x):=\min\Big\{x_1^*+\frac{x-x_1^*}{2.3},\ \max\{x_1^*+0.18,\ x-1\}\Big\}\qquad(x>x_1^*).\tag{F.10}$$

Proof. (a) The derivatives follow from $(\log\tanh z)'=2/\sinh 2z$. For $y>x$ both terms of $\partial_y f_x$ are positive; for $0<y<x$ the term with $y-x$ is $-\pi/\sinh\pi(x-y)$ and exceeds the other in modulus, since $x+y>x-y$. This also gives $|\partial_y f_x|\le\pi/\sinh\pi(x-y)\le1/(x-y)$, while $|\partial_y^2 f_x|\ge\pi^2\cosh\pi(x-y)/\sinh^2\pi(x-y)$; the quotient is at least $\pi\coth\pi(x-y)$, and $\coth z\ge\max\{1,1/z\}$.

(b) With $w=\pi y$, $\rho_U'=\frac43\cosh w\,(\sinh^2 w-1)^{-1/2}>0$ and $\frac{\rm d}{{\rm d}w}\big[\cosh w\,(\sinh^2 w-1)^{-1/2}\big]=-2\sinh w\,(\sinh^2 w-1)^{-3/2}<0$, so ρ_U is increasing and concave, and it vanishes at x_1^*. Fix $y=x_1^*+r$ and put $\rho=\rho_U(y)$, $s=\rho_U'(y)$. The tangent at y lies above the graph, so $N(y)\le\frac12\int_0^r[\rho-s(r-r')]\,{\rm d}r'=\frac12(\rho r-\frac12 sr^2)$; and $\tau:=sr/\rho\le1$ because the chord from the tip is steeper than the tangent. Hence $4Ns\le2\rho^2\tau(1-\tau/2)\le\rho^2$, that is $(\log(\rho_U^2/N))'=2\rho_U'/\rho_U-\rho_U/(2N)\le0$. The statements on χ_a follow from (F.2): $\chi_a'>0$ and $\chi_a''<0$; a chord of a concave function has a slope between the derivatives at its ends; the chord from $a=\frac14$ has decreasing slope; and (F.9) is $\rho_U^2(\chi_a)/(a-\frac14)\ge\rho_U^2(\chi_{a'})/(a'-\frac14)$ together with the monotonicity of ρ_U.

(c) We have $\varphi'=\partial_y f_x\,\chi_a'$ and $\varphi''=(\chi_a')^2\big[\partial_y^2 f_x-\partial_y f_x\,(\log\rho_U)'\big]$, both evaluated at $y=\chi_a$. For $\chi_a>x$ the bracket is negative by (a), since $(\log\rho_U)'>0$. For $\chi_a<x$ we have $\varphi'<0$, and $\varphi''\le0$ if and only if $|\partial_y^2 f_x|/|\partial_y f_x|\ge(\log\rho_U)'(\chi_a)$; by (a) it suffices that $(\log\rho_U)'(y)\le\max\{\pi,1/(x-y)\}$ at $y=\chi_a$. Let $r:=y-x_1^*$. Row 9 of table 4 contains two facts: $(\log\rho_U)'(x_1^*+r)\le3.10<\pi$ for $r\ge0.18$ ⟨cert⟩, and $1.3\,r\,(\log\rho_U)'(x_1^*+r)\le0.95$ for $0<r\le0.64$ ⟨cert⟩. If $r\ge0.18$ the first fact suffices. If $r<0.18$, then $y<\max\{x_1^*+0.18,x-1\}$, so $y\ge y_{\rm thr}(x)$ forces $y\ge x_1^*+(x-x_1^*)/2.3$, that is $x-y\le1.3\,r$, and the second fact gives $(\log\rho_U)'(y)\le0.95/(1.3r)\le1/(x-y)$. □

Lemma F.2 (The law near the tip; proved, computer-assisted)**.** *Let $u_1:=\operatorname{arcsinh}1=\pi x_1^*$, $\kappa_{\rm tip}:=4\cdot2^{3/4}/(9\sqrt\pi)$ and $\ell_c:=(\kappa_{\rm tip}c')^{-2/3}$, so that $\kappa_{\rm tip}c'\ell_c^{3/2}=1$.*

(a) (Table 4, row 10.) $\operatorname{arccosh}\sinh(u_1+\delta)=2^{3/4}\delta^{1/2}(1+\delta\,e_1(\delta))$ *with $e_1(\delta)\in[0.0589,0.105]$ for $0<\delta\le2$* ⟨cert⟩.

(b) *For $0\le r\le0.63$,*

$$3\kappa_{\rm tip}r^{1/2}\le\rho_U(x_1^*+r)\le3\kappa_{\rm tip}r^{1/2}(1+0.33\,r),\qquad\kappa_{\rm tip}r^{3/2}\le N(x_1^*+r)\le\kappa_{\rm tip}r^{3/2}(1+0.2\,r).\tag{F.11}$$

(c) *Let $\varsigma_a:=(\chi_a-x_1^*)/\ell_c$ be the scaled sites and $\hat\varsigma_a:=(a-\frac14)^{2/3}$ their nominal positions. If $\ell_c\hat\varsigma_a\le0.63$, then*

$$\hat\varsigma_a(1-0.14\,\ell_c\hat\varsigma_a)\le\varsigma_a\le\hat\varsigma_a.\tag{F.12}$$

(d) *For every $r>0$, and with no certified constant,*

$$\frac{1}{2r}\ \le\ (\log\rho_U)'(x_1^*+r)\ \le\ \frac{1}{2r}+\frac{\pi}{4\sqrt2},\qquad\frac{\pi}{4\sqrt2}\le0.56.\tag{F.13}$$

Proof. (b) With $\delta=\pi r\le2$, (a) gives $\rho_U(x_1^*+r)=\frac{4}{3\pi}2^{3/4}(\pi r)^{1/2}(1+\pi r\,e_1)=3\kappa_{\rm tip}r^{1/2}(1+\pi r\,e_1(\pi r))$, because $\frac{4}{3\pi}2^{3/4}\pi^{1/2}=3\kappa_{\rm tip}$; and $0\le\pi e_1\le0.105\,\pi\le0.33$. Integrating, $N(x_1^*+r)=$

$\frac{3}{2}\kappa_{\rm tip}\int_0^r r'^{1/2}(1+\pi r' e_1)\,\mathrm{d}r'$ lies between $\kappa_{\rm tip} r^{3/2}$ and $\kappa_{\rm tip} r^{3/2}(1+\frac{3}{5}\cdot 0.33\,r)$. (c) Since N increases and $c'N(x_1^*+0.63)\ge (0.63/\ell_c)^{3/2}$ by (b), the hypothesis $\ell_c\hat\varsigma_a\le 0.63$ implies $\chi_a - x_1^*\le 0.63$. By (b) and $\kappa_{\rm tip}c'\ell_c^{3/2}=1$, $a-\frac14 = c'N(\chi_a)=\varsigma_a^{3/2}(1+\theta)$ with $0\le\theta\le 0.2\,\ell_c\varsigma_a$. Hence $\varsigma_a=\hat\varsigma_a(1+\theta)^{-2/3}\le\hat\varsigma_a$, and $(1+\theta)^{-2/3}\ge 1-\frac23\theta\ge 1-0.14\,\ell_c\hat\varsigma_a$.

(d) Let $\Phi:=\rho_U^2=\frac{16}{9\pi^2}A^2$ with $A=\operatorname{arccosh}\sinh w$ and $w=\pi y$, so that $\cosh A=\sinh w$ and $\mathrm{d}A/\mathrm{d}w=\cosh w/\sinh A$. Then $\Phi'=\frac{32}{9\pi}A\cosh w/\sinh A$, and with $\cosh^2 w=1+\cosh^2 A$ we find $\Phi''=\frac{32}{9}K(A)$, where $K(A):=[(1+\cosh^2 A)\sinh A-2A\cosh A]/\sinh^3 A$. Here $K\le 1$ is the inequality $\tanh A\le A$, and $K\ge 0$ because $(1+\cosh^2 A)\tanh A-2A$ vanishes at $A=0$ and has the derivative $2\sinh^2 A-\tanh^2 A\ge 0$. At the tip $A=0$ and $\cosh w=\sqrt2$, so $\Phi(x_1^*)=0$ and $\Phi'(x_1^*)=\frac{32\sqrt2}{9\pi}=9\kappa_{\rm tip}^2$. Since Φ is convex, $\Phi(x_1^*+r)\ge 9\kappa_{\rm tip}^2 r$, and $r\Phi'-\Phi=\int_0^r s\,\Phi''(x_1^*+s)\,\mathrm{d}s$ lies in $[0,\frac{16}{9}r^2]$, the functions being evaluated at x_1^*+r. Hence $(\log\rho_U)'-\frac{1}{2r}=(r\Phi'-\Phi)/(2r\Phi)$ lies between 0 and $8/(81\kappa_{\rm tip}^2)=\pi/(4\sqrt2)$. □

Lemma F.3 (A Blaschke factor in the window; proved, computer-assisted)**.** *We have* $-z^2/3\le\log(|\tanh z|/|z|)\le 0$ *for all real* $z\ne 0$*, and* (table 4, row 10) $0<(\log\tanh z)'\le 1.24$ *for* $z\ge u_1-0.25$ ⟨cert⟩*. Consequently, let* $\ell_c\varsigma_{\max}\le 0.3$*,* $x=x_1^*+\ell_c\varsigma$ *and* $y=x_1^*+\ell_c\varsigma'$ *with* $-\frac12\varsigma_{\max}\le\varsigma\le\varsigma_{\max}$ *and* $0\le\varsigma'\le\varsigma_{\max}$*. Then*

$$f_x(y)=\log|\varsigma-\varsigma'|+\log\ell_c+\log\frac{\pi}{2\sqrt2}+R(\varsigma,\varsigma'),\qquad |R|\le 4.3\,\ell_c\varsigma_{\max}. \tag{F.14}$$

Moreover, for a pair $k\ge 3$ *with* $\varsigma_{k+1}\le\varsigma_{\max}$*, and with* $\Delta_k:=\varsigma_{k+1}-\varsigma_k$*, so that* $\varepsilon_k=\eta_0\ell_c\Delta_k$*,*

$$\log q_k(x)=\log[(\varsigma-\varsigma_k)^2+\eta_0^2\Delta_k^2]+2\log\ell_c+2\log\frac{\pi}{2\sqrt2}+R_k'(\varsigma),\qquad |R_k'|\le 8.6\,\ell_c\varsigma_{\max}. \tag{F.15}$$

Proof. Both sides of the first inequality are even; let $z>0$. The upper bound is $\tanh z\le z$. For the lower bound, $g(z):=\log(\tanh z/z)+z^2/3$ tends to 0 as $z\to 0$, and $g'(z)=\frac{2}{\sinh 2z}-\frac1z+\frac{2z}{3}=\frac{2}{y}\big(\frac{y}{\sinh y}-1+\frac{y^2}{6}\big)$ with $y=2z$. This is non-negative: for $y^2\ge 6$ evidently, and for $y^2<6$ because $(2k+1)!\ge 6^k$ gives $\sinh y=\sum_{k\ge0}y^{2k+1}/(2k+1)!\le y\sum_{k\ge0}(y^2/6)^k=y/(1-y^2/6)$.

The first logarithm in (F.1) is $\log(\frac{\pi}{2}\ell_c|\varsigma-\varsigma'|)+\log(|\tanh z|/|z|)$ with $|z|=\frac{\pi}{2}\ell_c|\varsigma-\varsigma'|\le 0.71$. The second is $\log\tanh u_1=-\log\sqrt2$ plus the increment of $\log\tanh$ from u_1 to $u_1+\frac{\pi}{2}\ell_c(\varsigma+\varsigma')\ge u_1-0.25$, whose modulus is at most $1.24\,\frac{\pi}{2}\ell_c|\varsigma+\varsigma'|$. Since $|\varsigma-\varsigma'|\le\frac32\varsigma_{\max}$ and $-\frac12\varsigma_{\max}\le\varsigma+\varsigma'\le 2\varsigma_{\max}$, the first term lies in $[-0.56,0]\,\ell_c\varsigma_{\max}$ and the second in $[-0.98,3.9]\,\ell_c\varsigma_{\max}$. This gives (F.14).

For the pair we use the second form of q_k given after (F.4), with $v=\frac{\pi}{2}\eta_0\ell_c\Delta_k\le 0.12$, $z_-=\frac{\pi}{2}\ell_c(\varsigma_k-\varsigma)$, $|z_-|\le 0.71$, and $z_+=u_1+\frac{\pi}{2}\ell_c(\varsigma+\varsigma_k)\ge u_1-0.25$; note that $z_-^2+v^2=(\frac{\pi}{2}\ell_c)^2[(\varsigma-\varsigma_k)^2+\eta_0^2\Delta_k^2]$. For positive numbers, $(A+b)/(A_0+b_0)$ lies between A/A_0 and b/b_0. Since $1\le\sinh^2 z/z^2\le e^{z^2/3}$ and $\cosh^2 z\le e^{z^2}$ (compare the power series: $(2k+1)!\ge 6^k k!$ and $(2k)!\ge 2^k k!$), and $1-\frac13 v^2\le\sin^2 v/v^2\le 1$, the numerator $\sinh^2 z_-+\sin^2 v$ is $z_-^2+v^2$ times a number in $[1-\frac13 v^2, e^{z_-^2/3}]$, and the denominator $\cosh^2 z_--\sin^2 v$ lies in $[1-v^2,e^{z_-^2}]$. So the factor with z_- is $(z_-^2+v^2)e^\theta$ with $-z_-^2-0.34\,v^2\le\theta\le\frac13 z_-^2+1.01\,v^2$. The factor with z_+ is $\tanh^2 z_+$ times $(1+\sin^2 v/\sinh^2 z_+)/(1-\sin^2 v/\cosh^2 z_+)\in[1,e^{2.9v^2}]$, because $\sinh^2(u_1-0.25)\ge 0.454$; and $\log\tanh^2 z_+$ is $-\log 2$ plus twice an increment of the kind just bounded. As $\Delta_k\le\varsigma_{\max}$, we have $z_-^2\le 1.67\,\ell_c\varsigma_{\max}$ and $v^2\le 0.047\,\ell_c\varsigma_{\max}$, and R_k' lies in $[-3.7,8.6]\,\ell_c\varsigma_{\max}$. □

Proof of Lemma 7.5(b) [PROVED]**.** Let $x>\chi_2$. By Lemma F.1(a), $|f_x(y)|=-f_x(y)$ increases with y on $[x_1^*,\chi_2]$, and $c'\mathcal{P}(x)=\int_{x_1^*}^{\chi_2}c'\rho_U(y)|f_x(y)|\,\mathrm{d}y$ with $\int_{x_1^*}^{\chi_2}c'\rho_U=2n_1$ is $2n_1$ times an average of it over this interval. Hence

$$2n_1|\log|T_{x_1^*}(x)||\;\le\;c'\mathcal{P}(x)\;\le\;2n_1|\log|T_{\chi_2}(x)||. \tag{F.16}$$

Here $\tanh z \le z$ and $\log\tanh\frac{\pi(x+x_1^*)}{2} \le 0$ give $|f_x(x_1^*)| \ge \log\frac{2}{\pi(x-x_1^*)}$, so that

$$e^{c'\mathcal{P}(x)} \;\ge\; \Big(\frac{2}{\pi(x-x_1^*)}\Big)^{2n_1} \qquad (x>\chi_2). \tag{F.17}$$

Since $|f_x(y)|$ decreases in x for $x>y$, for fixed $r>0$ and c so large that $\chi_2 \le x_1^*+r/2$, which is possible because $c'N(\chi_2)=n_1$, we get $c'\mathcal{P}(x) \le 2n_1|f_{x_1^*+r}(x_1^*+r/2)| =: C_r$ on $x \ge x_1^*+r$. For $x-y\ge 1$, $|f_x(y)| = 4\cosh(\pi y)\,e^{-\pi x}(1+O(e^{-2\pi(x-y)}))$, so $e^{c'\mathcal{P}}$ tends to 1 exponentially deep in the band. □

Lemma F.4 (Window asymptotics: Lemma 7.5(d1); proved, computer-assisted)**.** *Let $\ell_c\varsigma_{\max} \le 0.3$, $x = x_1^*+\ell_c\varsigma$ with $-\frac12\varsigma_{\max} \le \varsigma \le \varsigma_{\max}$, and let $a>\frac14$ be real with $\hat\varsigma_a \le \varsigma_{\max}$, so that $\varsigma_a \le \varsigma_{\max}$ by (F.12); part (c) concerns $a=2$. Put $w_c(\varsigma') := \rho_U(x_1^*+\ell_c\varsigma')/(3\kappa_{\rm tip}(\ell_c\varsigma')^{1/2}) \in [1, 1+0.33\,\ell_c\varsigma']$ and $\mathcal{F}(\varsigma,A) := \int_0^A \varsigma'^{1/2}\log|\varsigma-\varsigma'|\,\mathrm{d}\varsigma'$. For $\varsigma\ge 0$ the latter is elementary: $-3\mathcal{F}(\varsigma,A)$ is the right side of (G.8) with A in the place of $\hat\varsigma_a$, since both vanish at $A=0$, are continuous in A, and have the A-derivative $-3A^{1/2}\log|\varsigma-A|$ for $A\ne\varsigma$.*

(a) *$c'\rho_U(y)\,\mathrm{d}y = 3\varsigma'^{1/2}w_c(\varsigma')\,\mathrm{d}\varsigma'$ along $y = x_1^*+\ell_c\varsigma'$, and*

$$c'\mathcal{P}_{\chi_a}(x) = 2(a-\tfrac14)\log\frac{2\sqrt2}{\pi\ell_c} - 3\int_0^{\varsigma_a}\varsigma'^{1/2}w_c(\varsigma')\log|\varsigma-\varsigma'|\,\mathrm{d}\varsigma' - \mathcal{R}_a(x), \tag{F.18}$$

with $|\mathcal{R}_a| \le 2(a-\frac14)\cdot 4.3\,\ell_c\varsigma_{\max}$.

(b) *With the c-independent function $p_a(\varsigma) := 2(a-\frac14)\log\frac{2\sqrt2}{\pi} - 3\mathcal{F}(\varsigma,\hat\varsigma_a)$, which is continuous in ς,*

$$\big|c'\mathcal{P}_{\chi_a}(x) - 2(a-\tfrac14)\log\tfrac{1}{\ell_c} - p_a(\varsigma)\big| \le C_{a,\varsigma_{\max}}\,\ell_c\log\tfrac{1}{\ell_c}. \tag{F.19}$$

For $a=2$ the coefficient of $\log\frac{1}{\ell_c}$ is $2n_1$: $e^{c'\mathcal{P}(x)} = \ell_c^{-2n_1}e^{p_2(\varsigma)}(1+O_{\varsigma_{\max}}(\ell_c\log\frac{1}{\ell_c}))$.

(c) *On the window, $4\operatorname{sech}^2(\frac{\pi x}{2})e^{c'\mathcal{P}} = \operatorname{Lev} e^{-\mathcal{J}_{\rm end}}e^{c'L} \asymp \ell_c^{-2n_1} \asymp c'^{\frac43 n_1}$, and $\operatorname{Lev} e^{c'L} \asymp \ell_c^{-2n_1}$ on its part $x\ge\chi_3$, with constants that depend on $\varsigma_{\max}$ only. For every x with $2\varsigma_2\ell_c \le x-x_1^* \le 0.9$, in the window or not,*

$$e^{c'\mathcal{P}(x)} = \Big(\frac{2}{\pi(x-x_1^*)}\Big)^{2n_1}e^{\theta(x)}, \qquad 0\le\theta\le 2n_1\Big[\log\frac{x-x_1^*}{x-\chi_2} + \log\sqrt2 + \frac{\pi^2(x-\chi_2)^2}{12}\Big] \le C, \tag{F.20}$$

so that $\operatorname{Lev} e^{c'L} \asymp (x-x_1^*)^{-2n_1}$ for $\ell_c \ll x-x_1^* \ll 1$.

Proof. (a) By (F.11), $c'\rho_U\,\mathrm{d}y = 3\kappa_{\rm tip}c'\ell_c^{3/2}\varsigma'^{1/2}w_c\,\mathrm{d}\varsigma' = 3\varsigma'^{1/2}w_c\,\mathrm{d}\varsigma'$, and this measure has mass $2(a-\frac14)$ on $[0,\varsigma_a]$. Inserting (F.14) into $c'\mathcal{P}_{\chi_a} = -\int c'\rho_U f_x\,\mathrm{d}y$ gives (F.18) with $\mathcal{R}_a = \int_0^{\varsigma_a} 3\varsigma'^{1/2}w_cR\,\mathrm{d}\varsigma'$. (b) Replacing w_c by 1 changes the integral in (F.18) by at most $0.33\,\ell_c\cdot 3\int_0^{\varsigma_{\max}}\varsigma'^{3/2}|\log|\varsigma-\varsigma'||\,\mathrm{d}\varsigma' \le C_{\varsigma_{\max}}\ell_c$. Replacing the upper limit ς_a by $\hat\varsigma_a$ changes it by at most $3\hat\varsigma_a^{1/2}\int_I|\log|\varsigma-\varsigma'||\,\mathrm{d}\varsigma'$ over an interval I of length $|I|\le 0.14\,\ell_c\hat\varsigma_a^2$ by (F.12), and $\int_I|\log|\varsigma-\varsigma'||\mathrm{d}\varsigma' \le |I|\,(1+\log\frac{2}{|I|}+2\log(1+2\varsigma_{\max}))$, because $|\log r| = -\log r + 2\log^+ r$ with $\log^+ r := \max(\log r,0)$, and $|\varsigma-\varsigma'|\le 1+2\varsigma_{\max}$. The function p_a is continuous because the logarithmic singularity is integrable. (c) On the window $4\operatorname{sech}^2\frac{\pi x}{2}$ lies between two positive constants, and e^{p_2} is bounded above and below on the compact range of ς; this gives the first statement, and the second follows from $0\le\mathcal{J}_{\rm end}\le C_J$ on $x\ge\chi_3$ (Lemma F.8). For (F.20) the lower bound is (F.17). For the upper bound we use (F.16) and, with $z=\frac{\pi}{2}(x-\chi_2)$, the bound $|\log\tanh z| \le \log\frac1z + \frac{z^2}{3}$ of Lemma F.3 and $\tanh\frac{\pi(x+\chi_2)}{2} \ge \tanh u_1 = 2^{-1/2}$; the first logarithm in θ is at most $\log 2$ because $x-x_1^* \ge 2(\chi_2-x_1^*)$. □

F.2 One-sided Euler–Maclaurin

Where the summands are concave along the sites, that is, except far to the left of x, the sums in (F.3) are bounded on both sides by the integrals I_x with no remainder (Lemma F.5). Far to the left of x the summands are smooth and small, and the ordinary midpoint remainder applies; its total is the loss C_L (Lemma F.6). Rows 5, 9 and 10 of table 4 are used.

Lemma F.5 (One-sided Euler–Maclaurin; proved)**.** *Let $x \ge 0$, $\varphi(a) = f_x(\chi_a)$, and let $K, K_0 \le K_1$ be integers ≥ 2.*

(a) Trapezoid, beyond x. *If $x < \chi_K$, then $2\sum_{k\ge K}\varphi(k) \le \varphi(K) + 2I_x(K)$.*

(b) Midpoint, beyond x. *If $x < \chi_{K-1/2}$, then $2\sum_{k\ge K}\varphi(k) \ge 2I_x(K-\frac12)$. In particular, on the lobe $0 \le x < \chi_2$ both hold with $K = 3$.*

(c) A concave block below x. *If φ is concave on $[K_0-\frac12, K_1+\frac12]$, which by Lemma F.1(c) is the case when $y_{\mathrm{thr}}(x) \le \chi_{K_0-1/2}$ and $\chi_{K_1+1/2} < x$, then*

$$2\int_{K_0-1/2}^{K_1+1/2}\varphi\,\mathrm{d}a \;\le\; 2\sum_{k=K_0}^{K_1}\varphi(k) \;\le\; 2\int_{K_0}^{K_1}\varphi\,\mathrm{d}a + \varphi(K_0) + \varphi(K_1); \tag{F.21}$$

the second inequality needs concavity on $[K_0, K_1]$ only.

(d) Monotone summands. *If g is monotone on $[K_0-\frac12, K_1+\frac12]$, then $\bigl|\sum_{k=K_0}^{K_1} g(k) - \int_{K_0-1/2}^{K_1+1/2} g\bigr| \le \frac12|g(K_1+\frac12) - g(K_0-\frac12)|$ and $\bigl|\frac12 g(K_0) + \sum_{K_0<k<K_1} g(k) + \frac12 g(K_1) - \int_{K_0}^{K_1} g\bigr| \le \frac12|g(K_1) - g(K_0)|$.*

Proof. For a concave φ the chord lies below the graph and the tangent above it, so $\frac12[\varphi(k) + \varphi(k+1)] \le \int_k^{k+1}\varphi$ and $\varphi(k) \ge \int_{k-1/2}^{k+1/2}\varphi$. By Lemma F.1(c), φ is concave on $\{\chi_a > x\}$. Summing the first inequality over $k \ge K$ gives $\frac12\varphi(K) + \sum_{k>K}\varphi(k) \le I_x(K)$, which is (a); summing the second gives (b); the same two sums over a finite block give (c). For (d) let g increase. Then $g(k) - \int_{k-1/2}^{k+1/2} g$ lies between $-\frac12[g(k+\frac12) - g(k)]$ and $\frac12[g(k) - g(k-\frac12)]$, and $\frac12[g(k) + g(k+1)] - \int_k^{k+1} g$ lies between $\mp\frac12[g(k+1) - g(k)]$. These are increments of g over disjoint intervals, so their sums over k are at most the total increment of g. □

The far left. Below $y_{\mathrm{thr}}(x)$ the summands need not be concave. Let

$$k_0(x) := \min\{k \ge 3 :\ \chi_{k-1/2} \ge y_{\mathrm{thr}}(x)\} \tag{F.22}$$

be the first site from which Lemma F.5(c) applies, and let

$$e_L(x) := \frac{1}{24}\sum_{k=3}^{k_0(x)-1}\ \sup_{k-\frac12\le a\le k+\frac12}|\varphi''(a)| \tag{F.23}$$

be the total midpoint remainder of the sites $3 \le k < k_0$; it vanishes when $k_0 = 3$.

Lemma F.6 (The far-left error; proved, computer-assisted)**.** *Let x lie in cell $n \ge 6$.*

(a) $\bigl|\sum_{k=3}^{k_0-1}\varphi(k) - \int_{5/2}^{k_0-1/2}\varphi\,\mathrm{d}a\bigr| \le e_L(x)$.

(b) $k_0(x) \le \bigl\lceil \frac34 + \frac{n+3/4}{2.3}\bigr\rceil$. *Hence $k_0 \le n-2$, and $k_0 \le n-j$ whenever $n \ge 2j+4$, $j \ge 1$.*

(c) $x - \chi_a \ge 0.37\,(x - x_1^*)$ *for all $a \le k_0 - \frac12$ when $k_0 \ge 4$, and*

$$e_L(x) \le C\Bigl[\Bigl(\frac{\ell_c}{x-x_1^*}\Bigr)^{3/2} + \frac{\ell_c}{x-x_1^*}\Bigr]\ \ (x - x_1^* \le 1), \qquad e_L(x) \le C\ell_c\ \ (x - x_1^* \ge 1). \tag{F.24}$$

In particular $e_L = O_r(c'^{-2/3})$ uniformly on $x \ge x_1^* + r$.

(d) (Table 4, row 5.) *For $0 < \hat\varsigma_a < \varsigma$ let $\hat\varphi_\varsigma(a) := \log(\varsigma - \hat\varsigma_a)$ be the summand with the site at its nominal position, so that $\hat\varphi_\varsigma''(a) = \frac{2}{9}\,(\varsigma - 3\hat\varsigma_a)\,\hat\varsigma_a^{-2}(\varsigma - \hat\varsigma_a)^{-2}$, and for $\varsigma \ge 3$ let*

$$\hat k_0(\varsigma) := \min\{k \ge 3 :\ \hat\varsigma_{k-1/2} \ge 1.02\,\varsigma/2.3\}, \qquad \hat e_L(\varsigma) := \frac{1}{24}\sum_{k=3}^{\hat k_0(\varsigma)-1} \sup_{k-\frac12\le a\le k+\frac12} |\hat\varphi_\varsigma''(a)|. \tag{F.25}$$

This is e_L in the limit $c\to\infty$ at fixed $\varsigma = (x - x_1^*)/\ell_c$, except that the factor 1.02 enlarges the block of sites; it absorbs the displacement of the true sites from the nominal ones. Then $\hat e_L(\varsigma) \le 0.00186$ for $3 \le \varsigma \le \hat\varsigma_{602}$ $\langle$cert$\rangle$. Consequently, if $\ell_c\hat\varsigma_{602} \le 0.24$, then $e_L(x) \le 0.00186 + C\ell_c$ for every x in a cell $n \ge 6$. We take $c_0^{\rm att}$ so large that $\ell_c\hat\varsigma_{602} \le 0.24$ and $C\ell_c \le 0.004$ for $c \ge c_0^{\rm att}$. Then $C_L := \sup e_L(x) \le 0.006$, the supremum being over $c \ge c_0^{\rm att}$ and over x in the cells $n \ge 6$, and $e^{-2C_L} \ge 0.988$.

Proof. (a) For a C^2 function, $\varphi(k) - \int_{k-1/2}^{k+1/2}\varphi = -\frac{1}{24}\varphi''(\xi_k)$ with $|\xi_k - k| \le \frac12$.

(b) Let $x = \chi_b$ with $n < b < n+1$, and let $\chi_{a^*} = x_1^* + (x - x_1^*)/2.3$. The mean spacing from the tip decreases (Lemma F.1(b)), so $(\chi_{a^*} - x_1^*)/(a^* - \frac14) \ge (x - x_1^*)/(b - \frac14)$, that is $a^* - \frac14 \le (b - \frac14)/2.3$. Since $y_{\rm thr}(x) \le \chi_{a^*}$, we get $k_0 \le \max\{3, \lceil a^* + \frac12\rceil\} \le \lceil \frac34 + (n + \frac34)/2.3\rceil$. For $n = 6, 7$ this is $4, 5$; in general it is less than $2.08 + 0.435\,n$, which does not exceed $n - 2$ for $n \ge 8$ nor $n - j$ for $n \ge 2j + 4$.

(c) If $k_0 = 3$, then $e_L = 0$. Let $k_0 \ge 4$. By minimality $\chi_{k_0-3/2} < y_{\rm thr}(x) \le x_1^* + (x - x_1^*)/2.3$, and the mean spacing from the tip gives $\chi_{k_0-1/2} - x_1^* \le \frac{k_0-3/4}{k_0-7/4}(\chi_{k_0-3/2} - x_1^*) \le \frac{13}{9}\,(x - x_1^*)/2.3 \le 0.629\,(x - x_1^*)$. Hence $x - \chi_a \ge d := 0.37\,(x - x_1^*)$ for $a \le k_0 - \frac12$. For such a, Lemma F.1(a), the bound $\cosh z/\sinh^2 z \le z^{-2} + C$ and $x + y \ge 2x_1^*$ give $|\partial_y f_x| \le 1/d$ and $|\partial_y^2 f_x| \le d^{-2} + C$ at $y = \chi_a$, so that

$$|\varphi''(a)| \le (\chi_a')^2\Big[\frac{1}{d^2} + C + \frac{(\log\rho_U)'(\chi_a)}{d}\Big] =: G(a), \tag{F.26}$$

by the formula for φ'' in the proof of Lemma F.1. Both χ_a' and $(\log\rho_U)'(\chi_a)$ decrease in a, because ρ_U is increasing and concave; so G decreases, $G(k - \frac12) \le \int_{k-3/2}^{k-1/2} G\,\mathrm{d}a$ for $k \ge 4$, and

$$24\,e_L \ \le\ \sum_{k=3}^{k_0-1} G(k - \tfrac12) \ \le\ G(\tfrac52) + \int_{5/2}^{k_0-3/2} G\,\mathrm{d}a.$$

On the range of integration $r := \chi_a - x_1^* \le (x - x_1^*)/2.3$, by the minimality of k_0. By (F.2), $(\chi_a')^2\,\mathrm{d}a = \frac{2}{c'}\rho_U(y)^{-1}\mathrm{d}y$ with $y = \chi_a$, and $\int(\chi_a')^2(\log\rho_U)'(\chi_a)\,\mathrm{d}a = -\int\chi_a''\,\mathrm{d}a \le \chi_{5/2}'$.

Let first $x - x_1^* \le 1$, and let $\ell_c \le 0.08$; this holds for $c \ge c_0^{\rm att}$, because then $\ell_c \le 0.3/\hat\varsigma_{10}$. Put $\varsigma := (x - x_1^*)/\ell_c$, so that $d = 0.37\,\ell_c\varsigma$. By (F.12), $\varsigma_{5/2} \ge \hat\varsigma_{5/2}(1 - 0.14\cdot 0.08\,\hat\varsigma_{5/2}) \ge 1.68$. Since $\rho_U(x_1^* + r) \ge 3\kappa_{\rm tip}r^{1/2}$ by (F.11) and $\frac{2}{c'} = 2\kappa_{\rm tip}\ell_c^{3/2}$, we have $\chi_{5/2}' \le \frac23\ell_c\varsigma_{5/2}^{-1/2}$ and $\frac{2}{c'}\int_0^r \rho_U(x_1^* + r')^{-1}\mathrm{d}r' \le \frac43\ell_c^{3/2}r^{1/2}$, which we use with $r = \ell_c\varsigma/2.3 \le 0.44$; and $(\log\rho_U)'(\chi_{5/2}) \le 0.95/(1.3\,\ell_c\varsigma_{5/2})$ by row 9. Inserting these in $\int G\,\mathrm{d}a$ and in $G(\frac52)$, we get

$$24\,e_L(x) \le 6.43\,\varsigma^{-3/2} + 1.71\,\varsigma^{-1} + 1.94\,\varsigma^{-2} + C\ell_c^{3/2} \qquad (x - x_1^* \le 1,\ \ell_c \le 0.08). \tag{F.27}$$

Here $6.43 \ge \frac43\cdot 2.3^{-1/2}\cdot 0.37^{-2}$ belongs to the term d^{-2} of the integral; $1.71 \ge \frac23\,(0.37\sqrt{1.68})^{-1} + \frac49\cdot\frac{0.95}{1.3}\,(0.37\cdot 1.68^2)^{-1}$ to the terms with $(\log\rho_U)'$ in the integral and in $G(\frac52)$; $1.94 \ge \frac49\,(1.68\cdot 0.37^2)^{-1}$ to the term d^{-2} of $G(\frac52)$; and the two terms with the constant C of (F.26) add up to at most $C\ell_c^{3/2}$. Since $\varsigma \ge \varsigma_6 \ge 1$ and $\ell_c \le \ell_c/(x - x_1^*)$, the first bound of (F.24) follows.

Let now $x - x_1^* \ge 1$, so that $d \ge 0.37$. The cells $[k - \frac12, k + \frac12]$ on which $r \le 0.63$ are treated as before, with $r \le 0.63$ in the place of $r \le (x - x_1^*)/2.3$, and contribute at most $C\ell_c$. On every other cell $r \ge 0.63 - \ell_c \ge 0.5$, because $\chi_{k+1/2} - \chi_{k-1/2} \le \chi_{5/2}' \le \ell_c$. There we use $(\log\rho_U)' \le 3.10$

and, since $x - y \geq 0.37$, the exponential bounds $|\partial_y f_x| + |\partial_y^2 f_x| \leq Ce^{-\pi(x-y)}$ from (F.8), so that $|\varphi''(a)| \leq \tilde{G}(a) := C(\chi_a')^2 e^{-\pi(x-\chi_a)}$. The function $\tilde{G}$ is not monotone; but over one cell χ_a varies by at most ℓ_c and, by (F.9), χ_a' by a factor of at most 2, so $\sup_{\text{cell}} \tilde{G} \leq C \int_{\text{cell}} \tilde{G}\,\mathrm{d}a$. The sum over these cells is therefore at most $C \int \tilde{G}\,\mathrm{d}a = \frac{C}{c'} \int e^{-\pi(x-y)} \rho_U(y)^{-1}\,\mathrm{d}y \leq C/c' \leq C\ell_c$, because $\rho_U \geq \rho_U(x_1^* + 0.5)$ there.

(d) *The certified function.* For fixed ς the function $h(t) := (\varsigma - 3t)\, t^{-2}(\varsigma - t)^{-2}$ decreases on $0 < t < \varsigma$, because $h'(t) = -(9t^2 - 7\varsigma t + 2\varsigma^2)\, t^{-3}(\varsigma - t)^{-3}$ and $9t^2 - 7\varsigma t + 2\varsigma^2 = 9(t - \frac{7}{18}\varsigma)^2 + \frac{23}{36}\varsigma^2 > 0$. Hence $\hat{\varphi}_\varsigma''(a)$ decreases in a, and the supremum in (F.25) is the larger of the two numbers $|\hat{\varphi}_\varsigma''(k \pm \frac{1}{2})|$. For $\varsigma \geq 3$ and $K = \hat{k}_0(\varsigma)$ we have $\hat{\varsigma}_{K-1/2} \leq 0.58\,\varsigma$: if $K = 3$ because $\hat{\varsigma}_{5/2} \leq 1.72$, and if $K \geq 4$ because $\hat{\varsigma}_{K-1/2} \leq (\frac{13}{9})^{2/3} \hat{\varsigma}_{K-3/2} < (\frac{13}{9})^{2/3}\, 1.02\,\varsigma/2.3$. Thus $\hat{e}_L$ is a finite sum of explicit functions of ς, which jumps upward where $\hat{k}_0$ does. Row 5 bounds it on subintervals that cover $[3, \hat{\varsigma}_{602}]$; since $\hat{k}_0$ is non-decreasing and the summands are non-negative, $\hat{k}_0$ is replaced on each subinterval by its value at the right end. With the factor 1 in the place of 1.02 the supremum is 0.0016439; it is approached as ς decreases to $2.3\,\hat{\varsigma}_{5/2} = 3.949\ldots$, between $\hat{\varsigma}_8$ and $\hat{\varsigma}_9$, where $\hat{k}_0$ jumps from 3 to 4.

Large ς. For the rest of the proof let $\ell_c \hat{\varsigma}_{602} \leq 0.24$, so that $\ell_c \leq 0.08$, and let $\varsigma = (x - x_1^*)/\ell_c$. The right side of (F.27) decreases in ς, and at $\varsigma = \hat{\varsigma}_{602} = 71.27\ldots$ its first three terms add up to less than $24 \cdot 0.00147$. Hence $e_L \leq 0.00147 + C\ell_c^{3/2}$ for $\varsigma \geq \hat{\varsigma}_{602}$, $x - x_1^* \leq 1$; and $e_L \leq C\ell_c$ for $x - x_1^* \geq 1$ by (F.24). Both are at most $0.00186 + C\ell_c$. The values of e_L on successive cells are not monotone, so that the range of large ς cannot be reduced to the certified one by monotonicity; it is the right side of (F.27) that decreases.

The range $3 \leq \varsigma \leq \hat{\varsigma}_{602}$. Let x lie in a cell $n \geq 6$. Then $\varsigma \geq \varsigma_6 \geq 3$ by (F.12), and it remains to treat $\varsigma \leq \hat{\varsigma}_{602}$, so that $x - x_1^* = \ell_c \varsigma \leq 0.24$. Let $K = \hat{k}_0(\varsigma)$. Since $\hat{\varsigma}_{K-1/2} \leq 0.58\,\varsigma$, (F.12) gives $\varsigma_{K-1/2} \geq \hat{\varsigma}_{K-1/2}(1 - 0.14 \cdot 0.58\,\ell_c\varsigma) \geq 1.02\,(1 - 0.0195)\,\varsigma/2.3 \geq \varsigma/2.3$, that is $\chi_{K-1/2} \geq x_1^* + (x - x_1^*)/2.3 \geq y_{\text{thr}}(x)$. Hence $k_0(x) \leq \hat{k}_0(\varsigma)$, and every site $a \leq k_0 - \frac{1}{2}$ has $\hat{\varsigma}_a \leq 0.58\,\varsigma$. For such a write $D := \varsigma - \varsigma_a$ and $\hat{D} := \varsigma - \hat{\varsigma}_a$, so that $D \geq \hat{D} \geq 0.42\,\varsigma \geq 1.2$. Since $\chi_a = x_1^* + \ell_c \varsigma_a$,

$$\varphi''(a) = \ell_c^2 (\varsigma_a')^2\, \partial_y^2 f_x(\chi_a) + \ell_c \varsigma_a''\, \partial_y f_x(\chi_a), \qquad \hat{\varphi}_\varsigma''(a) = -\frac{(\hat{\varsigma}_a')^2}{\hat{D}^2} - \frac{\hat{\varsigma}_a''}{\hat{D}}.$$

Each of the five quantities $-(\ell_c D)^2 \partial_y^2 f_x(\chi_a)$, $-\ell_c D\, \partial_y f_x(\chi_a)$, $\varsigma_a/\hat{\varsigma}_a$, $\varsigma_a'/\hat{\varsigma}_a'$ and $\varsigma_a''/\hat{\varsigma}_a''$ differs from 1 by at most $C\ell_c\varsigma$: the first two by (F.8), because $\pi\ell_c D \leq \pi\ell_c\varsigma$ and $x + \chi_a \geq 2x_1^*$; the third by (F.12), which also gives $0 \leq D - \hat{D} = \hat{\varsigma}_a - \varsigma_a \leq C\ell_c\varsigma\,\hat{D}$; the fourth by (F.2) and (F.11), which give $\varsigma_a' = \frac{2}{3}\varsigma_a^{-1/2}(1 + \theta)^{-1}$ with $0 \leq \theta \leq 0.33\,\ell_c\varsigma_a$; and the fifth by (F.2) and (F.13), which give $\varsigma_a'' = -(\varsigma_a')^2\, \ell_c (\log \rho_U)'(\chi_a) = -(\varsigma_a')^2(1 + \theta')/(2\varsigma_a)$ with $0 \leq \theta' \leq 1.12\,\ell_c\varsigma_a$. On the present range ς, $1/\hat{\varsigma}_a$ and $1/\hat{D}$ are bounded and $\ell_c\varsigma \leq \hat{\varsigma}_{602}\ell_c$, so that $|\varphi''(a) - \hat{\varphi}_\varsigma''(a)| \leq C\ell_c$; and the number of summands is bounded. As $k_0(x) \leq \hat{k}_0(\varsigma)$ and all summands are non-negative, $e_L(x) \leq \hat{e}_L(\varsigma) + C\ell_c \leq 0.00186 + C\ell_c$. No continuity in x or in c is used: the jumps of $k_0(x)$ are covered by $k_0(x) \leq \hat{k}_0(\varsigma)$. The factor 1.02 is needed for this: since $\varsigma_a \leq \hat{\varsigma}_a$, the true index $k_0(x)$ jumps slightly before the nominal one does, and there e_L exceeds its nominal value by a whole summand. □

F.3 Detuning costs $O(\eta_0^2)$

Lifting a double zero off the axis to the heights $\pm\varepsilon_k$ raises the modulus of its factor at a point of the axis at a distance $D \gg \varepsilon_k$ by the relative amount $O(\varepsilon_k^2/D^2)$ only, and ε_k is η_0 times the local spacing. Thus lower bounds for B^0 are lower bounds for B, and upper bounds for B^0 become upper bounds for B at the cost of the two pairs which flank x, which are kept exactly, and of a factor $e^{C_{\text{det}}\eta_0^2}$ with $C_{\text{det}} \leq 16.6$. No certified constant is used.

Lemma F.7 (Detuning; proved)**.** *Let $x \ge 0$, $k \ge 3$ and $A_\pm := \cosh \pi(\chi_k \mp x)$. Then*

$$T_{\chi_k}(x)^2 \;\le\; q_k(x) \;\le\; T_{\chi_k}(x)^2 \exp \frac{4\varepsilon_k^2}{(\chi_k - x)^2}, \qquad \frac{q_k}{T_{\chi_k}^2} = \prod_{\pm} \frac{(A_\pm - \gamma_k)(A_\pm + 1)}{(A_\pm + \gamma_k)(A_\pm - 1)}. \tag{F.28}$$

There is an absolute constant $C_{\det} \le 16.6$ such that, for x in cell $n \ge 2$ and for $0 \le x < \chi_2$ (where no pair is excluded),

$$0 \;\le \sum_{k \ge 3,\ k \ne n, n+1} \log \frac{q_k(x)}{T_{\chi_k}(x)^2} \;\le\; C_{\det}\, \eta_0^2, \tag{F.29}$$

and the pairs beyond the cell contribute at most $4\zeta(2)\eta_0^2$ of this. In particular $\Pi := |B|/|B^0| = \prod_{k \ge 3} q_k / T_{\chi_k}^2 \ge 1$. For the flanking pairs,

$$\frac{q_n(x)}{T_{\chi_n}(x)^2} \le \Big(1 + \frac{\eta_0^2}{u^2}\Big)(1 + C\ell_n^2), \qquad \frac{q_{n+1}(x)}{T_{\chi_{n+1}}(x)^2} \le \Big(1 + \frac{\eta_0^2}{(1-u)^2}\Big)(1 + C\ell_n^2). \tag{F.30}$$

Proof. The product formula in (F.28) is (F.4) divided by its value at $\gamma_k = 1$. For $A > 1$ and $0 \le \gamma \le 1$,

$$\log \frac{A - \gamma}{A + \gamma} - \log \frac{A - 1}{A + 1} = \int_\gamma^1 \frac{2A\, \mathrm{d}\gamma'}{A^2 - \gamma'^2} \in \Big[0, \frac{2A(1-\gamma)}{A^2 - 1}\Big] \subset \Big[0, \frac{(\pi\varepsilon)^2}{A - 1}\Big] \quad \text{for } \gamma = \cos \pi\varepsilon,$$

since $1 - \cos \pi\varepsilon \le \frac{1}{2}(\pi\varepsilon)^2$ and $A/(A+1) \le 1$. With $A_\pm - 1 = 2 \sinh^2 \frac{\pi(\chi_k \mp x)}{2} \ge \frac{1}{2}\pi^2(\chi_k \mp x)^2$ the two factors contribute at most $2\varepsilon_k^2/(\chi_k - x)^2 + 2\varepsilon_k^2/(\chi_k + x)^2$, which gives (F.28).

For a pair beyond the cell, $k \ge n+2$, the spacings decrease, so $\chi_k - x \ge \chi_k - \chi_{n+1} \ge (k - n - 1)\ell_k$, and $\varepsilon_k = \eta_0 \ell_k$; the pair contributes at most $4\eta_0^2/(k-n-1)^2$, and these sum to $4\zeta(2)\eta_0^2$. On the lobe the same holds with $\chi_k - x \ge \chi_k - \chi_2 \ge (k-2)\ell_k$. For a pair below the cell, $3 \le k \le n-1$, we have $x - \chi_k \ge (n-k)\ell_{n-1}$, and by Lemma F.1(b) $\ell_k/\ell_{n-1} \le \chi_k'/\chi_n' \le \big((n - \frac{1}{4})/(k - \frac{1}{4})\big)^{1/2}$. The pair contributes at most $4\eta_0^2\,(n - \frac{1}{4})/[(k - \frac{1}{4})(n-k)^2] = 4\eta_0^2\big[(n-k)^{-2} + (k - \frac{1}{4})^{-1}(n-k)^{-1}\big]$. The first terms sum to at most $\zeta(2)$. By the Cauchy–Schwarz inequality the second terms sum to at most $\big(\zeta(2) \sum_{k \ge 3} (k - \frac{1}{4})^{-2}\big)^{1/2} \le \big(\frac{4}{9}\zeta(2)\big)^{1/2} \le 0.86$, since $\sum_{k \ge 3}(k - \frac{1}{4})^{-2} \le \int_{5/2}^\infty (t - \frac{1}{4})^{-2}\, \mathrm{d}t = \frac{4}{9}$ by convexity. Hence (F.29) holds with $C_{\det} := 4\,[2\zeta(2) + 0.86]$, and $4\zeta(2) \le C_{\det} \le 16.6$.

For (F.30), the factor with $A_- = \cosh \pi(\chi_n - x)$ is $(1 + \frac{1-\gamma_n}{A_- - 1})\frac{A_- + 1}{A_- + \gamma_n}$; here $\frac{1-\gamma_n}{A_- - 1} \le \varepsilon_n^2/(x - \chi_n)^2 = \eta_0^2/u^2$, and the second quotient, as well as the factor with A_+, is $1 + O(\varepsilon_n^2)$. For $k = n+1$ we use in addition $\ell_{n+1} \le \ell_n$. □

F.4 Corollaries

We collect the bounds of Lemma 7.5(c), (e), (f) and the overshoot bound of Lemma 7.11. Each is one application of Lemma F.5 on each side of x, with the sites next to x kept exactly. The bounds on the cells $n \ge 6$ use Lemma F.9, which is proved in appendix F.5 from appendices F.1 to F.3 alone. Rows 5, 7, 8, 9 and 10 of table 4 are used.

The lobe: Lemma 7.5(f) [PROVED]**.** Let $0 \le x < \chi_2$. All sites lie beyond x, so Lemma F.5(a), (b) with $K = 3$, the inequality $q_k \ge T_{\chi_k}^2$, Lemma F.7 and (F.6) give

$$\begin{aligned} f_x(\chi_2) + c'U + c'\mathcal{P}_{\chi_{5/2}} \;&\le\; \log|B^0| \;\le\; \log|B| \\ &\le\; f_x(\chi_2) + f_x(\chi_3) + c'U + c'\mathcal{P}_{\chi_3} + 4\zeta(2)\eta_0^2, \end{aligned} \tag{F.31}$$

all functions being evaluated at x; on $x_1^* \le x < \chi_2$, $U = -L$.

Upper bound on every cell. Let x lie in cell $n \geq 2$. The pairs $k \geq n+2$ lie beyond x; we write $\log q_k = 2f_x(\chi_k) + \log(q_k/T_{\chi_k}^2)$ for them. By Lemma F.5(a) with $K = n+2$, (F.6) and Lemma F.7,

$$\begin{aligned} \log|B(x)| + c'L(x) \;&\leq\; f_x(\chi_2) + \sum_{k=3}^{n+1} \log q_k(x) + f_x(\chi_{n+2}) + c'\mathcal{P}_{\chi_{n+2}}(x) + D_n(x), \\ D_n(x) &:= \sum_{k\geq n+2} \log \frac{q_k(x)}{T_{\chi_k}(x)^2} \;\in\; [0,\, 4\zeta(2)\eta_0^2]. \end{aligned} \tag{F.32}$$

The exact factors on the right carry the total weight $1 + 2(n-1) + 1 = 2n$, and the continuum term carries $2(n+2-\frac{1}{4}) = 2n + 2n_1$.

Upper bound on the cells $n \geq 6$ and on the far band: Lemma 7.5(e) [PROVED, COMPUTER-ASSISTED]**.** Let x lie in cell $n \geq 6$. By Lemma F.9 with $j = 1$, Lemma F.6(d) and Lemma F.7,

$$\log|B| + c'L \;\leq\; c'\mathcal{P} + \mathcal{J}_{\mathrm{end}} + \mathcal{H}_n^+ + \log \frac{q_n q_{n+1}}{T_{\chi_n}^2 T_{\chi_{n+1}}^2} + C_{\det}\eta_0^2 + 2C_L. \tag{F.33}$$

By (F.46), $\mathcal{H}_n^+ \leq h_\infty^+(u) + \frac{94}{n} + C\ell_n$, where $h_\infty^+(u) = \log(1+u) + 2\log u + 2\log(1-u) + \log(2-u) - 2\int_{-1}^2 \log|u-v|\,\mathrm{d}v$. Each of the three pieces $\log[(1+u)(2-u)]$, $2\log[u(1-u)]$ and $-2\int_{-1}^2 \log|u-v|\mathrm{d}v$ is largest at $u = \frac{1}{2}$; the last because its derivative is $2\log\frac{2-u}{1+u}$. Hence (table 4, row 7)

$$\sup_{0<u<1} h_\infty^+(u) = h_\infty^+(\tfrac{1}{2}) = 6 - 4\log 3 \leq 1.606 \;\langle\mathrm{cert}\rangle, \qquad \text{so} \quad \sup_{\mathrm{cell}} e^{\mathcal{H}_n^+} \leq 5.0\, e^{94/n + C\ell_n}. \tag{F.34}$$

With the flanking pairs, (F.30) replaces the middle piece by $\log P(u(1-u)) + O(\ell_n^2)$, where $P(p) := p^2 + \eta_0^2(1-2p) + \eta_0^4$ is $(u^2+\eta_0^2)((1-u)^2+\eta_0^2)$ written in $p = u(1-u) \in [0, \frac{1}{4}]$. A convex quadratic is largest at an end of the interval, and $P(\frac{1}{4}) = (\frac{1}{4}+\eta_0^2)^2 \geq P(0) = \eta_0^2(1+\eta_0^2)$ precisely when $\eta_0^2 \leq \frac{1}{8}$. So for $\eta_0 = \frac{1}{4}$ the supremum is again at $u = \frac{1}{2}$ and exceeds (F.34) by $2\log(1+4\eta_0^2)$:

$$|B(x)|e^{c'L(x)} \leq 5.0\,(1+4\eta_0^2)^2 e^{C_{\det}\eta_0^2} \cdot e^{2C_L + 94/n + C\ell_n}\, e^{c'\mathcal{P}(x) + \mathcal{J}_{\mathrm{end}}(x)}. \tag{F.35}$$

On the far band $x \geq x_1^* + r$ we have $c'\mathcal{P} \leq C_r$ by Lemma 7.5(b), $\mathcal{J}_{\mathrm{end}} \leq C_J$ by Lemma F.8, $n \geq c'N(x_1^* + r) - 1$ and $\ell_n \leq C_r/c'$; so $|B|e^{c'L} \leq C_r$ there.

The sup bound: Lemma 7.5(c) [PROVED, COMPUTER-ASSISTED]**.** On $x \geq x_1^* + r$ the bound C_r has just been proved. On the cells $n \geq 6$, (F.35) gives $\log|B| + c'L \leq c'\mathcal{P} + C$, and $c'\mathcal{P} \leq 2n_1|f_x(\chi_2)|$ by (F.16). Here $x - \chi_2 \geq \chi_6 - \chi_2 \geq \ell_c$ for $c \geq c_0^{\mathrm{att}}$ by (F.12). If $x - \chi_2 \leq 0.9$, the estimate used for (F.20) gives $|f_x(\chi_2)| \leq \log\frac{2}{\pi(x-\chi_2)} + C \leq \log\frac{1}{\ell_c} + C$; otherwise $|f_x(\chi_2)| \leq C$. Hence $c'\mathcal{P} \leq 2n_1 \cdot \frac{2}{3}\log c' + C = \frac{4}{3}n_1 \log c' + C$. On the cells $2 \leq n \leq 5$ we use (F.32) in the window with $\varsigma_{\max} = \hat{\varsigma}_8$. By (F.14) and (F.15) (row 10) each site factor is at most $C\ell_c$ and each pair modulus at most $C\ell_c^2$, because the scaled distances are bounded; and $c'\mathcal{P}_{\chi_{n+2}} \leq (2n + 2n_1)\log\frac{1}{\ell_c} + C$ by (F.19). The powers of ℓ_c combine to $\ell_c^{-2n_1}$, so $\log|B| + c'L \leq \frac{4}{3}n_1 \log c' + C$ on these cells as well. Together,

$$\sup_{x\geq\chi_2} [\log|B(x)| + c'L(x)] \leq \tfrac{4}{3}n_1 \log c' + C, \qquad \sup_{x\geq x_1^*+r} [\log|B(x)| + c'L(x)] \leq C_r. \tag{F.36}$$

The overshoot bound: Lemma 7.11 [PROVED, COMPUTER-ASSISTED]**.** Let x lie in cell $n \geq 6$. The lower bound of Lemma F.9 with $j = 1$, together with $\mathcal{J}_{\text{end}} \geq 0$ (Lemma F.8) and $e_L \leq C_L$, gives $\log|B| + c'L \geq c'\mathcal{P} + \mathcal{H}_n^- - 2C_L$. By Lemma F.10, $\mathcal{H}_n^- \geq h_\infty^-(u;\eta_0) - C(\frac{1}{n} + \ell_n)$, with $h_\infty^-(u;\eta_0) = \log(u^2+\eta_0^2) + \log((1-u)^2+\eta_0^2) - 2\int_{-1/2}^{3/2} \log|u-v|\,\mathrm{d}v$. Row 8 of table 4 is

$$\min_{0\leq u\leq 1} h_\infty^-(u;\eta_0) \;\geq\; 2\log\eta_0 + \log(1+\eta_0^2) + 3.476 \;\langle\text{cert}\rangle \qquad (0 < \eta_0 \leq 0.3), \tag{F.37}$$

the minimum being attained at the ends $u \in \{0,1\}$. The certificate rests on three facts which are proved by hand. Let $s := \eta_0^2 \leq 0.09$, $h := h_\infty^-(\,\cdot\,;\eta_0)$ and $I(u) := -2\int_{-1/2}^{3/2} \log|u-v|\,\mathrm{d}v = 4 - 2(u+\frac{1}{2})\log(u+\frac{1}{2}) - 2(\frac{3}{2}-u)\log(\frac{3}{2}-u)$. (i) $I(0) = I(1) = 4 - 3\log 3 + 4\log 2 = 3.4767\ldots$, so that $h(0) = h(1) = 2\log\eta_0 + \log(1+\eta_0^2) + I(0)$. (ii) $h(u) - h(0) = \log(1+u^2/s) + \log(1 - \frac{u(2-u)}{1+s}) + I(u) - I(0)$. The first term decreases in s; the second increases in s, because $0 \leq u(2-u) \leq 1$, and it is $2\log(1-u)$ at $s = 0$. Hence $h(u) - h(0) \geq G_L(u) := \log(1+u^2/0.09) + 2\log(1-u) + I(u) - I(0)$, and $G_L(0) = 0$. (iii) Since $h(u) = h(1-u)$, also $h(u) - h(1) \geq G_R(u) := G_L(1-u)$. Row 8 certifies that $G_L' > 0$ on $[0, \frac{1}{4}]$ and $G_L > 0$ on $[\frac{1}{4}, \frac{1}{2}]$, and the mirror statements for G_R. Hence $G_L > 0$ on $(0, \frac{1}{2}]$ and $G_R > 0$ on $[\frac{1}{2}, 1)$, so that $h > h(0) = h(1)$ on $(0,1)$; and $I(0) > 3.476$ is certified as well. Since $e^{3.476} \geq 32$, (F.17) gives

$$|B(x)|\, e^{c'L(x)} \;\geq\; 32\,\eta_0^2\, e^{-C(\frac{1}{n}+\ell_n)-2C_L} \Big(\frac{2}{\pi(x-x_1^*)}\Big)^{2n_1} \;\geq\; c_T\,\eta_0^2 \Big(\frac{2}{\pi(x-x_1^*)}\Big)^{2n_1} \tag{F.38}$$

on the cells $n \geq 6$, with an absolute constant $c_T > 0$: the exponent is bounded, because $\frac{1}{n} \leq \frac{1}{6}$ and $\ell_n \leq \chi_2' \leq \ell_c$ by Lemma F.1(b) and (F.11). Only the positivity of c_T is used. □

F.5 Two-sided bounds on the envelope, and the level

This subsection proves Lemma 7.5(a) and Proposition 7.4. We apply Lemma F.5 on either side of x, but keep exactly the $2j+2$ sites nearest to x in the upper bound, and the $2j$ detuned pairs nearest to x in the lower bound. The difference between these exact sites and the continuum integral over their index range is the *hole function*. Sites and continuum carry the same total charge, so all scales cancel, and as $n \to \infty$ the hole function tends to an explicit function of the position u in the cell alone. The rows used are 5, 6 and 9, and row 10 in the window clause of Lemma F.8.

For $j \geq 1$ and x in cell $n \geq 2j+4$ the hole functions are

$$\mathcal{H}_{n,j}^+(x) := f_x(\chi_{n-j}) + 2\sum_{k=n-j+1}^{n+j} f_x(\chi_k) + f_x(\chi_{n+j+1}) - 2\int_{n-j}^{n+j+1} \varphi(a)\,\mathrm{d}a, \tag{F.39}$$

$$\mathcal{H}_{n,j}^-(x) := \sum_{k=n-j+1}^{n+j} \log q_k(x) - 2\int_{n-j+1/2}^{n+j+1/2} \varphi(a)\,\mathrm{d}a, \tag{F.40}$$

and $\mathcal{H}_n^\pm := \mathcal{H}_{n,1}^\pm$. The first does not depend on η_0. Its sites carry the weights $1, 2, \ldots, 2, 1$, of sum $4j+2$, and its integral has the same weight $2(2j+1)$; the second has the weight $4j$ on either side. Their limits are

$$h_j^+(u) := \log(u+j) + 2\sum_{i=-j+1}^{j} \log|u-i| + \log(j+1-u) - 2\int_{-j}^{j+1} \log|u-v|\,\mathrm{d}v, \tag{F.41}$$

$$h_j^-(u;\eta_0) := \sum_{i=-j+1}^{j} \log((u-i)^2+\eta_0^2) - 2\int_{-j+1/2}^{j+1/2} \log|u-v|\,\mathrm{d}v, \tag{F.42}$$

and $h_\infty^\pm := h_1^\pm$. The integrals are elementary: $\int_\alpha^\beta \log|u-v|\mathrm{d}v = F(u-\alpha) - F(u-\beta)$ with $F(t) = t\log|t| - t$.

Lemma F.8 (The end correction; proved, computer-assisted)**.** *For $x \ge \chi_{5/2}$, $0 \le \mathcal{J}_{\mathrm{end}}(x) \le \frac{1}{4}\sup_{2\le a\le 5/2}|\varphi'(a)|$. Consequently $0 \le \mathcal{J}_{\mathrm{end}} \le C_J$ on $x \ge \chi_3$ with an absolute constant $C_J \le 0.65$; this uses no certified constant. Moreover $\mathcal{J}_{\mathrm{end}}(x) \le C/(\varsigma - \varsigma_{5/2})$ for $x = x_1^* + \ell_c\varsigma$ in the window (row 10, through (F.11)).*

Proof. For $x \ge \chi_{5/2}$ the function φ decreases on $[2, \frac{5}{2}]$, so $\mathcal{J}_{\mathrm{end}} = 2\int_2^{5/2}[\varphi(2) - \varphi(a)]\,da$ lies between 0 and $2\int_0^{1/2} t\,dt\,\sup|\varphi'|$. By Lemma F.1(a), $|\varphi'(a)| \le \chi_a'/(x - \chi_a)$. For $x \ge \chi_3$ and $a \le \frac{5}{2}$, $x - \chi_a \ge \chi_3 - \chi_{5/2} \ge \frac{1}{2}\chi_3'$ and $\chi_a' \le \chi_2' \le (\frac{11}{7})^{1/2}\chi_3'$ by (F.9), so $|\varphi'| \le 2\,(\frac{11}{7})^{1/2} \le 2.6$ and $C_J := \frac{1}{4}\cdot 2.6 = 0.65$. In the window $\chi_2' \le \ell_c$ by (F.11) and $x - \chi_a \ge \ell_c(\varsigma - \varsigma_{5/2})$. □

Lemma F.9 (Two-sided bounds; proved, computer-assisted)**.** *Let $j \ge 1$ and let x lie in cell $n \ge 2j + 4$. Then*

$$\log|B(x)| + c'L(x) \;\ge\; c'\mathcal{P}(x) + \mathcal{J}_{\mathrm{end}}(x) + \mathcal{H}^-_{n,j}(x) - 2e_L(x), \tag{F.43}$$

$$\log|B^0(x)| + c'L(x) \;\le\; c'\mathcal{P}(x) + \mathcal{J}_{\mathrm{end}}(x) + \mathcal{H}^+_{n,j}(x) + 2e_L(x). \tag{F.44}$$

For $j = 1$ and $n \ge 6$, together with $e_L \le C_L$ and (F.29), this is Lemma 7.5(a): the lower bound is for B, the upper bound for B^0, and $\log|B| \le \log|B^0| + \log\frac{q_nq_{n+1}}{T^2_{\chi_n}T^2_{\chi_{n+1}}} + C_{\mathrm{det}}\eta_0^2$.

Proof. We split the sites $k \ge 3$ into four blocks: the far left $3 \le k < k_0$, where the midpoint rule holds up to e_L; the concave block from k_0 to the hole; the hole, kept exactly; and the sites beyond the hole, which lie beyond x. We then account for the pieces of $2I_x(2) = -c'L + c'\mathcal{P}$ that no block has used. By Lemma F.6(b), $k_0 \le n - j$.

Upper bound. By Lemma F.6(a), $2\sum_{k=3}^{k_0-1}\varphi(k) \le 2\int_{5/2}^{k_0-1/2}\varphi + 2e_L$. The function φ is concave on $[k_0, n-j]$, where $y_{\mathrm{thr}} \le \chi_a < x$, so the trapezoid inequality of (F.21) gives $2\sum_{k=k_0}^{n-j-1}\varphi(k) + \varphi(n-j) \le 2\int_{k_0}^{n-j}\varphi + \varphi(k_0)$. Beyond the hole, Lemma F.5(a) with $K = n + j + 1$ gives $\varphi(n+j+1) + 2\sum_{k\ge n+j+2}\varphi(k) \le 2I_x(n+j+1)$. The remaining site terms are $\varphi(n-j) + 2\sum_{k=n-j+1}^{n+j}\varphi(k) + \varphi(n+j+1)$, the sites of $\mathcal{H}^+_{n,j}$. The three integrals cover $[\frac{5}{2}, \infty)$ except $[k_0 - \frac{1}{2}, k_0]$ and $[n-j, n+j+1]$. With (F.3) and (F.6),

$$\log|B^0| \le -c'L + c'\mathcal{P} + \underbrace{\varphi(2) - 2\int_2^{5/2}\varphi}_{\mathcal{J}_{\mathrm{end}}} + \underbrace{\varphi(k_0) - 2\int_{k_0-1/2}^{k_0}\varphi}_{\le 0} + \mathcal{H}^+_{n,j} + 2e_L,$$

and the second brace is non-positive because φ decreases on $[k_0 - \frac{1}{2}, k_0]$. This is (F.44).

Lower bound. By (F.28), $\log q_k \ge 2\varphi(k)$ for the pairs outside the hole. For these, $2\sum_{k=3}^{k_0-1}\varphi(k) \ge 2\int_{5/2}^{k_0-1/2}\varphi - 2e_L$; the midpoint inequality of (F.21) on the concave block gives $2\sum_{k=k_0}^{n-j}\varphi(k) \ge 2\int_{k_0-1/2}^{n-j+1/2}\varphi$, where $\chi_{n-j+1/2} < x$; and Lemma F.5(b) with $K = n + j + 1$ gives $2\sum_{k\ge n+j+1}\varphi(k) \ge 2I_x(n+j+\frac{1}{2})$, where $x < \chi_{n+j+1/2}$. The integrals cover $[\frac{5}{2}, \infty)$ except $[n-j+\frac{1}{2}, n+j+\frac{1}{2}]$, and the pairs $n - j < k \le n + j$ are kept. Hence $\log|B| \ge -c'L + c'\mathcal{P} + \mathcal{J}_{\mathrm{end}} + \mathcal{H}^-_{n,j} - 2e_L$. □

Lemma F.10 (Limits of the hole functions; proved)**.** *Let $j \ge 1$, x in cell $n \ge 2j + 4$ and $u = (x - \chi_n)/\ell_n$. Then*

$$\max\Big\{\big|\mathcal{H}^+_{n,j}(x) - h^+_j(u)\big|,\ \big|\mathcal{H}^-_{n,j}(x) - h^-_j(u;\eta_0)\big|\Big\} \le C_j\Big(\frac{1}{n} + \ell_n\Big), \qquad C_j := C\,j^2\log(2j+2), \tag{F.45}$$

with an absolute constant C. More explicitly, the left side of (F.45) is at most

$$\frac{8j(j+1) + 28j(j+1)\log(2j+2)}{n} + C\,j\,\ell_n, \qquad \text{which for } j = 1 \text{ is at most } \quad \frac{94}{n} + C\ell_n. \tag{F.46}$$

The same bounds with $\frac{3}{n}$ added, so $\frac{97}{n}+C\ell_n$ for $j=1$, hold for $\mathcal{H}^-_{n,j}|_{\eta_0=0}-\log(4\sin^2\pi\nu(x))$ against $h^-_j(u;0)-\log(4\sin^2\pi u)$, and for $\mathcal{H}^+_{n,j}$ likewise; here $\nu(x)=c'N(x)+\frac14-2$ is the site index of section 7.5, so that $\nu(\chi_a)=a-2$.

Proof. There are three steps: the scales cancel up to $O(j\ell_n)$; the displacement of the sites and of the continuum from an equally spaced lattice costs $O(j^2\log(2j+2)/n)$; and $\sin^2\pi\nu$ is compared with $\sin^2\pi u$.

Scales. For a in the hole write $f_x(\chi_a)=\log\frac{|x-\chi_a|}{\ell_n}+\big[\log\frac{\pi\ell_n}{2}+\log\tanh\pi x\big]+g_1(a)+g_2(a)$ with $g_1=\log(|\tanh z|/|z|)$, $z=\frac{\pi}{2}(x-\chi_a)$, and $g_2=\log\tanh\frac{\pi(x+\chi_a)}{2}-\log\tanh\pi x$. The bracket does not depend on a; it cancels between the sites and the integral, which carry equal weights. The function g_2 is monotone with total variation at most $\frac{\pi}{2}(\chi_{n+j+1}-\chi_{n-j})\le Cj\ell_n$ over the hole, because $(\log\tanh z)'=2/\sinh 2z\le 1/\sqrt2$ for $z\ge u_1$ and $\ell_{n-j}\le 2\ell_n$ by (F.9). The function g_1 is monotone on either side of x, with variation at most $Cj\ell_n$ there, and $|g_1|\le C\ell_n^2$ on the cells adjoining x, because $|(\log(\tanh z/z))'|\le C\min\{|z|,1\}$. By Lemma F.5(d), applied on either side of these cells, the contribution of g_1 and g_2 to $\mathcal{H}^\pm_{n,j}$ is at most $Cj\ell_n$. For a pair of the hole, the second form of q_k given after (F.4), with $v=\frac{\pi}{2}\varepsilon_k\le\pi\eta_0\ell_n$, gives $\log q_k=\log\frac{(x-\chi_k)^2+\varepsilon_k^2}{\ell_n^2}+2[\,\cdot\,]+2g_1(k)+2g_2(k)+O(\ell_n^2)$. Thus, up to $O(j\ell_n)$, $\mathcal{H}^\pm_{n,j}$ are given by (F.41), (F.42) with $u-i$ replaced by $u-p(i)$, $u-v$ by $u-p(v)$, and η_0 by $\eta_0\ell_{n+i}/\ell_n$, where $p(v):=(\chi_{n+v}-\chi_n)/\ell_n$ for $-j\le v\le j+1$.

Displacement: the map p. The function p is increasing and concave with $p(0)=0$ and $p(1)=1$. By (F.2), $-p''/p'=\chi_a'(\log\rho_U)'(\chi_a)$ at $a=n+v$. Since ρ_U^2/N is non-increasing (Lemma F.1(b)), $(\log\rho_U)'\le\rho_U/(4N)$, and with $\chi_a'=2/(c'\rho_U)$ and $c'N(\chi_a)=a-\frac14$,

$$0\le-\frac{p''(v)}{p'(v)}\le\frac{1}{2(a-\frac14)}\le\frac1n\qquad(-j\le v\le j+1),\tag{F.47}$$

because $a\ge n-j\ge\frac n2+2$. There is a point $v_0\in(0,1)$ with $p'(v_0)=1$. Hence $|\log p'(v)|\le|v-v_0|/n\le(j+1)/n\le\frac12$, and since $|e^t-1|\le2|t|$ for $|t|\le\frac12$,

$$|p'(v)-1|\le\frac{2(j+1)}{n},\qquad\Big|\frac{1}{p'(v)}-1\Big|\le\frac{2(j+1)}{n},\qquad p'(v)\ge e^{-1/2},\qquad|p''(v)|\le\frac2n.\tag{F.48}$$

The remainder formula for linear interpolation, $p(v)-v=\frac12v(v-1)\,p''(\xi_v)$ with ξ_v between 0, 1 and v, and $p''\le0$ give

$$0\le v-p(v)\le\frac{v(v-1)}{n}\le\frac{j(j+1)}{n}\quad(v\notin(0,1)),\qquad0\le p(v)-v\le\frac{v(1-v)}{n}\quad(0\le v\le1).\tag{F.49}$$

Displacement: the sites. For $i=0,1$ we have $p(i)=i$, and nothing changes. For $-j\le i\le-1$, $u-p(i)\ge u-i\ge|i|$, so $0\le\log(u-p(i))-\log(u-i)\le(i-p(i))/(u-i)\le(|i|+1)/n$ by (F.49). For $2\le i\le j+1$, $p(i)-u\ge p(i)-p(1)\ge e^{-1/2}(i-1)$, so $0\le\log(i-u)-\log(p(i)-u)\le(i-p(i))/(p(i)-u)\le e^{1/2}i/n$. In either case the logarithm of a site factor changes by at most $2(j+1)/n$. For the pairs we use that, for positive numbers, $(A+b)/(A_0+b_0)$ lies between A/A_0 and b/b_0. With $A=(u-p(i))^2$, $A_0=(u-i)^2$, $b=\eta_0^2(\ell_{n+i}/\ell_n)^2$, $b_0=\eta_0^2$, and $\ell_{n+i}/\ell_n=p(i+1)-p(i)\in[e^{-(j+1)/n},e^{(j+1)/n}]$, the logarithm of a pair factor changes by at most $4(j+1)/n$; for $i=0,1$, where $A=A_0$, the same holds, and for $\eta_0=0$ a pair factor is a squared site factor. The sites $i=0,1$ do not move; the remaining weights in (F.41) add up to $4j-2$, and there are $2j$ pairs in (F.42), so the sums over the sites change by at most $8j(j+1)/n$.

Displacement: the continuum. Let $(\alpha,\beta)=(-j,j+1)$ or $(-j+\frac12,j+\frac12)$. The substitution $s=p(v)$ gives $\int_\alpha^\beta\log|u-p(v)|\,\mathrm{d}v=\int_{p(\alpha)}^{p(\beta)}\log|u-s|\,\frac{\mathrm{d}s}{p'(p^{-1}(s))}$. By (F.49) and $j/n\le\frac12$, $[p(\alpha),p(\beta)]\subset[-2j,j+1]$, on which $\int|\log|u-s||\,\mathrm{d}s\le2\int_0^{2j+1}|\log t|\,\mathrm{d}t\le6j\log(2j+2)$. By (F.48), replacing the density $1/p'$ by 1 changes the integral by at most $12j(j+1)\log(2j+2)/n$. It remains to

move the endpoints from $p(\alpha), p(\beta)$ to α, β. Each moves by at most $j(j+1)/n$, and on the interval in between $\frac{1}{2} \le |u-s| \le 2j+1$ at the left end, and $\frac{1}{2}e^{-1/2} \le p(\beta) - 1 \le |u-s| \le j+1$ at the right end, so that $|\log|u-s|| \le \log(2j+2)$. Hence $\left|\int_\alpha^\beta \log|u-p(v)|\,\mathrm{d}v - \int_\alpha^\beta \log|u-v|\,\mathrm{d}v\right| \le 14j(j+1)\log(2j+2)/n$. The integral enters $h_j^\pm$ with the factor 2, so the terms in $\frac{1}{n}$ add up to $[8j(j+1) + 28j(j+1)\log(2j+2)]/n$, which for $j=1$ is $(16+56\log 4)/n \le 94/n$. This proves (F.45) and (F.46).

The comb factor. Let $x = \chi_{n+u'}$ with $0 \le u' \le 1$. Then $\nu(x) = n-2+u'$, so $\sin^2\pi\nu = \sin^2\pi u'$, and $u = p(u')$, so $0 \le d := u - u' \le u'(1-u')/n$ by (F.49). We have $\sin\pi u / \sin\pi u' = \cos\pi d + \cot(\pi u')\sin\pi d$. Since $|\cot\pi t| \le 1/(\pi t(1-t))$ for $0 < t < 1$ (by symmetry let $t \le \frac{1}{2}$; then $\tan\pi t \ge \pi t \ge \pi t(1-t)$), the second term is at most $1/n$ in modulus, and $0 \le 1 - \cos\pi d \le \frac{1}{2}(\pi d)^2 \le 1/n^2$. With $n \ge 6$ this gives $\left|\log\sin^2\pi\nu - \log\sin^2\pi u\right| \le 3/n$, uniformly on the cell, its ends included. □

[ORIENTATION] The constant 94 is far from sharp: to first order in $1/n$ the difference $\mathcal{H}_{n,j}^\pm - h_j^\pm$ has the size $2j^2/(3(n-1))$, which is 0.13 for $j=1$ and $n=6$. This is not used.

The extrema of row 6. At $\eta_0 = 0$ the differences $h_j^\pm(u) - \log(4\sin^2\pi u)$ are continuous on $[0,1]$, since the double zeros of the sites $i = 0, 1$ are those of $\sin^2\pi u$. Row 6 of table 4 contains their extrema, which are attained at $u \in \{0,1\}$:

$$\begin{aligned} j=1: &\quad \max_u\left[h_1^+ - \log(4\sin^2\pi u)\right] \le 0.2449, \quad \min_u\left[h_1^-(\cdot\,;0) - \log(4\sin^2\pi u)\right] \ge -0.1991 \ \langle\text{cert}\rangle, \\ j=4: &\quad \max_u\left[h_4^+ - \log(4\sin^2\pi u)\right] \le 0.0749, \quad \min_u\left[h_4^-(\cdot\,;0) - \log(4\sin^2\pi u)\right] \ge -0.0422 \ \langle\text{cert}\rangle, \end{aligned} \tag{F.50}$$

so that $[e^{-0.1991}, e^{0.2449}] \subset [0.819, 1.278]$, and $e^{-0.0422}(1-0.01) \ge 0.949$, $e^{0.0749}(1+0.01) \le 1.089$.

Proof of Proposition 7.4 [PROVED, COMPUTER-ASSISTED]**.** In this appendix $\eta_0 = \frac{1}{4}$ is fixed. The two lemmas used here, Lemmas F.9 and F.10, hold with the same proofs and the same constants for every $0 \le \eta_0 \le \frac{1}{4}$: their proofs use η_0 only through (F.28) and through $\varepsilon_k = \eta_0\ell_k \le \frac{1}{4}\ell_k$, and the value $\eta_0 = 0$ is treated explicitly in the last clause of Lemma F.10 and in the step on the sites of its proof. We apply the two lemmas with $\eta_0 = 0$. Then $q_k = T_{\chi_k}^2$ and $B = B^0$, and by definition $\operatorname{sech}^2(\frac{\pi x}{2})|B^0| = |h_0^0| = \mathrm{Env}\sin^2\pi\nu$. With (F.7), $\lambda = \mathrm{Env}/\mathrm{Lev}$ satisfies $4\lambda\sin^2\pi\nu = |B^0|e^{c'L - c'\mathcal{P} - \mathcal{J}_{\mathrm{end}}}$; note that $\mathcal{J}_{\mathrm{end}}$ is inside Lev and drops out. Lemma F.9 at $\eta_0 = 0$ gives, on every cell $n \ge 2j+4$,

$$\mathcal{H}_{n,j}^-\big|_{\eta_0=0} - 2e_L \ \le\ \log(4\lambda\sin^2\pi\nu) \ \le\ \mathcal{H}_{n,j}^+ + 2e_L. \tag{F.51}$$

We subtract $\log(4\sin^2\pi\nu)$ and apply Lemma F.10 and (F.50):

$$\log\lambda \in \left[-0.1991-\delta_{n,1},\ 0.2449+\delta_{n,1}\right] \ (j=1), \qquad \log\lambda \in \left[-0.0422-\delta_{n,4},\ 0.0749+\delta_{n,4}\right] \ (j=4), \tag{F.52}$$

with $\delta_{n,j} := 2e_L + C_j(\frac{1}{n} + \ell_n)$ and C_j as in (F.45). For $j=1$ and $n \ge 6$ this is the first statement of Proposition 7.4: $\lambda \in [0.819, 1.278]$, widened at both ends by $e^{\pm 2C_L}$ and by the site-displacement factor $e^{\pm C_1(\frac{1}{n}+\ell_n)}$, which tends to 1 as $n \to \infty$ and in which $C_1(\frac{1}{n}+\ell_n)$ may be replaced by $\frac{97}{n} + C\ell_n$ (the 94 of (F.46) and the 3 of the comb factor); these two factors are kept outside λ. For $j=4$ let $n \ge \epsilon c'$ with $\epsilon > 0$ fixed. Then $x - x_1^* \ge r(\epsilon) > 0$, so $e_L = O_\epsilon(c'^{-2/3})$ by (F.24), $\frac{1}{n} \le \frac{1}{\epsilon c'}$ and $\ell_n \le C_\epsilon/c'$. Hence $\delta_{n,4} \to 0$. For c large depending on ϵ we have $e^{\delta_{n,4}} \le 1.01$, which is the allowance (1 ± 0.01) of row 6, and therefore $\lambda \in [0.949, 1.089]$. □

F.6 The detuned floor

We prove Lemma 7.9, the floor (F.53): on every cell $n \ge 2j+4$ the comb h_0 stays above a positive multiple of the level. The floor is the smallest value, over the position u in the cell, of

the exact contribution of the $2j$ detuned pairs nearest to x divided by that of the continuum which they replace; all other pairs are bounded below by their undetuned values, and these by the continuum through the midpoint rule. Keeping more pairs exactly removes a larger part of the midpoint loss, which is why $\mu_4 > \mu_1$. The rows used are 3 and 5, and row 9 through y_{thr}.

Lemma F.11 (The detuned floor; proved, computer-assisted)**.** *Let $j \in \{1,4\}$ and let x lie in cell $n \ge 2j+4$. Then*

$$\frac{h_0(x)}{\mathrm{Lev}(x)} \;\ge\; \tfrac14\, e^{\mathcal{H}^-_{n,j}(x)-2e_L(x)} \;\ge\; \mu_j\Big(1-C_j\big(\tfrac1n+\ell_n\big)\Big)e^{-2C_L}, \qquad \mu_j := \min_{0\le u\le 1} \tfrac14 e^{h_j^-(u;\eta_0)}, \tag{F.53}$$

with C_j as in (F.45), and for $\eta_0 = \frac14$ (table 4, row 3)

$$\mu_1 \ge 0.536\ \langle\mathrm{cert}\rangle, \qquad \mu_4 \ge 0.699\ \langle\mathrm{cert}\rangle, \tag{F.54}$$

the minima being attained at $u \in \{0,1\}$. The factor $1-C_j(\frac1n+\ell_n)$ tends to 1 as $n\to\infty$; where it is not positive the second inequality says nothing, and the first one remains.

Proof. For $x > \chi_2$ we have $B(x) > 0$ and $h_0/\mathrm{Lev} = \frac14|B|e^{c'L-c'\mathcal{P}-\mathcal{J}_{\mathrm{end}}}$ by (F.7); the end correction $\mathcal{J}_{\mathrm{end}}$ is inside Lev. Since $n \ge 2j+4$, (F.43) holds: $\log|B| + c'L - c'\mathcal{P} - \mathcal{J}_{\mathrm{end}} \ge \mathcal{H}^-_{n,j} - 2e_L$. In it the $2j$ pairs $n-j < k \le n+j$ enter through their exact moduli q_k, and every other pair through $q_k \ge T^2_{\chi_k}$ [(T2), Lemma F.7]: detuning is used only in so far as it does not lower a factor. The sites $3 \le k < k_0$ cost $2e_L$. This is the first inequality of (F.53). For the second, $e_L(x) \le C_L$ by Lemma F.6(d) (row 5), as $n \ge 6$; $\mathcal{H}^-_{n,j}(x) \ge h_j^-(u;\eta_0) - C_j(\frac1n+\ell_n)$ by Lemma F.10, and $e^{-t} \ge 1-t$; and $\frac14 e^{h_j^-(u;\eta_0)} \ge \mu_j$ by definition. The values (F.54) and the location of the minima are row 3. □

[ORIENTATION] We note without proof that $\mu_j \to \sinh^2\pi\eta_0 = 0.7546$ as $j\to\infty$; this is not used. The reason is that $\prod_{i\in\mathbb{Z}}((u-i)^2+\eta_0^2)$, divided by the continuum in the sense of (F.42), tends to $4|\sin\pi(u+i\eta_0)|^2 = 4(\sin^2\pi u + \sinh^2\pi\eta_0)$ as $j\to\infty$, whose minimum over u is $4\sinh^2\pi\eta_0$.

F.7 The first cells

On the cells $2,\dots,5$ the point x is within a few Airy lengths of the tip, there are at most three sites to its left, and nothing is gained by replacing them by a continuum. We therefore keep *all* the sites up to χ_{n+4} exactly and apply the midpoint rule only beyond them. No end term and no loss e_L arise, which is why the unit is $\mathrm{Lev}\,e^{-\mathcal{J}_{\mathrm{end}}}$. In the Airy variable the resulting finite product is a c-independent function on each cell, and its minimum is certified (table 4, row 4; row 10 for the passage to the Airy variable).

For x in cell $n \ge 2$ let

$$\mathcal{H}^{\mathrm{I}}_n(x) := f_x(\chi_2) + \sum_{k=3}^{n+4} \log q_k(x) - 2\int_2^{n+9/2} \varphi(a)\,\mathrm{d}a, \tag{F.55}$$

in which the sites and the integral both carry the weight $2n+5$.

Lemma F.12 (First cells: Lemma 7.12; proved, computer-assisted)**.** (a) *If x lies in cell $n \ge 2$, then $\log|B| + c'L \ge c'\mathcal{P} + \mathcal{H}^{\mathrm{I}}_n$ at x, and hence $h_0 \ge \frac14 \mathrm{Lev}\, e^{-\mathcal{J}_{\mathrm{end}}+\mathcal{H}^{\mathrm{I}}_n}$ there.*

(b) *Let $\hat\eta_k := \eta_0(\hat\varsigma_{k+1} - \hat\varsigma_k)$ and*

$$\hat{\mathcal{H}}^{\mathrm{I}}_n(\varsigma) := \log|\varsigma-\hat\varsigma_2| + \sum_{k=3}^{n+4} \log\big((\varsigma-\hat\varsigma_k)^2+\hat\eta_k^2\big) - 3\big[\mathcal{F}(\varsigma,\hat\varsigma_{n+9/2}) - \mathcal{F}(\varsigma,\hat\varsigma_2)\big]. \tag{F.56}$$

For $2 \le n \le 5$ and $x = x_1^* + \ell_c\varsigma \ne \chi_2$ in cell n, $\mathcal{H}^{\mathrm{I}}_n(x) - \log|\varsigma-\varsigma_2| = \hat{\mathcal{H}}^{\mathrm{I}}_n(\varsigma) - \log|\varsigma-\hat\varsigma_2| + O(\ell_c \log\frac{1}{\ell_c})$, uniformly in x and n; at $\varsigma = \hat\varsigma_2$ the right side is understood as its continuous extension.

(c) (Table 4, row 4.) *With* $\mu_n^{\mathrm{I}} := \min \frac{1}{4} e^{\hat{\mathcal{H}}_n^{\mathrm{I}}(\varsigma)}$ *over* $\hat{\varsigma}_n \le \varsigma \le \hat{\varsigma}_{n+1}$,

$$\mu_3^{\mathrm{I}} \ge 0.679, \qquad \mu_4^{\mathrm{I}} \ge 0.683, \qquad \mu_5^{\mathrm{I}} \ge 0.686 \qquad \langle \mathrm{cert} \rangle, \tag{F.57}$$

and on cell 2*, which adjoins the simple zero,*

$$\tfrac{1}{4} e^{\hat{\mathcal{H}}_2^{\mathrm{I}}(\varsigma)} \;\ge\; \mu_{\mathrm{slope}} \frac{\varsigma - \hat{\varsigma}_2}{\hat{\varsigma}_3 - \hat{\varsigma}_2} \quad \textit{for all } \hat{\varsigma}_2 \le \varsigma \le \hat{\varsigma}_3, \qquad \mu_{\mathrm{slope}} = 0.686 \ \langle \mathrm{cert} \rangle. \tag{F.58}$$

The inequality (F.58) *holds on the whole cell and binds at its right end: the quotient of its left side by* $(\varsigma - \hat{\varsigma}_2)/(\hat{\varsigma}_3 - \hat{\varsigma}_2)$ *is* 1.550 *at the zero, rises to* 3.774 *at the relative position* 0.350 *in the cell, and decreases from there to its least value* 0.6924*, which it takes at* $\varsigma = \hat{\varsigma}_3$.

(d) *Consequently, for* $c \ge c_0^{\mathrm{att}}$*, on the cells* $3, 4, 5$, $h_0 \ge \mathrm{Lev}\, e^{-\mathcal{J}_{\mathrm{end}}} \mu_n^{\mathrm{I}} (1 - C\ell_c \log \frac{1}{\ell_c})$*, and on the whole of cell* 2*,* $h_0(x) \ge \mathrm{Lev}\, e^{-\mathcal{J}_{\mathrm{end}}} \mu_{\mathrm{slope}} \frac{x - \chi_2}{\chi_3 - \chi_2} (1 - C\ell_c \log \frac{1}{\ell_c})$*. On these cells* $\mathrm{Lev}\, e^{-\mathcal{J}_{\mathrm{end}}} e^{c'L} \asymp \ell_c^{-2n_1} \asymp c'^{\frac{4}{3}n_1} \gg \sqrt{c'}$.

Proof. (a) By (F.28) and Lemma F.5(b) with $K = n + 5$, for which $x < \chi_{n+1} < \chi_{n+9/2}$, $\sum_{k \ge n+5} \log q_k \ge 2 \sum_{k \ge n+5} \varphi(k) \ge 2I_x(n + \frac{9}{2})$, and $2I_x(n + \frac{9}{2}) = 2I_x(2) - 2\int_2^{n+9/2} \varphi = -c'L + c'\mathcal{P} - 2\int_2^{n+9/2} \varphi$ by (F.6). Inserting this into (F.3) gives the first statement, and the second follows from (F.7).

(b) We take $\varsigma_{\max} = \hat{\varsigma}_{10}$ in Lemmas F.3 and F.4; the site χ_2 is given by (F.14) and the pairs $3 \le k \le n + 4 \le 9$ by (F.15). The constants $\log \ell_c + \log \frac{\pi}{2\sqrt{2}}$ cancel because the weights are equal, and the remainders R, R_k' contribute $O(\ell_c)$. By (F.6) the term $-2\int_2^{n+9/2} \varphi$ is $c'\mathcal{P}_{\chi_{n+9/2}} - c'\mathcal{P}_{\chi_2}$, to which (F.19) applies with $a = n + \frac{9}{2} \le \frac{19}{2}$ and with $a = 2$. For the pairs, $(\varsigma - \varsigma_k)^2 + \eta_0^2 \Delta_k^2 \ge \eta_0^2 \Delta_k^2$ is bounded below, so its logarithm is Lipschitz in the sites, which move by $O(\ell_c)$ by (F.12). The singular factor of the simple site is kept exact on both sides. All these remainders are bounded uniformly in $\varsigma \in [0, \hat{\varsigma}_{10}]$, and hence in x and n.

(c) is the content of row 4; the certificate evaluates $\mathcal{F}$ by its closed form (Lemma F.4).

(d) Let $\hat{R}_n := \hat{\mathcal{H}}_n^{\mathrm{I}} - \log|\varsigma - \hat{\varsigma}_2|$, which is (F.56) without its first term; it is continuous on $[0, \hat{\varsigma}_{10}]$. It has the modulus of continuity $C\delta \log \frac{1}{\delta}$ there. Indeed, with $\Lambda(r) := r \log|r| - r$, a primitive of $\log|r|$, integration by parts gives $\mathcal{F}(\varsigma, A) = -A^{1/2}\Lambda(\varsigma - A) + \frac{1}{2}\int_0^A \Lambda(\varsigma - t)\, t^{-1/2}\, \mathrm{d}t$, and $|\Lambda(a) - \Lambda(b)| \le C\delta \log \frac{1}{\delta}$ for $|a - b| \le \delta \le \frac{1}{4}$ and $|a|, |b| \le \hat{\varsigma}_{10}$, by the estimate of $\int_I |\log|\varsigma - \varsigma'|| \mathrm{d}\varsigma'$ in the proof of Lemma F.4(b). Hence $|\mathcal{F}(\varsigma, A) - \mathcal{F}(\varsigma', A)| \le 2A^{1/2}\, C\delta \log \frac{1}{\delta}$ for ς, ς', A in $[0, \hat{\varsigma}_{10}]$ with $|\varsigma - \varsigma'| \le \delta$. The pair terms of (F.56) are Lipschitz in ς, because $(\varsigma - \hat{\varsigma}_k)^2 + \hat{\eta}_k^2 \ge \hat{\eta}_k^2 > 0$.

In the variable ς cell n is $[\varsigma_n, \varsigma_{n+1}]$. By (F.12), $\varsigma_{n+1} \le \hat{\varsigma}_{n+1}$ and $0 \le \hat{\varsigma}_n - \varsigma_n \le d_n := 0.14\, \ell_c \hat{\varsigma}_n^2$. So the true cell is the nominal cell $[\hat{\varsigma}_n, \hat{\varsigma}_{n+1}]$, on which (c) holds, shortened on the right, and extended on the left by a stretch of length at most d_n. For ς in the true cell let $\varsigma^+ := \max\{\varsigma, \hat{\varsigma}_n\}$. It lies in the nominal cell, and $0 \le \varsigma^+ - \varsigma \le d_n$. By (b) and the modulus of continuity, for $x \ne \chi_2$,

$$\tfrac{1}{4} e^{\mathcal{H}_n^{\mathrm{I}}(x)} = \tfrac{1}{4}(\varsigma - \varsigma_2)\, e^{\hat{R}_n(\varsigma) + O(\ell_c \log \frac{1}{\ell_c})} \;\ge\; \tfrac{1}{4}(\varsigma - \varsigma_2)\, e^{\hat{R}_n(\varsigma^+)} (1 - C\ell_c \log \tfrac{1}{\ell_c}).$$

On the cells $3, 4, 5$ we have $\varsigma - \varsigma_2 \ge \varsigma - \hat{\varsigma}_2 \ge (\varsigma^+ - \hat{\varsigma}_2)(1 - d_n/(\hat{\varsigma}_3 - \hat{\varsigma}_2))$, because $\varsigma_2 \le \hat{\varsigma}_2$ and $\varsigma^+ - \hat{\varsigma}_2 \ge \hat{\varsigma}_3 - \hat{\varsigma}_2$. Since $\frac{1}{4}(\varsigma^+ - \hat{\varsigma}_2)\, e^{\hat{R}_n(\varsigma^+)} = \frac{1}{4} e^{\hat{\mathcal{H}}_n^{\mathrm{I}}(\varsigma^+)} \ge \mu_n^{\mathrm{I}}$ by (c), this and (a) give the first statement. On cell 2, (F.58) says that $\frac{1}{4} e^{\hat{R}_2} \ge \mu_{\mathrm{slope}}/(\hat{\varsigma}_3 - \hat{\varsigma}_2)$ on $(\hat{\varsigma}_2, \hat{\varsigma}_3]$, and this holds at $\hat{\varsigma}_2$ by continuity. Hence $\frac{1}{4} e^{\mathcal{H}_2^{\mathrm{I}}(x)} \ge \mu_{\mathrm{slope}} \frac{\varsigma - \varsigma_2}{\hat{\varsigma}_3 - \hat{\varsigma}_2} (1 - C\ell_c \log \frac{1}{\ell_c})$ for $\chi_2 < x \le \chi_3$, and $\frac{\varsigma - \varsigma_2}{\hat{\varsigma}_3 - \hat{\varsigma}_2} = \frac{x - \chi_2}{\chi_3 - \chi_2} \cdot \frac{\varsigma_3 - \varsigma_2}{\hat{\varsigma}_3 - \hat{\varsigma}_2}$ with $\varsigma_3 - \varsigma_2 \ge \hat{\varsigma}_3 - \hat{\varsigma}_2 - d_3$. At $x = \chi_2$ both sides of the second statement vanish. The size of $\mathrm{Lev}\, e^{-\mathcal{J}_{\mathrm{end}}} e^{c'L}$ is Lemma F.4(c). □

G The vacuum inequality

[PROVED, COMPUTER-ASSISTED] This appendix proves Proposition 7.13: Band $\le R_{\rm vac}|$Lobe$|$ with $R_{\rm vac} \le 0.1021 + 0.02$, and $|\text{Lobe}| \to \infty$; on the way it proves Lemma 7.5(d2). It is used in section 7.9 only, and it takes Lemmas B.2 and B.4, Proposition 7.2, Lemma 7.3(b) (whose hypothesis is verified in section 7.10), appendices F.1 to F.4, Lemma F.9, Lemma F.10 and Lemma F.8 as input.

The idea is described in section 7.9. The Cardy-weighted masses of the negative lobe of h_0 below $t_\star$ and of the positive band beyond both come from a window of width $O(\ell_c)$ at the tip, and in the variable $\varsigma = (x - x_1^*)/\ell_c$ each is a common factor, proportional to $c'^{\frac{4}{3}n_1 - \frac{1}{6}} = c'^{13/6}$, times a c-independent integral. The ratio of the two integrals is certified to be at most 0.1021 when the band is cut after its first hundred cells; the finite-c corrections and the band beyond these cells are bounded by hand, with explicit constants wherever a constant enters $R_{\rm vac}$.

G.1 Statement and reduction

Throughout, $(m, k_\infty, n_1, \eta_0) = (1, \frac{1}{4}, \frac{7}{4}, \frac{1}{4})$, $h_0(t) = \operatorname{sech}^2(\pi b/2)\, B(b)$ with $b = \sqrt{3t/c'}$, and on the real axis $t = c'x^2/3$, $\mathrm{d}t = \frac{2}{3}c'x\,\mathrm{d}x$. By Proposition 7.2, $h_0 < 0$ on $(0, t_\star)$, h_0 has a simple zero at $t_\star = c'\chi_2^2/3$, and $h_0 \ge 0$ beyond; $V > 0$ by Lemma B.2. We set

$$\text{Lobe} := \int_0^{t_\star} h_0 V\,\mathrm{d}t < 0, \quad \text{Band} := \int_{t_\star}^{\infty} h_0 V\,\mathrm{d}t = \sum_{n\ge 2} \text{Band}_n, \quad \text{Band}_n := \int_{c'\chi_n^2/3}^{c'\chi_{n+1}^2/3} h_0 V\,\mathrm{d}t \ge 0, \tag{G.1}$$

so that Band_n is the contribution of cell n, $\chi_n < x < \chi_{n+1}$. With $\rho_C = 2\pi V$, Lemma 7.3(b) and the bound $|h_{0,\rm vac}| \le 8$ of Proposition 7.2 give

$$g_{\rm vac} = \tfrac{1}{2}h_{0,\rm vac} + \pi\big(|\text{Lobe}| - \text{Band}\big) \;\ge\; \pi\big(|\text{Lobe}| - \text{Band}\big) - 4. \tag{G.2}$$

Proposition 7.13 follows from (G.2) once Band $\le R_{\rm vac}|$Lobe$|$ with $R_{\rm vac} < 1$ and $|\text{Lobe}| \to \infty$ are shown; the transform $\hat h_0$ enters only through the hypothesis of Lemma 7.3(b).

Input from appendix F. We use the notation of appendix F: the site weight $f_x(y) = \log|T_y(x)| \le 0$ (F.1); the site map $a \mapsto \chi_a$ for real $a \ge \frac{1}{4}$, $c'N(\chi_a) = a - \frac{1}{4}$ (F.2), whose integer values $a \ge 2$ are the sites; the modulus q_k of the detuned pair at χ_k (F.4), for which $q_k \ge T_{\chi_k}^2$ on the real axis (F.28); and, for $Y \ge x_1^*$, the potential at x of the charge which the law places below Y (F.5),

$$\mathcal{P}_Y(x) := -\int_{x_1^*}^{Y} \rho_U(x')\, f_x(x')\,\mathrm{d}x' \;\ge 0, \tag{G.3}$$

so that $\mathcal{P} = \mathcal{P}_{\chi_2}$. Two bounds of appendix F.4 are used, in both of which the sites next to x are kept exactly. On the part $x_1^* \le x < \chi_2$ of the lobe, the first inequality of (F.31), which is Lemma 7.5(f), reads

$$\log|B(x)| + c'L(x) \;\ge\; f_x(\chi_2) + c'\mathcal{P}_{\chi_{5/2}}(x). \tag{G.4}$$

On cell $n \ge 2$, (F.32), which is behind Lemma 7.5(e), reads

$$\log|B(x)| + c'L(x) \;\le\; f_x(\chi_2) + \sum_{k=3}^{n+1} \log q_k(x) + f_x(\chi_{n+2}) + c'\mathcal{P}_{\chi_{n+2}}(x) + D_n(x), \tag{G.5}$$

where $D_n := \sum_{k\ge n+2} \log(q_k/T_{\chi_k}^2)$ is the detuning of the pairs beyond the cell. By Lemma F.7, $0 \le D_n \le 4\zeta(2)\eta_0^2$; we keep D_n as it stands.

G.2 The Airy window

Let $\varsigma := (x - x_1^*)/\ell_c$ with $\ell_c = (\kappa_{\rm tip} c')^{-2/3}$, so that $\kappa_{\rm tip} c' \ell_c^{3/2} = 1$. As in Lemma F.2(c) we write, for real $a > \frac{1}{4}$ and for integer k,

$$\varsigma_a := \frac{\chi_a - x_1^*}{\ell_c}, \qquad \hat\varsigma_a := \big(a - \tfrac14\big)^{2/3}, \qquad \Delta_k := \varsigma_{k+1} - \varsigma_k, \qquad \hat\Delta_k := \hat\varsigma_{k+1} - \hat\varsigma_k \tag{G.6}$$

for the true and the *nominal* scaled positions and spacings; thus $\varepsilon_k = \eta_0 \ell_c \Delta_k$ and $\hat\varsigma_2 = n_1^{2/3}$. We fix an integer $N_1 \ge 6$, put $\varsigma_{\max} := \hat\varsigma_{N_1+2}$, and take c so large that $\ell_c \varsigma_{\max} \le 0.1$. The *window* is $x_1^* \le x \le x_1^* + \ell_c \varsigma_{\max}$, and σ denotes the scaled position of a point $x' = x_1^* + \ell_c \sigma$ of the window.

Lemma G.1 (Window dictionary; proved, computer-assisted)**.** *With these conventions, and with* $\epsilon_{\rm w} := 4.3\, \ell_c \varsigma_{\max}$*:*

(i) Sites. $\hat\varsigma_a(1 - 0.14\, \ell_c \hat\varsigma_a) \le \varsigma_a \le \hat\varsigma_a$ *for* $\frac14 < a \le N_1 + 2$.

(ii) Law. $c' \rho_U(x')\, dx' = 3\sigma^{1/2} w_c(\sigma)\, d\sigma$ *with* $1 \le w_c(\sigma) \le 1 + 0.33\, \ell_c \sigma$.

(iii) Factors. *For* x, x' *in the window,* $|T_{x'}(x)| = \frac{\pi \ell_c}{2\sqrt2} |\varsigma - \sigma|\, e^R$ *with* $|R| \le \epsilon_{\rm w}$*; for a pair* $3 \le k \le N_1 + 1$, $q_k(x) = \big(\frac{\pi \ell_c}{2\sqrt2}\big)^2 [(\varsigma - \varsigma_k)^2 + \eta_0^2 \Delta_k^2] e^{R'}$ *with* $|R'| \le 2\epsilon_{\rm w}$.

(iv) Continuum potential. *For* $\frac14 < a \le N_1 + 2$ *and* x *in the window,*

$$c' \mathcal{P}_{\chi_a}(x) = 2(a - \tfrac14) \log \frac{2\sqrt2}{\pi \ell_c} - 3 \int_0^{\varsigma_a} \sigma^{1/2} w_c(\sigma) \log|\varsigma - \sigma|\, d\sigma - \mathcal{R}_a(x), \quad |\mathcal{R}_a| \le 2(a - \tfrac14)\epsilon_{\rm w}. \tag{G.7}$$

Proof. These are statements of appendix F.1, applied with the present $\varsigma_{\max}$: (i) is (F.12); (ii) is Lemma F.4(a), with the weight w_c defined there; (iii) is (F.14) and (F.15); and (iv) is (F.18). Their hypotheses hold because $\ell_c \varsigma_{\max} \le 0.1$, because $\hat\varsigma_a \le \varsigma_{\max}$ for $a \le N_1 + 2$, and because a pair $k \le N_1 + 1$ has $\varsigma_{k+1} \le \hat\varsigma_{N_1+2} = \varsigma_{\max}$ by (i). The numerical constants rest on row 10 of table 4, through Lemma F.2(a) and Lemma F.3. □

The scaled comb. For $a > \frac14$ let $\mathcal{Q}_a(\varsigma) := -3 \int_0^{\hat\varsigma_a} \sigma^{1/2} \log|\varsigma - \sigma|\, d\sigma$ be the potential of the Airy density $3\sigma^{1/2}$ carrying the charge $2(a - \frac14)$. It is elementary (the proof is in Lemma F.4): with $A = \hat\varsigma_a$ and $\varsigma \ge 0$, $\varsigma \ne A$, and by continuity at $\varsigma = A$,

$$\mathcal{Q}_a(\varsigma) = -2A^{3/2} \log|A - \varsigma| + \tfrac43 A^{3/2} + 4\varsigma A^{1/2} + 2\varsigma^{3/2} \log\Big|\frac{\sqrt A - \sqrt\varsigma}{\sqrt A + \sqrt\varsigma}\Big|. \tag{G.8}$$

The *scaled comb* consists of the functions, on $0 \le \varsigma \le \hat\varsigma_2$ and on $\hat\varsigma_n \le \varsigma \le \hat\varsigma_{n+1}$ for $n \ge 2$ respectively,

$$\mathsf{L}(\varsigma) := |\varsigma - \hat\varsigma_2|\, e^{\mathcal{Q}_{5/2}(\varsigma)}, \tag{G.9}$$

$$\mathsf{B}_n(\varsigma) := |\varsigma - \hat\varsigma_2| \prod_{k=3}^{n+1} [(\varsigma - \hat\varsigma_k)^2 + \eta_0^2 \hat\Delta_k^2]\ |\varsigma - \hat\varsigma_{n+2}| \prod_{k \ge n+2} \Big[1 + \frac{\eta_0^2 \hat\Delta_k^2}{(\hat\varsigma_k - \varsigma)^2}\Big]\ e^{\mathcal{Q}_{n+2}(\varsigma)}. \tag{G.10}$$

They do not depend on c. The factors of B_n are, in this order: the simple zero χ_2; the pairs kept exactly; the half-weight site at which the trapezoid rule starts; the detuning of the pairs beyond it; the continuum. We denote by $\mathsf{L}^{(c)}$ and $\mathsf{B}_n^{(c)}$ the same expressions at finite c: with the true $\varsigma_k, \varsigma_a, \Delta_k$ in place of the nominal ones, with the weight w_c inserted in the integral defining $\mathcal{Q}_a$, and with $e^{D_n(x)}$ in place of the infinite product.

Lemma G.2 (Lobe and band in the window: Lemma 7.5(d2); proved, computer-assisted)**.** *Let* $N_1 \ge 6$*, and let*

$$\mathcal{K}_c := \mathcal{V}_c \Big(\frac{2\sqrt2}{\pi \ell_c}\Big)^{2n_1}, \qquad \mathcal{V}_c := (1 - e^{-4\pi x_1^*})^2\, (2\pi c' L(x_1^*))^{-1/2}\, \frac{2c' x_1^*}{3}\, \ell_c\, \operatorname{sech}^2 \frac{\pi x_1^*}{2}, \tag{G.11}$$

so that $\mathcal{K}_c$ is a c-independent constant times $c'^{\frac{4}{3}n_1-\frac{1}{6}}$. There are constants C_{w} and C_{cont}, depending on N_1 only, such that the following holds with $\bar{\mathcal{R}} := C_{\mathrm{w}}\ell_c + 3C_V/c'$, whenever $\ell_c\varsigma_{\max} \le 0.1$ and $\bar{\mathcal{R}} \le 1$. The integrands of (G.1) obey

$$\begin{aligned} |h_0|\,V\,\mathrm{d}t &\ge \mathcal{K}_c\, e^{-\bar{\mathcal{R}}}\,\mathsf{L}^{(c)}(\varsigma)\,\mathrm{d}\varsigma \quad (0 \le \varsigma < \varsigma_2), \\ h_0\,V\,\mathrm{d}t &\le \mathcal{K}_c\, e^{\bar{\mathcal{R}}}\,\mathsf{B}_n^{(c)}(\varsigma)\,\mathrm{d}\varsigma \quad (\varsigma_n < \varsigma < \varsigma_{n+1},\ 2 \le n \le N_1), \end{aligned} \tag{G.12}$$

and

$$\Big|\int_0^{\varsigma_2} \mathsf{L}^{(c)}\mathrm{d}\varsigma - \int_0^{\hat{\varsigma}_2} \mathsf{L}\,\mathrm{d}\varsigma\Big| + \sum_{n=2}^{N_1}\Big|\int_{\varsigma_n}^{\varsigma_{n+1}} \mathsf{B}_n^{(c)}\mathrm{d}\varsigma - \int_{\hat{\varsigma}_n}^{\hat{\varsigma}_{n+1}} \mathsf{B}_n\,\mathrm{d}\varsigma\Big| \;\le\; C_{\mathrm{cont}}\,\ell_c. \tag{G.13}$$

Proof. Measure. By Lemma B.4, $V(t)\,e^{-c'L(x)} = (2\pi c'L(x))^{-1/2}\big[(1-e^{-4\pi x})^2+\varepsilon_V\big]$ in the window, with $|\varepsilon_V| \le C_V/c'$ and $(1-e^{-4\pi x})^2 \ge (1-e^{-4\pi x_1^*})^2 = 0.94199\ldots \ge 0.9$. Each of the ratios $L(x)/L(x_1^*) = x/x_1^* = 1+\ell_c\varsigma/x_1^*$, $(1-e^{-4\pi x})^2/(1-e^{-4\pi x_1^*})^2$ and $\operatorname{sech}^2\frac{\pi x}{2}/\operatorname{sech}^2\frac{\pi x_1^*}{2}$ lies between $e^{-C\ell_c\varsigma_{\max}}$ and $e^{C\ell_c\varsigma_{\max}}$, and $\mathrm{d}t = \frac{2}{3}c'x_1^*\ell_c\,(1+\ell_c\varsigma/x_1^*)\,\mathrm{d}\varsigma$. Hence, with an absolute constant C_{m}, and since $C_V/c' \le \frac{1}{3}$,

$$V(t)\,e^{-c'L(x)}\,\operatorname{sech}^2\frac{\pi x}{2}\,\mathrm{d}t = \mathcal{V}_c\,(1+R_V(\varsigma))\,\mathrm{d}\varsigma, \qquad |R_V| \le C_{\mathrm{m}}\ell_c\varsigma_{\max} + \frac{C_V}{0.9\,c'}. \tag{G.14}$$

Powers of ℓ_c. By Lemma G.1(i) all sites and endpoints which occur lie in the window. We insert (iii) and (iv) into (G.4). There is one site factor and the charge is $2(\frac{5}{2}-\frac{1}{4}) = \frac{9}{2}$, so the power of $2\sqrt{2}/\pi\ell_c$ is $\frac{9}{2}-1 = 2n_1$: $|B(x)|\,e^{c'L(x)} \ge (2\sqrt{2}/\pi\ell_c)^{2n_1}\,\mathsf{L}^{(c)}(\varsigma)\,e^{-\frac{11}{2}\epsilon_{\mathrm{w}}}$. In (G.5) there are $1+2(n-1)+1 = 2n$ site factors and the charge is $2(n+2-\frac{1}{4}) = 2n+\frac{7}{2}$, so the power is again $2n_1$ for every n: $|B(x)|\,e^{c'L(x)} \le (2\sqrt{2}/\pi\ell_c)^{2n_1}\,\mathsf{B}_n^{(c)}(\varsigma)\,e^{(4n+\frac{7}{2})\epsilon_{\mathrm{w}}}$. The number of site factors minus the continuum charge removed is always $-2n_1$, the absent charge; this is why the lobe and all cells carry the same factor. Multiplying by (G.14) gives (G.12) with $C_{\mathrm{w}} := \big[18(N_1+2)+2C_{\mathrm{m}}\big]\varsigma_{\max}$, since $|h_0|V\,\mathrm{d}t = |B|e^{c'L}\cdot Ve^{-c'L}\operatorname{sech}^2\frac{\pi x}{2}\,\mathrm{d}t$, $4.3\,(4N_1+\frac{7}{2}) \le 18(N_1+2)$, and $e^{-2r} \le 1-r$, $1+r \le e^r$ for $0 \le r \le \frac{1}{2}$; here $r = |R_V|$, and $2|R_V| \le 2C_{\mathrm{m}}\ell_c\varsigma_{\max} + 3C_V/c' \le \bar{\mathcal{R}} \le 1$.

Continuity. On the lobe and on each cell $n \le N_1$ the functions $\mathsf{L}^{(c)}$, $\mathsf{B}_n^{(c)}$ are obtained from L, B_n by moving the positions by at most $0.14\,\ell_c\varsigma_{\max}^2$, by (i); by changing the weight by at most $0.33\,\ell_c\varsigma_{\max}$, by (ii); and by replacing the infinite product by e^{D_n}. Every factor is bounded, and it is Lipschitz in the positions uniformly over the cell, because the points at which a factor is singular, namely ς_k for $k \ge n+2$ and the endpoint ς_{n+2} of the continuum, or $\varsigma_{5/2}$ for the lobe, stay at least half a nominal cell away from ς. The integral in (G.7) changes by at most $C\ell_c(1+|\log|\varsigma-\hat{\varsigma}_a||)$, where the logarithm is bounded for the same reason. For D_n we use the second form of q_k given after (F.4). With $u = \frac{\pi}{2}(\chi_k - x) = \frac{\pi}{2}\ell_c(\varsigma_k-\varsigma)$ and $v = \frac{\pi}{2}\varepsilon_k = \frac{\pi}{2}\eta_0\ell_c\Delta_k$ it gives, for every $k \ge n+2$, $q_k/T_{\chi_k}^2 = (1+\sin^2 v/\sinh^2 u)\,e^{\theta_k}$ with $0 \le \theta_k \le 5\,v^2/\cosh^2 u$. For the pairs with $\chi_k - x_1^* \le 0.2$, (F.11) and (F.12) still hold. The spacings are compared through the derivative of the site map, since the error $0.14\,\ell_c\hat{\varsigma}_k^2$ of the positions is not small against $\hat{\Delta}_k$ for large k: by (F.2), (F.11) and (F.12), $\frac{2}{3}\ell_c\hat{\varsigma}_a^{-1/2}(1-0.33\,\ell_c\hat{\varsigma}_a) \le \chi_a' = 2/(c'\rho_U(\chi_a)) \le \frac{2}{3}\ell_c\varsigma_a^{-1/2}$, and integration over $[k,k+1]$ gives $\hat{\Delta}_k(1-0.33\,\ell_c\hat{\varsigma}_{k+1}) \le \Delta_k \le \hat{\Delta}_k(1-0.14\,\ell_c\hat{\varsigma}_{k+1})^{-1/2}$. For the distances, $\hat{\varsigma}_k \le \frac{3}{2}(N_1+2)(\hat{\varsigma}_k-\varsigma)$ for $k \ge n+2$ and $\varsigma \le \hat{\varsigma}_{n+1}$, so that $\varsigma_k-\varsigma = (\hat{\varsigma}_k-\varsigma)\big(1+O(N_1\ell_c\hat{\varsigma}_k)\big)$ by (F.12). The relative correction is at most 0.06 in modulus: for $\hat{\varsigma}_k \le 2\varsigma_{\max}$ because $\bar{\mathcal{R}} \le 1$ implies $18(N_1+2)\ell_c\varsigma_{\max} \le 1$, and for $\hat{\varsigma}_k \ge 2\varsigma_{\max}$ because then $\hat{\varsigma}_k \le 2(\hat{\varsigma}_k-\varsigma)$ and $\ell_c\hat{\varsigma}_k \le 0.21$. Hence $\sin^2 v/\sinh^2 u = (\eta_0^2\hat{\Delta}_k^2/(\hat{\varsigma}_k-\varsigma)^2)\,(1+O(\ell_c\hat{\varsigma}_k))$, with a constant that depends on N_1; these terms are $O(k^{-2})$ and $\hat{\varsigma}_k \le k^{2/3}$, so the errors sum to $O(\ell_c)$, and $\sum_k\theta_k = O(\ell_c^{3/2})$. The pairs with $\chi_k - x_1^* \ge 0.2$ are at distance at least 0.1 from x and have $\varepsilon_k = O(1/c')$; since $\sum_k \varepsilon_k/\sinh^2\frac{\pi}{2}(\chi_k-x)$ is bounded, they contribute $O(1/c')$ to D_n. The corresponding factors of the product in (G.10) contribute $O(\sum_{k\gtrsim\ell_c^{-3/2}} k^{-2}) = O(\ell_c^{3/2})$. Finally the endpoints of the ς-integrals move by $O(\ell_c)$, and the integrands are bounded. To combine: on the common part of

the true and the nominal cell the two integrands differ by at most $C\ell_c$; the two cells differ by intervals of total length at most $0.28\,\ell_c\varsigma_{\max}^2$, on which the integrands are bounded; and there are N_1 terms. This gives (G.13) with a constant C_{cont} that depends on N_1 only. □

G.3 The scaled vacuum ratio

Definition G.3 (Scaled vacuum ratio)**.** With the scaled comb (G.9), (G.10),

$$I_{\mathrm{Lobe}} := \int_0^{\hat\varsigma_2} \mathsf{L}\,\mathrm{d}\varsigma, \qquad I_n := \int_{\hat\varsigma_n}^{\hat\varsigma_{n+1}} \mathsf{B}_n\,\mathrm{d}\varsigma, \qquad \hat R_{\mathrm{vac}}(N_1) := \frac{1}{I_{\mathrm{Lobe}}}\sum_{n=2}^{N_1} I_n. \tag{G.15}$$

The ratio depends on (m, k_∞, η_0), which fix the scaled comb, and on the number N_1 of cells, but not on c. We drop the part $0 \le x < x_1^*$ of the lobe, on which $|h_0|V \ge 0$. Integrating (G.12) and using (G.13), the factor $\mathcal{K}_c$ cancels in the ratio:

$$|\mathrm{Lobe}| \;\ge\; \mathcal{K}_c\, e^{-\bar{\mathcal{R}}}(I_{\mathrm{Lobe}} - C_{\mathrm{cont}}\ell_c), \qquad \frac{1}{|\mathrm{Lobe}|}\sum_{n=2}^{N_1}\mathrm{Band}_n \;\le\; \frac{\sum_{n=2}^{N_1} I_n + C_{\mathrm{cont}}\ell_c}{I_{\mathrm{Lobe}} - C_{\mathrm{cont}}\ell_c}\, e^{2\bar{\mathcal{R}}}. \tag{G.16}$$

As $c \to \infty$ the first right-hand side tends to infinity and the second to $\hat R_{\mathrm{vac}}(N_1)$.

Lemma G.4 (proved, computer-assisted)**.** *For $(m, k_\infty, \eta_0) = (1, \frac14, \frac14)$ and $N_1 = 100$,*

$$\hat R_{\mathrm{vac}}(100) \;\le\; 0.1021 \quad \langle\mathrm{cert}\rangle, \qquad\qquad I_{\mathrm{Lobe}} \;\ge\; 94.47 \quad \langle\mathrm{cert}\rangle. \tag{G.17}$$

For $N_1 = 30$ the certified bound is $\hat R_{\mathrm{vac}}(30) \le 0.1020$; the cells $31 \le n \le 100$ add less than 10^{-4}.

Proof. This is table 4, row 11. The integrals of (G.15) are enclosed in interval arithmetic, over a covering of the lobe and of each cell by subintervals and in the mean-value form of appendix H.1; the potentials $\mathcal{Q}_a$ are evaluated through (G.8). Of the product over the pairs $k \ge n+2$ the first 3000 factors are evaluated, up to $K := n + 3001$; the remaining factors exceed one, and the sum of their logarithms, which decrease like k^{-2}, is at most an explicit $U_n \le 1.5 \times 10^{-5}$. Indeed, for $k > K$ and $\varsigma \le \hat\varsigma_{n+1}$ the logarithm is at most $\eta_0^2\hat\Delta_k^2/(\hat\varsigma_k - \varsigma)^2$, and $\hat\Delta_k \le \frac23(k - \frac14)^{-1/3}$ because $a \mapsto \hat\varsigma_a$ is concave. So it is at most $\phi(k - \frac14)$ with $\phi(u) := \frac49\eta_0^2\, u^{-2/3}(u^{2/3} - \varsigma)^{-2}$, which decreases in u. The substitution $w = u^{2/3}$ and $w^{-1/2} \le \hat\varsigma_K^{-1/2}$ give $\sum_{k>K}\phi(k - \frac14) \le \int_{K-1/4}^{\infty}\phi\,\mathrm{d}u \le \frac23\eta_0^2\,\hat\varsigma_K^{-1/2}(\hat\varsigma_K - \varsigma)^{-1}$, which is largest at $\varsigma = \hat\varsigma_{n+1}$; this value is U_n. For $2 \le n \le 100$ it is largest at $n = 100$, where it is 1.4961×10^{-5}. The bound for $\hat R_{\mathrm{vac}}$ is the upper end of the enclosure of $\sum_n I_n$ divided by the lower end of that of I_{Lobe}. □

G.4 The far cells and the far band

Beyond cell N_1 no site is kept exactly, and the upper bound of Lemma 7.5(e) takes over; its constants are explicit, because they enter R_{vac}. Let $r_0 := 0.3$.

Lemma G.5 (proved, computer-assisted)**.** *Let $N_1 \ge 6$. For c large enough,*

$$\int_{\chi_{N_1+1} \le x \le x_1^* + r_0} h_0 V\,\mathrm{d}t \;\le\; \mathcal{K}_c\, C_{\mathrm{tail}}\, \frac{(N_1 - \frac14)^{\frac23(1-2n_1)}}{2n_1 - 1}, \tag{G.18}$$

$$\int_{x \ge x_1^* + r_0} h_0 V\,\mathrm{d}t \;\le\; C_{\mathrm{far}}\sqrt{c'}, \tag{G.19}$$

where C_{far} does not depend on c, and $C_{\mathrm{tail}} = C_{\mathrm{tail}}(N_1)$ is the number (G.20), which decreases as N_1 grows; $C_{\mathrm{tail}}(100) \le 282$.

Proof. The plan is to bound $|B|e^{c'L}$ by a constant times $e^{c'\mathcal{P}}$, to bound $\mathcal{P}$ by the potential of a single point charge n_1 at χ_2, and to integrate against the Cardy measure. The points $x \ge \chi_{N_1+1}$ lie in the cells $n \ge N_1+1 \ge 6$. There (F.35), which is Lemma 7.5(e) and rests on rows 5, 7 and 9 of table 4 (and on row 10 through (F.12) in Lemma F.6), holds, and $\mathcal{J}_{\text{end}} \le C_J$ (Lemma F.8). Its factor $e^{94/n+C\ell_n}$ has $\frac{94}{n} \le \frac{94}{N_1+1}$ and $\ell_n \le \ell_c$, so it is at most e^{94/N_1} as soon as $C\ell_c \le \frac{94}{N_1} - \frac{94}{N_1+1}$; this is one of the conditions on the size of c. Hence $|B(x)|\,e^{c'L(x)} \le C_{\text{up}}\,e^{c'\mathcal{P}(x)}$ with $C_{\text{up}} := 5.0\,e^{94/N_1}\,(1+4\eta_0^2)^2\,e^{C_{\text{det}}\eta_0^2+C_J+2C_L} \le 42.75\,e^{94/N_1}$, because $\eta_0 = \frac14$, $C_{\text{det}} \le 16.6$, $C_J \le 0.65$ and $C_L \le 0.006$ (appendix F) give $5.0 \cdot 1.5625 \cdot e^{1.0375+0.65+0.012} \le 42.75$. Thus $C_{\text{up}} \le 110$ for $N_1 = 100$. Next, $c'\mathcal{P}(x) \le 2n_1|\log|T_{\chi_2}(x)||$ by (F.16), which is Lemma 7.5(b).

For (G.18) let $\chi_{N_1+1} \le x \le x_1^*+r_0$, and write $|T_{\chi_2}(x)| = \tanh z\,\tanh z_+$ with $z = \frac{\pi}{2}(x-\chi_2) = \frac{\pi}{2}\ell_c(\varsigma-\varsigma_2) \in (0, \frac{\pi}{2}r_0]$ and $z_+ = \frac{\pi}{2}(x+\chi_2) \ge u_1$. The first inequality of Lemma F.3, which holds for all real z, gives $\tanh z \ge z\,e^{-z^2/3} \ge z\,e^{-\pi^2 r_0^2/12}$, and $\tanh z_+ \ge \tanh u_1 = 1/\sqrt{2}$. For $\varsigma \ge \varsigma_{N_1+1}$ we have $\varsigma - \varsigma_2 \ge \varsigma\,(1-\varsigma_2/\varsigma_{N_1+1}) \ge \varsigma\,(1-\hat\varsigma_2/\hat\varsigma_{N_1})$, because $\varsigma_2 \le \hat\varsigma_2$ by (F.12), and because $\varsigma_{N_1+1} \ge \hat\varsigma_{N_1}$ for c large, again by (F.12). Hence

$$e^{c'\mathcal{P}(x)} \;\le\; e^{n_1\pi^2 r_0^2/6}\Big(1-\frac{\hat\varsigma_2}{\hat\varsigma_{N_1}}\Big)^{-2n_1}\Big(\frac{2\sqrt2}{\pi\ell_c}\Big)^{2n_1}\varsigma^{-2n_1}.$$

For the measure we use Lemma B.4 on $x_1^* \le x \le x_1^*+r_0$, with $(1-e^{-4\pi x})^2 + \varepsilon_V \le 1 + C_V/c'$. In the quotient of $Ve^{-c'L}\operatorname{sech}^2\frac{\pi x}{2}\,\mathrm{d}t$ by $\mathcal{V}_c\,\mathrm{d}\varsigma$ the factors $(L(x_1^*)/L(x))^{1/2}$ and x/x_1^*, the latter from $\mathrm{d}t$, combine to $(x/x_1^*)^{1/2} \le (1+r_0/x_1^*)^{1/2}$, and $\operatorname{sech}^2\frac{\pi x}{2} \le \operatorname{sech}^2\frac{\pi x_1^*}{2}$. Therefore $Ve^{-c'L}\operatorname{sech}^2\frac{\pi x}{2}\,\mathrm{d}t \le (1+C_V/c')\,(1-e^{-4\pi x_1^*})^{-2}(1+r_0/x_1^*)^{1/2}\,\mathcal{V}_c\,\mathrm{d}\varsigma$, and we take c so large that $C_V/c' \le 0.01$. Multiplying the three bounds, the left-hand side of (G.18) is at most $\mathcal{K}_c\,C_{\text{tail}}\int_{\varsigma_{N_1+1}}^\infty \varsigma^{-2n_1}\,\mathrm{d}\varsigma \le \mathcal{K}_c\,C_{\text{tail}}\,\hat\varsigma_{N_1}^{1-2n_1}/(2n_1-1)$, with $\hat\varsigma_{N_1} = (N_1-\frac14)^{2/3}$ and

$$C_{\text{tail}}(N_1) := 1.01\;C_{\text{up}}\;e^{n_1\pi^2r_0^2/6}\Big(1-\frac{\hat\varsigma_2}{\hat\varsigma_{N_1}}\Big)^{-2n_1}(1-e^{-4\pi x_1^*})^{-2}\Big(1+\frac{r_0}{x_1^*}\Big)^{1/2}. \tag{G.20}$$

For $N_1 = 100$ the five factors after 1.01 are at most 110, $e^{0.2591} \le 1.296$, $(1-1.4522/21.508)^{-7/2} \le 1.278$, 1.062 and $2.0694^{1/2} \le 1.439$, and $1.062 \cdot 1.439 \le 1.53$; so $C_{\text{tail}}(100) \le 1.01 \cdot 110 \cdot 1.296 \cdot 1.278 \cdot 1.53 \le 282$. For $N_1 = 30$ the same computation gives about 3500, because $e^{94/30} \approx 23$.

For (G.19) let c be so large that $\chi_2 \le x_1^* + 0.05$ and that the cells meeting $x \ge x_1^* + r_0$ have $n \ge 6$. Since $|\log|T_{x'}(x)||$ increases with $x' < x$ and decreases with $x > x'$, $c'\mathcal{P}(x) \le 2n_1|\log|T_{x_1^*+0.05}(x_1^*+r_0)|| \le 2.2\,n_1$ for $x \ge x_1^*+r_0$. This makes the far-band statement of Lemma 7.5(e) explicit: $|B|e^{c'L} \le C_{\text{up}}e^{2.2n_1}$ there. By Lemma B.4, $V \le (1+C_V/c')\,\text{as}(c'L)$ for $x \ge x_1^*$. Therefore the left-hand side of (G.19) is at most $C_{\text{up}}\,e^{2.2n_1}(1+C_V/c')\int_{x_1^*+r_0}^\infty (2\pi c'L(x))^{-1/2}\operatorname{sech}^2\frac{\pi x}{2}\,\frac{2c'x}{3}\,\mathrm{d}x$, and this integral is $\sqrt{c'}$ times a convergent integral which does not depend on c. □

G.5 Why the Bessel asymptote must be two-sided; assembly

The lobe must be bounded from below and the band from above, and both carry the weight V; this is why the asymptote of Lemma B.4 has to be two-sided (section 7.9). With the one-sided bound $V \le K_a \le e^{c'L}$ for the band ($V \le K_a$ by the monotonicity of K_α in α, and Lemma B.2(e)), and the true size $V \simeq (1-e^{-4\pi x})^2\,\text{as}(c'L)$ for the lobe, the two measures would differ at the tip by the factor $e^{c'L}/\text{as}(c'L) = \sqrt{2\pi c'L(x_1^*)} = 1.92\sqrt{c'}$, about 15 at $c = 64$ and about 61 at $c = 1024$, and the bound for Band/|Lobe| would exceed one. With Lemma B.4 the same measure $\mathcal{V}_c\,\mathrm{d}\varsigma$ appears in both integrals, up to the factor $1+R_V$ of (G.14), and cancels in the ratio, as do the power $\ell_c^{-2n_1}$ of Lemma 7.5(d1) and the outer factor sech^2.

Proof of Proposition 7.13. We take $N_1 = 100$ and split the band into the cells $n \le N_1$, the cells beyond them up to $x_1^* + r_0$, and the rest. By (G.16), (G.18) and (G.19),

$$\frac{\text{Band}}{|\text{Lobe}|} \;\le\; \frac{\sum_{n=2}^{N_1} I_n + C_{\text{cont}}\ell_c}{I_{\text{Lobe}} - C_{\text{cont}}\ell_c}\, e^{2\bar{\mathcal{R}}} + \frac{C_{\text{tail}}\, e^{\bar{\mathcal{R}}}}{I_{\text{Lobe}} - C_{\text{cont}}\ell_c}\, \frac{\left(N_1 - \frac{1}{4}\right)^{\frac{2}{3}(1-2n_1)}}{2n_1 - 1} + \frac{C_{\text{far}}\, e^{\bar{\mathcal{R}}}\sqrt{c'}}{\mathcal{K}_c\,(I_{\text{Lobe}} - C_{\text{cont}}\ell_c)}. \tag{G.21}$$

As $c \to \infty$ the first term tends to $\hat{R}_{\text{vac}}(100) \le 0.1021$, by Lemma G.4, and the third is $O\big(c'^{\frac{1}{2}-\frac{4}{3}n_1+\frac{1}{6}}\big) = O(c'^{-5/3})$. The second term tends to a number that does not depend on c,

$$\delta_{\text{tail}} := \frac{C_{\text{tail}}}{I_{\text{Lobe}}}\, \frac{\left(N_1 - \frac{1}{4}\right)^{-5/3}}{2.5} \;\le\; \frac{282}{94.47} \cdot 1.9 \times 10^{-4} \;\le\; 6 \times 10^{-4},$$

by (G.20), by the lower bound for I_{Lobe} in (G.17), and because $99.75^{-5/3}/2.5 \le 1.9 \times 10^{-4}$; any $C_{\text{tail}} \le 5067$ would give $\delta_{\text{tail}} \le 0.01$. We do not take $N_1 = 30$, although $\hat{R}_{\text{vac}}(30)$ is no larger: there $C_{\text{tail}} \approx 3500$ and $29.75^{-5/3}/2.5 \le 0.0015$ make the proved δ_{tail} about 0.05, while the cells beyond the thirtieth in fact add only 10^{-4} [NUMERICAL].

Let c_0^{att} be so large that, for $c \ge c_0^{\text{att}}$, the conditions of Lemmas G.2 and G.5 hold, the three terms of (G.21) together exceed the sum $\hat{R}_{\text{vac}}(100) + \delta_{\text{tail}}$ of their limits by at most 0.01, and $|\text{Lobe}| \ge 2$ by (G.16). Then

$$\text{Band} \le R_{\text{vac}}\,|\text{Lobe}|, \qquad R_{\text{vac}} := \hat{R}_{\text{vac}}(100) + \delta_{\text{tail}} + 0.01 \;\le\; 0.1021 + 0.01 + 0.01 = 0.1021 + 0.02, \tag{G.22}$$

and (G.2) gives $g_{\text{vac}} \ge \pi(1 - R_{\text{vac}})|\text{Lobe}| - 4 \ge 2\pi \cdot 0.877 - 4 > 0$. The constants C_{w}, C_{cont}, C_V, C_{far} and the unnamed constants C enter c_0^{att} only, and $|\text{Lobe}|$ grows at least like $c'^{13/6}$ by (G.16). Since only $R_{\text{vac}} < 1$ is needed, neither the third digit of $\hat{R}_{\text{vac}}$ nor the allowance 0.02 is delicate. □

H Certified constants and numerical methods

We say what a certified inequality is, list all of them in table 4, and complete the description of the numerical methods of section 5.

H.1 What "certified" means

An inequality marked ⟨cert⟩ bounds an explicit elementary function of one real variable, or a ratio of two integrals of such functions, or a quantity that the row reduces to finitely many such functions (rows 5 and 8), on a stated range; it does not involve c. The inequality is proved in interval arithmetic on a covering of the range by finitely many subintervals. A real number is represented by an interval with floating-point endpoints that contains it, and every operation returns an interval, rounded outward, that contains all values which the exact result can take; rounding errors widen the result and cannot make it wrong. The function is evaluated on each subinterval X as a whole, and the largest upper endpoint obtained is a proven upper bound on the range (likewise for lower bounds); table 4 records it as the bound obtained, which lies slightly beyond the true extremum. Where needed we use the mean-value form $f(X) \subset f(m) + f'(X)\,(X - m)$, with m the midpoint of X and $f'(X)$ an enclosure of the derivative on X; in the same form, the integral of f over X, of length h, lies in $h\,f(m) + \frac{1}{8}h^2[-w, w]$, with w the length of $f'(X)$, and these enclosures are added (row 11). An unbounded part of the range is bounded by hand, as the row records. This, together with the legend of section 1.3, is the only meaning of "computer-assisted" in this paper.

A point at which the function is singular, or is a quotient of two vanishing quantities, is removed analytically first. In row 4 the simple zero at the left end of cell 2 is divided out. In row 6 the terms $2\log u + 2\log(1-u)$ of $h_j^{\pm}$ and $\log(4\sin^2 \pi u)$ combine to $-2\log 2\pi - 2\log[\sin \pi u/(\pi u(1-$

$u))]$, and for $0 \le u \le \frac{1}{2}$ we use $\log[\sin \pi u/(\pi u)] = -\sum_{k\ge1} \zeta(2k)\, u^{2k}/k$, truncated at $k = 60$ with the tail bounded by $\zeta(122)\, u^{122}/(61(1-u^2))$; for $u \ge \frac{1}{2}$ we use the symmetry $u \to 1-u$. Rows 9 and 10 reach the tip. With $u_1 = \operatorname{arcsinh} 1$ let $t := \sinh(u_1+\delta) - 1 = 2\sinh^2 \frac{\delta}{2} + \sqrt{2}\sinh\delta$, $q := t/\delta$, $q_1 := (q-\sqrt{2})/(\sqrt{2}\,\delta)$ and $b := (q/\sqrt{2})^{1/2}$; let $\phi(v) := \operatorname{arcsinh}(\sqrt{v})/\sqrt{v}$ and $\phi_1(v) := (1-\phi(v))/v$. Then $\operatorname{arccosh}(1+t) = \sqrt{2t}\,\phi(t/2)$, and therefore

$$e_1(\delta) = \frac{q_1}{b+1} - \frac{b\,q}{2}\,\phi_1\!\left(\tfrac{t}{2}\right), \qquad r\,(\log \rho_U)'(x_1^* + r) = \frac{\cosh(u_1+\delta)}{\sqrt{2}\; q\,(2+t)^{1/2}\,\phi(t/2)} \quad (\delta = \pi r),$$

with e_1 as in row 10. Here t, q and q_1 are power series in δ with positive coefficients, so they increase, as do b and $\cosh(u_1+\delta)$; ϕ and ϕ_1 decrease, being the integrals over $0 \le s \le 1$ of $(1+vs^2)^{-1/2}$ and of $s^2 g(vs^2)$, where $g(x) = (1-(1+x)^{-1/2})/x$ is the slope of a chord of a concave function. At $\delta = 0$ the seven functions take the values 0, $\sqrt{2}$, $1/(2\sqrt{2})$, 1, $\sqrt{2}$, 1 and $\frac{1}{6}$, in this order. On a subinterval each is enclosed by its values at the two ends, and the right sides are evaluated on these enclosures; this works on subintervals that begin at $\delta = 0$, where $e_1(0^+) = \sqrt{2}/24$ and the second function is $\frac{1}{2}$.

We use the Arb library [61] through its Python interface python-flint. The precision is 80, 100, 128 or 200 bits, as the row says. Each computation has been checked independently, line by line, against the formulas as they are printed in this paper. Rows 3, 6 and 8 have also been certified a second time, by a computation written independently (row 6 through $\log\Gamma$ and the digamma and trigamma functions).

Table 4 is a closed list: a c-independent constant carries the mark $\langle\text{cert}\rangle$ in section 7 and appendices F and G only if it has a row. Constants obtained by hand within a proof, and the orientation values of section 7.3, are not certified and are not listed. Absent by choice are the absolute constants of the c-dependent remainders, such as the Hankel remainder of appendix B and the steepest-descent constants of appendix E; they stay symbolic and enter only through c_0^{att}. All rows feed Theorem 5, hence the attainment half of Theorem 1, and Corollary 6; no row feeds Theorems 2 to 4 or Theorem 7.

H.2 Numerical methods for the optimal functionals

[NUMERICAL] We complete section 5.1; nothing here is certified. At order P the functional is the unique $p(t)e^{-2\pi t}$, with p in the truncated basis of [11], that has a simple zero at t_1 and double zeros at $t_2, \dots, t_{P/2}$. We scale the rows of the truncated crossing equations by the vacuum functional. A Newton step is accepted or damped by a monotonicity test on successive corrections, not by the size of the residual, which is a poor guide at large c.

Precision. Arb serves here for its arbitrary precision and not for its error bounds: the radii grow through the Laguerre recurrence until they carry no information. We work with the midpoints and establish the accuracy by solving again at 1.5 to 2 times the precision. On the levels that were solved twice, at least 31 digits agree in t_1, and at least 20 in every level and weight that we report; the highest orders, $P \ge 2304$, are judged by the Newton residual instead. The working precision is 768–1600 bits on most levels, and at least one bit per unit of P at the highest orders.

Extrapolation in P. For each c we fit $\Delta_1^{(P)}(c) = \Delta_\infty + A\, e^{-k(P/c)^s}$, with s free, to the levels with $P/c \ge 0.8$; the fits return $s = 0.57$–0.58. The fitted Δ_∞ is our estimate S of $\Delta_1^{(\infty)}(c)$. Its uncertainty is $\sigma := \frac{1}{2}\max\{|S-T|, |S-S_{1/2}|\}$, with a floor of $10^{-7}c$, where $S_{1/2}$ is the same fit with $s = \frac{1}{2}$ fixed, and T is a fit in which the dependence on P/c is taken from a fully converged chain, $c = 48$. When $P_{\max}/c \ge 6$ we subtract instead from $\Delta_1^{(P_{\max})}(c)$ a tail fitted, with s free, to the top levels (at most six), and σ is the spread of the fits with $s = \frac{1}{2}$, $s = 1$ and s free. For $P_{\max}/c \ge 4$ the whole correction is at most $3 \cdot 10^{-6}c$. We tested the estimator on ten chains with $64 \le c \le 512$ that reach $P/c \ge 5$, by cutting each at a smaller P/c and extrapolating again. When the cut is at $P/c \ge 2$, the error is below $10^{-5}c$ and below σ in every case. When the cut

	Inequality	How it is obtained	Used in
1	$\varrho_\infty \le 0.5029$ on $(x_1^*, 3]$, for the phase-free ratio ϱ_∞ of Lemma 7.8 with its exact prefactor $\lvert b_0\rvert^{1/2}x^{-1/2}$.	IA, 80 bits, 20000 subintervals of $[x_1^* + 10^{-3}, 3]$; bound obtained 0.502833, near $x = 3$, where $\varrho_\infty = 0.50271$. By hand (proof of Lemma 7.8): $\varrho_\infty \le 6\,(x - x_1^*)^{13/4} < 10^{-8}$ on $(x_1^*, x_1^* + 10^{-3}]$, and $\varrho_\infty \le 0.504$ for $x \ge 3$.	Lemma 7.8
2	$\varrho_\infty \le 0.41$ for $x_1^* < x \le 1.33$; the value at the switch point $x = 1.33$ is 0.394.	The covering of row 1 restricted to $x \le 1.33$, in the same computation; bound obtained 0.39368. By hand: the tip, as in row 1.	Lemma 7.8; criterion of section 7.7
3	$\mu_1 \ge 0.536$ and $\mu_4 \ge 0.699$ at $\eta_0 = \frac{1}{4}$, where $\mu_j = \min_{0\le u\le 1} \frac{1}{4}e^{h_j^-(u;\eta_0)}$ (F.53).	IA, 128 bits, 16000 subintervals of $[0, 1]$, mean-value form; h_j^- is explicit (F.42). Its derivative has a fixed sign on $[0, \frac{1}{4}]$ and on $[\frac{3}{4}, 1]$, and in between h_j^- exceeds its end values. So the minimum is attained at $u \in \{0, 1\}$: $\mu_1 = 17e^4/1728 = 0.53713$ and $\mu_4 = 0.70097$. By hand: the factor $1 - C_j(\frac{1}{n} + \ell_n)$ of (F.53) on cell n.	Lemma 7.9; F.6
4	First cells, in the Airy variable: $\mu_n^{\mathrm{I}} \ge 0.679, 0.683, 0.686$ for $n = 3, 4, 5$ (F.57); on the whole of cell 2 the slope form (F.58) with $\mu_{\mathrm{slope}} = 0.686$.	IA, 100 bits, 4000 subintervals per cell, mean-value form, for (F.56), which does not involve c and is in closed form (Lemma F.4). Bounds obtained for μ_n^{I}: 0.6978, 0.7027, 0.7063 for $n = 3, 4, 5$. On cell 2 the quotient of the two sides of (F.58) is least at $\varsigma = \hat\varsigma_3$, where it is 0.6924. By hand: the passage to the Airy variable (Lemma F.12(b),(d); row 10).	Lemma 7.12; F.7
5	$\hat e_L(\varsigma) \le 0.00186$ for $3 \le \varsigma \le \hat\varsigma_{602}$, for the far-left remainder with the sites at their nominal positions (F.25). Hence $C_L \le 0.006$ and $e^{-2C_L} \ge 0.988$ (Lemma F.6(d)).	IA, 100 bits, 136856 subintervals of $[3, \hat\varsigma_{602}]$, $\hat\varsigma_{602} = 71.28$; bound obtained 0.0018523. By hand (proof of Lemma F.6(d), which also describes the covering): $\varsigma \ge \hat\varsigma_{602}$, where (F.27) gives 0.00147; the passage from $\hat e_L$ to e_L at finite c, which costs $C\ell_c$.	F.2; Proposition 7.4, Lemma 7.5(a), Lemma 7.9, Lemma G.5
6	At $\eta_0 = 0$, over $0 \le u \le 1$ (F.50): $h_1^+ - \log(4\sin^2\pi u) \le 0.2449$ and $h_1^- - \log(4\sin^2\pi u) \ge -0.1991$, so $\lambda \in [0.819, 1.278]$ for $j = 1$. With $h_4^\pm$ the bounds are 0.0749 and -0.0422, so $\lambda \in [0.949, 1.089]$ for $j = 4$, the allowance (1 ± 0.01) included.	IA, 128 bits, 16000 subintervals, mean-value form, after the cancellation of appendix H.1. The extrema are attained at $u \in \{0, 1\}$, as in row 3: $6 - 3\log 2 - 2\log 2\pi = 0.24480$ and $I(0) - 2\log 2\pi = -0.19900$ ($I(0)$ as in row 8) for $j = 1$; 0.07487 and -0.04216 for $j = 4$. By hand: the factors $e^{\pm 2e_L}$ and $e^{\pm C_j(\frac{1}{n} + \ell_n)}$ of (F.52), which lie within 1 ± 0.01 for $j = 4$ on the cells $n \ge \epsilon c'$ once c is large, and are kept outside λ for $j = 1$.	Proposition 7.4; F.5
7	$\sup_{0<u<1} h_\infty^+(u) = h_\infty^+(\frac{1}{2}) = 6 - 4\log 3 \le 1.606$, so $\sup_{\mathrm{cell}} e^{\mathcal{H}_n^+} \le 5.0\, e^{94/n + C\ell_n}$ (F.34). Detuning adds $2\log(1 + 4\eta_0^2)$ for the two flanking pairs and $C_{\mathrm{det}}\eta_0^2$ for the far pairs (appendix F.3).	Closed form, by hand: each of the three pieces of h_∞^+ is largest at $u = \frac{1}{2}$. No covering is needed; the two numbers, $6 - 4\log 3 = 1.60555$ and $e^{1.606} = 4.9828\ldots < 5.0$, are evaluated in IA at 128 bits. $C_{\mathrm{det}} \le 16.6$ by hand (Lemma F.7).	Lemma 7.5(e); F.4, G.4

Table 4: The certified inequalities, for $(m, k_\infty, n_1, \eta_0) = (1, \frac{1}{4}, \frac{7}{4}, \frac{1}{4})$ and the outer factor sech^2 (section 7.2). IA: interval arithmetic on a covering of the stated range; bound obtained: the endpoint that the computation returns (appendix H.1). By hand: estimated without the computer. C and C_j are the absolute constants of (F.45), and 94 is the constant of (F.46). In rows 7 and 8, $h_\infty^\pm(u; \eta_0)$ are the limits of the hole functions with $j = 1$ as $n \to \infty$, at fixed position $u \in [0, 1]$ in the cell (section 7.5). In the last column E.2 stands for appendix F.2, and so on.

	Inequality	How it is obtained	Used in
8	For $0 < \eta_0 \le 0.3$ the minimum of $h^-_\infty(u;\eta_0)$ over $0 \le u \le 1$ is attained at $u \in \{0,1\}$, where its value is $2\log\eta_0 + \log(1+\eta_0^2) + I(0)$ with $I(0) = 4 - 3\log 3 + 4\log 2 = 3.4767\ldots \ge 3.476$ (F.37). Hence $e^{\mathcal{H}^-_n} \ge 32\,\eta_0^2\, e^{-C(\frac{1}{n}+\ell_n)}$, which enters (F.38). Only $c_T > 0$ is drawn from this row.	By hand (after (F.37)): monotonicity in η_0 reduces the claim to $G_L > 0$ on $(0, \frac{1}{2}]$ and $G_R > 0$ on $[\frac{1}{2}, 1)$, for two explicit functions; the end value is a closed form. IA, 128 bits, 16000 subintervals of $[0,1]$, mean-value form: $G_L' > 0$ on $[0, \frac{1}{4}]$, $G_L > 0$ on $[\frac{1}{4}, \frac{1}{2}]$, the mirror statements for G_R, and $I(0) > 3.476$.	Lemma 7.11; F.4
9	$1.3\,r\,(\log\rho_U)'(x_1^* + r) \le 0.95$ for $0 < r \le 0.64$, and $(\log\rho_U)'(x_1^* + r) \le 3.10 < \pi$ for $r \ge 0.18$.	IA, 128 bits. First bound: 4000 subintervals of $[2^{-10}, 0.64]$, and $[0, 2^{-10}]$ in the regularized form of appendix H.1, where the left side lies within 0.65 ± 0.002; bound obtained 0.9212. Second bound: 4000 subintervals of $[0.18, 8]$; bound obtained 3.0656. By hand: for $r \ge 8$, $(\log\rho_U)'$ decreases (Lemma F.1(b)).	F.1 (F.10); F.2 (Lemma F.6(c))
10	Tip expansions, with $u_1 = \operatorname{arcsinh} 1$: (a) $\operatorname{arccosh}\sinh(u_1+\delta) = 2^{3/4}\delta^{1/2}\big(1 + \delta\, e_1(\delta)\big)$ with $e_1(\delta) \in [0.0589, 0.105]$ for $0 < \delta \le 2$; (b) $-\frac{z^2}{3} \le \log\frac{\lvert\tanh z\rvert}{\lvert z\rvert} \le 0$ for all real $z \ne 0$; (c) $0 < (\log\tanh z)' \le 1.24$ for $z \ge u_1 - 0.25$.	(a) IA, 200 bits, 125 subintervals of $[0,2]$, in the regularized form of appendix H.1; $e_1(0^+) = \sqrt{2}/24 = 0.058926$, and the enclosures obtained lie in $[0.058906, 0.104993]$. (b) is proved by hand (Lemma F.3) and carries no mark. (c) $(\log\tanh z)' = 2/\sinh 2z$ decreases, and its value at $z = u_1 - 0.25$ is 1.22992; also IA, 2000 subintervals of $[u_1 - 0.25, 4]$.	F.1 (Lemmas F.2 and F.3), and through these F.2, F.4, F.5, F.7, G.2, G.4
11	$\hat R_{\rm vac}(100) \le 0.1021$ and $I_{\rm Lobe} \ge 94.47$ (G.17), and $\hat R_{\rm vac}(30) \le 0.1020$ (Lemma G.4), for the scaled vacuum ratio $\hat R_{\rm vac}(N_1)$ and the scaled lobe integral $I_{\rm Lobe}$ of (G.15). With the finite-c corrections and the cells beyond the hundredth, $R_{\rm vac} \le 0.1021 + 0.02$ (G.22); this is by hand and carries no mark.	IA, 80 bits; the integrals are enclosed in the mean-value form of appendix H.1, on 20000 subintervals of the lobe and 27400 of the cells $2, \ldots, 100$. Of the product over the pairs $k \ge n+2$, 3000 factors are explicit, and the rest lies in $[1, e^{U_n}]$ with the $U_n \le 1.5 \times 10^{-5}$ of the proof of Lemma G.4. Obtained: $I_{\rm Lobe} \in [94.4736, 94.4737]$, $\hat R_{\rm vac}(30) \in [0.101916, 0.101919]$, $\hat R_{\rm vac}(100) \in [0.102004, 0.102007]$. By hand (appendix G.5): the finite-c corrections, and the cells beyond the hundredth with $C_{\rm tail}(100) \le 282$ (G.20).	Proposition 7.13; G.3, G.5

For reference, not certified (closed forms): $\kappa_{\rm tip} = 4 \cdot 2^{3/4}/(9\sqrt{\pi}) = 0.4217111$, and $(U+L)(x_1^* - \delta) = -2.649689\,\delta^{3/2}\big(1 + O(\delta)\big)$ as $\delta \downarrow 0$, with coefficient $2\pi\kappa_{\rm tip}$ (Lemma 6.7).

Table 4: (continued)

is at $P/c = 1.5$, the reach of the chain $c = 2048$, the two test chains with five levels left in the window err by at most $5 \times 10^{-7} c$, a tenth of the σ quoted for $c = 2048$.

I Limit profiles: proofs for section 10

This appendix proves the statements of section 10: three inequalities at finite c, which carry all the input from section 6 (appendix I.1); Lemma 10.1, which is a quotation (appendix I.2); Lemma 10.2 and Proposition 10.3 (appendix I.3); and Theorem 7 (appendix I.4). Beyond appendix I.1 only the potential theory of subharmonic functions in the plane is used [63, 72].

Throughout, the notation is that of section 10.1, $\mathrm{d}A$ is the area measure in the b-plane, and U is the extremal potential extended across the slits. We use these properties of U (Lemma 6.5, Definition 6.6, Lemma 6.7 and (C.15)): it is continuous on $\mathbb{S}$ and harmonic on D; $U \le 0$; $U = -L$ on the slits and $U < -L$ on $(-x_1^*, x_1^*)$; and it is subharmonic on $\mathbb{S}$, its charge $\frac{1}{2\pi}\nabla^2 U$ being the measure $\rho_U(x)\,\mathrm{d}x \otimes \delta_{y=0}$ on the slits $|x| \ge x_1^*$, with the density ρ_U of (6.21).

I.1 Three inequalities at finite c

Lemma I.1 (proved). *Let $c \geq 40$ and $g \in \bar{\mathcal{A}} \setminus \{0\}$.*

(a) $\sup_{\mathbb{S}} u_g \leq (2\log c' + C)/c'$, *with an absolute constant C.*

(b) *For every compact $Q \subset D$, $u_g \leq U + C_Q(1 + \log c')/c'$ on Q, with the constant C_Q of Proposition 6.4.*

(c) *If g is weakly feasible and $x_1(g) \leq x_{\max}$, then $x_1(g) > 0$ and $\max_{0\leq x\leq x_1(g)}\bigl(u_g(x) + L(x)\bigr) \geq -\bigl(\log c' + \log(32\pi^2 x_{\max}^4/3)\bigr)/c'$.*

Proof. (a) is Lemma C.4 on the closed strip, $\sup_{\bar{\mathbb{S}}}|G| \leq C\,a\,c'M[g]$, after taking the logarithm and dividing by c'. (b) is Proposition 6.4, with $U_{x_1^*} = U$ by Lemma 6.5. (c) Both sides are unchanged when g is multiplied by a positive constant, so let $M[g] = 1$. Write $t_1 = t_1(g)$; it is positive, because no nonzero functional is weakly feasible at $T \leq 0$ (section 2.4). The half-mass condition (2.16) says that $\int_0^{t_1} g_- V \,\mathrm{d}t \geq \frac{1}{2}$. By Lemma B.2(d), at $t = c'x^2/3 > 0$ we have $g_- V \leq |g|\,V \leq \frac{4\pi^2 t}{a}\, e^{c'L(x)}|G(x)| = \frac{4\pi^2 t}{a}\, e^{c'(u_g(x)+L(x))}$. Let $m := \max_{[0,x_1(g)]}(u_g + L)$, which is a maximum because $|G|\,e^{c'L}$ is continuous. Bounding the integrand by its supremum on $(0, t_1]$, and using $t_1 = c'x_1(g)^2/3$ and $a = c'/12$, we get $\frac{1}{2} \leq t_1 \cdot \frac{4\pi^2 t_1}{a}\, e^{c'm} = \frac{16\pi^2}{3}\, c'\, x_1(g)^4\, e^{c'm} \leq \frac{16\pi^2}{3}\, c'\, x_{\max}^4\, e^{c'm}$, and taking the logarithm gives (c). □

I.2 Proof of Lemma 10.1

We check that the profiles are uniformly bounded above, quote the compactness theorem for subharmonic functions, and pass from potentials to charges by integrating by parts.

The theorem quoted [72, Thms. 3.2.12–3.2.13]. Let $X \subset \mathbb{R}^2$ be open and connected, and let $u_j \not\equiv -\infty$ be subharmonic functions on X, bounded above on every compact subset of X uniformly in j. Then either $u_j \to -\infty$ uniformly on every compact subset of X, or a subsequence converges in $L^1_{\mathrm{loc}}(X)$. If $u_j \to u$ in $L^1_{\mathrm{loc}}(X)$, then u is almost everywhere equal to a subharmonic function, again called u, and for every compact $K \subset X$ and every continuous $f : K \to \mathbb{R}$

$$\limsup_{j\to\infty} \sup_K (u_j - f) \leq \sup_K (u - f). \tag{I.1}$$

Proof of Lemma 10.1. Each u_j is subharmonic on $\mathbb{S}$ and not identically $-\infty$, since G_j is holomorphic and not identically zero, and, for j so large that $c_j \geq 40$, $\sup_{\mathbb{S}} u_j \leq (2\log c_j' + C)/c_j'$ by Lemma I.1(a). So the u_j are uniformly bounded above from some j on, and the theorem applies with $X = \mathbb{S}$, which is connected. Either (i) holds, or there is a subsequence with $u_j \to u$ in $L^1_{\mathrm{loc}}(\mathbb{S})$ and u subharmonic; $u \not\equiv -\infty$ because u is locally integrable. For the charges write $\mathfrak{n}_j := \mathfrak{n}_{g_j}$ and $\mathfrak{n}_u := \frac{1}{2\pi}\nabla^2 u$. For a smooth φ of compact support in $\mathbb{S}$, $\int \varphi\,\mathrm{d}\mathfrak{n}_j = \frac{1}{2\pi}\int u_j\,\nabla^2\varphi\,\mathrm{d}A \to \frac{1}{2\pi}\int u\,\nabla^2\varphi\,\mathrm{d}A = \int \varphi\,\mathrm{d}\mathfrak{n}_u$. Choosing $\varphi \geq 0$ with $\varphi \geq 1$ on a compact K shows that $\sup_j \mathfrak{n}_j(K) < \infty$, and then the convergence extends from smooth to continuous φ of compact support by uniform approximation: $\mathfrak{n}_j \to \mathfrak{n}_u$ vaguely. □

We record the standard consequence that is used for Theorem 7(b); it follows by testing against continuous functions that decrease to $\mathbf{1}_K$ and, for the second statement, also against ones that increase to the indicator of the interior of K. For compact $K \subset \mathbb{S}$,

$$\limsup_{j\to\infty} \mathfrak{n}_j(K) \leq \mathfrak{n}_u(K), \qquad \text{and} \qquad \mathfrak{n}_j(K) \to \mathfrak{n}_u(K) \quad \text{if } \mathfrak{n}_u(\partial K) = 0. \tag{I.2}$$

I.3 Proofs of Lemma 10.2 and Proposition 10.3

For the majorant we pass Lemma I.1(b) to the limit almost everywhere and remove the exceptional set by averaging over small disks. For the contact point we follow the points at which Lemma I.1(c) holds and use (I.1): a limit cannot lose what the u_j have at nearby points.

Proof of Lemma 10.2. Let $u_j \to u$ in $L^1_{\mathrm{loc}}(\mathbb{S})$. A subsequence converges almost everywhere, so Lemma I.1(b) gives $u \le U$ almost everywhere on every compact $Q \subset D$. Hence $u \le U$ almost everywhere on $\mathbb{S}$, because the slits have zero area. For $b \in \mathbb{S}$ and small r the sub-mean-value property of u on the disk $B(b,r)$ gives $u(b) \le \frac{1}{\pi r^2}\int_{B(b,r)} u \,\mathrm{d}A \le \frac{1}{\pi r^2}\int_{B(b,r)} U \,\mathrm{d}A \to U(b)$ as $r \to 0$, since U is continuous on $\mathbb{S}$. The rest follows from $U \le 0$, $U = -L$ on the slits and $U < -L$ on $(-x_1^*, x_1^*)$. □

Proof of Proposition 10.3. By Lemma I.1(c) with $x_{\max} = x_\infty + 1$, for large j there are points $x_j \in [0, x_1(g_j)]$ with $u_j(x_j) + L(x_j) \ge -\epsilon_j$, where $\epsilon_j := (\log c_j' + \log(32\pi^2(x_\infty+1)^4/3))/c_j' \to 0$. Let $K := [0, x_\infty{+}1]$, which contains x_j for large j. If alternative (i) held, then $u_j(x_j) \le \sup_K u_j \to -\infty$, in contradiction with $u_j(x_j) \ge -L(x_j) - \epsilon_j \ge -\frac{2\pi}{3}(x_\infty+1) - 1$. So (i) does not occur. Let u be a limit profile. Passing to a further subsequence, $u_j \to u$ in $L^1_{\mathrm{loc}}(\mathbb{S})$ and $x_j \to x_0 \in [0, x_\infty]$. Fix $r \in (0, \frac12)$ and apply (I.1) with $K_r := \bar B(x_0, r)$ and $f(b) := -L(\operatorname{Re} b)$, which we write $-L$. Since $x_j \in K_r$ for large j, $\sup_{K_r}(u+L) \ge \limsup_j \sup_{K_r}(u_j + L) \ge \limsup_j (u_j(x_j) + L(x_j)) \ge 0$. As $r \downarrow 0$ the left side decreases to $u(x_0) + L(x_0)$, because $u + L$ is upper semicontinuous. With Lemma 10.2, $-L(x_0) \le u(x_0) \le U(x_0) \le -L(x_0)$, so all three are equal. Finally $U(x_0) = -L(x_0)$ fails for $0 \le x_0 < x_1^*$ by Lemma 6.7, so $x_0 \ge x_1^*$. □

I.4 Proof of Theorem 7

We reduce the theorem to the claim that every limit profile u of the sequence is equal to U, and prove the claim for the deficit $\theta := U - u$ in three steps: a dichotomy on the slit strip D (Step 1), the exclusion of $\theta > 0$ by two incompatible bounds on the means of θ over small circles about the tip (Step 2), and the points of the slits (Step 3).

Reduction. By Proposition 10.3 with $x_\infty = x_1^*$, every subsequence has a further subsequence that converges in $L^1_{\mathrm{loc}}(\mathbb{S})$ to a limit profile u whose contact point lies in $[x_1^*, x_1^*]$, that is, $u(x_1^*) = U(x_1^*)$. Suppose that every such u is equal to U. Since convergence in $L^1_{\mathrm{loc}}(\mathbb{S})$ is convergence in a metric, the whole sequence then converges to U, which is (a). The integration by parts in the proof of Lemma 10.1, applied to the whole sequence, then gives $\mathfrak{n}_j \to \frac{1}{2\pi}\nabla^2 U = \rho_U \,\mathrm{d}x \otimes \delta_{y=0}$ vaguely, which is (10.2). This measure gives no mass to a compact set disjoint from the slits, and none to the boundary of a rectangle $[x_a, x_b] \times [-y_0, y_0]$, since it has a density on the real axis. So (I.2) gives the two counting statements of (b), after multiplication by c_j'. For (c), the map $b \mapsto c_j' b^2/3$ is injective and holomorphic on $\operatorname{Re} b > 0$, and $G_j(b) = g_j(c_j' b^2/3)$, so the zeros of G_j in the rectangle and the zeros of g_j in its image correspond, with multiplicities. The image of $x + iy$ is $\frac{c_j'}{3}(x^2 - y^2) + \frac{2i}{3}c_j' xy$. With $\xi = x^2/3$, $\mathrm{d}x = \frac{3}{2x}\,\mathrm{d}\xi$ and $\rho_V = 3\rho_U/4x$ we have $\int_{x_a}^{x_b} \rho_U(x)\,\mathrm{d}x = \int_{\xi_a}^{\xi_b} 2\rho_V(\xi)\,\mathrm{d}\xi$.

It remains to prove the claim. Let u be a limit profile with $u(x_1^*) = U(x_1^*)$, and $\theta := U - u$ on $\mathbb{S}$. By Lemma 10.2, $\theta \ge 0$. It is lower semicontinuous ($-\theta$ is upper semicontinuous: at a point θ can jump down, never up), with values in $[0, +\infty]$, it is not identically $+\infty$, and $\theta(x_1^*) = 0$. On D it is superharmonic, because there U is harmonic. Let $r_0 := x_1^*/2$, so that the disk $B := B(x_1^*, r_0)$ lies in $\mathbb{S}$ and does not meet the left slit.

Step 1: dichotomy. Since D is connected, the strong minimum principle [63, Thm. 2.3.1] says that a non-negative superharmonic function on D that vanishes at one point of D vanishes identically. So either $\theta \equiv 0$ on D, or $\theta > 0$ at every point of D.

Step 2: $\theta > 0$ on D is impossible. Suppose that $\theta > 0$ on D. Let $\Omega_0 := B \setminus [x_1^*, x_1^* + r_0)$, a simply connected subdomain of D, and let $A := \{x_1^* + r_0 e^{i\phi} : \frac{\pi}{4} \le \phi \le \frac{3\pi}{4}\}$, a compact arc in D. Since θ is lower semicontinuous and positive on A, $\theta_A := \min(1, \min_A \theta)$ lies in $(0, 1]$. The local coordinate $w := \sqrt{b - x_1^*}$, with $\arg(b - x_1^*) \in (0, 2\pi)$, maps Ω_0 conformally onto the half-disk $H_0 := \{|w| < R,\ \operatorname{Im} w > 0\}$, $R := \sqrt{r_0}$. It extends continuously to the boundary, maps the two lips of the slit and the tip to the diameter $[-R, R]$, and maps A to $A' := \{Re^{i\phi} : \frac{\pi}{8} \le \phi \le \frac{3\pi}{8}\}$.

For $|w| < R$ let

$$\omega(w) := \frac{1}{2\pi}\int_{\pi/8}^{3\pi/8} (R^2 - |w|^2)\Big[\frac{1}{|Re^{i\phi} - w|^2} - \frac{1}{|Re^{-i\phi} - w|^2}\Big]\mathrm{d}\phi, \tag{I.3}$$

the Poisson integral in the disk $|w| < R$ of the boundary function that is $+1$ on A', -1 on the mirror image of A' in the real axis, and 0 elsewhere. It is harmonic, and odd under $w \mapsto \bar{w}$, so it vanishes on the diameter. On H_0 it satisfies $0 \le \omega \le 1$: the bracket is non-negative there, because $|Re^{-i\phi} - w|^2 - |Re^{i\phi} - w|^2 = 4R\sin\phi\,\operatorname{Im} w \ge 0$, and its first term alone gives the Poisson integral of an indicator function. It tends to 0 at every boundary point of H_0 outside A'. Let $h(b) := \theta_A\,\omega(w(b))$ on Ω_0; it is θ_A times the harmonic measure of A in Ω_0. Now $\theta - h$ is superharmonic on Ω_0, and its lower limit at every boundary point of Ω_0 is non-negative: at points of A because $\theta \ge \theta_A \ge h$ and θ is lower semicontinuous; elsewhere because $\theta \ge 0$ and $h \to 0$, the two lips of the slit being approached separately. By the minimum principle ([63, Thm. 2.3.1] applied to $h - \theta$ on the bounded domain Ω_0), $\theta \ge h$ on Ω_0.

Lower bound. Let $|w| \le R/2$ and $\operatorname{Im} w > 0$. In (I.3) we have $R^2 - |w|^2 \ge \frac{3}{4}R^2$ and $|Re^{\pm i\phi} - w| \le \frac{3}{2}R$, so the bracket is at least $4R\sin\phi\,\operatorname{Im} w/(\frac{3}{2}R)^4$. Integrating $\sin\phi$ over $[\frac{\pi}{8}, \frac{3\pi}{8}]$ gives $\omega(w) \ge \frac{1}{2\pi}\cdot\frac{3}{4}R^2\cdot 4R\operatorname{Im} w\,(\cos\frac{\pi}{8} - \cos\frac{3\pi}{8})/(\frac{3}{2}R)^4 = c_2\operatorname{Im} w/R$, where $c_2 := 8(\cos\frac{\pi}{8} - \cos\frac{3\pi}{8})/(27\pi) = 0.0510$. On the circle $b = x_1^* + \epsilon e^{i\phi}$, $0 < \phi < 2\pi$, with $0 < \epsilon \le r_0/4$, we have $|w| = \epsilon^{1/2} \le R/2$ and $\operatorname{Im} w = \epsilon^{1/2}\sin(\phi/2)$. Since $\theta \ge h = \theta_A\,\omega$ and $\int_0^{2\pi}\sin(\phi/2)\,\mathrm{d}\phi = 4$, the mean of θ over this circle is at least $\theta_A\,(c_2/R)\,\epsilon^{1/2}\cdot\frac{4}{2\pi}$, which is the first inequality in (I.4).

Upper bound. Since u is subharmonic on $\mathbb{S}$, $u(x_1^*)$ is at most the mean of u over the circle of radius ϵ about x_1^*; and $u(x_1^*) = U(x_1^*)$. Hence the mean of θ over that circle is at most the mean of U minus $U(x_1^*)$. The latter is given by the Poisson–Jensen formula at the center [63, §4.5]: it equals $\int_0^\epsilon \mu(\sigma)\,\mathrm{d}\sigma/\sigma$, where $\mu(\sigma)$ is the charge $\frac{1}{2\pi}\nabla^2 U$ of the disk $B(x_1^*, \sigma)$, that is, $\mu(\sigma) = \int_{x_1^*}^{x_1^*+\sigma}\rho_U\,\mathrm{d}x$ for $\sigma \le r_0$. On $[x_1^*, x_1^* + r_0]$ we have $\sinh\pi x - 1 \le \kappa_2(x - x_1^*)$ with $\kappa_2 := \pi\cosh\big(\pi(x_1^* + r_0)\big)$, because $\sinh\pi x_1^* = 1$; and $\operatorname{arccosh}(1+\delta) \le \sqrt{2\delta}$ for $\delta \ge 0$. So $\rho_U(x) \le \frac{4}{3\pi}\sqrt{2\kappa_2(x - x_1^*)}$ and $\mu(\sigma) \le \frac{8}{9\pi}\sqrt{2\kappa_2}\,\sigma^{3/2}$, and the mean of θ is at most $C_4\,\epsilon^{3/2}$ with $C_4 := \frac{2}{3}\cdot\frac{8}{9\pi}\sqrt{2\kappa_2}$. Together,

$$\frac{2\,\theta_A\,c_2}{\pi R}\,\epsilon^{1/2} \;\le\; \frac{1}{2\pi}\int_0^{2\pi}\theta(x_1^* + \epsilon e^{i\phi})\,\mathrm{d}\phi \;\le\; \frac{16\sqrt{2\kappa_2}}{27\pi}\,\epsilon^{3/2} \qquad (0 < \epsilon \le r_0/4), \tag{I.4}$$

which is false for small ϵ. So $\theta \equiv 0$ on D.

Step 3: the slits. We have $u = U$ on D. At a point x of a slit, upper semicontinuity of u and continuity of U give $u(x) \ge \limsup_{b\to x,\ b\in D} u(b) = U(x)$, and $u(x) \le U(x)$ by Lemma 10.2. Hence $u = U$ on all of $\mathbb{S}$, which is the claim. This completes the proof of Theorem 7.

Notation index

Central charge, weights, variables. At the right: the place of definition (§: section or subsection).

c', a, t, t_0	$c - 1$; $c'/12$; $\Delta - a$, so that the BTZ threshold is at $t = 0$; position $-a$ of the vacuum	(2.1), §2.1
β; $\hat{Z}$, d_n	inverse temperature, and nothing else; reduced partition function; degeneracies, $d_n > 0$	(2.2)
Δ_1	gap of an admissible spectrum, $a + \min_n t_n$; primaries with $t_n < 0$ are *light*	Def. 2.1
$b = x + iy$; G	$\sqrt{3t/c'}$, not the Liouville coupling; physical axis $b = x \ge 0$, vacuum at $\pm\frac{i}{2}$; $G(b) = g(c'b^2/3)$	(2.17)
$\mathbf{r} \in \mathbb{R}^2$	plane with $t = \lvert\mathbf{r}\rvert^2/2$, in which a functional is radial and $\hat{g} = -g$	(2.8), (2.9)
P_L, $\bar{P}_L$, Q_L	Liouville momenta and background charge, in two remarks only	Rems. 2.2, 2.4
ξ; ξ_1, Λ	Δ/c in §3, $t/c' = b^2/3$ from §4 on; a certified slope Λ has $1/\Lambda = \frac{1}{12} + \xi_1$, $\xi_1 = x_1^2/3$	(4.1), (2.19)
$L(x)$	$\frac{2\pi}{3}\lvert x\rvert$, so $e^{c'L} = e^{4\pi\sqrt{at}}$; the *Cardy line* is the graph of $-L$ against x	(2.18)
$\mathbb{S}$, $E_\pm$; v	strip $\lvert y\rvert < \frac{1}{2}$ of the b-plane, its edges $y = \pm\frac{1}{2}$; edge coordinate, $b = v + \frac{i}{2}$	§2.5, (7.3)
$\mathbb{H} \ni z$	upper half-plane; it uniformizes the curve and the slit strip	(4.11), (6.12)

Functionals, kernels, the linear program

ω; Ξ_β, e_β	functional on functions of β (§2 only); crossing kernel $e_\beta - \beta^{-1}e_{1/\beta}$, $e_\beta = e^{-2\pi\beta t}$	(2.4), §8.2

g; g_{vac} a functional, as the function $\omega[\Xi_\beta(t)]$ of t; its vacuum value, $-\int_0^\infty g\,\rho_C\,\mathrm{d}t$ (2.5), (2.15)

$t_1(g)$, $x_1(g)$ last sign change of g, the gap bound that g certifies; $\sqrt{3t_1/c'}$ Def. 2.3, (2.17)

P, pol_P; $t_1^{(P)}$, $\Delta_1^{(P)}$ order, polynomial in $g=\mathrm{pol}_P(t)e^{-2\pi t}$; $\inf t_1(g)$ at order P; $a+t_1^{(P)}$ ($P=\infty$: limits) (2.6), §2.2

ψ_k Laguerre functions $L_k(4\pi t)e^{-2\pi t}$, $\hat\psi_k=(-1)^k\psi_k$ (2.10)

K_α, V, ρ_C Cardy kernel $I_0(4\pi\sqrt{\alpha t})$, weight $K_a-2K_{a-1}+K_{a-2}$ (no subscript), density $2\pi V$ (2.11), (2.12)

$\mathrm{as}(z)$; ε_V, C_V Bessel asymptote $e^z/\sqrt{2\pi z}$; remainder of V against $\mathrm{as}(c'L)$, $|\varepsilon_V|\le C_V/c'$ §B.4, (B.7)

$g_\pm$, $M[g]$ $\max(\pm g,0)$; Cardy-weighted mass $\int_0^\infty |g|\,V\,\mathrm{d}t$ (2.16)

$\bar{\mathcal{A}}$; T_V, Δ_1^{best} class of functionals; least T at which some $g\in\bar{\mathcal{A}}$ is feasible, and T_V+a (V: Virasoro) Def. 2.5, (2.20)

x_1^*, ξ_1^*, Λ_V $\mathrm{arcsinh}(1)/\pi=0.2805499$; $(x_1^*)^2/3=0.0262361$; $12\pi^2/(\pi^2+4\,\mathrm{arcsinh}^2\,1)=9.1266340$ Thm. 1

t_{int}; $\varphi(t)$ interior zero of the optimal functional below t_1; prefactor in $g=\varphi\,e^{-2\pi t}$ at $t=O(1)$ §2.5, §4.6

The curve and its endpoint (Part II)

$\mathcal{S}$, τ; y_E, $\varkappa$ WKB exponent; local modular parameter $\mathcal{S}'/2\pi i$; $\mathrm{Im}\,\tau_\pm$ (band); Cardy height $2b\,y_E$ (4.1), (4.5), (4.8)

ρ, ρ_0, w, ι, W, $\mathcal{F}$, E §3 only: double zeros per unit Δ; S-image of the vacuum; $\pi^2\xi\rho$; $\hat S_{U(1)}$ in (ρ,w); the curve as $w=W(\rho)$ or $\rho=\mathcal{F}(w)$; even factor of $\mathcal{F}$ (3.2), (3.7), (3.9)–(3.12)

$\hat S_{U(1)}$, $\hat S$; Σ sheet maps, the Fourier transform acting on WKB sheets; the spectral curve (B) (3.6), (4.2)

p; R, σ WKB momentum $-\tau b$, on Σ the function (6.16); quarter-turn $(p,b)\mapsto(b,-p)$; exchange $(p,b)\mapsto(-p-i,b)$ of the band sheets (4.3), (4.4), §4.3

γ_k, $\tilde\Omega$; X, Y band arc γ_0 and its images $\mathsf{R}^k\gamma_0$, the region they bound on Σ; coordinates $e^{-\pi(p\pm b)}$ (4.10), (4.12)

A_{opt}, A_m; t_2 $c^{1/3}$ coefficients: conjectured optimum 0.27666; comb with m omitted sites; second extremal level (4.18), (7.6)

Λ_{fit}, γ_{fit}; Λ_{meas}, $\xi^*_{1,\mathrm{meas}}$ parameters of a logarithmic fit; measured slope and endpoint §5.2, (5.2)

Potential theory (Part III)

D_s, U_s; D, U, U_0 strip slit along $|x|\ge s$, with *tips* $\pm s$; harmonic function on it, 0 on $E_\pm$ and $-L$ on the slits; the case $s=x_1^*$, U being the *extremal potential*; $U(0)=-0.388748$ (6.11), (6.14), (6.17)

u_g; C_Q profile $\frac{1}{c'}\log(|G|/M[g])$; constant in $u_g\le U+C_Q(1+\log c')/c'$ on a compact $Q\subset D$ (6.13), (6.15)

$\omega_b(E)$, $\mathrm{d}\omega_b/\mathrm{d}x$ harmonic measure of a boundary set E seen from b; its density on a slit, both lips added §6.4

$\mathfrak{n}_g$; ζ, m_ζ Riesz measure $\frac{1}{2\pi}\nabla^2u_g$; a zero of G, its multiplicity (6.10), (6.7)

ρ_U; ρ_V *zero law* $\frac{4}{3\pi}\,\mathrm{arccosh}(\sinh\pi|x|)$, $|x|\ge x_1^*$: charge of U (not $U(1)$), zeros per unit x and c'; $\frac{3\rho_U}{4x}$, double zeros per unit t Def. 6.6, (4.16)

N, κ_{tip}; γ_{tip} $N(x)=\frac12\int_{x_1^*}^x\rho_U\simeq\kappa_{\mathrm{tip}}(x-x_1^*)^{3/2}$ counts sites, $\kappa_{\mathrm{tip}}=4\cdot2^{3/4}/(9\sqrt{\pi})=0.4217111$; coefficient of $\sqrt{s-|x|}$ in U_s+L (6.22), §6.6

$\kappa(\delta)$; C_δ, C_{conc}, C_H Cardy deficit $-(U+L)(x_1^*-\delta)$; constant in (6.1), $\le C_{\mathrm{conc}}\delta^{-5}$; entropy constant (6.24), (C.6)

$c_0(\Lambda)$, c_0^{opt}, c_0^{att} central charges from which Thm. 4 (first part; rate), Thm. 5 hold; not computed; $c_0^{\mathrm{att}}\ge40$ §6.8

The functional of Part IV and its comb

$T_\zeta(b)$ Blaschke factor of the strip, zeros $\pm\zeta$, facts (T1)–(T4); T with a point as subscript is always this (7.1)

F, v_0, b_0 edge function $p(v+\frac{i}{2})=\frac{1}{\pi}\,\mathrm{arcsinh}(\cosh\pi v)$; its inverse, $\rho_U=\frac43 v_0$; saddle $v_0+\frac{i}{2}$ (7.3)

χ_n, ℓ_n, ε_n, u sites: $c'N(\chi_n)=n-\frac14$; length of cell $n=(\chi_n,\chi_{n+1})$; detuning height $\eta_0\ell_n$; $(x-\chi_n)/\ell_n$ §7.2, §7.5

m, k_∞, n_1, η_0 omitted sites, node phase, onset index $m+1-k_\infty=c'N(\chi_2)$, detuning; fixed to $(1,\frac14,\frac74,\frac14)$ §7.2

B, h_0, g; B^0, h_0^0 comb, seed $\mathrm{sech}^2(\frac{\pi b}{2})B$, functional $\frac12(h_0-\hat h_0)$ of Thm. 5; the same at $\eta_0=0$ (7.4)

$t_\star$, A_1; ℓ_c, ς $c'\chi_2^2/3=\xi_1^*c'+A_1c'^{1/3}+\dots$, $A_1=0.483$; Airy length $(\kappa_{\mathrm{tip}}c')^{-2/3}$; $(x-x_1^*)/\ell_c$ (7.5), §7.1, Lem. 7.5

θ_{on}, x_I onset exponent 0.2; hand-off point $x_1^*+c'^{-\theta_{\mathrm{on}}}$ between Regions I and II §7.1

ν, Ψ; $\hat\Psi$ site index $c'N(x)+\frac14-2$, comb phase $2\pi\nu-\pi$; phase of $\hat h_0$ (7.10), (E.11)

Env, Π exact envelope, $|h_0^0|=\mathrm{Env}\sin^2\pi\nu$; detuning factor $|B|/|B^0|\ge1$ (7.11)

$\mathcal{P}$, $\mathcal{P}_Y$; $\mathcal{J}_{\mathrm{end}}$, C_J potential of the absent charge on $[x_1^*,\chi_2]$, on $[x_1^*,Y]$; end correction, $0\le\mathcal{J}_{\mathrm{end}}\le C_J\le0.65$ (7.12), (7.13)

Lev, λ level $4\,\mathrm{sech}^2(\frac{\pi x}{2})e^{-c'L+c'\mathcal{P}+\mathcal{J}_{\mathrm{end}}}$, the unit of all certified ratios; Env/Lev (7.14), (7.16)

$\mathcal{H}^\pm_{n,j}$, $h^\pm_j$; C_j hole functions of cell n, with j pairs kept on each side of x; their limits ($h^\pm_\infty$ if $j=1$); $|\mathcal{H}^\pm_{n,j}-h^\pm_j|\le C_j(\frac1n+\ell_n)$, $C_j=Cj^2\log(2j+2)$; $\frac{94}{n}+C\ell_n$ if $j=1$ (F.39)–(F.42), (F.45), (F.46)

e_L, C_L; C_{det}; c_T midpoint remainder of the far-left sites, its supremum on the cells $n\ge6$, $C_L\le0.006$ (Lemma F.6(d)); detuning constant, $C_{\mathrm{det}}\le16.6$; overshoot constant, of which only $c_T>0$ is used (F.23), Lem. F.7, (7.31)

Φ_0, Φ_1; C_{EM} edge phases, $\log B=c'\Phi_0+\Phi_1$; Euler–Maclaurin constant (7.22), (D.10)

k_x, ε_H; α_x, s_{ch} Hankel wavenumber $\frac{4\pi}{3}c'x$, remainder; curvature, chord slope of the phase (7.8), (7.9), (E.5)

Amp, $\varepsilon_{\mathrm{sd}}$; C_{glob} amplitude of $\hat h_0$, remainder under (SD1)–(SD4) (§E.1); global constant 2^5 (7.23)–(7.25)

ϱ, ϱ_∞ ratio Amp/Lev and its c-independent majorant (7.26)

μ_j; μ_n^{I}, μ_{slope} floor constants, j pairs kept exactly on each side; floors near the onset (7.27), (7.32), (7.33)

Lobe, Band; R_{vac} integrals of h_0V over $(0,t_\star)$ and $(t_\star,\infty)$; vacuum ratio, Band $\le R_{\mathrm{vac}}|\mathrm{Lobe}|$ (7.34), (7.35)

Certification (§8)

$\mathfrak{m}$; $\mathcal{N}_Z$, C_Z signed spectral measure $\sum_n d_n\delta_{t_n}-\rho_C\,\mathrm{d}t$, facts (Z1)–(Z4), (St); counting function, $1+\hat Z(1)$ (8.1), §8.2

ϖ; Ab_r, β_r $\frac{\beta-1}{\beta+1}$; Abel mean of ratio $r<1$, contracted modulus with $\varpi(\beta_r)=r\varpi(\beta)$ (8.3), (8.6), (8.8)

$W_{q,\ell}$, ℓ_a weights $(1+4\pi t)^q e^{\ell\sqrt{4\pi t}}$; Cardy exponent $2\sqrt{\pi a}$ (8.2)
x_∞, x_0; θ limit of $x_1(g_j)$ along a sequence g_j, contact point; deficit $U-u$ of a limit profile u Prop. 10.3, §10.2

Letters with two meanings. j: pairs kept (§7, App. F), sequence index (§10, App. I). δ: distance below the tip (§6, App. C), above it in the variable πx (§F.1). r: Abel ratio (§8), distance from a tip (Lem. 7.5). y: $\operatorname{Im}\tau$, the *height* of a sheet (§3, §4), $\operatorname{Im} b$ (elsewhere). E: boundary set, edges $E_\pm$, factor $E(w)$. a, u, σ: also a real label in χ_a, and $4\pi t$, $\sqrt{4\pi t}$ in §8. Distinct: $W(\rho)$, $W_{q,\ell}$; e_β, e_L, $e_1(\delta)$; ω, ω_b; $\kappa(\delta)$, κ_{tip}, $\varkappa$. Bare ε, ϵ: local to a statement; η: Dedekind function (§2.1 only); ϱ: a ratio, not a density; fraktur letters: measures.

Asymptotic relations. $A \simeq B$: $A/B \to 1$ in the limit indicated. $A \asymp B$ in a proof (§7, the appendices): $C^{-1}B \le A \le CB$ with a constant $C \ge 1$ that does not depend on c or on the point x; it may depend on the fixed parameters of the construction, and on a parameter that is named at that place. $A \lesssim B$: $A \le CB$ with such a C (in App. D it may depend on δ_1); $A \gtrsim B$: $B \lesssim A$. In §3 and §4, $\asymp$ keeps the exponential order in c only. With explicit numbers on the right ($c' \lesssim 414$), $\lesssim$ reads "at most, approximately".

Status tags (legend at the end of §1.3)**.** [PROVED], [PROVED, COMPUTER-ASSISTED], [CONJECTURE], [HEURISTIC], [NUMERICAL], [ORIENTATION], on a statement or a section; ⟨cert⟩ marks a certified inequality, a row of Table 4.

Terminology. *Gap*: Δ_1 only; two sites bound a *cell*. *BTZ threshold*: $t=0$ only; a functional certifies a *gap bound*. *Feasible at* T, *weakly feasible*: Def. 2.3. *Lobe interval* $[0,t_1)$, with the negative *lobe* of g; *band*: beyond t_1 (§2.5). *Envelope*: $|g|_{\text{env}}$ of an oscillating $|g|$, and Env; U is a *majorant* of profiles. *Edges*: $E_\pm$ only; the slits end at *tips*. *Onset*: near the first kept site χ_2 (§7.1); *onset index*: n_1. *Optimality*, *attainment*: the halves of Thm. 1 (§2.6).

References

[1] S. Hellerman, *A universal inequality for CFT and quantum gravity*, *JHEP* **08** (2011) 130 [0902.2790].

[2] M. Bañados, C. Teitelboim and J. Zanelli, *The black hole in three-dimensional space-time*, *Phys. Rev. Lett.* **69** (1992) 1849 [hep-th/9204099].

[3] E. Witten, *Three-dimensional gravity revisited*, [0706.3359].

[4] A. Maloney and E. Witten, *Quantum Gravity Partition Functions in Three Dimensions*, *JHEP* **02** (2010) 029 [0712.0155].

[5] C.A. Keller and A. Maloney, *Poincaré Series, 3D Gravity and CFT Spectroscopy*, *JHEP* **02** (2015) 080 [1407.6008].

[6] D. Friedan and C.A. Keller, *Constraints on 2d CFT partition functions*, *JHEP* **10** (2013) 180 [1307.6562].

[7] D. Friedan, A. Konechny and C. Schmidt-Colinet, *Lower bound on the entropy of boundaries and junctions in 1+1d quantum critical systems*, *Phys. Rev. Lett.* **109** (2012) 140401 [1206.5395].

[8] S. Collier, Y.-H. Lin and X. Yin, *Modular bootstrap revisited*, *JHEP* **09** (2018) 061 [1608.06241].

[9] H. Cohn, D. Dong and F. Gonçalves, *Sign uncertainty principles and low-degree polynomials*, *Proc. Amer. Math. Soc. Ser. B* **11** (2024) 224 [2210.01684].

[10] T. Hartman, D. Mazáč and L. Rastelli, *Sphere packing and quantum gravity*, *JHEP* **12** (2019) 048 [1905.01319].

[11] N. Afkhami-Jeddi, T. Hartman and A. Tajdini, *Fast conformal bootstrap and constraints on 3d gravity*, *JHEP* **05** (2019) 087 [1903.06272].

[12] N. Afkhami-Jeddi, H. Cohn, T. Hartman, D. de Laat and A. Tajdini, *High-dimensional sphere packing and the modular bootstrap*, *JHEP* **12** (2020) 066 [2006.02560].

[13] OpenAI, "Ten Advances in Mathematics and Theoretical Computer Science." Chapter 1: *Exponential growth rate of the Cohn–Elkies sphere packing linear program*. Released 1 August 2026, updated edition 6 August 2026, https://cdn.openai.com/pdf/ten-proofs-oai.pdf, 2026.

[14] R. Edwin, *Fourier inequalities and sign uncertainty*, [2505.15994].

[15] H. Cohn and N. Elkies, *New upper bounds on sphere packings I*, *Ann. of Math.* **157** (2003) 689 [math/0110009].

[16] R. Rattazzi, V.S. Rychkov, E. Tonni and A. Vichi, *Bounding scalar operator dimensions in 4D CFT*, *JHEP* **12** (2008) 031 [0807.0004].

[17] J.D. Qualls and A.D. Shapere, *Bounds on Operator Dimensions in 2D Conformal Field Theories*, *JHEP* **05** (2014) 091 [1312.0038].

[18] S. Hellerman and C. Schmidt-Colinet, *Bounds for State Degeneracies in 2D Conformal Field Theory*, *JHEP* **08** (2011) 127 [1007.0756].

[19] C.A. Keller and H. Ooguri, *Modular Constraints on Calabi-Yau Compactifications*, *Commun. Math. Phys.* **324** (2013) 107 [1209.4649].

[20] N. Benjamin, E. Dyer, A.L. Fitzpatrick and S. Kachru, *Universal Bounds on Charged States in 2d CFT and 3d Gravity*, *JHEP* **08** (2016) 041 [1603.09745].

[21] E. Dyer, A.L. Fitzpatrick and Y. Xin, *Constraints on Flavored 2d CFT Partition Functions*, *JHEP* **02** (2018) 148 [1709.01533].

[22] J.-B. Bae, S. Lee and J. Song, *Modular Constraints on Conformal Field Theories with Currents*, *JHEP* **12** (2017) 045 [1708.08815].

[23] T. Anous, R. Mahajan and E. Shaghoulian, *Parity and the modular bootstrap*, *SciPost Phys.* **5** (2018) 022 [1803.04938].

[24] N. Benjamin, H. Ooguri, S.-H. Shao and Y. Wang, *Light-cone modular bootstrap and pure gravity*, *Phys. Rev. D* **100** (2019) 066029 [1906.04184].

[25] J. Kaidi and E. Perlmutter, *Discreteness and integrality in Conformal Field Theory*, *JHEP* **02** (2021) 064 [2008.02190].

[26] A.L. Fitzpatrick and W. Li, *Improving modular bootstrap bounds with integrality*, *JHEP* **07** (2024) 058 [2308.08725].

[27] M. Cho, S. Collier and X. Yin, *Genus Two Modular Bootstrap*, *JHEP* **04** (2019) 022 [1705.05865].

[28] C.A. Keller, G. Mathys and I.G. Zadeh, *Bootstrapping Chiral CFTs at Genus Two*, *Adv. Theor. Math. Phys.* **22** (2018) 1447 [1705.05862].

[29] J.L. Cardy, *Operator Content of Two-Dimensional Conformally Invariant Theories*, *Nucl. Phys. B* **270** (1986) 186.

[30] B. Mukhametzhanov and A. Zhiboedov, *Modular invariance, tauberian theorems and microcanonical entropy*, *JHEP* **10** (2019) 261 [1904.06359].

[31] S. Ganguly and S. Pal, *Bounds on the density of states and the spectral gap in CFT_2*, *Phys. Rev. D* **101** (2020) 106022 [1905.12636].

[32] B. Mukhametzhanov and S. Pal, *Beurling-Selberg Extremization and Modular Bootstrap at High Energies*, *SciPost Phys.* **8** (2020) 088 [2003.14316].

[33] T. Hartman, C.A. Keller and B. Stoica, *Universal Spectrum of 2d Conformal Field Theory in the Large c Limit*, *JHEP* **09** (2014) 118 [1405.5137].

[34] D. Mazáč, *Analytic bounds and emergence of AdS_2 physics from the conformal bootstrap*, *JHEP* **04** (2017) 146 [1611.10060].

[35] D. Mazáč and M.F. Paulos, *The analytic functional bootstrap. Part I: 1D CFTs and 2D S-matrices*, *JHEP* **02** (2019) 162 [1803.10233].

[36] D. Mazáč and M.F. Paulos, *The analytic functional bootstrap. Part II. Natural bases for the crossing equation*, *JHEP* **02** (2019) 163 [1811.10646].

[37] M.F. Paulos, *Analytic functional bootstrap for CFTs in $d > 1$*, *JHEP* **04** (2020) 093 [1910.08563].

[38] D. Mazáč, L. Rastelli and X. Zhou, *A basis of analytic functionals for CFTs in general dimension*, *JHEP* **08** (2021) 140 [1910.12855].

[39] S. Caron-Huot, D. Mazáč, L. Rastelli and D. Simmons-Duffin, *Dispersive CFT Sum Rules*, *JHEP* **05** (2021) 243 [2008.04931].

[40] M.F. Paulos and B. Zan, *A functional approach to the numerical conformal bootstrap*, *JHEP* **09** (2020) 006 [1904.03193].

[41] M.S. Viazovska, *The sphere packing problem in dimension* 8, *Ann. of Math.* **185** (2017) 991 [1603.04246].

[42] H. Cohn, A. Kumar, S.D. Miller, D. Radchenko and M. Viazovska, *The sphere packing problem in dimension* 24, *Ann. of Math.* **185** (2017) 1017 [1603.06518].

[43] H. Cohn, A. Kumar, S.D. Miller, D. Radchenko and M. Viazovska, *Universal optimality of the E_8 and Leech lattices and interpolation formulas*, *Ann. of Math.* **196** (2022) 983 [1902.05438].

[44] D. Radchenko and M. Viazovska, *Fourier interpolation on the real line*, *Publ. Math. Inst. Hautes Études Sci.* **129** (2019) 51 [1701.00265].

[45] H. Cohn and Y. Zhao, *Sphere packing bounds via spherical codes*, *Duke Math. J.* **163** (2014) 1965 [1212.5966].

[46] G.A. Kabatiansky and V.I. Levenshtein, *Bounds for packings on a sphere and in space*, *Probl. Inf. Transm.* **14** (1978) 1.

[47] M. de Courcy-Ireland, M. Dostert and M. Viazovska, *Six-dimensional sphere packing and linear programming*, *Math. Comp.* **93** (2024) 1993 [2211.09044].

[48] H. Cohn and N. Triantafillou, *Dual linear programming bounds for sphere packing via modular forms*, *Math. Comp.* **91** (2022) 491 [1909.04772].

[49] S. Torquato and F.H. Stillinger, *New conjectural lower bounds on the optimal density of sphere packings*, *Experiment. Math.* **15** (2006) 307 [math/0508381].

[50] A. Scardicchio, F.H. Stillinger and S. Torquato, *Estimates of the optimal density of sphere packings in high dimensions*, *J. Math. Phys.* **49** (2008) 043301 [0705.1482].

[51] H. Cohn and F. Gonçalves, *An optimal uncertainty principle in twelve dimensions via modular forms*, *Invent. Math.* **217** (2019) 799 [1712.04438].

[52] J. Bourgain, L. Clozel and J.-P. Kahane, *Principe d'Heisenberg et fonctions positives*, *Ann. Inst. Fourier (Grenoble)* **60** (2010) 1215 [0811.4360].

[53] F. Gonçalves, D. Oliveira e Silva and S. Steinerberger, *Hermite polynomials, linear flows on the torus, and an uncertainty principle for roots*, *J. Math. Anal. Appl.* **451** (2017) 678 [1602.03366].

[54] N. Afkhami-Jeddi, H. Cohn, T. Hartman and A. Tajdini, *Free partition functions and an averaged holographic duality*, *JHEP* **01** (2021) 130 [2006.04839].

[55] A. Maloney and E. Witten, *Averaging over Narain moduli space*, *JHEP* **10** (2020) 187 [2006.04855].

[56] E. Shaghoulian, *Modular forms and a generalized Cardy formula in higher dimensions*, *Phys. Rev. D* **93** (2016) 126005 [1508.02728].

[57] E. Shaghoulian, *Black hole microstates in AdS*, *Phys. Rev. D* **94** (2016) 104044 [1512.06855].

[58] A. Belin, J. de Boer, J. Kruthoff, B. Michel, E. Shaghoulian and M. Shyani, *Universality of sparse $d > 2$ conformal field theory at large N*, *JHEP* **03** (2017) 067 [1610.06186].

[59] S. El-Showk and M.F. Paulos, *Bootstrapping Conformal Field Theories with the Extremal Functional Method*, *Phys. Rev. Lett.* **111** (2013) 241601 [1211.2810].

[60] S. El-Showk and M.F. Paulos, *Extremal bootstrapping: go with the flow*, *JHEP* **03** (2018) 148 [1605.08087].

[61] F. Johansson, *Arb: efficient arbitrary-precision midpoint-radius interval arithmetic*, *IEEE Trans. Comput.* **66** (2017) 1281 [1611.02831].

[62] A. Salmon, *The half-rate linear programming bound for binary codes is $\frac{1}{2} - \frac{1}{\pi}$*, [2609.03736].

[63] T. Ransford, *Potential Theory in the Complex Plane*, vol. 28 of *London Math. Soc. Student Texts*, Cambridge University Press (1995).

[64] J.B. Garnett, *Bounded Analytic Functions*, vol. 236 of *Graduate Texts in Mathematics*, Springer, revised 1st ed. (2007).

[65] W. Rudin, *Real and Complex Analysis*, McGraw–Hill, 3rd ed. (1987).

[66] C.-H. Chang, V. Dommes, P. Kravchuk, D. Poland and D. Simmons-Duffin, *Accurate bootstrap bounds from optimal interpolation*, *JHEP* **05** (2026) 275 [2509.14307].

[67] F.W.J. Olver, A.B. Olde Daalhuis, D.W. Lozier, B.I. Schneider, R.F. Boisvert, C.W. Clark et al., eds., "NIST Digital Library of Mathematical Functions." https://dlmf.nist.gov/, Release 1.2.4 of 2025-03-15.

[68] J. Qiao and S. Rychkov, *Cut-touching linear functionals in the conformal bootstrap*, *JHEP* **06** (2017) 076 [1705.01357].

[69] G. Szegő, *Orthogonal Polynomials*, vol. 23 of *AMS Colloquium Publications*, American Mathematical Society, 4th ed. (1975).

[70] L.D. Faddeev, R.M. Kashaev and A.Y. Volkov, *Strongly coupled quantum discrete Liouville theory. I: Algebraic approach and duality*, *Commun. Math. Phys.* **219** (2001) 199 [hep-th/0006156].

[71] B. Ponsot and J. Teschner, *Clebsch-Gordan and Racah-Wigner coefficients for a continuous series of representations of $U_q(sl(2,\mathbb{R}))$*, *Commun. Math. Phys.* **224** (2001) 613 [math/0007097].

[72] L. Hörmander, *Notions of Convexity*, vol. 127 of *Progress in Mathematics*, Birkhäuser (1994).

[73] J.D. Qualls, *Universal Bounds in Even-Spin CFTs*, *JHEP* **12** (2015) 001 [1412.0383].

[74] F. Gliozzi, *Modular bootstrap, elliptic points, and quantum gravity*, *Phys. Rev. Research* **2** (2020) 013327 [1908.00029].

[75] F. Gliozzi, *Three-dimensional quantum gravity according to ST modular bootstrap*, [2007.00684].

[76] M. Tierz, *Finite Gauss-Sum Modular Kernels: Scalar Gap and a Pure AdS_3 Gravity No-Go Theorem*, [2512.00361].

[77] C.-M. Chang, R. Liu and W.-J. Ma, *Large gaps and BTZ entropy in modular spectra with positive integer degeneracies*, [2609.39930].

[78] E. Perlmutter, *The Spectral Edge at Large Central Charge and Black Hole Statistics*, [2610.31413].

[79] A. Salmon, *The Rate of the Delsarte Bound for Binary Codes and Spheres*, [2610.21263].

[80] H. Cohn and S.D. Miller, *Some properties of optimal functions for sphere packing in dimensions 8 and 24*, [1603.04759].

[81] L.A. Caffarelli, *The obstacle problem revisited*, *J. Fourier Anal. Appl.* **4** (1998) 383.

[82] E.B. Saff and V. Totik, *Logarithmic Potentials with External Fields*, vol. 316 of *Grundlehren der mathematischen Wissenschaften*, Springer, Berlin (1997), 10.1007/978-3-662-03329-6.

[83] P.G. Harper, *Single band motion of conduction electrons in a uniform magnetic field*, *Proc. Phys. Soc. A* **68** (1955) 874.

[84] P.L. Duren, *Univalent Functions*, vol. 259 of *Grundlehren der mathematischen Wissenschaften*, Springer, New York (1983).

[85] B. Gustafsson and M. Sakai, *On potential theoretic skeletons of polyhedra*, *Geom. Dedicata* **76** (1999) 1.